636.2 + 636.4 : 591.872 : 591.185.34 : 591.487

MEDEDELINGEN LANDBOUWHOGESCHOOL
WAGENINGEN • NEDERLAND • 77-13 (1977)

A QUALITATIVE AND QUANTITATIVE INVESTIGATION OF OLFACTORY AND NASAL RESPIRATORY MUCOSAL SURFACES OF COW AND SHEEP BASED ON VARIOUS ULTRASTRUCTURAL AND BIOCHEMICAL METHODS

B. P. M. MENCO
Department of Animal Physiology, Agricultural University, Wageningen, The Netherlands

(Received 4-IV-1977)

H. VEENMAN & ZONEN B.V. – WAGENINGEN – 1977

Mededelingen Landbouwhogeschool
Wageningen 77-13 (1977)
(Communications Agricultural University)
is also published as a thesis

CONTENTS

Abbreviations

The present list only provides abbreviations which are regularly used throughout the whole text.

BSA:	bovine serum albumine
EM:	electron microscopy
EOG:	electro-olfactogram
ESR:	electron spin resonance
HVEM:	high-voltage transmission electron microscope
K:	1,000 times magnified
Na^+-K^+-ATPase:	sodium-potassium adenosine triphosphatase
SEM:	scanning electron microscope
TEM:	transmission electron microscope

9(2) + 2 axonemal structure: the inner ciliary structure which consists of nine peripheral microtubular doublet subfibers and two single central microtubular subfibers

GENERAL INTRODUCTION

Many hypotheses have been developed to account for the process of olfaction (for reviews see MOULTON and BEIDLER, 1967; DAVIES, 1971 and POYNDER, 1974), but at the present time none of them has been verified. The olfactory organ demonstrates very interesting receptor properties. It interacts with a great variety of compounds, called odorants (STAHL, 1973).

Appropriate biochemical and biophysical methods including the separation of sensory surfaces should be able to provide important evidence about receptive mechanisms and attempts to use such techniques have begun in recent years (e.g. KOCH and NORRING, 1969; ASH and SKOGEN, 1970; KOYAMA et al., 1971; KOROLEV and FROLOV, 1973; MENCO et al., 1974; MARGOLIS, 1975). Techniques for separating receptor structures have also been suggested by OTTOSON (1970), but sofar none of these methods has yielded a pure fraction of receptor endings (see DODD, 1974). The present account will deal mainly with the anatomy of the bovine olfactory epithelium emphasizing prospects for isolating receptor moieties. The adjacent nasal respiratory epithelium has also been investigated since, like the olfactory bipolar nervous cells such respiratory cells bear cilia. In the latter case, however, they are motile, rather than sensory, thus enabling a determination of features which are specific for the olfactory cilia and a comparison between two adjacent epithelium types allows such specific characterizations (LUCAS and DOUGLAS, 1934; SLEIGH, 1974).

The cow has been used as an experimental animal, since the size of its olfactory organ and the availability of samples seemed most convenient for this work. Some of the studies presented here were carried out on sheep. Indications for behaviour towards odorants in cows have been reviewed by ERNST and PUSHKARSKII (1975).

In Chapter 1, the distal processes of both epithelium types are described, using different microscopical methods, including light microscopy, scanning electron microscopy, thin section transmission electron microscopy and thick section high-voltage transmission electron microscopy. This latter method was used in the hope that it would permit olfactory cilia to be followed over their whole lengths. In this chapter some attention will also be devoted to macroscopic observations.

Chapter 2 deals with the results of freeze-etch and electron spin resonance studies on both epithelium types. Both techniques allow predictions of some of the molecular properties of the receptive area through investigation of intact tissue in vitro.

Chapter 3 deals with a quantitative analysis of the morphological data. Statistical methods are used where it is possible. Several features of the olfactory nerve endings are compared for different nasal areas and for adult as opposed to juvenile animals. Special emphasis is placed on the ciliary processes.

Olfactory and respiratory cilia are also compared with each other. Furthermore, estimates for possible receptor concentrations based chiefly on freeze-etch results are presented.

Such quantitative information is important for biochemical work, since it indicates whether one can consider nerve ending preparations as homogeneous or if one has to take into account that biochemical preparations may contain morphologically different nerve ending types. Furthermore, some ideas about receptor quantities which might be isolated can be obtained.

Finally, Chapter 4 deals with attempts to isolate peripheral receptor membranes. The conventional criteria used by others for assessing the purity of the fractions have been shown to be inadequate (DODD, 1974); this prompted us to initiate anatomical studies on the bovine olfactory mucosa, so as to provide ourselves with a more adequate basis for future biochemical studies.

1. MACROSCOPIC AND MICROSCOPIC STUDIES ON BOVINE NASAL EPITHELIUM USING LIGHT MICROSCOPY, LOW- AND HIGH-VOLTAGE TRANSMISSION AND SCANNING ELECTRON MICROSCOPY

1.1. INTRODUCTION

The ultrastructure of the vertebrate olfactory epithelium has been explored by many authors, both by transmission and scanning electron microscopy. Papers on transmission electron microscopy include reviews by DE LORENZO (1970), REESE and BRIGHTMAN (1970), GRAZIADEI (1971b, 1973a, 1974a, 1974b), VINNIKOV (1974), ALTNER and KOLNBERGER (1975) and ANDRES (1975) and extensive investigations by HEIST et al. (1967), SEIFERT (1970), YAMAMOTO (1976) and LOO (1977). Scanning electron microscopy has been carried out by GRAZIADEI (1970, 1971b, 1973a, 1975) on turtle, frog, dog, catfish and garfish; by GRAZIADEI and GRAZIADEI (1976) on mudpuppy and tiger salamander; by ADAMS and MCFARLAND (1971) and ADAMS (1972) on mouse; by BERTMAR (1972) on sea trout; by CONTICELLO et al. (1973) on guinea pig; by KANDA et al. (1973) on man and guinea pig; by BREIPOHL et al. (1973a, 1973b, 1974a, 1974b) on goldfish and chicken; by WATERMAN and MELLER (1973a, 1973b) on goldhamster embryo; by ANDREWS (1974) on rat; by SHIMAMURA and TOH (1974) on rabbit; by ANDRES (1975) on caiman, goldfish and rhesus monkey; by ZEISKE et al. (1976) on cyprinodontoid fish and by LENZ (1976) on man, rabbit and sheep.

Neither transmission nor scanning electron microscopy has been applied to the ox, an animal which is suitable for biochemical studies on the olfactory system because of its size and availability (DODD, 1970; KOYAMA et al., 1971).

Although the general ultrastructure of the peripheral olfactory system in all vertebrates investigated sofar, particularly in mammals, seems to be almost identical (GRAZIADEI, 1973a, 1974a), a thorough anatomical investigation of the olfactory surface of the species selected was considered essential for further biochemical studies. Without such anatomical knowledge a proper identification of sensory structures is virtually impossible. Ciliated nasal respiratory epithelium (LUCAS and DOUGLAS, 1934; NEGUS, 1958; STOCKINGER, 1963; OKANO and SUGAWA, 1965; MATULIONIS and PARKS, 1973) was selected as a tissue for comparison with the olfactory tissue, which is also ciliated. The presence of respiratory cilia has also been demonstrated with the scanning electron microscope (BARBER and BOYDE, 1968; ADAMS, 1972; LENZ, 1972; GRAZIADEI, 1975). In the present study the structure of both epithelium types and particularly of their cilia has been compared using several methods, including macroscopic observations, light microscopy, scanning electron micro-

scopy, and transmission electron microscopy, with normal and high-voltage instruments. Scanning and high-voltage techniques allow clarification of the three dimensional organization of the tissue types under investigation.

1.2. Materials and methods

1.2.1. *Methods identical for all microscopic investigations*

Observations were made on olfactory and respiratory mucosae obtained from the heads of five cows and ten calves (younger than two weeks) of both sexes. Heads were obtained from local slaughterhouses between one and four hours after the animals had been slaughtered. This delay is probably acceptable in view of the fact that in frogs (though they are poikilothermic animals) motility of respiratory and olfactory cilia in isolated epithelium patches has been observed up to five hours after the animal had been killed (own observations).

Heads were cut sagittally with a bandsaw or an axe. From this point on methods were varied slightly during the course of the work. Most of these variations did not seem to be detrimental to sample observations.

Cold Karnovsky's (1965) fixative (3% glutaraldehyde, 3% formaldehyde prepared from paraformaldehyde, 0.01% $CaCl_2$-buffered with 0.075 M Na-cacodylate/HCl to pH = 7.0) was pipetted gently on the epithelium surface in situ. A neutral pH was chosen, since indicator paper (range 6–8), when applied to the epithelium surface, showed a pH value of 7.0. Heads were transported to the laboratory after this treatment and the tissue was further fixed (in situ) at 4°C for a total of about two hours.

Subsequently, portions from the areas under investigation were dissected and left standing in fixative for a further two hours. Pieces of mucosa up to 0.5 cm^2 in area were selected and used for all the types of microscopic investigations employed here. These areas were not considered to be too large for an adequate fixation for the transmission studies, since the zone under investigation only forms the upper 100 μm layer of the mucosa. One advantage of this procedure is that damage caused to the surface during the preparation is minimized. During the fixation tissue blocks were either very gently agitated or left alone. Following aldehyde fixation blocks were rinsed in the same buffer used in fixation, although the aldehyde was now replaced by 6% (w/v) sucrose. The rinsing sequence was as follows: 30 seconds, 30 minutes, 1 hour, 6 hours and once more 6 hours, respectively. Subsequently, blocks were fixed for one hour in 1% OsO_4 made up in the same buffer as used for aldehyde fixation, except that 4.5% sucrose was present. The blocks were then rinsed again.

Much of the tissue material, used in the present work, was fixed in non-buffered OsO_4 instead of in a buffered solution. No investigations were done on the effects of pH and variation in osmolarity.

Dehydration was usually carried out with ethanol with propylene oxide as clearing agent, but occasionally acetone was used.

1.2.2. *Preparation of sections for high-voltage transmission observation*

The procedures followed here were chiefly adapted from techniques described in GLAUERT's review (1974). For high voltage electron microscopy block staining was applied during dehydration and clearing procedures. Tissue blocks were left for 24 hours at 60 °C in absolute ethanol containing 2% (w/v) uranyl acetate (LOCKE et al., 1971) and 1.5% (v/v) glacial acetic acid (LOCKE and KRISHNAN, 1971). The blocks were subsequently cleared in propylene oxide. The selected tissue blocks were then embedded in Araldite according to standard techniques (GLAUERT and GLAUERT, 1958). Araldite blocks appropriate for electron microscopic transmission observations were selected under a light microscope by observing sections (2–5 μm) stained at 60 °C with 'Paragon' stain (Gurr).

These sections and sections for electron microscope observation were cut with a Reichert ultramicrotome with glass knives made with a LKB knife maker. Thick sections prepared for high-voltage electron microscopy were not stretched with chloroform before taking them up with the grids from the water. Before the next thick section was made ultrathin sections were cut until thin sections again had a gold-silver appearance. This ensured adequate thick section surfaces. Sections were attached to Formvar/carbon coated 75 mesh hexagonal grids.

In order to ensure maximal contact between staining solutions and the sections on the grids during staining procedures, staining solutions were deaerated with a water pump before use, thus preventing the formation of air bubbles on the sections. All staining was carried out by inserting rings made from plastic tubing (Viton) of 1 cm diameter and 3 mm height, containing 3 to 4 grids in beakers with the staining or washing solutions. Sections were stained with lead citrate (VENABLE and COGGESHALL, 1965) for 1 hour. They were then washed once in 0.02% NaOH (w/v), twice in distilled water and restained with alcoholic uranyl acetate (see above) for 1 hour at 60 °C. They were washed once in 50% ethyl alcohol and twice in distilled water. Subsequently, the sections were restained in a lead citrate solution for 1 hour and washed again as above. In the case that lead carbonate precipitates were formed, grids were quickly rinsed in 0.05% (v/v) HNO_3 (FARVARD and CARASSO, 1973) and then rinsed with distilled water. Staining of thick sections up to 2 μm could readily be evaluated at 125 kV in a Hitachi 125 E electron microscope. After staining the grids were recoated with Formvar and carbon on both sides (sandwiched). With this method no drift was observed in sections up to 10 μm thick at 1,000 kV.

Sections were examined in an AEI-EM7 High-Voltage Electron Microscope at the Department of Material Sciences of Birmingham University. Generally, they were observed at 1,000 kV with a 20 μm aperture. Stereopair micrographs were prepared by tilting the sample stage over adequate angles, selected from a table prepared by BEESTON (1972).

1.2.3. *Preparation of ultrathin sections for normal transmission electron microscope observation*

Samples selected for thin section transmission electron microscopy were chiefly treated according to the procedures described for the HVEM. Deviations will be described in the following section.

The ultrathin sections were stretched with chloroform vapour before attaching them to Formar/carbon coated 75 mesh hexagonal grids. They were stained with the same staining solutions as used for the HVEM work, but in this case they were exposed twice for only one minute to lead citrate (before and after the uranyl acetate staining) and during 4 to 8 minutes to uranyl acetate. The uranyl acetate solutions employed here consisted of a saturated solution in 50% aqueous ethyl alcohol containing 1.5% (v/v) glacial acetic acid, or a 25% uranyl acetate solution in absolute methanol (STEMPAK and WARD, 1964). With the latter method Formvar-coated grids had to be used. At the beginning of the present study Parlodion-coated grids were used, but since Parlodion dissolves in methanol this method had to be discontinued.

Sections were examined in a Hitachi 125E electron microscope at 125 kV usually with a 20 μm aperture. Occasionally they were examined in a JEM 7 or a JEM 200 electron microscope at 100 kV.

1.2.4. *Preparation of sections for light microscopic observation*

The best 'Paragon' stained sections were mounted in Polymount (Staines) and examined and photographed with a Vickers 55 light microscope. Kodacolor II was used for the photography.

1.2.5. *Preparations of tissue blocks for examination in a scanning electron microscope*

Except when block staining was applied, samples for scanning and transmission electron microscopy were treated together until ethyl alcohol dehydration. Scanning samples to be freeze-dried were also cleared with propylene oxide. After dehydration and subsequent clearing, samples for transmission and scanning studies were separated by dissecting small tissue pieces from the 0.5 cm^2 blocks to be used for transmission studies. The remainder was used for scanning studies and processed further in various ways.

Since neither a critical drying point apparatus nor a sputter-coater were available at the onset of this study, blocks selected for scanning electron microscopy were also processed in different ways during this study.

Blocks to be freeze-dried were first processed through a graded series of propylene oxide/benzene or acetone/benzene mixtures, depending on the dehydration method used (modified after NØRREVANG and WINGSTRAND, 1970). Subsequently, samples were coated with gold/palladium (Polaron) by evaporation, while revolving and tilting. In later experiments samples were dried in a Polaron E 3000 Critical Drying Point Apparatus. After dehydration with ethyl alcohol, blocks were processed through a graded series of amyl acetate and critical point dried from liquid CO_2 (LEWIS and NEMANIC, 1973).

FIG. 1A and B. General survey of the posterior region of the respiratory and olfactory areas in a one week old male calf (*A*) and a two year old steer (*B*). Insets show the upper jaws of both animals; the nasal regions of interest are indicated by an ellipse. The ethmoturbinates (E and Ec) show yellow pigmented olfactory (Olf) and pale respiratory (Resp) epithelium. The cribriforum plate (Cp) contains only olfactory epithelium. The olfactory area of the adult animal (*B*) is more elongated and more darkly pigmented than the olfactory area of the calf (*A*). Cc: cerebral cavity; E1-6: six endoturbinates; Ec: ectoturbinate appearing behind endoturbinates; N: nasopharynx.

As soon as possible after drying, samples were coated in a Polaron Diode Sputtering Device Type E 5000 with a 20 nm–40 nm gold layer (ECHLIN, 1975).

Tissue blocks were examined in a Cambridge Mk 2A Stereoscan microscope, usually at 30 kV. Stereopair micrographs were prepared by tilting the sample stage over 5° to 7°.

1.2.6. *Account of the amount of tissue material used*

Out of a total of 72 blocks of Araldite embedded tissue 42 proved to contain the required epithelium surface. Fewer usable blocks were obtained from cows than from calves.

Out of a total of 35 samples prepared, twenty-five containing the required olfactory or respiratory surface were used for study in the scanning electron microscope. This does not mean that the specimens selected contained only ciliated surfaces, but at least some ciliated surface was present.

In the transmission studies three to four grids, each containing 5 to 10 sections, were prepared from each usable block. Thus about 800 thin sections were studied in total.

High-voltage transmission studies on thick sections were carried out on eight of the best blocks. About 40 grids, each bearing 5 to 10 sections varying in thickness from 0.5–10 μm, were prepared. Thus, in total about 300 sections were made, and thicknesses between 2.5–5 μm appeared to be most suitable for this type of study.

1.2.7. *Materials*

All chemicals employed were obtained from British Drug Houses and were of analytical grade unless otherwise stated.

1.3. RESULTS

1.3.1. *Macroscopic appearance*

A general macroscopic view of bovine juvenile and adult nasal cavities in relation to the rest of the head is presented in the insets of Fig. 1A and B respectively, while the rest of these figures depict a closer view upon the anterior respiratory (white area) and posterior olfactory (yellow area) epithelia of the ethmoturbinates in both age groups. The nasal septum has been dissected away. This dissection slightly damaged the adult turbinate surface.

The olfactory region is pale yellow in juvenile animals and turns brownish-yellow with age. Transition areas between the respiratory and olfactory epithelium are clearly visible. The olfactory area is separated from the brain cavity by the cribriform plate which is also covered with olfactory epithelium; in the calf this epithelium part is relatively larger than in the adult animal. The whole olfactory area seems to change shape with age.

In the sagittal plane the olfactory area increased approximately by identical factors as the rest of the snout, thus suggesting postnatal development of the

olfactory area. However, exact olfactory surface areas were not determined. Whether or not growth of the olfactory area reflects an increase in the total number of nerve endings is the subject of microscopical investigations described in the discussion of this chapter and in Chapter 3.

1.3.2. *General histology of the bovine nasal mucosa*

Fig. 2 presents light micrographs of the ox respiratory (Fig. 2A) and olfactory (Fig. 2B) epithelium at approximately identical magnifications. Figs. 3 and 4 compare these types of epithelium by scanning and thick section, but not high-voltage, electron microscopy. The two epithelium types appear quite different with these microscopic methods in spite of the fact that both contain ciliated surfaces. Freeze-etch techniques have revealed additional ultrastructural differences which cannot be detected with any of the other microscopical techniques (see Chapter 2).

In the respiratory epithelium cilia are implanted on non-sensory columnar cells (Fig. 4A) and form a metachronal surface pattern caused by their beating action (Fig. 3A in particular). Proximally, basal cells are visible and under this basal cell layer the inconspicuous basal membrane is found, followed by the lamina propria which contains collagen fibers. The ultrastructure of this epithelium type is described in detail by STOCKINGER (1963), OKANO and SUGAWA (1965) and MATULIONIS and PARKS (1973).

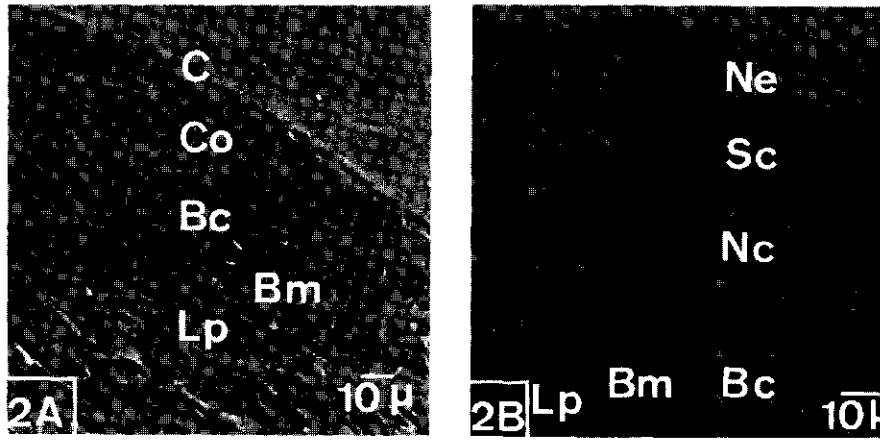

FIG. 2A and B. Light micrographs of columnar respiratory epithelium (*A*) and pseudostratified olfactory epithelium (*B*). (*A*) is taken from the nasal turbinates of a male calf, (*B*) is from the cribriform plate of an adult steer. Cilia (C) of the nervous epithelium originate from knob shaped nerve endings (Ne); the cilia of the respiratory epithelium are parallel to each other. The height of the respiratory epithelium is here about half that of the olfactory epithelium. Bc: basal cells; Bm: basal membrane (not visible here); Co: columnar cells; Lp: lamina propria; Nc: nerve cell perikaryon layer; Sc: supporting cell perikaryon layer. Micrographs were made after colour negatives, taken from Araldite embedded, Paragon stained thick sections.

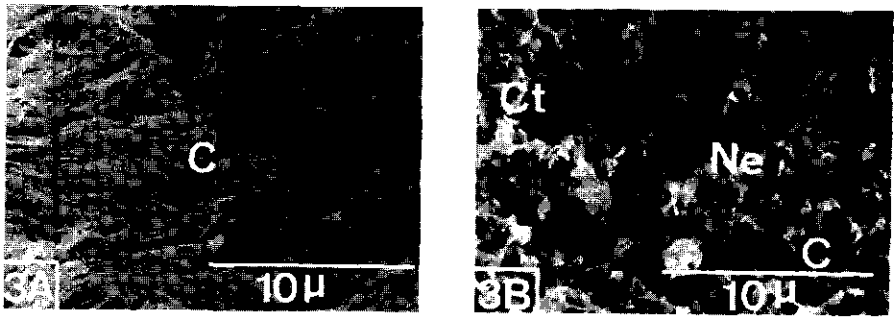

FIG. 3A and B. SEM views of (*A*) respiratory epithelium from calf septum and (*B*) olfactory epithelium from calf ethmoturbinate. Cilia (C) are present in both photographs. In the respiratory epithelium they are fixed during their effective stroke. In the olfactory epithelium they consist of two parts, a short initial part and a long ciliary taper (Ct). Here they originate from dendritic nerve endings (Ne) and alternate with supporting cell microvilli (Mv). The olfactory epithelium has a more fuzzy appearance than the respiratory epithelium which is due to mucus remnants. Both preparations were freeze-dried, Au/Pd-rotary evaporated and viewed under 45°. The olfactory preparation was gently scraped between drying and coating.

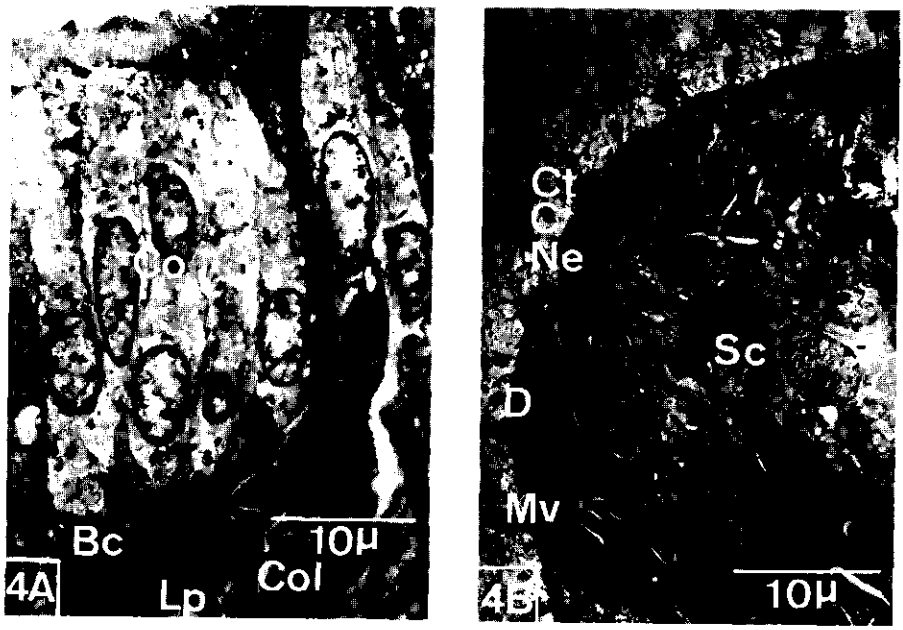

FIG. 4A and B. Thick section transmission electron micrographs of (*A*) respiratory epithelium from the septum of an adult steer and (*B*) olfactory epithelium from the cribriform plate. In (*A*) narrow, dark, vacuolated cells and lighter, non-vacuolated cells are seen. The lamina propria (Lp) contains collagen (Col) fibers. Olfactory ciliary tapers can be followed for about 13 μm. They run parallel to the epithelium surface. Note the heterogeinity of the olfactory surface. D: dendrite. For other legends see Figs. 2 and 3.

The bipolar olfactory sensory cells possess knob-shaped nerve endings (frequently called terminal swellings or olfactory vesicles) which usually expand somewhat above the epithelium surface. These knobs also bear cilia. At their base these cilia resemble respiratory cilia, but after 1 to 2 μm they taper to a smaller diameter (FRISCH, 1967) which is then maintained over a length which has yet to be determinded, although estimates for three macrosmatic species are elegantly calculated by SEIFERT (1970). Using morphometric methods he estimated their length to be about 50 μm in cat, dog and rabbit.

Apart from these cilia projecting from the nerve endings, the surface of the olfactory area is also covered with microvilli which originate form supporting (sustentacular) cells. These two cell types, the nervous and the supporting cells, form the major population of the upper cell layers of the olfactory epithelium (Figs. 2B, 3B and 4B). In Fig. 4B ciliary tapers are seen to run parallel to the epithelium surface and perpendicular to the microvilli. These microvilli frequently form bush-shaped structures.

Three zones of nuclei can be seen in Fig. 2B. The upper zone contains the nuclei of the supporting cells. The nuclei of the nerve cells are found in the central zone and the nuclei of the basal cells in the lower zone (GRAZIADEI, 1973a).

The respiratory epithelium is thinner than the olfactory epithelium (see also Chapter 3) and the cilia are probably embedded in a different mucus environment since scanning micrographs (e.g. Figs. 3A and 3B) more often reveal unremoved mucus in the olfactory than in the respiratory samples.

The rest of this chapter will be devoted to a more detailed description of the two types of epithelium.

1.3.3. *Structure of the bovine respiratory epithelium*

1.3.3.1. Scanning electron microscopy of the bovine respiratory epithelium

Figures 3A and 5 represent the surfaces of the ox nasal respiratory mucosa. The cilia are clearly arranged in a wave-like pattern, suggesting that they were beating at the moment of fixation. This has also been shown in SEM studies of this type of epithelium in several other species (BARBER and BOYDE, 1968; ADAMS, 1972; INOUE, 1974; GRAZIADEI, 1975).

Recently, the scanning technique has also frequently been applied to human nasal respiratory epithelium (AMENDOLEA et al., 1972; MYGIND and BRETLAU, 1973; OKUDA and KANDA, 1973; ŠVEJDA and ŠAFÁŘ, 1974) because this technique may have useful prospects for diagnostic purposes.

In Fig. 3A cilia are shown fixed in their effective stroke, while in Fig. 5 they are fixed in their recovery stroke (LENZ, 1972). In the posterior nasal area from which our preparations originate, the cilia usually form a thick uninterrupted carpet. This contrasts with the situation in the anterior area (LENZ, 1972; MYGIND and BRETLAU, 1973) where large areas are covered with a squamous epithelium type.

FIG. 5. Scanning electron micrograph of septal respiratory epithelium (adult, female). The cilia are probably fixed during their recovery stroke. Compare this figure with Fig. 3A. The preparation was freeze-dried and Au/Pd-rotary evaporated. 0° tilt.

Fig. 6. depicts a stereo view of a portion of respiratory epithelium. Some secretory products (probably from goblet cells) or cellular debris are present on and between the cilia. Distally these cilia taper slightly.

1.3.3.2. Transmission electron microscopy of the bovine respiratory epithelium

Figs. 4A and 7 show the main features of the respiratory epithelium as seen by TEM methods. Dark cells represent old degenerating cells. They are intensely vacuolated and usually of a smaller diameter than the lighter and presumably younger cells. Mitochondria in the dark cells are round while in

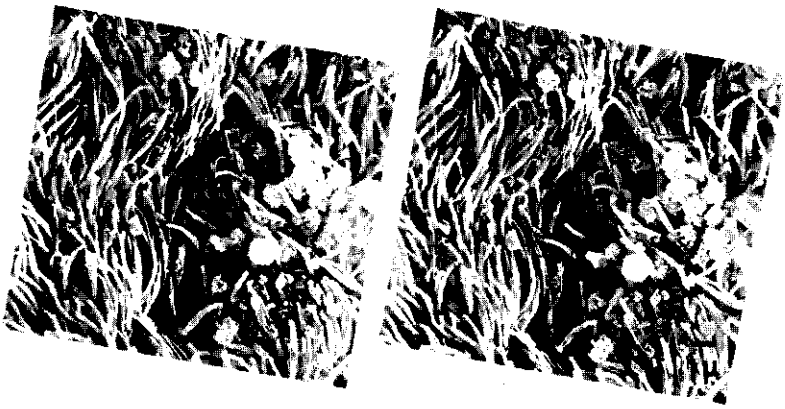

FIG. 6. Stereopair of ethmoturbinal respiratory epithelium (calf). Many cilia taper at their tips. Some agglutinated mucus or cellular debris is present on the surface. Stereopair figures may be viewed without any additional aid. They should be held at a distance of about 30 cm before the eyes on a still surface. Staring for about one minute at the photographs should reveal the stereo image. In case no satisfactory stereo representation can be obtained, a pocket stereo viewer may be of help. The preparation was critical point dried and Au-sputter-coated. Tilting angle: 6° (0°–6°).

the lighter cells they are elongated. Cilia of the two cell types do not differ markedly. Ciliary basal bodies contain short striated rootlets at their base, and at their central region they contain internal dots and basal feet (Figs. 7 and 8), which is the case in many other types of basal bodies (WOLFE, 1972). The axoneme doublets possess arms (Fig. 9) which contain dynein, a Mg^{++}-activated ATPase, thought to be responsible for ciliary motion (GIBBONS, 1965; STEPHENS and EDDS, 1976).

The axonemal structure is embedded in a matrix which is less dense than that matrix of olfactory cilia (Figs. 25 and 34). A more extensive comparison between the two cilia types will be presented in later sections (Chapter 3, Table VI and Summary, Table XVII and Fig. 56). Respiratory cilia are very similar to other motile cilia in their ultrastructural design (WARNER, 1972, 1974).

Multivesicular bodies are present in the apical cell part (Fig. 7). These organelles are also present in the olfactory supporting cells (Fig. 24). Sometimes respiratory cilia contain small vesicles (Fig. 7). Also other structures, such as microvilli sometimes form vesicles (Fig. 8).

Goblet cells, secreting granular mucogen droplets of varying electron densities are presented in Fig. 10. Here again, darker and lighter cells can be distinguished. Some mucogen droplets contain dense spherical bodies, rather similar to those encountered in bovine nasal respiratory submucosal glands as described by BOZARTH and STRAFUSS (1974). YAMAMOTO (1976) noticed the presence of such bodies in the olfactory secretion droplets of rabbit and bat.

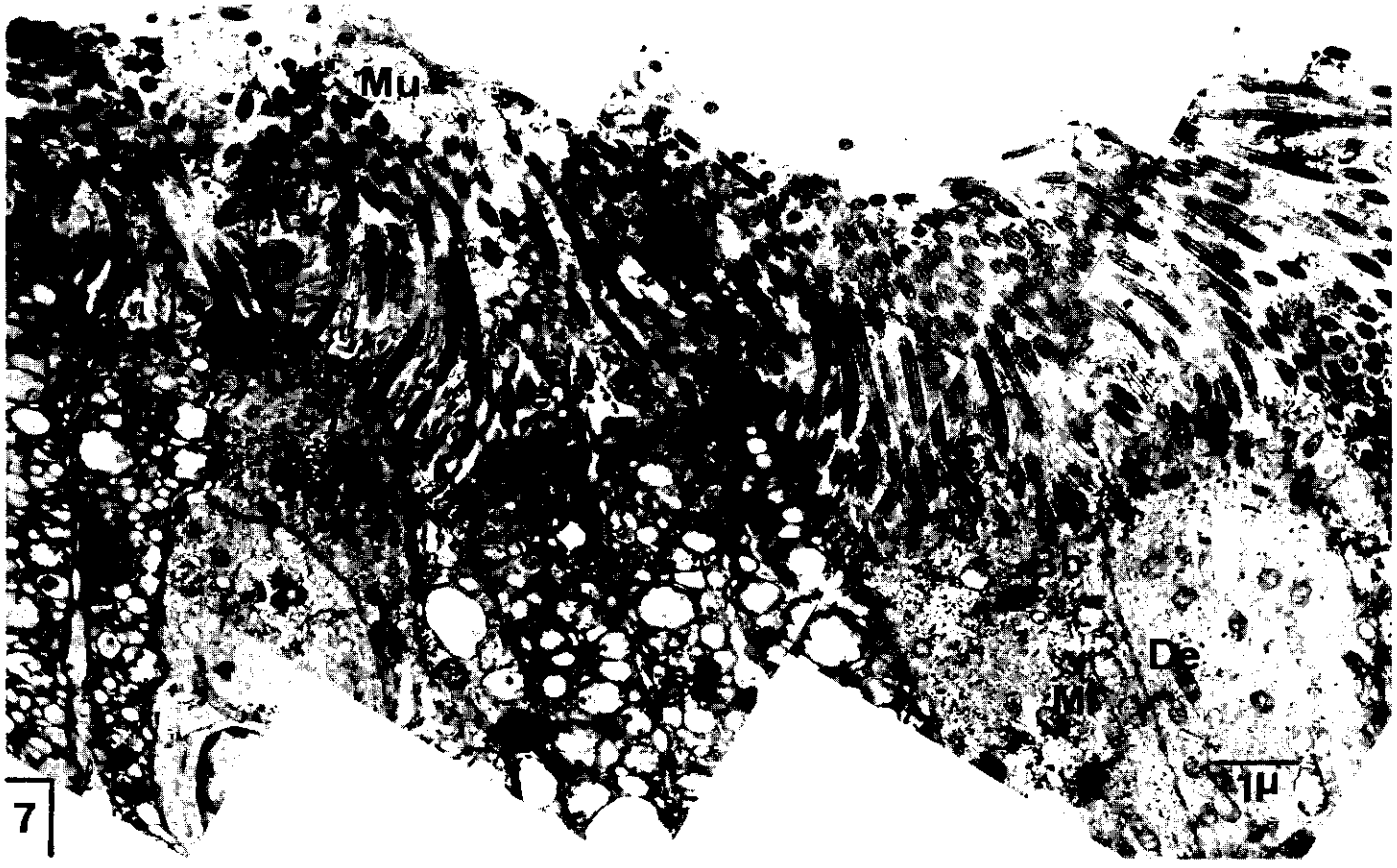

FIG. 7. Compound TEM picture of bovine respiratory epithelium (adult, septal). Dark cells in lysis contain swollen mitochondria (Mi) and multivesicular bodies (Mb). Lighter cells contain elongated mitochondria with cristae generally parallel to the epithelium surface. The membranes between two light cells display several desmosomes (De). Basal bodies (Bb) contain a central dense dot (compare with Figs. 25 and 34). Ciliary (C) axonemal structures seem like stairs due to the presence of arms and radial links. Some cilia are vesiculated (Ve). Mu: mucus; Mv: microvilli.

FIG. 8. Respiratory cilia (adult septal). Basal bodies (Bb) contain two rootlet types (R1 and R2). R2 is the basal foot. Bars formed by doublet arms and radial links are clearly visible between the central and peripheral microtubuli. A granulated area is present on the membrane near the base of the cilia: the ciliary necklace (Nl). For other legends see Fig. 7.

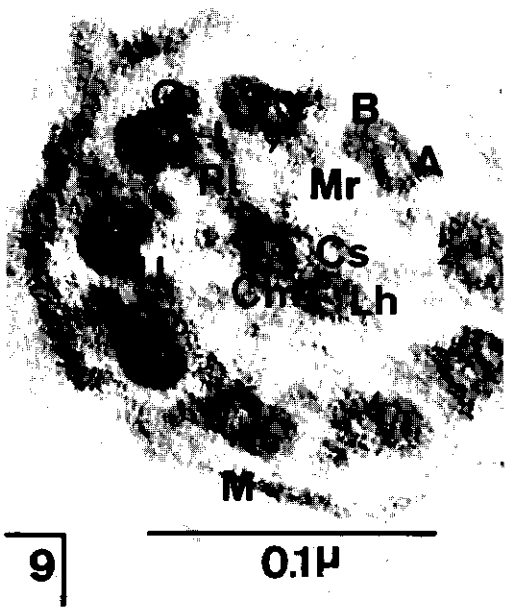

FIG. 9. Cross-section of a respiratory cilium (adult, septal). A: doublet subfiber A; B: doublet subfiber B; Cmt: central microtubular subfibers; Cs: central sheath; I: inner dynein containing arms; Il: inter doublet link; Lh: link head; M: membrane; Mr: matrix region; O: outer dynein containing arms; Rl: radial link; 1–9: nine microtubular doublets. Nomenclature as used by WARNER (1972, 1974).

FIG. 10. Two secretory goblet cells surrounded by cilia bearing columnar cells (adult, nasal ethmoturbinal epithelium). The two cells are in different stages of the secretory process. They contain mucogen (Mu) droplets of various densities. These droplets occasionally contain dense spherical dots (thin arrow). Some cilia (C) show tapering tips (heavy arrow; compare with Fig. 6).

An atypical brush cell, also found in the olfactory epithelium (Fig. 27, HVEM stereopair), was occasionally observed in the nasal respiratory epithelium.

Ciliary axonemes lacking individual membranes were encountered at numbers sometimes up to about 120 within one microvillous membrane (Fig. 11). These aggregates are of respiratory origin, as is indicated by the arm-bearing doublets in the inset of Fig. 11, and also by the fact that these structures are implanted on columnar cells as we have observed in unpublished photographs. Moreover the absence of supporting cells and the mutual linking of these axonemal sacs by tight junctions are indicative of the non-sensory nature. At places where microvilli originate from these sacs, these aggregates are surrounded by an internal cell coat which is less dense here than for the rest of the ciliary aggregate.

1.3.4. *Structure of the bovine olfactory epithelium*

1.3.4.1. Scanning electron microscopy of the bovine olfactory epithelium

1.3.4.1.1. General anatomy

Most SEM studies on the mammalian olfactory mucosa show only the long tapering distal parts of the olfactory cilia. The present study also shows the

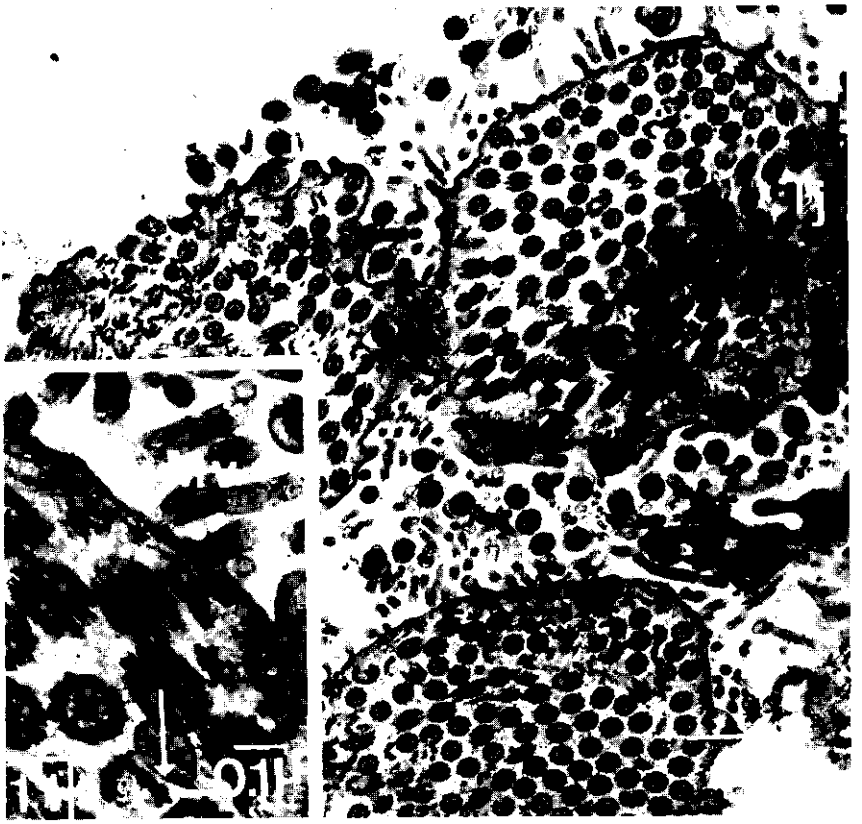

FIG. 11. Ciliary aggregates within microvillous membranes (adult, septal respiratory epithelium). The same tissue sample at higher magnification (inset) shows that the layer abutting the aggregate membrane is darker than the rest of the aggregate matrix. Microvillar membranes are less dense than the membranes surrounding the rest of the aggregate. Aggregates are connected by tight junction (Tj) containing membranes. The inset shows further that the microtubular doublets do contain dynein arms.

nerve endings from which the cilia originate, including the more proximal parts of the cilia. In some cases this appearance was obtained without any special treatment. In other cases the tissue blocks were gently scraped with a razor blade after freeze-drying but before gold/palladium coating, thus permitting the outline of intact nerve endings to be seen (diagram of Fig. 12).

Cilia originating from nerve endings are shown in Figs. 13, 14, 15, 17 and 19B. Generally, the surface of the olfactory cilia appears to be of a more complex structure than the membrane surface of respiratory cilia. However, this difference is less pronounced in the ox than, e.g. in amphibians (GRAZIADEI and GRAZIADEI, 1976). The granulated appearance might be caused by mucus remnants, but could also indicate some functional specialization of the receptor membrane itself. In the latter case, the granulated appearance is perhaps

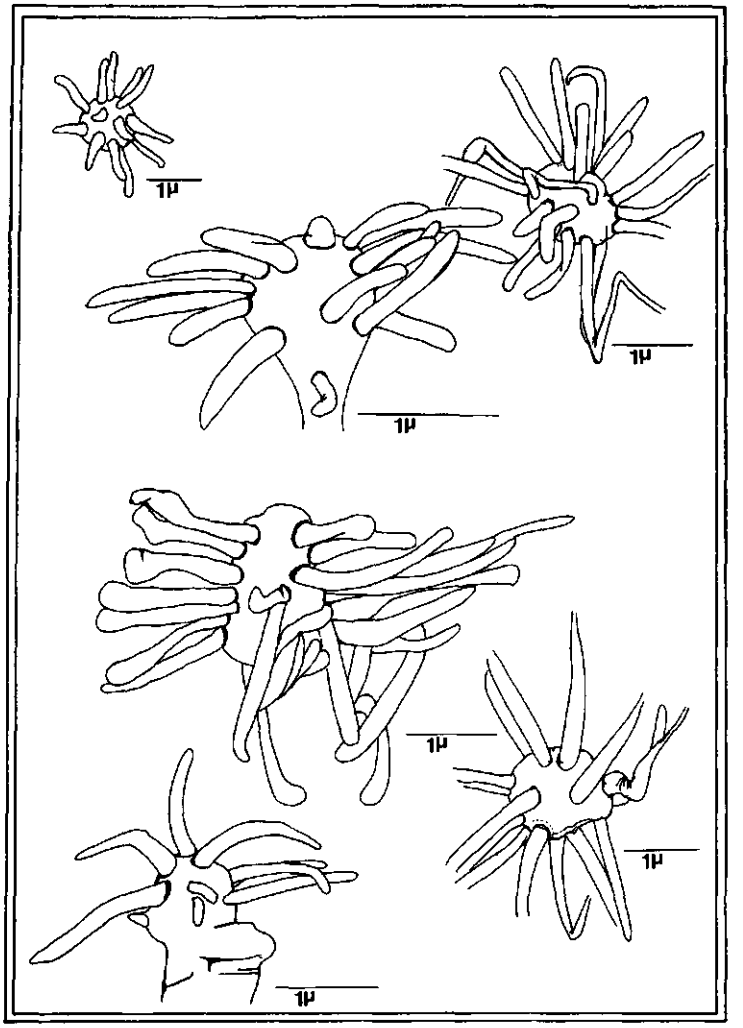

FIG. 12. Some outlines of olfactory nerve endings with the proximal, parts of their cilia, as observed by SEM.

associated with the particles seen within the olfactory nerve membranes when using freeze-etch techniques (Chapter 2).

The nerve endings in Fig. 14 bear cilia, which end in club-shaped knobs. These knobs could be formed by breaking of the distal ciliary parts, but on the other hand could also represent real ciliary tips since club-shaped tips are also seen in sectioned (Figs. 35 and 39) and freeze-etch (Fig. 49) preparations.

One cilium of a nerve ending in Fig. 14 clearly reveals a ciliary necklace (GILULA and SATIR, 1972), a feature which, as far as we know, has not been

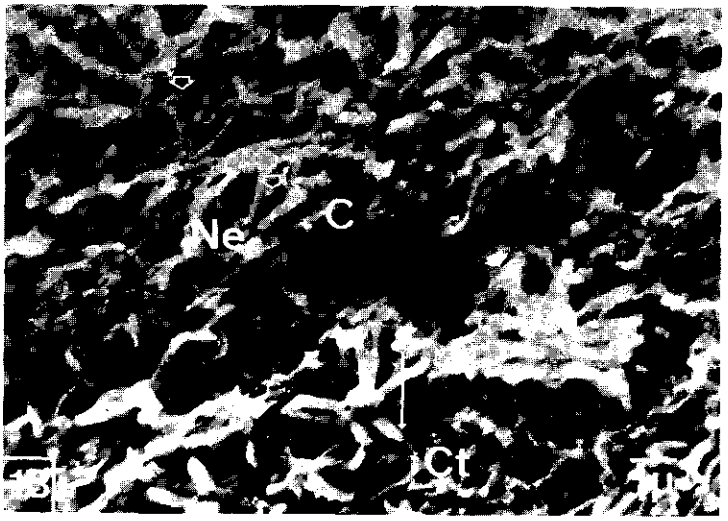

FIG. 13. Olfactory epithelium surface (calf, cribriform plate). One very regular nerve ending (heavy arrow) is seen amidst several other nerve endings. Another nerve ending shows a tapering cilium (thin arrow). Nerve endings and cilia show light dots on their surface (open arrows). For legends see Fig. 3. The preparation was freeze-dried, Au-sputter-coated and viewed under 45°.

observed with this technique before. These necklaces, consisting of about 6 strands, were seen regularly (Table VI in Chapter 3). The fact that they are made visible with this technique suggests that they contain a rather rigid surface structure which is neither obscured by the metal coating nor by the relatively poor resolving capacity (about 10 nm) of the scanning electron microscope. Since the necklace features may be correlated with characteristics revealed by the freeze-etch technique (Chapters 2 and 3, Tables I and VI), it is possible that the presence of membrane particles may also affect the SEM appearance of receptive membranes in general, as is seen in Fig. 15 (inset). However, granule diameters are about 40 nm – four times as big as those of freeze-etch particles (Table I in Chapter 2). With regard to the question whether they are really membrane surface structures, deep etching could possibly provide an answer. Generally, this granulation is obscured by excess coating. In addition this nerve ending contains some pore like structures, which could represent the openings of endocytotic vesicles as seen e.g. in Figs. 24 and 31A.

The main part of Fig. 15 shows a transition area between the olfactory and respiratory epithelium surface. In this figure a patch containing nerve endings with cilia which are broken or not fully developed, as well as the microvilli of supporting cells is abutted by a zone of respiratory cilia. A clear spatial arrangement of supporting cells and nerve endings as observed by GRAZIADEI (1975) in some lower vertebrates was not found. Stereopairs of these transition areas are shown in Fig. 16. Respiratory cilia seem to beat over the olfactory

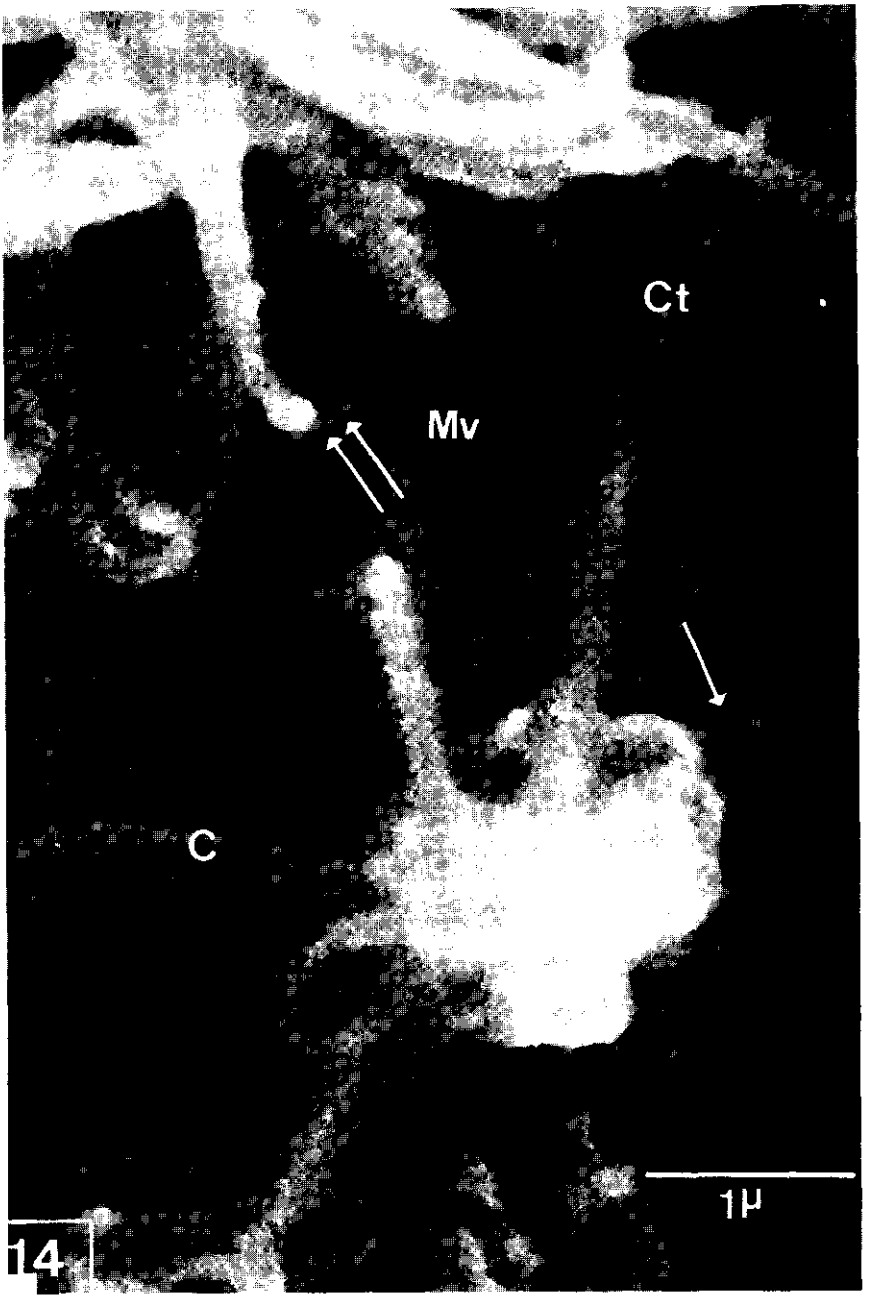

FIG. 14. Olfactory nerve endings (calf, ethmoturbinal). One nerve ending shows a cilium with a visible ciliary necklace (arrow). Ciliary tips are club shaped (double arrow). Compare this figure with Figs. 26, 35, 39 and 49. For legends see Fig. 3. The preparation was freeze-dried, Au/Pd-rotary evaporated and viewed under 45°.

epithelium although the extent of a possible mucus flow caused by this beating over the olfactory epithelium is presumably of little significance.

Nerve endings often have a regular structure (Figs. 12 and 13) which is also discernable in transmission electron micrographs, e.g. in Fig. 43 (OKANO, 1965; OKANO et al., 1967; FRISCH, 1967; SEIFERT, 1970). The apical surface of the olfactory knob is usually devoid of cilia. Scanning micrographs, like those presented here, allow counting of the total number of cilia per nerve ending,

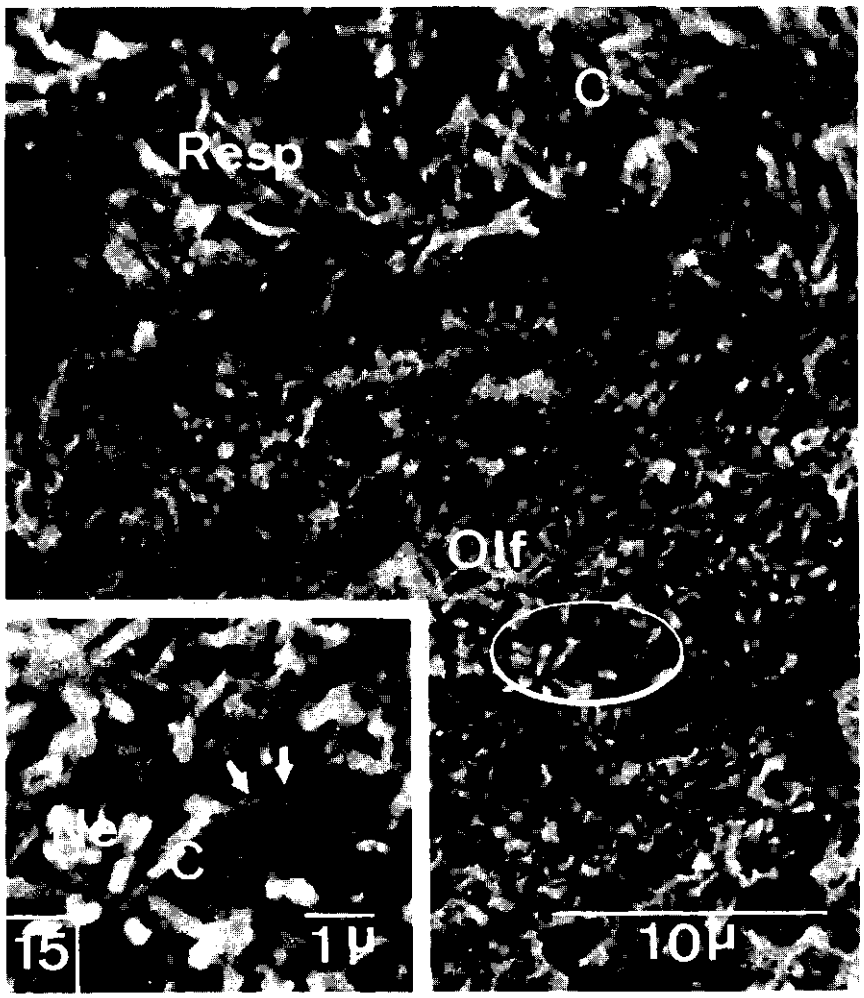

FIG. 15. Transition zone between olfactory and respiratory epithelium (calf, ethmoturbinal). Long respiratory cilia (Resp) are fixed while waving over the olfactory epithelium (Olf). The inset (encircled area at higher magnification) shows a nerve ending with a very granulated appearance and some pore like structures (arrow). Nerve ending density here is about 4.10^6 nerve endings/cm^2. For other legends see Fig. 3. The preparation was freeze-dried, Au-sputter-coated and viewed under 0°.

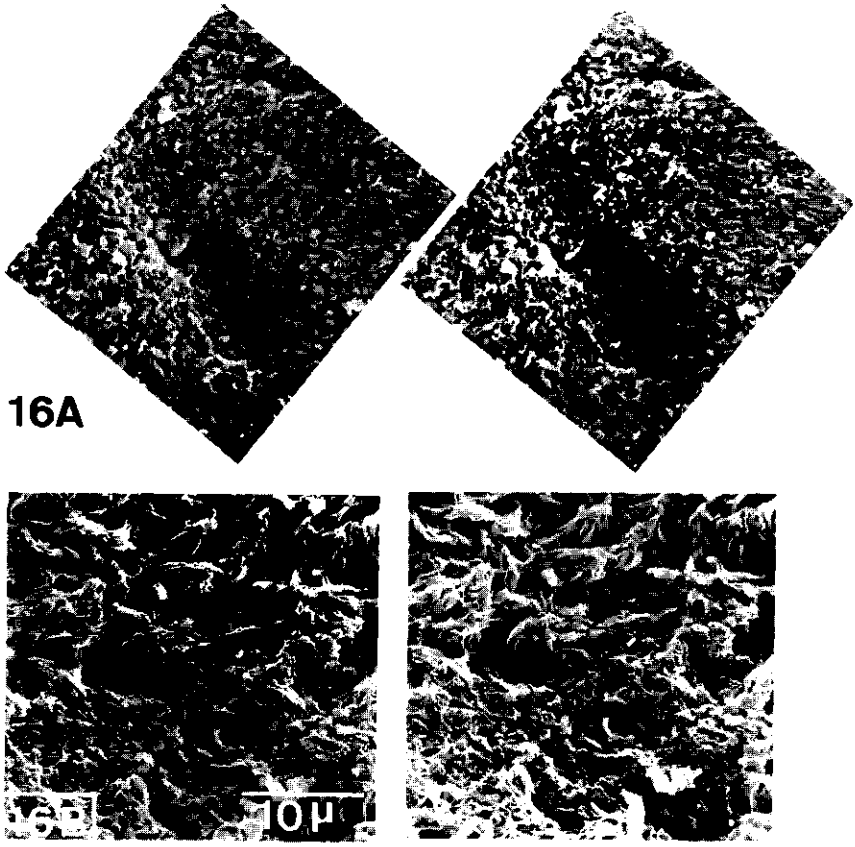

FIG. 16. Stereopairs of transition zone between olfactory and respiratory epithelium (calf, ethmoturbinal). The structured upper areas represent respiratory areas while the lower parts depict olfactory epithelium. (*A*) Tilting angle: 6° (0°–6°); (*B*) Tilting angle: 6° (0°–6°). Preparations were critical point dried and Au-sputter-coated.

although approximately 1/4–2/5 of the cilia remains obscured behind the nerve ending and parts of other (visible) cilia. The results of these measurements will be presented in Chapter 3.

Figs. 17A and B show the complex construction of the surface of the olfactory epithelium in the cow. A similar photograph of frog olfactory epithelium has been presented previously (F. JOURDAN in: HOLLEY, 1975), but the nerve endings themselves can be distinguished more easily in the present figure. The scanning beam was focussed on a canyon-shaped crack in the epithelium, thus allowing an oblique view of the mucus layer. On the mucus surface the narrow distal portions of olfactory cilia (Fig. 17A, left) show indications of alignment (ANDREWS, 1974). The surface is not visibly covered by a terminal film, as has been described by ANDRES (1975). The mucus layer itself has a very fluffy ap-

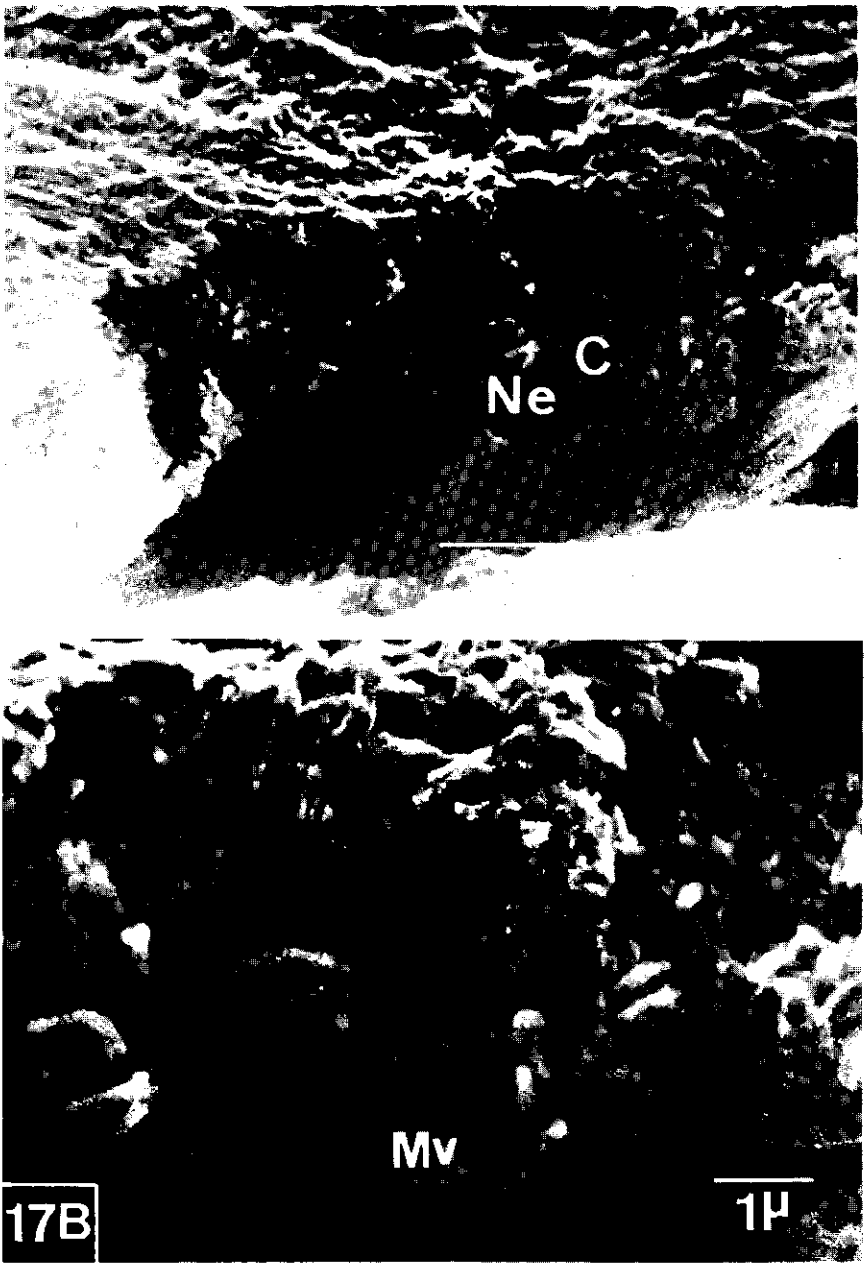

FIG. 17. (*A*) Oblique view of the mucus layer of olfactory epithelium (calf, septal); (*B*): detail. The edge of a crack which developed during the sample preparation is shown. The ciliary tapers (Ct) on the surface are locally aligned in parallel (compare with Fig. 43). The cilia contain a fuzzy surface coat (see *B*). For other legends see Fig. 3. The preparation was freeze-dried, Au/Pd-rotary evaporated and viewed under 45°.

pearance and contains nerve endings, broken proximal parts of cilia, ciliary tapers, microvilli of supporting cells, mucus remnants and cavities. Again, the surfaces of the cilia appear structured. Details of cellular structures beneath the mucus layer are not revealed. This mucus face clearly illustrates the complex situation which is met in attempting to isolate pure receptor site fractions.

Fig. 18 shows the surface of an epithelium in which the nerve endings are obscured by ciliary processes and mucus. One distal cilium segment can be followed over approximately 18 μm. Such distal structures often show spheres, probably corresponding to the ciliary vesicles which are frequently observed in sectioned material (Figs. 24, 31A, 40A and B, 41 and 43) and in freeze-etch material (Fig. 50). Part of a terminal film (ANDRES, 1975) may be observed in this presentation. Once more the complexity of the surface is obvious.

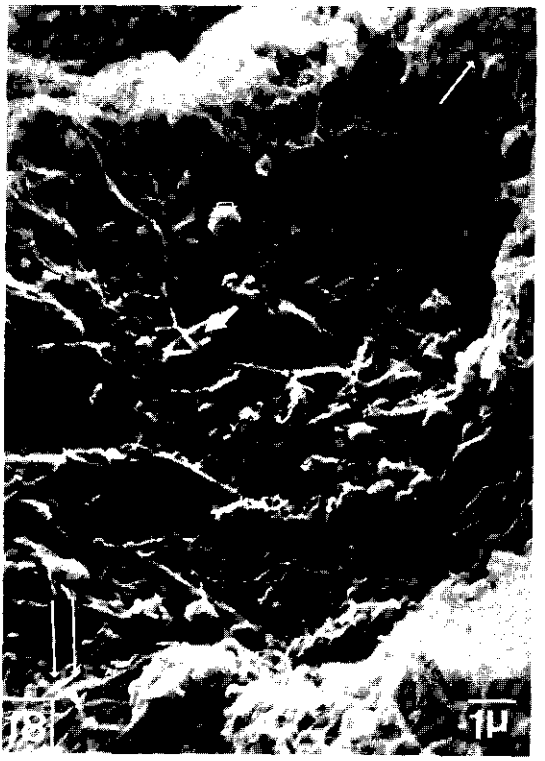

FIG. 18. Olfactory ciliary tapers (calf, ethmoturbinal). Little spheres are present on the tapers (open arrow), which are possibly identical to the vesicles seen in transmission micrographs (Figs. 24, 40, 41 and 43) and freeze-etch micrographs (Fig. 50). One taper (heavy arrow) can be followed over about 18 μm. At the top right hand corner part of a terminal film is shown (thin arrow) and at the bottom left hand corner an area with the tapers aligned parallel is seen (two thin arrows). The preparation was critical point dried, Au-sputter-coated and viewed under 30°.

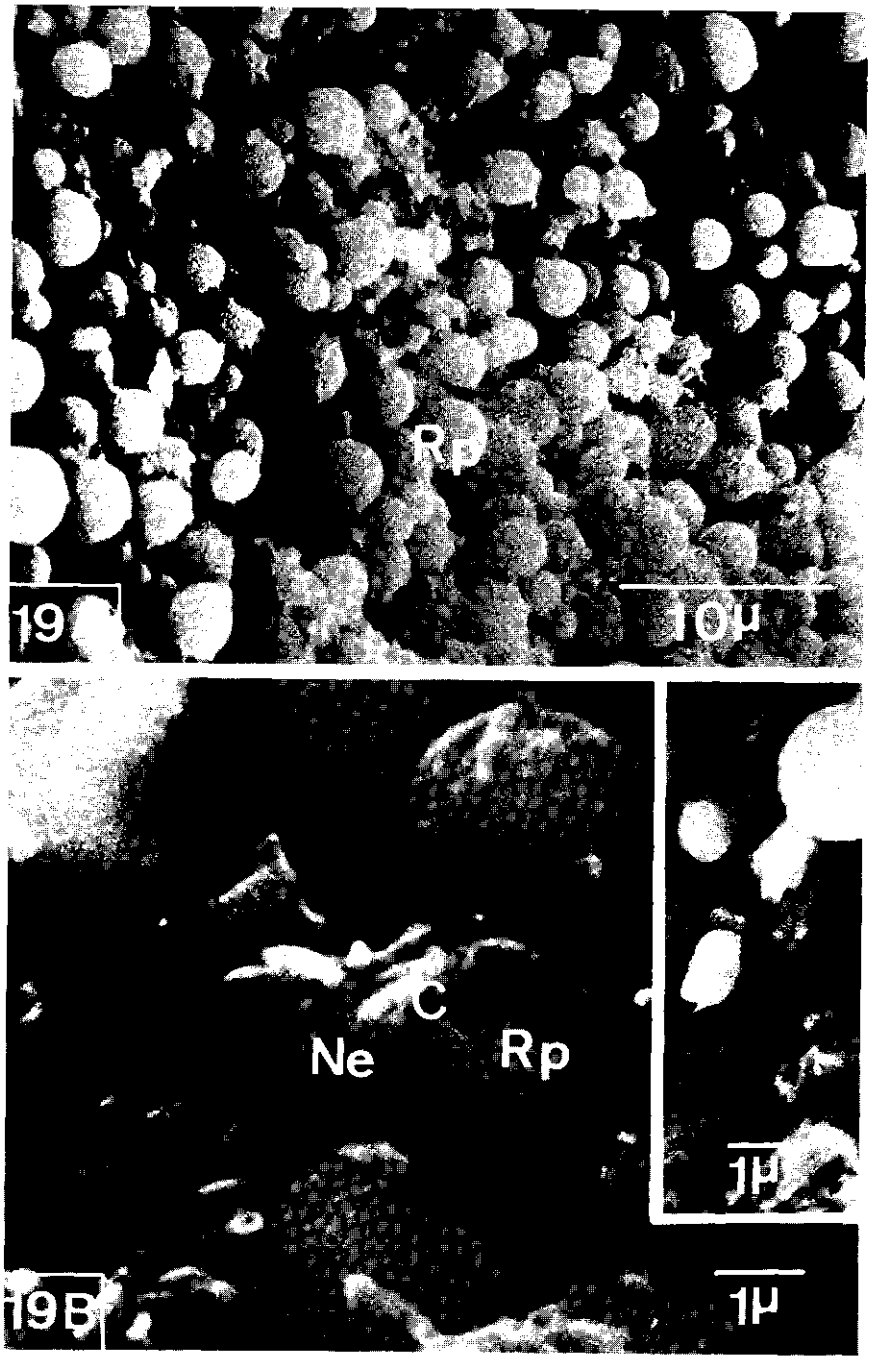

FIG. 19. Regenerated or newly formed area of olfactory epithelium on the ethmoturbinate of an adult cow at low (*A*) and higher (*B*) magnifications. Recently formed nerve endings (Ne) bearing cilia (C), are surrounded by rounded projections (Rp). These rounded projections have a larger diameter than fully developed nerve endings (compare with Fig. 28). *B* shows that the rounded projections bear a surface structure. The inset of *B* shows that in some instances these rounded projections are surrounded by microvilli of supporting cells. The preparation was freeze-dried, Au/Pd-rotary evaporated and viewed under 45°.

1.3.4.1.2. Temporal and spatial differences in the surface of the bovine olfactory epithelium as shown by the scanning electron microscope

Fig. 19, obtained from samples of an adult animal, shows upon increasing magnification nerve endings surrounded by rounded projections. These rounded projections are similar to those observed in hamster embryo nasal pits by WATERMAN and MELLER (1973a). Comparing our observations with those on the hamster leads to the conclusion that the rounded projections in Fig. 19 represent nerve endings, containing centrioles which are about to form cilia. The idea that we are dealing with a relatively young area agrees with the observation that the nerve endings in Fig. 19B bear cilia which may yet form tapers. However, breaking of the distal parts cannot be excluded a priori. Apically at this presumably newly formed nerve ending a developing cilium can be seen. The inset of Fig. 19B demonstrates that the rounded projections probably do not represent expanded supporting cells. Moreover, smooth young nerve endings have a larger diameter than cilium-bearing nerve endings, as has been demonstrated with transmission studies (Fig. 28, HVEM-stereopair and several photographs which are not presented; WATERMAN and MELLER, 1973a; CUSCHIERI and BANNISTER, 1975; KERJASCHKI and HÖRANDNER, 1976).

In Fig. 20 epithelia from the septum, cribriform plate and nasal turbinates obtained from three calves are compared. At neither magnification presented do these patches resemble each other, although they underwent exactly the same treatment. Some of the samples show glands (Fig. 20; IC: septum calf 3, and IE: cribriform plate calf 3), while others do not.

At higher magnification some areas (Figs. 20; IIC, IIE, IIF and IIG) show mainly tapers, while others (Fig. 20; IIA and IIB) show nerve endings and the more proximal parts of cilia. Some patches have plaques, probably of a mucous nature (Fig. 20; C, D and F), whereas other areas hardly seem to show any mucus (Fig. 20; E and G). There is no clear system in these differences. They are probably due to local momentary activities at the time of fixation. These variations may also be caused by local variations in the mucus composition. It is impossible to establish if these local differences are caused by temporal or spatial alterations. It cannot be excluded that these differences represent artefacts.

1.3.4.2. High-voltage and normal transmission electron microscopy of the bovine olfactory mucosa

1.3.4.2.1. General description of the mucosa

The ultrastructural organization of bovine olfactory epithelium is generally identical to that of other mammals. In the present section a general description of this tissue will be presented, while following sections will trace the nervous processes from the axonal parts to the tips of cilia in greater detail. Attention will be devoted mainly to ciliary structures since they are thought to possess the receptor sites (OTTOSON and SHEPHERD, 1967). Relevant informa-

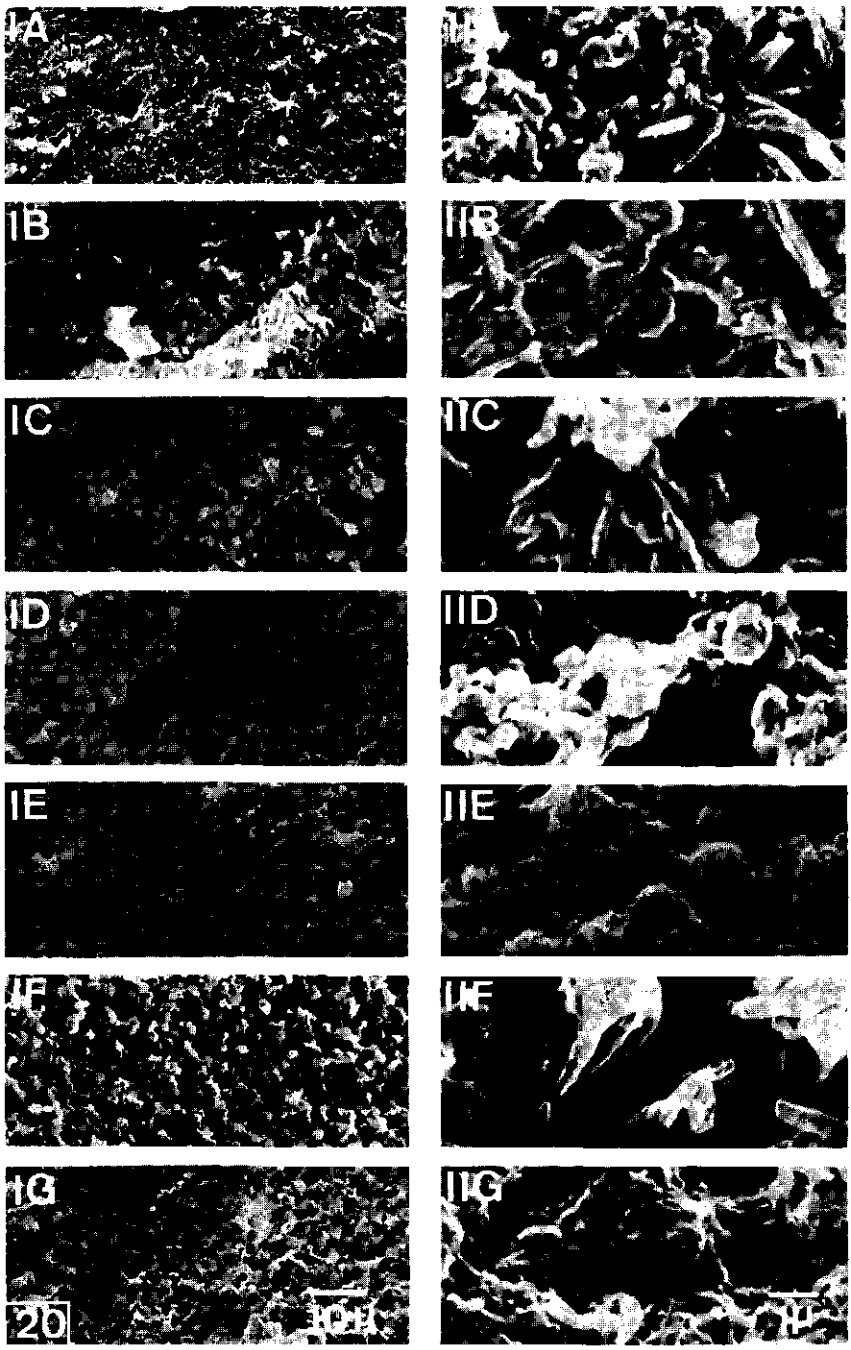
IA
IB
IC
ID
IE
IF
IG
20

tion about the supporting cells, Bowman glandular cells and some other cell types will also be included.

The collage of Fig. 21 (taken from the same block as Fig. 4B) traverses the mucosa from the lamina propria to the terminal film of the mucosa. The lamina propria and basal membrane located proximally, are just visible on the right. Above these structures one observes dark basal cells and light processes which are the subnuclear feet of supporting cells. These contain dense inclusions, probably pigment granules.

The three to four central layers of more rounded nuclei are neural while the three to four top layers of more irregular shaped nuclei belong to supporting cells. However, a proper separation between the cell types remains difficult since the section might be oblique. Supporting cells are heavily vacuolated. The neural cell bodies have peri-nuclear cytoplasm which contains swollen cisternae of endoplasmatic reticulum. Some axonal processes can be followed for several microns. Apically, pale dendrites and dense supporting cells are visible. Sometimes dendrites appear to be adjacent to one another (see also GRAZIADEI, 1971a). Enclosing of dendrites by supporting cells as has been described by BREIPOHL et al. (1974c) for mouse cannot be excluded either.

One cell, probably a supporting cell, is undergoing lysis. The mucus layer contains olfactory cilia and microvilli. Top right of Fig. 21 shows part of a terminal film.

1.3.4.2.2. A description of the non-ciliary part of the olfactory mucosa

Some details of apical and proximal regions are presented in Fig. 22. Both micrographs in this figure show glands of Bowman sectioned axially and horizontally, respectively. The ciliary-microvillar region contains many membranous vesicles (see page 42). Supporting cells shown in Fig. 22A are heavily vacuolated. Fig. 22B depicts axonal processes surrounded by Schwann sheaths. Moreover some glandular cells, which appear to be secreting, may be seen. These glands probably belong to the mucous type (YAMAMOTO, 1976). Furthermore, supporting cell feet, basal cells and the lamina propria can be observed in this figure. Axonal and dendritic processes have a similar appearance as those in other animals (see the references in the INTRODUCTION to this chapter and Figs. 23 and 51). Both cell compartments as well as the nerve endings themselves (Figs. 23–26) contain numerous microtubuli.

FIG. 20. Series of SEM pictures of olfactory epithelium obtained from different areas of several bovines, prepared at the same time under identical conditions. All samples are shown at two magnifications. This series demonstrates the apparent heterogeneity of the epithelium surface. **A.** *Calf 1; septum* (viewed under 0°); **B.** *Calf 2;* septum (viewed under 6°, respectively 0°); **C.** *Calf 3;* septum (viewed under 0°); **D.** *Calf 1; cribriform plate* (viewed under 0°, respectively 6°); **E.** *Calf 3; cribriform plate* (viewed under 0°); **F.** and **G.** *Calf 3; transition area between cribriform plate and ethmoturbinates* (viewed under 0°). For further explanation see text page 25. The preparations were critical point dried and Au-sputter-coated.

FIG. 21. Compound picture representing a complete survey of bovine olfactory epithelium in an oblique plane of section (steer, cribriform plate). The epithelium is about 90 μm thick and consists of one basal (Bc), about four neural (Nc) and about three supporting (Sc) cell layers, as indicated by their nuclei. The perikaryon cytoplasm of the olfactory neurons is alternately vacuolated and condensed. One supporting cell (arrow) undergoes degeneration. Microvilli form bush-shaped formations (Mv). A: axons; Bm: basal membrane; C: olfactory cilia, including their tapering processes; D: dendrites of the olfactory neurons; Lp: lamina propria; Ne: olfactory dendritic nerve endings; Scr: secretion or pigment droplets; Sf: supporting cell feet; Tf: terminal film.

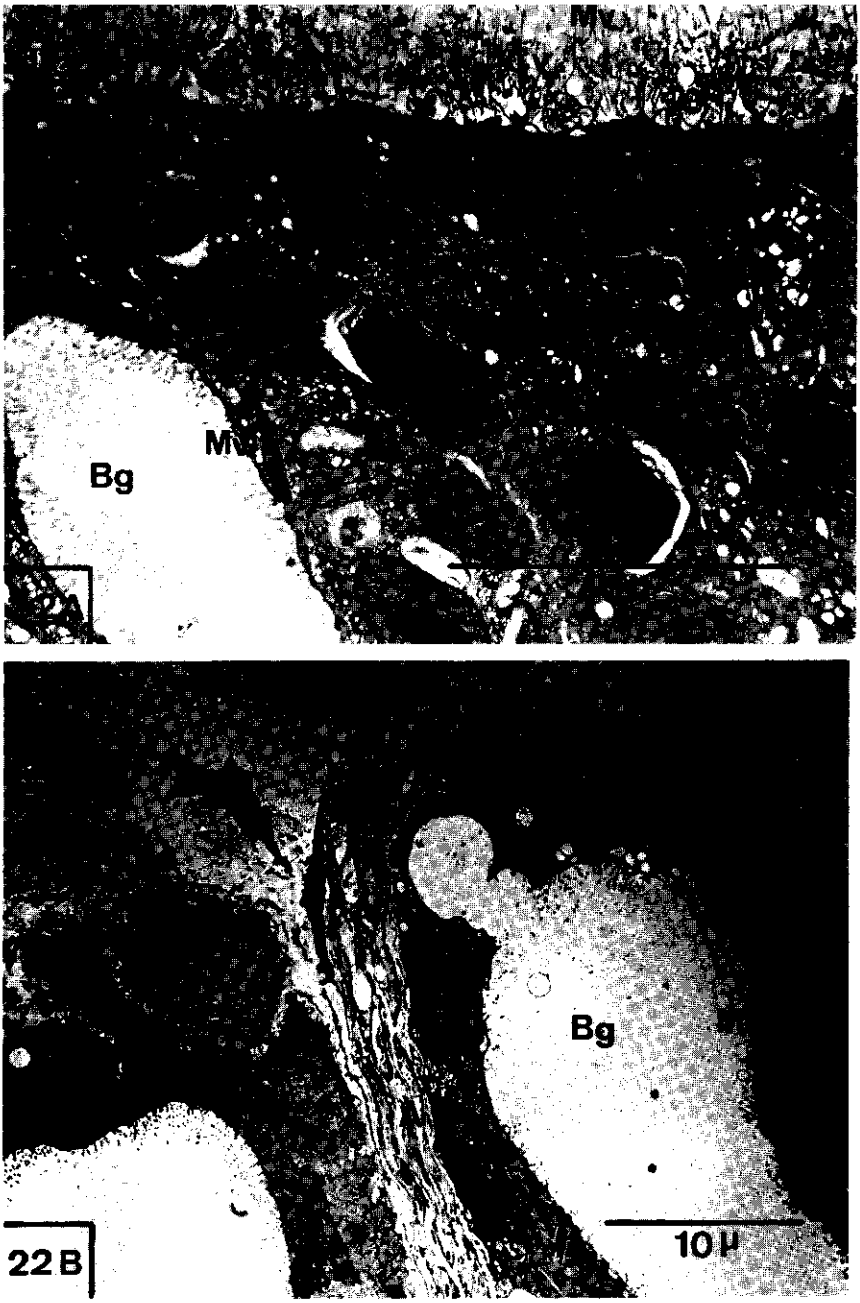

FIG. 22. Olfactory epithelium (calf, ethmoturbinal). (*A*) Sectioned perpendicular and (*B*) parallel to the epithelium surface, at basal cell (Bc) level. The supporting cells (Sc) in (*A*) are very vacuolated. Their microvilli (Mv) are positioned perpendicular to the epithelium surface, while the olfactory cilia (C) run parallel to this surface. They bear vesicles (Cv). Both sections contain Bowman glands (Bg). The cells of these glands bear short microvilli (Mv). The axon bundle (A) in *B* is abutted on both sides by such glands. The lumen of these glands contains a slightly granulated mass. The light processes in *B* are supporting cell feet (Sf). These surround a basal cell. On the left side of these feet some collagen fibers (Col) of the lamina propria can be seen.

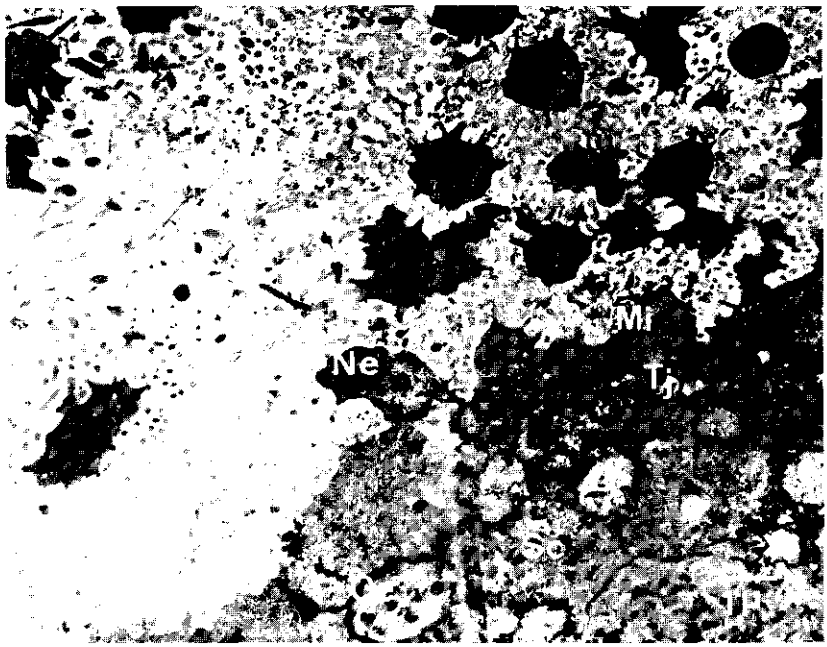

FIG. 23. Distal region of bovine olfactory epithelium (calf, cribriform plate). Dendrites (D) are separated by supporting cells (Sc). Dendrites and nerve endings (Ne) contain centrioles (Ce) over their whole observed lengths. Mitochondria (Mi) are most frequently observed at the level where the nerve endings leave the epithelium surface. The nerve endings and dendrites are stacked with microtubuli, apparently chiefly orientated in a direction perpendicular to the epithelium surface. Tight junctions (Tj) connect supporting cells and nervous cells at this level. Both supporting cells and nervous cells bear microvilli (Mv). Cilia (C) formation only occurs at some distance from the surface.

In the nerve endings, microtubuli sometimes seem to be surrounded by an electron-lucent halo (Fig. 25). The nerve endings also frequently contain endocytotic vesicles (Figs. 24, 25, 31A and 32A). These vesicles often occur close to the outer surface of the nerve endings (Figs. 24 and 31A) and contain in many cases smaller vesicles (Fig. 32A). The nerve ending coat is fairly often of a microvillous nature (Figs. 25 and 26).

Fig. 27 shows stereopair micrographs (HVEM) of the apical part of an atypical brush cell which is positioned close to a nerve ending. These brush cells are similar to the ones seen in the respiratory epithelium (page 15).

1.3.4.2.3. Temporal and spatial differences in the bovine olfactory epithelium as seen by transmission methods

In addition to a part of a normal nerve ending and a microvillous bush, the stereopair of Fig. 28 shows part of a rounded projection. This structure is probably comparable to the ones seen in Fig. 19 and by WATERMAN and MELLER (1973a) in hamster embryo. The dark spots inside this projection represent

FIG. 24. Olfactory nerve endings and their mucous environment from ethmoturbinal and (inset) septal areas (calf). Endocytotic vesicles (Ev) are present within the nerve endings. They sometimes accumulate near the nerve ending surface (main photograph). One vesicle might be formed newly (arrow). Their openings could be the pits seen in the nerve ending of the inset of Fig. 15. The nerve ending is probably young, since it contains a fibrogranular microtubuli pool (Fg; see text page 47). A supporting cell shows a multivesicular body (Mb). These are also present in the respiratory epithelium (Fig. 7). The inset shows a granular mass (G) present in the mucus (Mu). Ciliary matrices (C) are much denser here than matrices of respiratory cilia (Fig. 8). Several types of ciliary proximal and taper (Ct) cross-sections are observed: 9(2) + 2 (single arrow); 4 microtubular subfibers (double arrow); 2 subfibers (heavy arrow); 1 subfiber (open arrow). Large numbers of ciliary vesicles (Cv) are present. Mv: microvilli; Tj: tight junction.

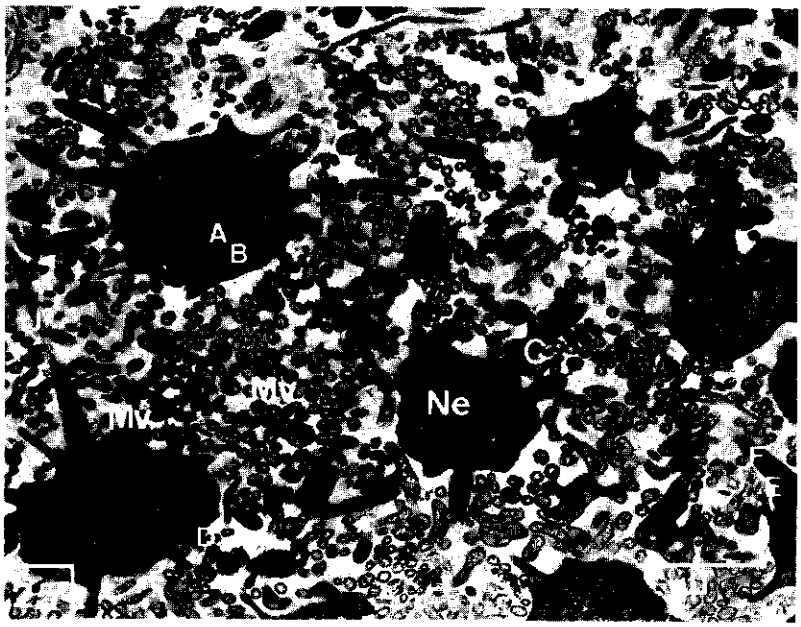

FIG. 25. Nerve ending from the same area, but more distally, as Fig. 23. Nerve ending (Ne) microtubuli are electron dense and surrounded by an electron-lucent halo. The lettering (small capital letters) of the ciliary sections corresponds to that of Fig. 34. For further explanation of these sections see also legends of Fig. 34. The nerve endings contain short microvilli (Mv). Supporting cell microvilli (also Mv) are much more electron-lucent than nervous structures.

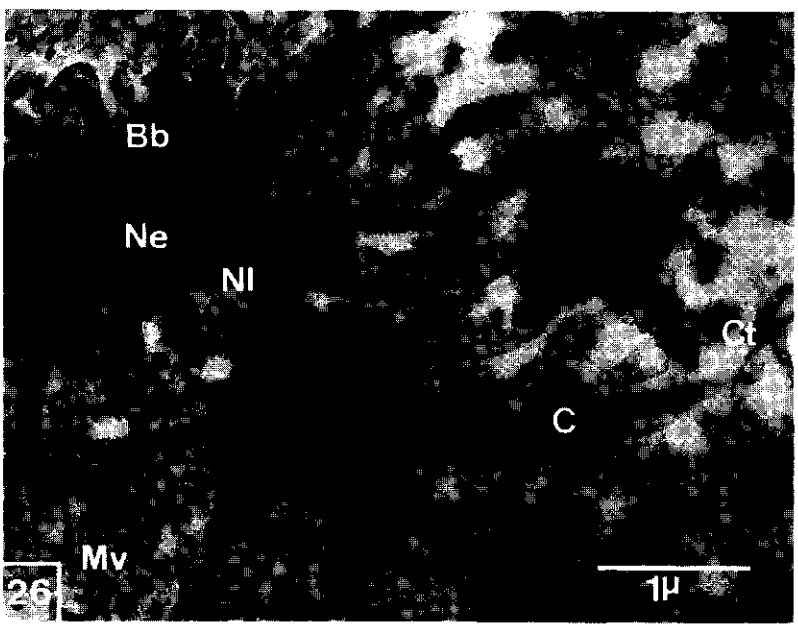

FIG. 26. HVEM picture of a thicker section (about 1 μm) of the same area as Fig. 25. Note that virtually the whole nerve ending lumen (Ne) consists of microtubuli and basal bodies (Bb). Cilia (C) very clearly contain necklaces (Nl). Ct: ciliary tapers; Mv: microvilli.

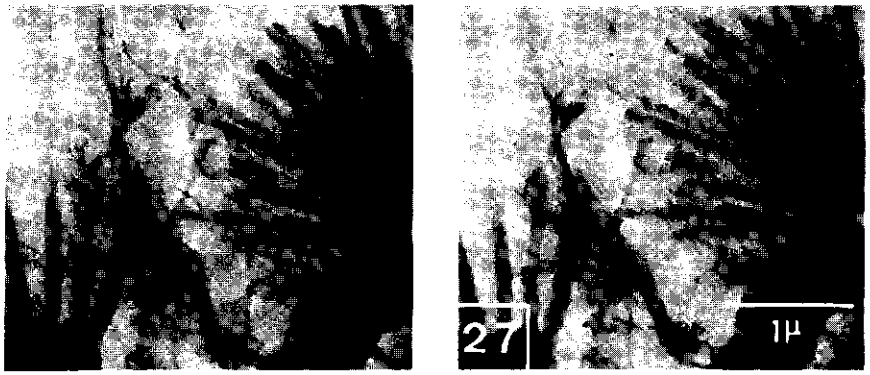

FIG. 27. High voltage stereopair of the brushes of an atypical brush cell and of olfactory cilia (adult, cribriform plate). Brushes of this appearance may be seen in olfactory as well as in respiratory samples. The section diameter was about 3 μm. Tilting angle: 2°.

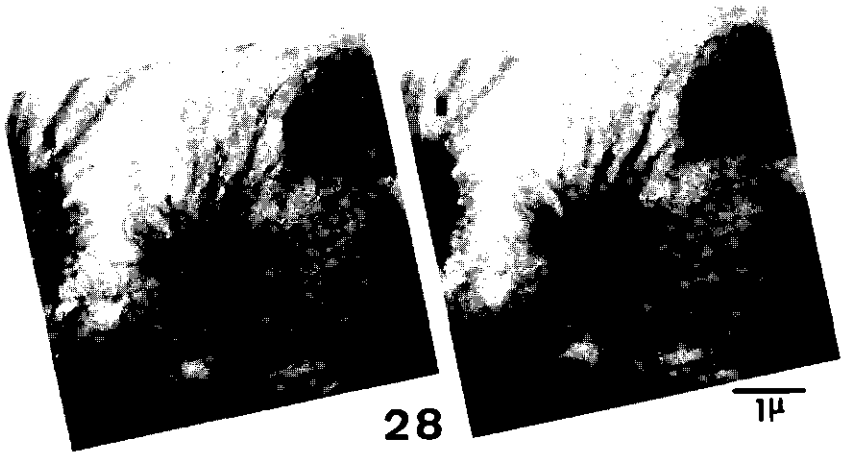

FIG. 28. High voltage stereopair of two nerve endings, one butted and one not (calf, ethmoturbinal). The latter nerve ending contains centrioles but no cilia and probably represents the rounded projections of Fig. 19. The nerve endings are separated by a bush-shaped supporting cell microvillous structure. The ciliated nerve ending contains numerous small microvilli. The diameter of this section was about 3 μm. Tilting angle: 3.5°.

centrioles which will give rise to cilia at a later stage. The presence of such projections suggests the existence of temporal differences in the epithelium surface. Fig. 29 shows a type of nerve ending which may represent an immature stage since all its cilia are approximately of the same length and lack tapers. The cilia end in club-shaped knobs. This seems typical of ciliary tips at all stages (Figs. 35 and 39) and is seen irrespective of the technique used (Figs. 14 and 49). Further indications of temporal differences between nerve endings are the presence of fibrogranular microtubular pools (Fig. 30). These pools and

FIG. 29. Newly formed olfactory cilia (calf, ethmoturbinal). The cilia here have all the same length (about 2.3 μm) and end in club-shaped tips (compare with Fig. 39). The nerve ending is filled with centrioles, which are just discernable.

the centriole replication figure in the inset of Fig. 32C suggest that centriole replication leading to ciliogenesis (ROTER DIRKSEN, 1971) may occur inside the nerve ending.

Besides these temporal differences, olfactory epithelia also often show spatial differences (as seen in Fig. 20 in scanning observations). Figs. 31 and 32 show some of the diverse appearances of this epithelium and its nerve endings. In these cases samples were not prepared at the same time. In adult animals the epithelium seems to be more heterogeneous than in the calf. This might be related to age differences of the nerve ending, but it seems also likely that older animals more frequently contain pathological features.

Nerve endings are sometimes devoid of cilia while centrioles are present (Figs. 31B and 32B). Such nerve ending structures have a smaller diameter than rounded projections seen in recently formed areas (Figs. 19 and 28). Also ciliary axonemes are present within the cytoplasm of the terminal knob of dendrites (Fig. 31C), although not as conspicuously as in the respiratory cells (Fig. 11).

The structure of mitochondria, nuclei, endoplasmatic reticulum as well as the overall appearance of the epithelium differs much as a comparison of the three areas of Fig. 31 reveals. A closer view on the nerve ending (Fig. 32) supports this conclusion.

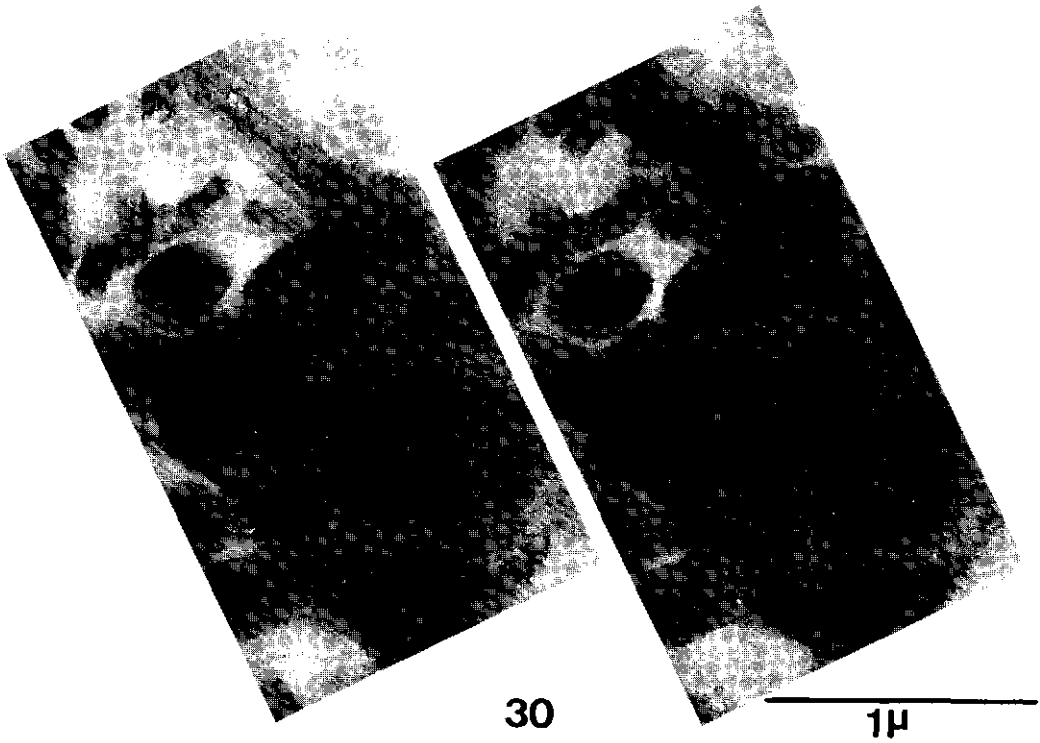

FIG. 30. High voltage stereopair of an olfactory nerve ending containing a bag-shaped fibrogranular centriole precursor mass (calf, septal). The necklace of the cilium in the upper part of the photographs, surrounds the whole cilium. Basal bodies are shown with their basal feet and some other rootlets (see Fig. 34). The section diameter was about 1 μm. Tilting angle: 1.5°.

1.3.4.2.4. Ciliary and microvillous structures

Ciliary structures are usually comprised of an intracellular part, the basal body, and an extracellular part, the cilium itself. Olfactory cilia form no exception. The main difference between olfactory cilia and other types of cilia is that the former possess in addition to proximal axonemal structures of normal appearance, long distal parts (FRISCH, 1967) of a small diameter which contain a reduced number of microtubuli. Basal bodies which have not yet formed cilia, are usually called centrioles. Fig. 33 shows these olfactory cilia with respect to the nerve ending from which they originate in a stereo-micrograph.

Cross-sections of basal bodies and cilia are presented in Fig. 34. Places from where cross-sections were taken are marked in Fig. 25. The following description will follow the cilium from basal body to the ciliary tip. Basal body triplets, consisting of A, B and C subfibers are shown in Fig. 34A, followed by a section of the basal body part which contains centrally an electron-

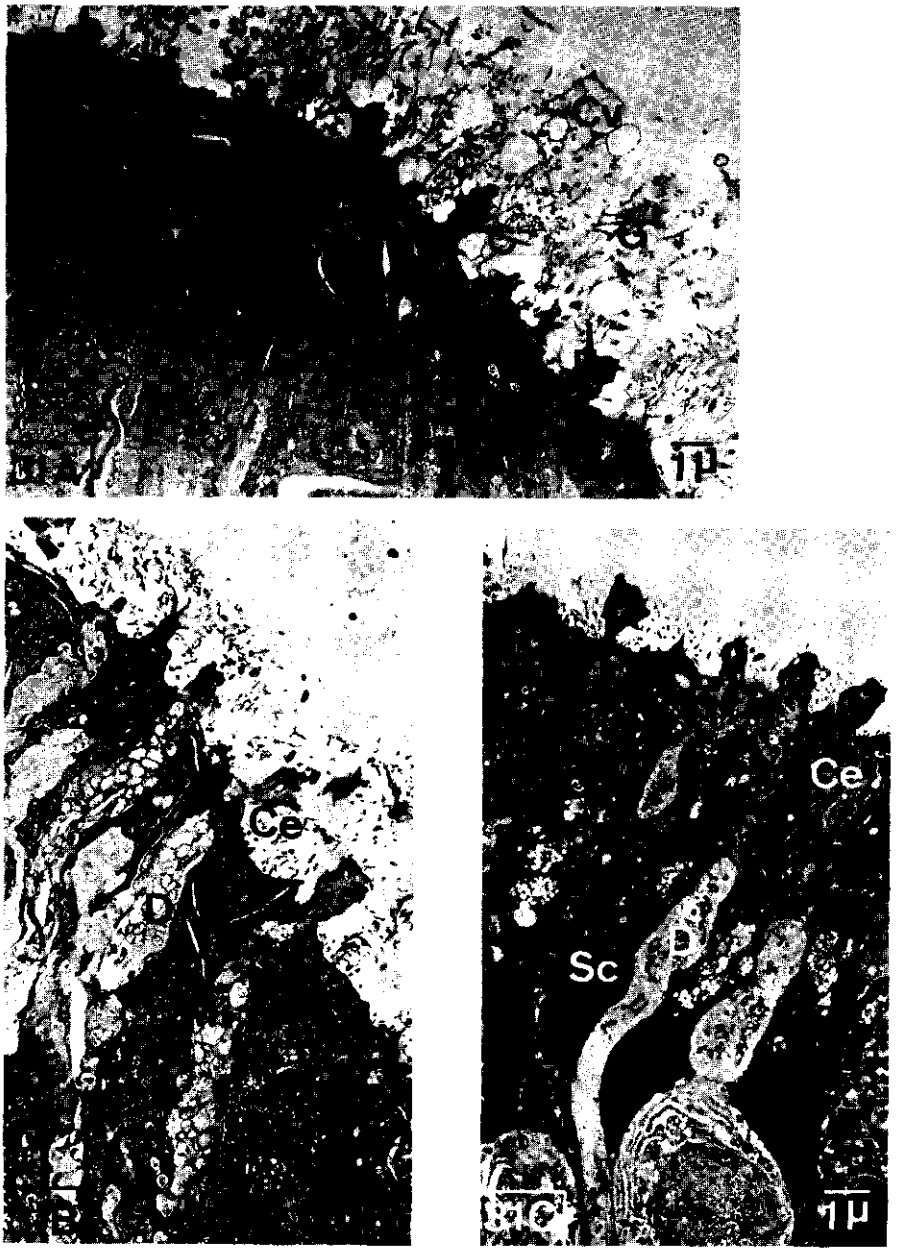

FIG. 31. Some examples of the apical region of bovine olfactory epithelium. **A**. *Calf, septal*: The mucus layer contains many ciliary vesicles (Cv). Nerve endings contain endocytotic vesicles (Ev). A granulated area (G) as in Fig. 24, is present in the mucus layer. Supporting cells (Sc) are vesiculated. Cilia (C) are normally developed. **B**. *Cow, cribriform plate*: The nervous dendrites (D) contain swollen mitochondria (Mi). The supporting cells here are vesiculated as well and contain elongated mitochondria. The nerve endings have few cilia, but contain many centrioles (Ce). Dendritic structures might make mutual contact here. **C**. *Cow, ethmoturbinate*: Supporting cells here are dark and contain dark nuclei. Their perinuclear cytoplasm contains vesiculated regions. Nerve endings contain several ciliary axonemes within their lumen (compare with Fig. 11). Centrioles can be seen in the dendrites. Fully developed cilia are not present.

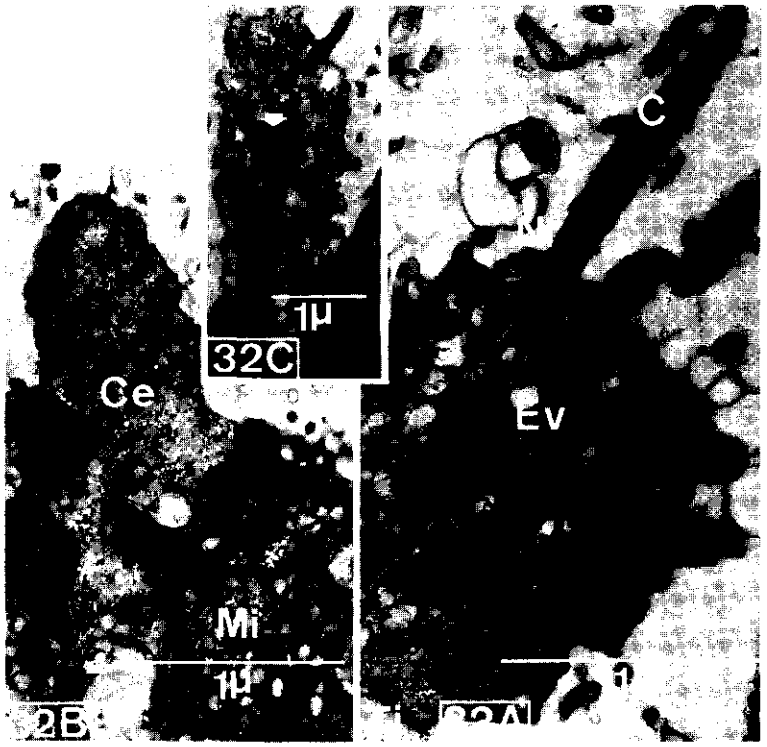

FIG. 32. Some examples of olfactory nerve endings. **A.** *Calf, ethmoturbinal*: The nerve ending contains many endocytotic vesicles (Ev). Several of them contain a second vesicle within their lumen. The latter vesicles have a darker lumen than the surrounding vesicle. Cilia (C) show necklaces (Nl). A tight junction (Tj) can be seen. **B.** *Cow, cribriform plate:* This nerve ending contains several centrioles (Ce) and/or basal bodies, but no cilia. Mitochondria (Mi) are big and round. **C.** *Calf, cribriform plate:* The centriole (arrow) in this nerve ending depicts a replication figure.

dense dot (Fig. 34B) and a section of the basal foot (Fig. 34C). The basal foot, consisting of one or two rootlets, is one of the two rootlet types present on the olfactory basal bodies.

The more distal rootlet type (Fig. 34D) exhibits unstriated filaments which are attached to every microtubular triplet or doublet and which end in a dense dot. These rootlets display a pin-wheel pattern (OKANO, 1965; YAMAMOTO, 1976) and form an angle of about 60° with the tangent through the doublet. They frequently appear attached to the nerve ending membrane (Figs. 25 and 35). The C-microtubule subfiber, the outermost subfiber (PITELKA, 1974) disappears at this level, as can be seen better in OKANO's (1965) paper. In Fig. 34A and C the inner core of the basal body and the surrounding nerve ending mass have identical electron densities, while the triplet and doublet-containing ring is more electron-lucent.

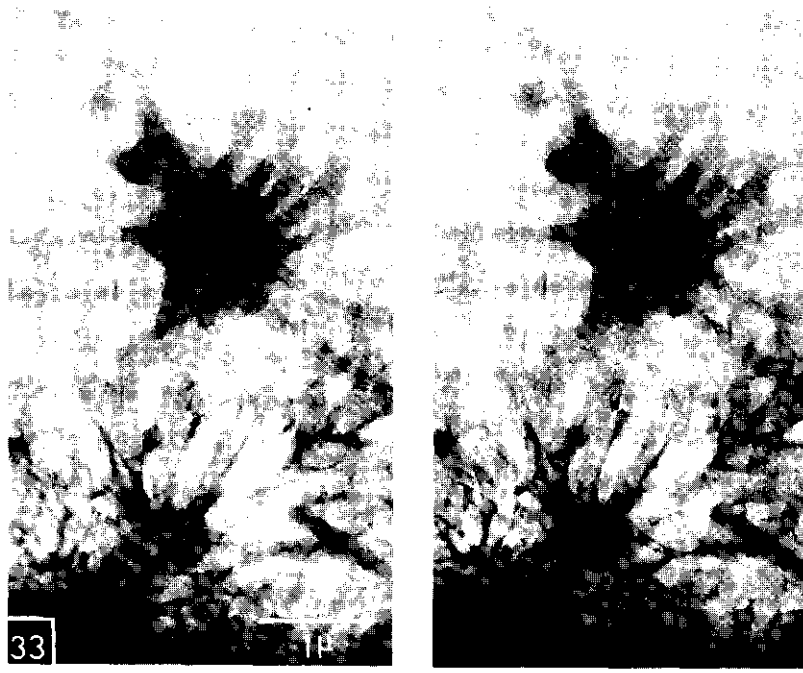

FIG. 33. A high-voltage stereopair of an olfactory nerve ending (calf, ethmoturbinal). Parts of most cilia belonging to this nerve ending are shown but the connection with the epithelium surface cannot be seen. The section diameter was about 2.5 μm. Tilting angle: 1°.

FIG. 34. Cross-sections of olfactory cilia at various distances between basal bodies and tapering distal ciliary segments. **A.** *Basal body triplets* (calf, septal): A (innermost), B and C (outermost) microtubular subfibers are present. The A and B subfibers are maintained in the cilia. **B.** *Basal body with central dot* (calf, septal). **C.** *Basal body with basal foot* (calf, septal): **B** and **C** are both sectioned near the central region of the basal body. In this case no clear triplets can be seen at this level, though C-subfibers usually disappear somewhat more distally in the basal body (see text page 37). The microtubular subfibers are contained within an electron-lucent ring. They are linked by dense bars. **D.** *Basal body rootlets displaying a pinwheel pattern* (calf, septal): These rootlets are present distally of the basal feet. They are frequently seen attached to the cell membrane (Figs. 25 and 35). They form an angle of about 60° with the tangent through the microtubular doublets or triplets from which they originate. Their cytoplasmic endings contain a dense dot. **E.** *Basal plate* (calf, septal): The basal plate is electron-denser than the rest of the ciliary matrix and contains an even denser membranous edge. This basal plate appears at a level where the cilium leaves the nerve ending. Doublets here are linked together, probably by nexin, and contain small arms in their centers. These arms make Y-shaped connections with the ciliary membrane. **F.** *Cilium, still lacking central subfibers* (calf, septal). **G.** *Complete cilium* (calf, septal): The 9 outer doublets and two inner subfibers are all present here. Note the absence of dynein containing arms on the doublets, although some kind of structure might be attached (compare with Fig. 9). **H** and **I.** *Distal deviations of the 9(2) + 2 structure* (calf, septal): Note the absence of dynein arms and the relative density of the ciliary matrix. **J.** *Ciliary transition zone* (calf, septal): This transition zone is intermediate between complete axonemal structures and the tapers, with just one or two subfibers (see Fig. 37).

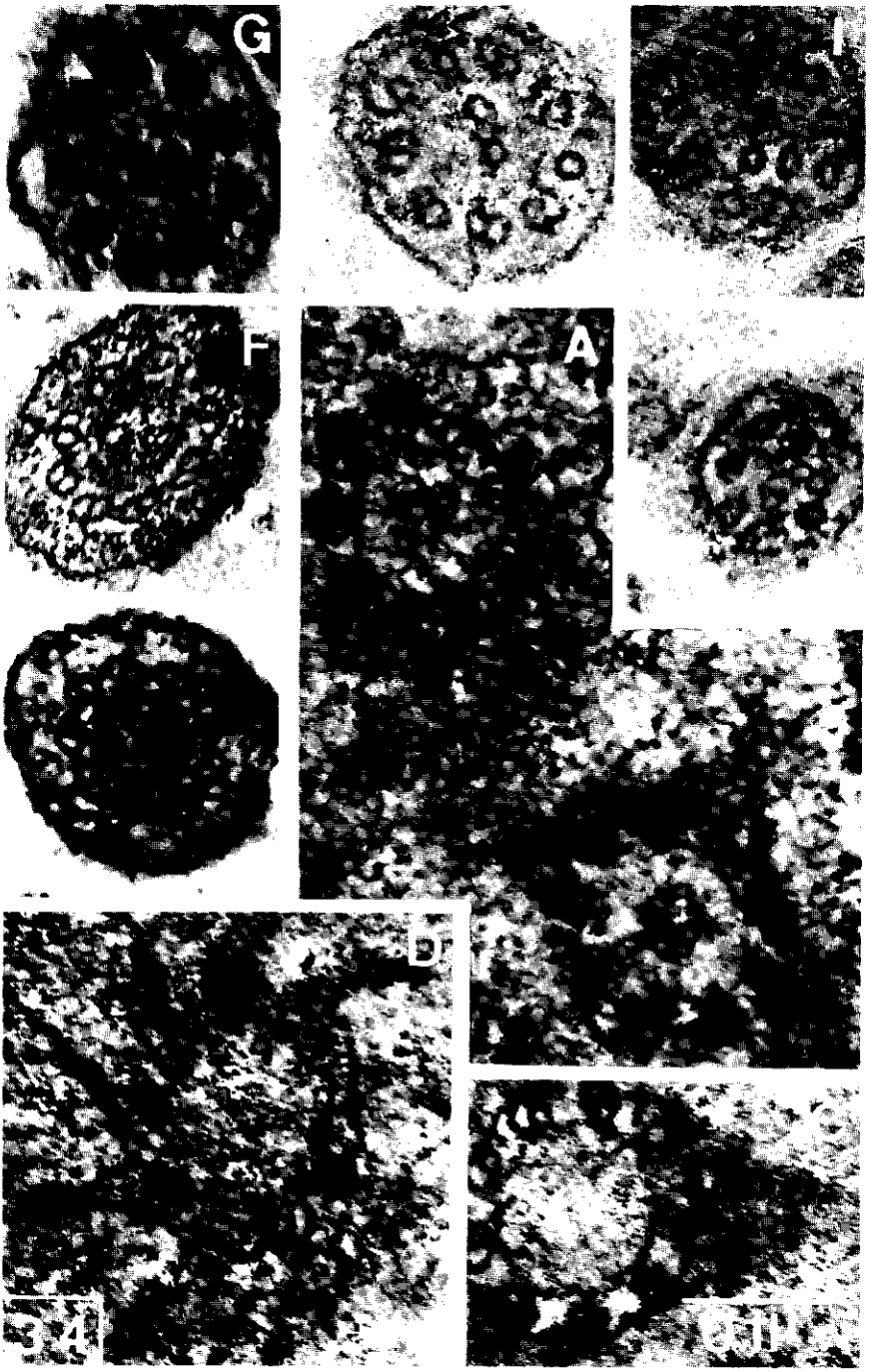
G
F
A
B

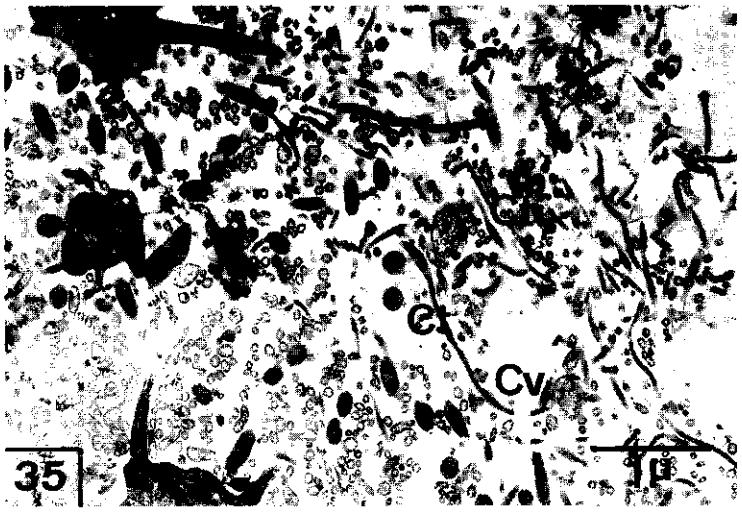

FIG. 35. Olfactory nerve endings, depicting many of their structures (calf, cribriform plate). This section is from the same area as Figs. 23 and 25. Ciliary tapers (Ct) show ciliary vesicles (Cv) and ciliary tips (Cti). They make frequently contact, both mutual and with supporting cell microvilli. A basal plate (arrow) is clearly visible here.

FIG. 36. Olfactory cilium (calf, septal). The cilium stands on a base, containing the basal body. The membrane of the necklace (Nl) area contains big particles (double arrows). The membrane area of the initial cilium part is very rippled. The ciliary taper also contains particles (inset, single arrow) which are smaller than in the necklace area. On places where mucus fibers adhere to the ciliary membrane, membrane areas are less dense than elsewhere (heavy arrow). The ciliary matrix does not reveal any clear structure also not in the tapering region. Therefore it is not possible to indicate from which subfibers of the original 9(2) + 2 axonemal figure the taper microtubular subfibers originate. The matrix is very dense as compared to the respiratory ciliary matrix (Figs. 8 and 9). A taper cross-section containing four microtubular subfibers is present (thin arrow).

FIG. 37. Ciliary taper cross-sections (calf, septal). The cross-sections contain 2–4 microtubular subfibers, each containing 13 subunits (inset). Where two subfibers remain, they are connected by electron-dense material. The inner membrane lamina is more electron dense than the outer membrane lamina. Mucus fibers are attached to the ciliary cross-sections.

FIG. 38. Ciliary tapers and microvilli (calf, cribriform plate). The diameter of the main taper in this figure changes from top to bottom from 0.09 μm, via 0.16 μm to 0.03 μm, with a varying number of microtubules. The taper membrane is particulated (arrows) as may also be seen in Fig. 36.

Fig. 34E shows a cilium (probably sectioned at basal plate level) which just emerged from the nerve ending. The central pair of microtubuli is still not present here. The doublets are linked by a protein called nexin (STEPHENS and EDDS, 1976) and at their center they are connected to the ciliary membrane. The basal plate is darker than the rest of the axonemal matrix and possesses an even denser edge. In Fig. 34F the central pair of subfibers is not yet present. This section is cut just above the basal plate. The inner membrane lamina is more dense than the outer lamina. The other sections in Fig. 34 follow the cilium through its initial course until just beyond the region where it starts tapering and where the microtubular structure is reduced from the 9(2) + 2 axonemal structure (see Fig. 9), via the various kinds of intermediate structures to finally just one or two fibers (Figs. 35–38). It could not be established whether the remaining microtubuli in the ciliary tapers are the inner singlet fibers or remnants of outer doublets (Fig. 36). In contrast to respiratory cilia (Figs. 9 and 11) microtubular doublets in bovine olfactory cilia do not appear to possess arms (Fig. 34E–J). The axonemal matrix appears to be less ordered than respiratory axonemal matrices (compare for example Figs. 25 and 34 to Figs. 8 and 9). The microtubuli within the tapers are connected by a fibrillar structure. The outer ciliary membrane lamina (depicted in Fig. 37) is less dense than the inner membranous lamina. For details on dimensions of microtubules and membranes of the cilia, see Chapter 3 (Table V).

Some ciliary tips are shown in Fig. 35 and, at a higher magnification, in the thick section of Fig. 39. They are club-shaped (OKANO, 1965; DE LORENZO, 1970) and have a cap of material, which is more electron-lucent than the rest of the ciliary tip.

Cilia often stand on a base (Fig. 36), which encloses the major part of the basal body. Ciliary necklace particles are also shown in Fig. 36. In the tapering area the membrane shows particles, which are smaller than the necklace particles and which might correspond to the particles as seen by freeze-etch methods (Chapter 2). In addition to these particles the ciliary membrane appears to be characteristically rippled. Some microvilli and strands of mucus seem to be attached to the ciliary membrane. At places where such attachment occurs the membrane is less dense.

Besides cilia and microvilli the mucus layer contains several other structures, such as granulated areas (Fig. 24, inset, and 31A) and various types of vesicles (Figs. 40A, B and 41, inset). Some of these vesicles contain axonemal remnants (Fig. 40B), whilst others do not (Fig. 40A). In the latter figure tapers, bearing pale vesicles instead of denser club-shaped structures at their tips, make mutual contact. The vesicles here contain many different types of inclusions. In other figures which are not presented here, club-shaped tips could be seen which may also make contact with such vesiculated tips. Fig. 40A shows inside the vesicles and adjacent to their membranes relatively dense layers. The photographs presented here indicate that most of these vesicles are of ciliary origin. Fig. 41 (inset) shows that they often occur on the ciliary tapers, most of which run parallel to each other and to the epithelium surface (Figs. 41 and 43).

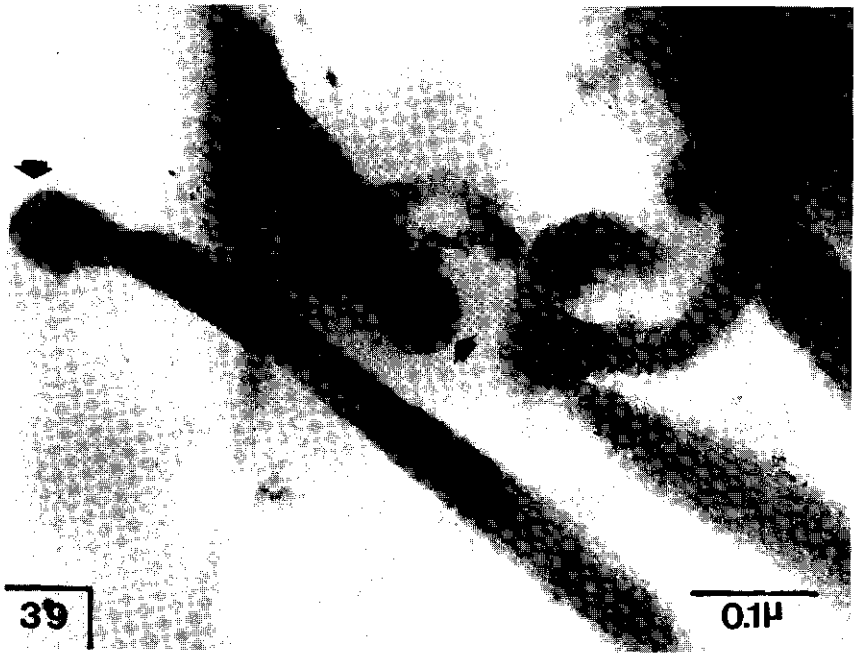

FIG. 39. Thick section of club-shaped ciliary tips (adult, cribriform plate). The tips appear to be covered with an electron-lucent cap (arrows).

The olfactory mucus layer includes microvilli originating from supporting cells (Fig. 42). They appear to look rather similar to the microvilli of the respiratory mucosa (Fig. 11, inset). In contrast to NAESSEN's (1971) observations on guinea pig no clear inner structure is discernable here. On the outside of these microvilli strands of mucus are found to adhere. The topography of these microvilli between ciliary structures is shown in the lower right hand corner of Fig. 41A, which is sectioned just under the level where cilia sprouting oc-

FIG. 40. Olfactory ciliary tapers and vesicles (calf, septal). *A*. The majority of the vesicles probably represent ciliary tips. Their membranes have different appearances. They also contain different inclusions. Two of the vesicles, with adhering taper parts, make mutual contact. Several other forms of ciliary contacts can be seen. *B*. A ciliary vesicle on a taper. This vesicle contains microtubuli.

FIG. 41. Olfactory mucus layer (calf, septal). The main figure is a high-voltage micrograph. Inset is taken by a TEM. Section thickness was about 1 μm. The photograph shows nerve endings (Ne) from the region where they just emerge from the epithelium surface (the dense part of the photograph) until their most distal ciliary taper ends (see also inset). These ciliary tapers (Ct) frequently bear vesicles (Cv). Vesicles here often have an internal structure. Several nerve endings contain fibrogranular microtubuli pools (Fg) and centrioles (small dark spots inside the nerve endings). Some areas show only cross-sections of microvilli (Mv); this is the case close to the epithelium surface (compare with Fig. 23). Note the electron-lucent pockets (arrow) in the mucus layer, which show no structure.

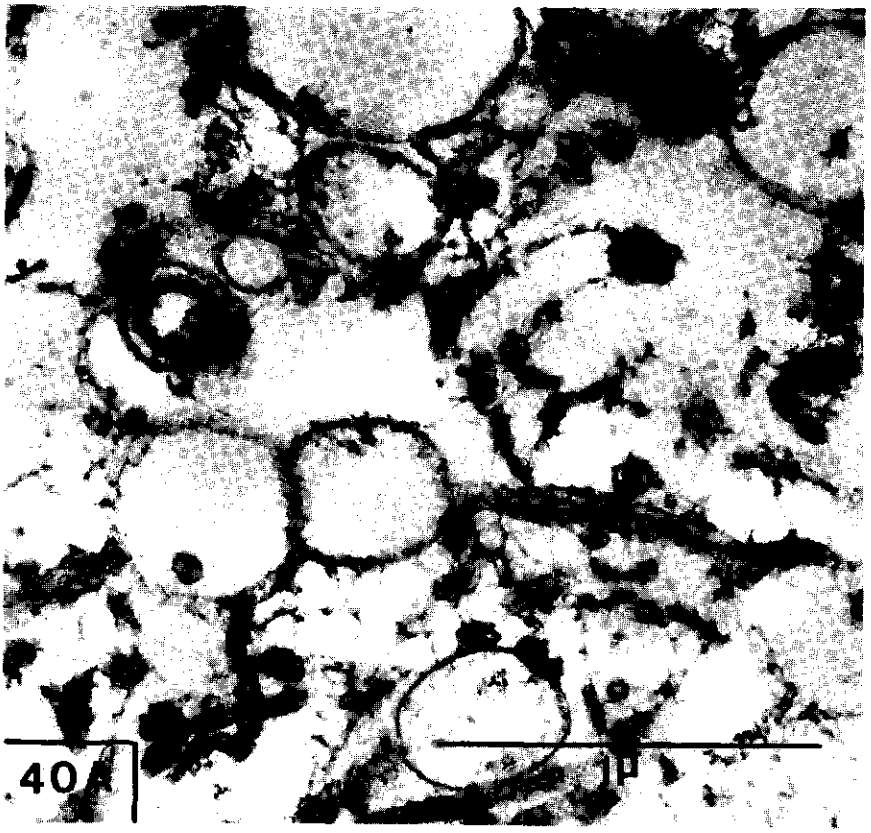
40A
1μ


40B
0.1μ

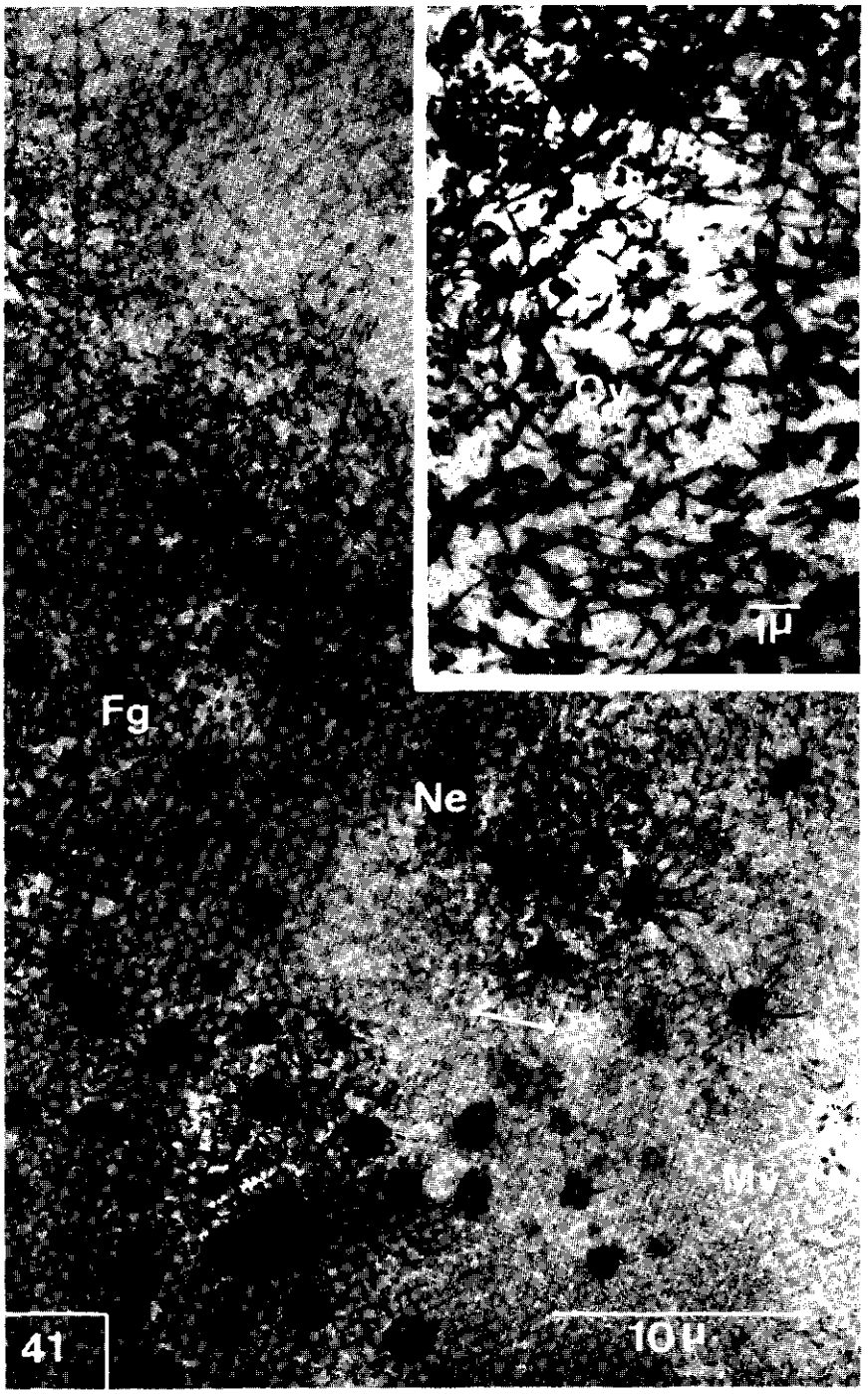
Fg
Ne
1μ
10μ
41

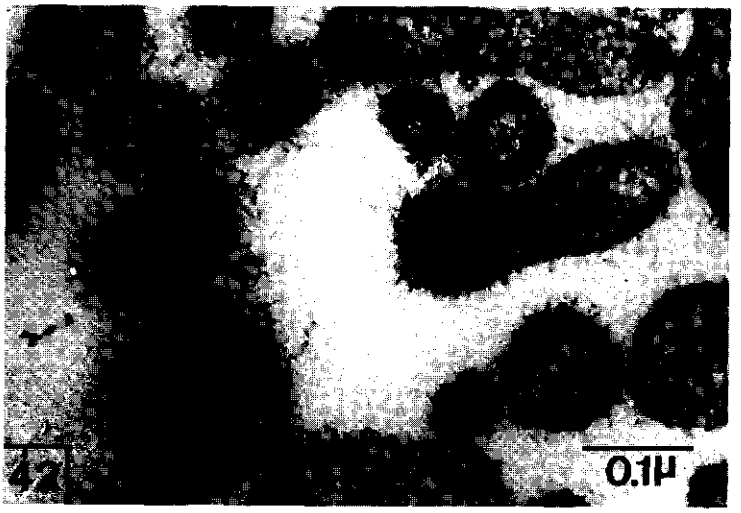

FIG. 42. Microvilli of supporting cells (calf, septal). They do not show a clear internal structure. A mucus coat adheres to their outer membrane surfaces. Compare these cross-sections with those of Fig. 11 (inset).

curs. Nerve endings can be followed traversing this picture all the way until only tapers remain. In the center of the picture cilia and microvilli are found together, while the inset shows a part depicting mainly ciliary tapers and vesicles.

Inside the nerve endings the presence of fibrogranular microtubular pools is noticeable.

In addition to the structures described above, some figures (Figs. 41 and 43) demonstrate areas which are optically empty. These 'bubbles' are surrounded by ciliary tapers and microvilli (Fig. 43). Furthermore, Fig. 43 shows clearly the complexity of the epithelium surface and should be compared with the scanning micrographs of Fig. 17. Ciliary tapers appear to form rather complex structures in which surrounding, crossing-over and traversing occurs. They usually run in groups.

1.4. DISCUSSION

1.4.1. *General*

The results presented in this chapter confirm and extend the observations made by several other authors on the epithelium types described here (for references see INTRODUCTION). In the present discussion the main attention will be devoted to the ciliary structures and to growth and turnover of the olfactory area. Some other relevant observations will be discussed too.

1.4.2. *Expansion and turn-over of the olfactory epithelium*

Whether or not growth of the olfactory epithelium area (Fig. 1), reflects an increase in the number of nerve endings or a fragmentation of the original area could not be assessed indisputably. However, as will be shown in Chapter 3, nerve ending densities in young and adult animals are fairly similar, which may indicate that during growth of the animal the total number of nerve endings increases proportionally with the rest of the head. KOLB's (1971) results on the olfactory area of several bat species indicate also such a proportional relationship between the total number of nerve endings and the size of the olfactory area.

Some evidence for a proportional post-natal development is provided by the scanning micrographs of Fig. 19, which illustrate the situation in an adult animal, and by the HVEM stereopair of Fig. 28. The nerve ending structures in these figures have similar appearances as those observed in embryonal (WATERMAN and MELLER, 1973a; CUSCHIERI and BANNISTER, 1975; KERJASCHKI and HÖRANDNER, 1976) and juvenile (OKANO et al., 1973, 1976; FURUTA et al., 1975) tissues of several other mammalian species. Only in kittens such cilium deprived nerve ending structures could not be detected (FURUTA et al., 1974). Furthermore, the centriole replication figures of Figs. 24, 30, 32B (inset) and 41A indicate ciliary renewal (ROTER DIRKSEN, 1971). This means that centriole supply occurs both by centriole transport (HEIST et al., 1967; HEIST and MULVANEY 1968; MULVANEY and HEIST, 1971a) from elsewhere to the nerve ending and by centriole replication inside the nerve ending. In the vomeronasal organ cilia development does not continue beyond this centriole multiplication stage (KOLNBERGER and ALTNER, 1971). All these features indicate postnatal renewal or addition of nervous material in the olfactory epithelium, although pathological features cannot be excluded.

These findings seem to confirm recent publications concerning cellular turnover (MOULTON et al., 1970; MOULTON, 1974, 1975) and regeneration processes in the olfactory area (MULVANEY and HEIST, 1971b; GRAZIADEI, 1973b; MATULIONIS, 1975, 1976; YAMAMOTO et al., 1976). The reappearance of the olfactory nerve (OLEY et al., 1975) and of the olfactory epithelium (BEDINI et al., 1976) after transection of the olfactory nerve in pigeons accompanied the reappearance of an electrical response. Previous experiments (TAKAGI, 1971) in frog could not show this effect. The olfactory epithelium appears to be transient. Most likely postnatal expansion does occur.

1.4.3. *Nasal epithelium surface structures*

1.4.3.1. Endocytotic vesicles within the olfactory nerve ending

BAKHTIN (1975) suggests that the endocytotic vesicles, as seen in Figs. 24, 31A and 32A, have an autolytic role, whereas DE LORENZO (1970) suggests that they are pinocytotic. The fact that they are so frequently found near the nerve ending surface suggests the latter role. The existence of several types of vesicles cannot be excluded. Fig. 15 (inset) probably shows openings of such vesicles.

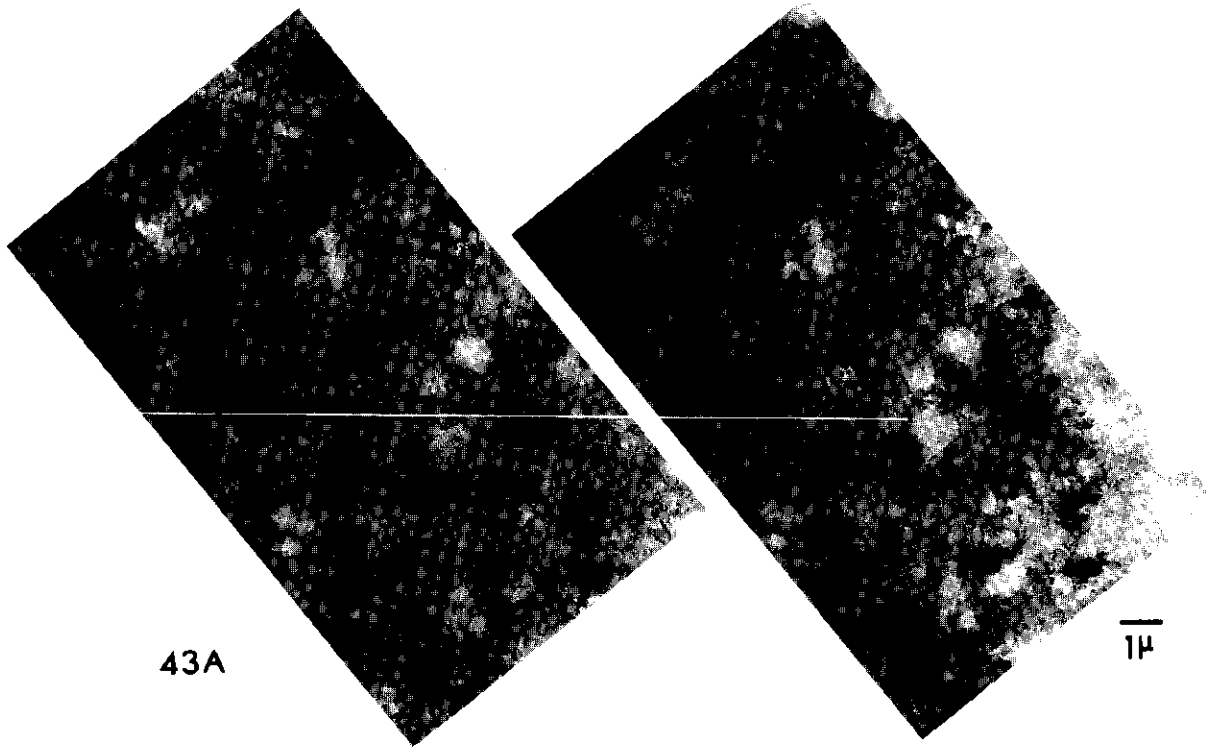

FIG. 43. HVEM micrographs of olfactory mucus surface (calf, septal). *A*: stereopair and *B*: higher magnification of (*A*). Note particularly the many organelle-free patches within the mucus layer (thin arrow), which are surrounded by ciliary tapers and supporting cell microvilli. One ciliary bundle (two arrows) is seen to surround other ciliary bundles. This picture shows the complexity of the olfactory mucous surface. In the complete micrograph, from which this picture is a detail, cilia could be followed over approximately 30 μm. Compare this picture with Fig. 17. The diameter of the section was about 4 μm. Tilting angle: 3°.

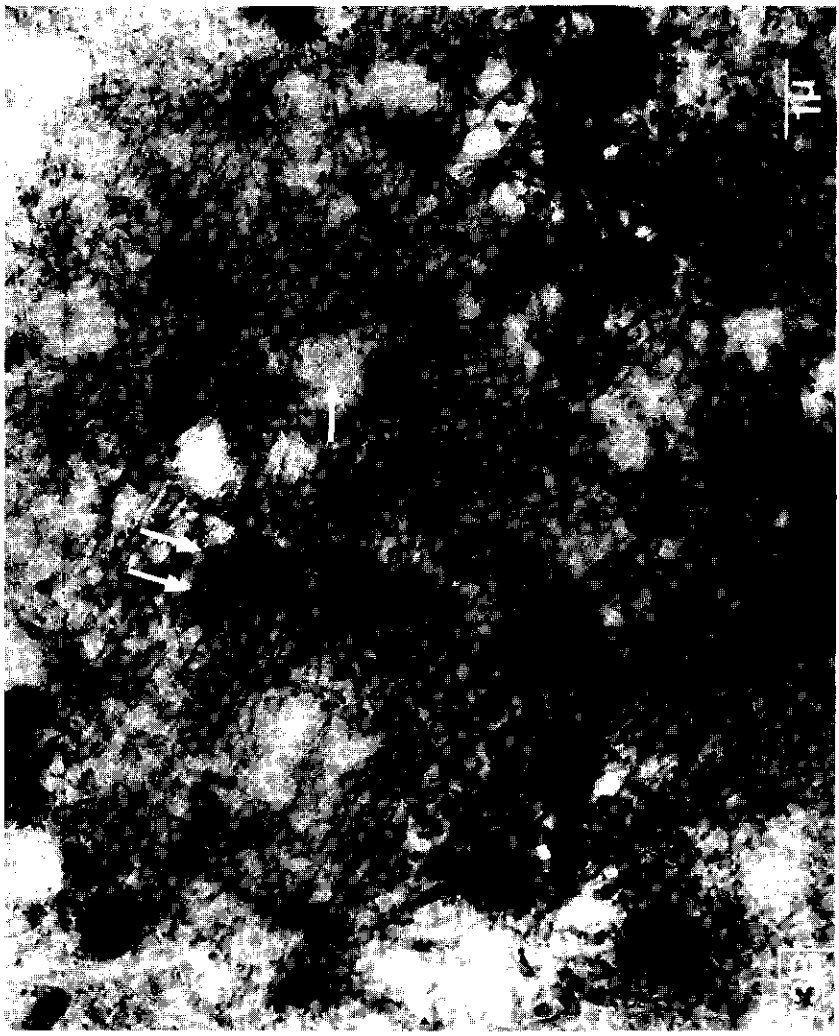

FIG. 43B.

1.4.3.2. Brush cell

The brush cell, occasionally found in both nasal respiratory epithelium and olfactory epithelium (Fig. 27; HEIST et al., 1967; ANDRES, 1969; JOURDAN, 1975), is also found in other types of ciliated epithelium, e.g. tracheal epithelium (ANDREWS, 1974; JEFFERY and REID, 1975). YAMAMOTO (1976) devotes an extensive discussion to the presence of this cell type. ANDRES (1969) considered this cell to be of nervous origin. Recently it has been found, that microvilli of apparently similar brush cells in intestinal epithelium contain actin (MOOSEKER and TILNEY, 1975).

1.4.3.4. Ciliary structures

1.4.3.4.1. General

Olfactory cilia are a specialized cilium type like the receptive structures of most other sensory organs in virtually all eukaryotes (THURM, 1969; ATEMA, 1973, 1975; BARBER, 1974; VINNIKOV, 1974). Most mammalian olfactory cilia contain the normal nine doublets plus the two central microtubule axonemal structure over a distance of 1–3 μm beyond the necklace. Distally from this proximal segment with its complete axonemal structure the cilia form tapers characterized by a smaller diameter and containing fewer microtubules. The major parts only contain one or two microtubular subfibers in mammals. This prolonged tapering represents a ciliary modification typically encountered in olfactory epithelium of several vertebrate taxa, e.g. mammals (FRISCH, 1967; SEIFERT, 1970) and amphibians (REESE, 1965). It may be compared to the characteristic ciliary modifications observed in the outer segments of vertebrate visual cells and insect antennal hairs.

1.4.3.4.2. Axonemal aggregates

The ciliary aggregates found in the respiratory (Fig. 11) as well as in the olfactory epithelium (Fig. 31C) are not a unique feature. Similar aggregates have been found in the olfactory epithelium of several lower vertebrates, expecially in fishes (BRONSHTEIN and PYATKINA (1966) as quoted by VINNIKOV, 1969, 1974; SCHULTE, 1972; GRAZIADEI, 1973a; LOWE, 1974; LOWE and MACLEOD, 1975) and in mammals (OKANO, 1965; YAMAMOTO, 1976). In the latter study the ciliary membrane is present around axonemal structures within the olfactory nerve ending knob. Since these structures were only found irregularly it is possible that these aggregates in both mammalian epithelium types represent a pathological feature.

1.4.3.4.3. Basal bodies

Basal bodies in both epithelium types, the respiratory as well as the olfactory, apparently belong to the Type I basal bodies of PITELKA (1974), since their basal plates approximately level with the nerve ending membrane region where the latter is deflected upward to become the ciliary membrane. Also only one plate is present per cilium. The major difference between the basal bodies of the two kinds of cilia is the presence of short striated rootlets on the basal bodies of respiratory cilia (Fig. 8), while such rootlets are absent on olfactory nervous basal bodies (Figs. 25 and 34). Big striated rootlets on olfactory basal bodies as seen by, for example, OKANO (1965), SEIFERT (1970) and YAMAMOTO (1976) in several mammals, were never observed in the bovine. The latter author devotes an extensive discussion to the presence of such rootlets on olfactory cilia. At basal foot level the basal bodies of both cilium types contain a dense dot (Figs. 7, 25 and 34). These dots are probably associated with the presence of RNA in basal bodies (HARTMAN, 1975).

1.4.3.4.4. Ciliary axonemal and membrane structures

Cross-sections of bovine olfactory cilia as seen in Fig. 34 are similar to those seen in a variety of other vertebrates (OKANO, 1965; DE LORENZO, 1970; SEIFERT, 1970; KRATZING, 1972; YAMAMOTO, 1976). The major difference when compared with similar cross-sections of respiratory cilia (Fig. 9) is the absence in the olfactory cilia of arms on the axonemal doublets. This feature corresponds to the situation in most other vertebrates (BANNISTER, 1965; OKANO, 1965; HEIST et al., 1967; SEIFERT, 1970; KRATZING, 1972, 1975; THEISEN, 1973). In bovines and some other mammals no motility of olfactory cilia has been observed, in contrast to ciliary movements seen in the respiratory area (LUCAS and DOUGLAS, 1934). In some other animals, however, olfactory cilia do contain arms or armlike structures, for example in the frog (BRONSHTEIN, 1964 as quoted by VINNIKOV, 1969, 1974; REESE, 1965) and most noticeably in lamprey (THORNHILL, 1967). Thus it appears that the absence of these arms is a common, but not universal feature of olfactory cilia. In frog, motility of the olfactory cilia may easily be observed and has been reported by several authors (BRONSHTEIN, 1964 as quoted by VINNIKOV, 1974; REESE, 1965). The present author filmed such movement (MENCO, 1976; film available from the foundation TELEAC). Respiratory cilia are known to be motile in virtually all cases studied (NEGUS, 1958). In instances of motile olfactory ciiia (frog) their beatings show lower frequencies than in the case of respiratory cilia (MENCO, unpublished).

Motile cilia contain a protein, called dynein (GIBBONS, 1965), whereas in immotile cilia, such as abnormal human spermatozoa (AFZELIUS, et al., 1975; BACCETTI et al., 1975) this protein is lacking. Concomitant with this lack is the absence of the doublet arms. These arms are also missing in abnormal and immotile cilia of the human respiratory tract (AFZELIUS, 1976; PEDERSEN and MYGIND, 1976) which may be the cause of other pathological conditions encountered in these patients. The abnormal respiratory cilia described by AFZELIUS (1976) show a dense ciliary matrix just as olfactory cilia. Possibly there exists a relationship between the absence of arms and the density of the ciliary matrix.

Dynein is located in the arms (AFZELIUS, 1959; GIBBONS, 1965; STEPHENS and LEVINE, 1970; SUMMERS, 1975; STEPHENS and EDDS, 1976). This protein is a Mg^{++}-ATPase, which is apparently responsible for motility of the cilia.

The absence of arms and the probably corresponding absence of dynein in olfactory cilia may indicate that the main function of the axonemes in the olfactory cilia is not related to the propagation of motility, in contrast to the situation in respiratory cilia. KERJASCHKI (1976) recently came to a similar conclusion on the basis of observations on ciliary tapers, using tannic acid fixation.

ATEMA (1973) has proposed that the axonemes contain the receptive moiety, though later (ATEMA, 1975) he restricts their possible function to a participation in the transduction process. In agreement with the opinion expressed by several other authors (see DODD, 1974) he now suggests, that this moiety is

located in the ciliary membrane, rather than in the axoneme. OLSEN (1975) links the microtubules with the cyclic AMP system which is most likely partially incorporated in the cell membrane. Some evidence for the presence of such a cAMP system in olfactory mucosal preparations is presented by BITENSKY (1972), KURIHARA and KOYAMA (1972) and MENEVSE et al. (1974). MINOR and SAKINA (1973) and MENEVSE et al. (1976) indicate the involvement of cyclic nucleotides in the olfactory receptive process using electrophysiological methods.

Cyclic nucleotides were found to be involved in the visual system (MIKI et al., 1974; GORIDIS et al., 1975), in the audiosensory system (AHLSTROM et al., 1975), in chemotaxis (KONIJN, 1974), in vertebrate taste (KURIHARA, 1972; MENEVSE et al., 1974; CAGAN, 1976) and in insect chemoreception (DALEY and VANDE BERG, 1976; VANDE BERG, 1975) and thus to be as common in sensory processes as the presence of microtubular structures.

Regarding the function of microtubules in chemoreception, it is interesting to note that substances which depolymerize tubulins inhibit proper functioning of chemotactic behaviour (BANDMAN et al., 1973; EDELSON and FUDENBERG, 1973; LEVANDOVSKY et al., 1975) and responses to sex pheromones in insect olfaction (BLOCK and BELL, 1974). JACKSON and LEE (1965) observed degeneration of vertebrate olfactory receptors after treatment with colchicine, a microtubule depolymerizing agent. The relevance of the microtubular system to the electrical properties of the cell is indicated by the finding that a disorganized microtubular structure in a cockroach mechanoreceptor was accompanied by the loss of electrophysiological responses (MORAN and VARELA, 1971). In ciliary axonemal structures binding sites for colchicine and other vinca-alkaloids are blocked (MARGULIS, 1973) and can only be exposed after solubilization of the axoneme (STEPHENS and LEVINE, 1970). Since up till now it has been impossible to isolate olfactory cilia (see Chapter 4), nothing is known about the binding of such agents to the microtubular singlet fibers in the ciliary tapers. The cases mentioned above could concern both cytoplasmic and membrane-attached microtubules. They may indicate that non-axonemal microtubules are in some way involved in the transduction process.

A possible model for this signal-transduction can be constructed. After interaction of odorants with receptor sites, cyclase systems are activated to form cyclic nucleotides. Regulated by cyclic nucleotide phosphodiesterases these nucleotides activate one or more protein kinase types, which are directly linked to the microtubular system. The extended length of these microtubules could serve as a system which transmits signals over ciliary distances as great as 200 μm in the frog (REESE, 1965) and 50–60 μm in some macrosmatic mammalian species (SEIFERT, 1970) to the nerve ending knob. Here the signal is further processed together with signals obtained from other cilia belonging to the same cell. This hypothesis is derived from ATEMA's (1973, 1975) and OLSEN's (1975) hypotheses. The presence of lateral contacts between nerves of the peripheral olfactory system, at virtually all levels (at ciliary, dendritic as well as at axonal levels) suggests the existence of lateral interactions between the olfactory

nerves, as has been dicussed by DE LORENZO (1970). This author actually claimed to observe synaptic contacts between dendrites. A signal perceived by one cell may be evaluated by a number of cells. However, our freeze-etch studies (Chapter 2) did not yield further evidence for the presence of such contacts.

If the ciliary and nerve ending knob membrane contains the receptive moiety as well as the stimulus transmitting moiety (which may also be located in the microtubules) then the axonemal microtubules would probably have a different role, although the possibility of a combined function of the ciliary membrane and the axonemal structures in stimulus transmission cannot be excluded. If the membrane plays the major role in stimulus transmission, then the most important function of the axonemal structures could be those of a cyto-skeleton to hold that membrane (BANNISTER, 1965). This could be envisaged in view of the fact that the tapers grow in a sticky mucus (of unknown viscosity) and seem nevertheless well stretched along their observed lengths (Figs. 18, 41 and 43).

The ratio of length to diameter of the tapers can be 1,000 to 2,000 (for tapers of 100 to 200 μm long with a diameter of 0.1 μm). Without a cytoskeleton it seems unlikely that the receptive membrane could bridge such distances. Therefore it is suggested that microtubuli have this function anyway. In addition they could have any of the other functions.

Another remaining question concerns the formation of the cilia and their tapers. Are they formed at their proximal ends, so that growth occurs from the basal body region, or are packages of microtubular protein added to their distal ends? Some of the ciliary vesicles could be involved in ciliary growth. They do contain microtubular structures in some instances (Fig. 40B). SEIFERT (1970) and NAESSEN (1971) think that these vesicles are degenerative structures. It might just as well be that at least part of them has a functional role (OKANO, 1965), e.g. participation in growth processes. They could also represent artefacts. Biochemical and physiological work is necessary in assessing possible roles for these vesicles. They are observed here in virtually all olfactory samples with section (Figs. 22A, 24, 31A, 32A, 35, 40A, B, 41 and 43) as well as with freeze-etch techniques (Figs. 50A and B). In the latter the freshest possible samples were obtained. Current freeze-etch work indicates the possibility of different types of such vesicles (MENCO, unpublished). Vesicle formation is also observed in the respiratory epithelium (Figs. 7 and 8).

Ciliary tips may be involved in the growth of the cilia as well. The caps on the ciliary tips (Fig. 39) may contain enzymes, similar to the acrosomal caps in spermatozoa (see e.g. review FAWCETT, 1975). These enzymes could be mucus digesting, which serves to make the mucus less viscous, thus facilitating ciliary outgrowth. In this context it is worth noting that OKANO (1965) noticed in dog several different types of tips, nearly all of them vesiculated. Respiratory cilia might not need such caps, since they can move the mucus actively and they are much shorter (length/diameter ratio $\approx$ 50). Moreover, there is a difference in character of the mucus between the two types of epithelium as is indicated

by our scanning experiments (Fig. 3A, B). Mucus remains were more distinctly observed on the olfactory than on the respiratory epithelium surface, which confirms a report by GRAZIADEI and GRAZIADEI (1976). Histochemical studies showed that the mucus types differ in composition (CUSCHIERI and BANNISTER, 1974), though definite information about the mucus composition is still lacking. The mucus is probably of a heterogeneous nature as is indicated by the presence of different inclusion types (Figs. 24 inset, 31A and 43). These inclusions could also be foreign material, which has intruded the mucus from the surface.

The high-voltage electron microscope technique has been applied with the aim of establishing total lengths of cilia. This objective has not been realized, although cilia could be followed over longer distances than with other techniques (Fig. 43). Therefore, the estimates of SEIFERT (1970) for some macrosmatic species (rabbit, cat and dog) remain the most accurate values available. He estimated, using morphometric methods, that the cilia in these species are about 50–60 μm long. The high-voltage technique allows a better observation of the mutual relationship between individual cilia as well as their relationship to supporting cell microvilli. Moreover, as with SEM observations, it appeared possible to make a more accurate assessment of the total number of cilia per nerve ending than had been possible sofar. Consequently, it seems to us that the use of thick sections, enhanced by the stereo representation, yields information which would have been difficult to obtain by other techniques.

1.4.3.5. Electron-lucent mucus inclusions

The electron-lucent mucus inclusions are the most interesting features revealed by the HVEM technique (Figs. 41 and 43). They are surrounded by ciliary tapers and microvilli and might represent small gas pockets. Photographs, however, cannot prove such a suggestion and leave their nature open to speculation. In our opinion these inclusions could represent gaseous bubbles passing the mucus surface in the time span between slaughter and fixation, thus reflecting tissue deterioration. Alternatively they might represent air pockets taken up from the outside. Whatever their origin, they influence the spatial organization of both cilia and microvilli. The occurrence of these bubbles could conceivably indicate that odorant-receptor interaction occurs, at least partially, in the gaseous phase. The bubbles then would function as odorant carriers. This hypothesis would facilitate explanations of odorant transport. Odorants may have to pass the probably aqueous mucus before they are in a position to interact with membrane receptor sites. Most odorants are fairly hydrophobic, though they usually do contain a polar group. The receptor sites could be proteins as well as phospholipids. The phospholipid molecules contain polar headgroups orientated to the periphery of the bilayers (SINGER and NICOLSON, 1972). As a consequence, odorants, when interacting with this phospholipid moiety of the bilayers, first meet these headgroups. The polar ends of the odorants could then interact with the headgroups, while the non-polar parts interact with the fatty acid parts of the phospholipids (CHERRY et al., 1970). In the case of proteinaceous receptor sites the situation is different since

conceivably the protein molecules expose hydrophobic as well as hydrophilic parts at the membrane-mucus interface. The interaction between odorants and phospholipids could also occur via pore formation (DAVIES, 1971). Pores could just as well be present in the proteins (SINGER, 1975), for example as hydrophobic cores.

Alternatively, the electron-lucent pockets could also represent an accumulation of electron-lucent material, which is not penetrated by cilia, or holes which remained after certain materials disappeared during fixation. They then reflect artefacts.

2. A FREEZE-ETCH AND ELECTRON SPIN RESONANCE STUDY ON NASAL EPITHELIUM OF COW AND SHEEP

2.1. INTRODUCTION

There are indications that olfactory receptor sites are at least partially of proteinaceous nature (GETCHELL and GESTELAND, 1972; GENNINGS et al., 1976, 1977; MENEVSE et al., 1977). These proteins are most likely embedded in the ciliary membrane which can be envisaged as a fluid mosaic bilamellar structure (SINGER and NICOLSON, 1972). In view of the fact that most odorants are amphiphilic molecules containing relative large hydrophobic moieties, the phospholipid parts of the membrane may also play a role in the odour perception process (DODD, 1974).

Since it is well established that intramembranous particles, seen with freeze-etch or freeze-fracture techniques as developed by MOOR et al., (1961) are in most instances proteinaceous (BRANTON, 1971; GRANT and MCCONNELL, 1974; SEGREST et al., 1974; VERKLEIJ and VERVERGAERT, 1975; ZINGSHEIM and PLATTNER, 1976), the presence of such particles in the nerve ending membranes of the peripheral olfactory organ might provide evidence for the existence of proteins in those olfactory neuronal membranes. These proteins may have a function in odour reception processes.

Characteristics of the olfactory epithelium have been compared with those of the nasal respiratory epithelium, because the columnar cells in the latter tissue type are also covered with cilia (MATULIONIS and PARKS, 1973; Chapter 1). Olfactory cilia are of nervous origin (GRAZIADEI, 1973a; Chapter 1), while the cilia in the respiratory epithelium lack a sensory function, but are instead responsible for moving mucus as indicated by their active motion (Chapter 1).

In addition to the freeze-etch studies both epithelium types have been studied using the electron spin resonance technique. This technique provides information about the molecular environment of a nitroxide labeled molecule after its incorporation into the tissue. Unfortunately the information obtained is affected by the fact that nitroxide spin labels, as initially synthesized by STONE et al. (1965), probably bind to many other cellular components in addition to the receptive membranes. Another disadvantage is that the spin labels are rather bulky, and might therefore distort their environment. In spite of its limitations this technique has been applied to many other biological tissues and has provided a considerable amount of information about label environments (see reviews by JOST et al., 1971; HOLMES, 1973; KEITH et al., 1973 and BERLINER, 1976).

2.2. Materials and methods

2.2.1. *Freeze-etch studies*

Bull heads were obtained from local slaughterhouses. They became available within two hours after killing. The heads were split sagittally and cold Karnovsky's (1965) fixative (pH = 7.0) was gently applied to the exposed nasal area.

Subsequently, portions from the areas under investigation were dissected and left to fix for another hour at 4 °C. After fixation, tissue blocks were washed in the same buffer as used for fixation, the fixative being replaced by 6% sucrose. Washing solutions were renewed after intervals of one minute, one hour, one hour and two hours respectively. The fixed tissue samples then were impregnated for 24–36 hours with 20% glycerol, made up in the same buffer as above (0.075 M Na-cacodylate containing 0.1% $CaCl_2$). This solution was renewed after two hours.

The tissue blocks were attached to gold stubs (3 mm diameter) in such a way that the razor blade would fracture perpendicularly to the ciliated epithelium surface. Blocks were fractured, etched and replicated by platinum and carbon evaporation in a Balzer's GA-6 Freeze-Etching Device according to standard techniques (Fisher and Branton, 1975).

Replicas were transferred to distilled H_2O which was replaced by a cleaning solution (10% commercial bleach). They were left to clean for 3 hours. The bleach was then replaced by H_2O through 5 washings. In turn water was replaced by 25% H_2SO_4 and the replicas were left to be cleaned for another three hours. Through five washings the sulfuric acid was again replaced by distilled water. The replicas were collected on Formvar/carbon coated grids and examined in a Hitachi-125E electron microscope at 125 kV, usually with a 20 μm objective aperture.

The nomenclature of Branton et al. (1975) is used throughout this study, the P-face (PF) being the A-face in former studies and the E-face (EF) being the former B-face. Shadows appear white in the photographs.

2.2.2. *Electron spin resonance studies*

Sheep heads were obtained from local slaughterhouses. The heads were cut sagitally and the nasal area of interest was dissected. All preparative treatments were carried out at 4 °C. Nasal mucosa from the septum was used for spin label incorporation.

The labels used were 12- and 16-doxylstearic acid (Synvar Chemicals, Palo Alto, California). The absolute ethanol, in which the labels were dissolved, was evaporated with nitrogen and the remaining label was emulsified either in an ice-cold Krebs-C physiological salt solution (Krebs, 1950) or in 0.05 M Tris-HCl (Sigma), pH = 7.0 made up to an approximately equiosmotic medium with 0.9% NaCl.

Label incorporation was started within five hours after slaughter. Incorporation periods lasted from one to three days. Most experiments were carried out

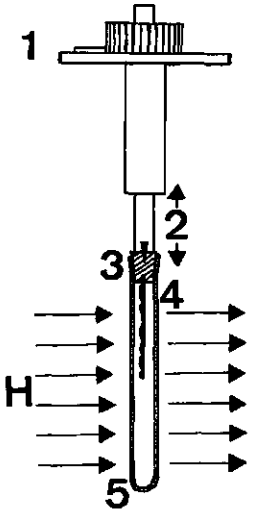

FIG. 44. Goniometer device used in electron spin resonance experiments. 1. Goniometer; 2. Adjustable Teflon rod; the direction of movement is indicated by the arrows; 3. Rubber bung with slit to hold sample containing microscope cover slide. The bung is attached to the Teflon rod with a pin; 4. Sample containing cover slide; 5. Quartz ESR loading tube. The arrows indicate the direction of the magnetic field (H), with the glass slide perpendicular to the magnetic field in the illustration.

on tissue slices, attached to a microscope cover slide. These slides were stuck in a closed quartz loading tube, which was attached to a goniometer (Fig. 44). ESR spectra were recorded parallel and perpendicular to the magnetic field (LIBERTINI et al., 1969). Excess label was removed by dipping the incubated tissue slices ten times in Krebs-C or buffer solutions. During this procedure the washing solutions were three times renewed. It was difficult to assess incorporation, since most of the label was removed after rinsing, even after the long incubation times used. The signal to noise ratio became very poor then.

In some experiments the mucosa was gently scraped with a spatula (KOCH and NORRING, 1969; DODD, 1970). The obtained material should contain most of the receptive fractions, although this receptive fraction represents only a very small amount of the scraped material (Chapter 4).

In this case label incorporation was carried out for 30 minutes only. Tissue concentrations used were 100 mg wet weight/ml. Tissue suspensions were collected in Pasteur pipettes from which the spectra were recorded. Usually in both types of experiments a label concentration of 5×10^{-4} M was maintained. Label incubation with exchange from bovine serum albumine (BSA, Fraction V; HUBBELL and MCCONNELL, 1968) and without spin label exchange from BSA did not make any difference.

In some instances, after recording of spectra, tissue samples were incubated crudely with odorous compounds and the spectra were recorded once more. The odorants used were: (+)-citronellol (International Flavors and Fragances, Naarden), 1-butyric acid and CCl_4. Only 1-butyric acid, which is water soluble, could be mixed with buffer or physiological salt solutions. CCl_4 stimulation was carried out by adding a droplet of this compound in the sample containing loading tube (Fig. 44). (+)-Citronellol was in some instances emulsified with the sample containing dispersions (in 1/50 or 1/150 v/v ratios). The spectra

were recorded shortly after this addition. In the slide experiments, (+)-citronellol was vaporized over the epithelium surface. This was done by adding droplets of this compound to solid CO_2 in a wash bottle. Adding water to this mixture resulted in an odorous flow which was led through a piece of silicone tubing over the epithelium slices. In all these instances it would have been much better to link an olfactometer to the ESR apparatus, but such facilities were not available.

As a standard, 5.10^{-4} M 16-doxylstearic acid dissolved in dodecane was used. Spectra were recorded with a Decca Radar X-1 ESR Spectrometer, using 100 Kc/second, with a klystron frequency of 9.3 MHz. The magnet used was a Newport Instruments 7 In. Magnet. All spectra were obtained at room temperature. Odour stimulations were also carried out at room temperature.

2.2.3. *Materials*

Unless specifically mentioned, all chemicals were obtained either from British Drug Houses or from Sigma Inc. and were of analytical grade.

2.3. Results

2.3.1. *Freeze-etching*

Figures 45 and 46 show freeze-etch replicas of bovine olfactory epithelium while Fig. 47 shows a replica of the respiratory surface. The anatomical outlines of the freeze-etch features do not differ significantly from those of section transmission and scanning studies (Chapter 1) and tend to show similar differences between the two epithelium types as the two other methods (Chapter 3; Table VI).

The replicas of Figs. 45 and 46 show cilia protruding in various directions, while the replica of Fig. 47, showing the apical region of respiratory columnar cells, contains cilia perpendicular to the epithelium surface.

Observations in Figs. 45 and 46 which seem to indicate the olfactory nature of the cilia in these figures are: *1.* The cilia taper, as is indicated by the sudden change in diameter (Figs. 45C, 46B and C). The cilium shown in Fig. 46C exhibits a fracture face of a cross-section in the transition area where the cilium starts tapering, as is indicated by the two cross-section diameters present within this ciliary segment. *2.* The diameters of these cross-sections are in agreement with measurements of both cilia segments performed on the photographs obtained with other observation methods (Table VI). Olfactory cilia always taper in this animal whereas respiratory cilia usually do not as described in Chapter 1.

The nerve ending of Fig. 45C shows, juxtaluminally, part of a zonula occludens region which can be recognized by its typical ridges. In Fig. 45A on the right and in Fig. 48 similar ridges can be seen on fracture faces of supporting cells. These ridges consist of six to eight strands of rather large particles which often aggregate. Fig. 45C shows that these tight junction particles protrude

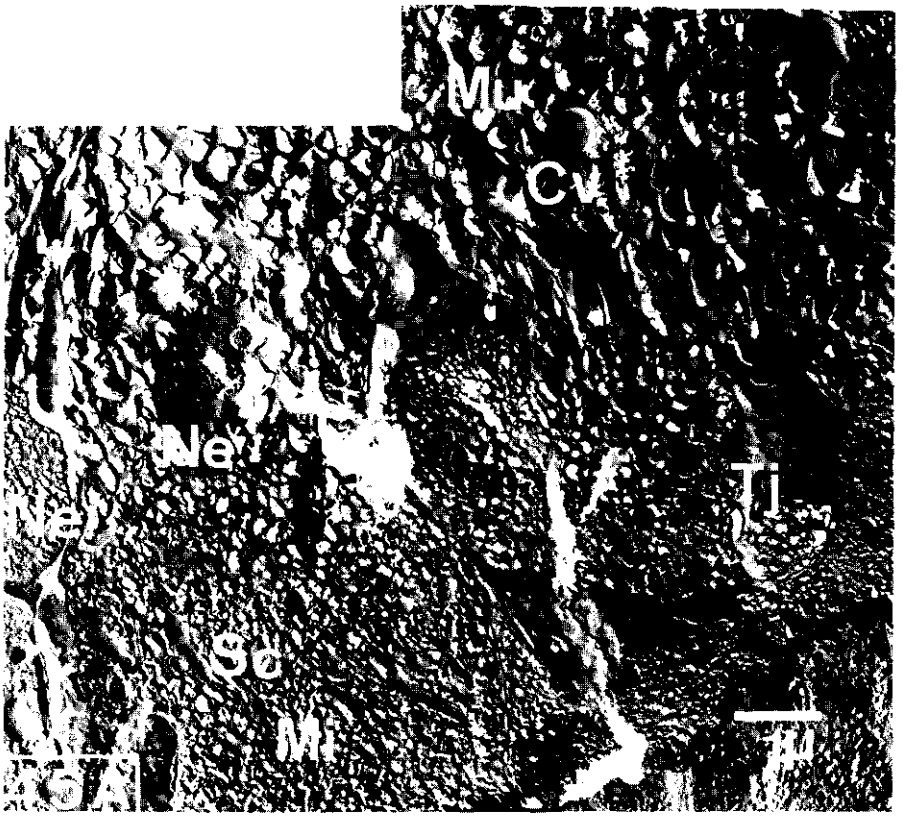

FIG. 45. Freeze-etch replicas of some olfactory nerve endings (calf). *B* and *C* are details of *A*. One of the nerve endings (Ne) of (*A*) shows at high magnification (*45C*) two ciliary (C) fragments. One of them shows the fracture face of the inner membranous lamina (PF = protoplasmic face), while the other one depicts the fracture face of the outer membranous lamina (EF = exo- or endoplasmic face). Another nerve ending (magnified in *B*) shows only cilia, which broke approximately at necklace (Nl) level. About 12 of them are present (*B*: 1-12). Tight junctions (Tj) are present both on nerve endings and on supporting cells (Sc). The arrow in *45C* points to a region where two other cells joined the nervous cell. Note the way this junctional line continues in *A*. Several desmosomes are present (arrows). P-faces of nervous cells, supporting cells, supporting cell microvilli (Mv) and olfactory cilia contain many particles, while E-faces are virtually devoid of particles. Note that the ciliary vesicles (Cv) contain particles as well. Mi: mitochondria; Mu: mucus.
For Figs. *45B* and *C* see pages 61, respectively 62.

deeply into the nerve ending plasmatic region and might be continuous with some structures close to the plasma membrane.

The fracture surface of the supporting cell of Fig. 48 contains round patches, suggesting the presence of pinocytotic vesicles under the surface or other surface irregularities.

Both olfactory and respiratory types of cilia contain necklaces in the region where the ciliary membrane joins the plasma membrane of the cell surface

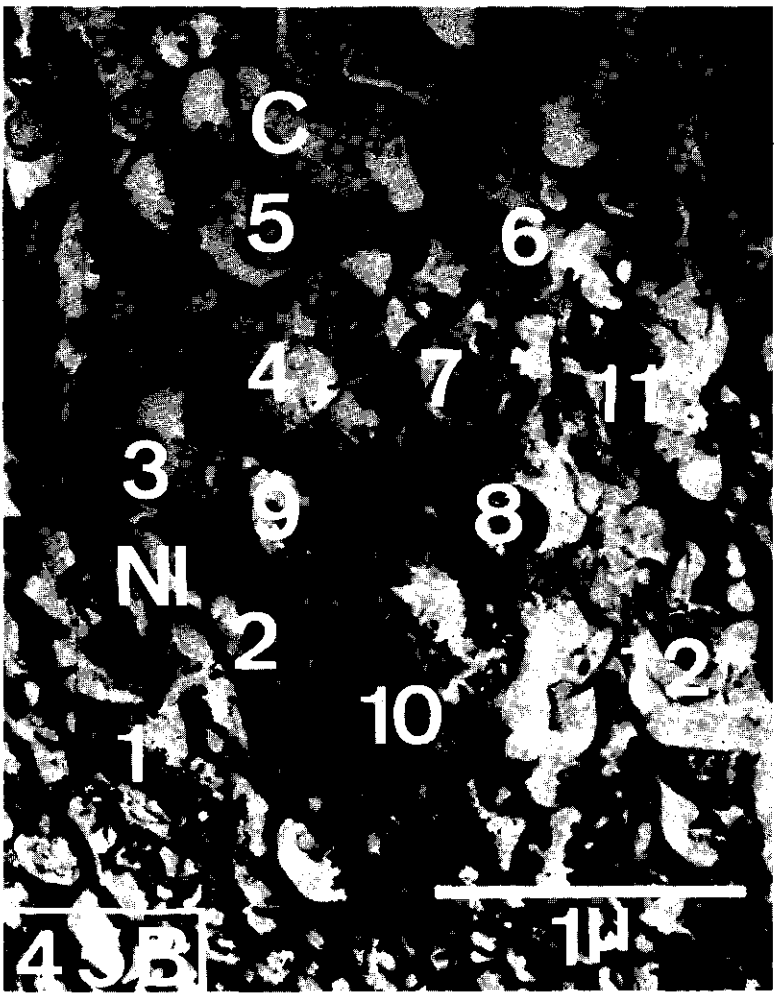

FIG. 45B.

(Figs. 45, 46 and 47). The strand spacing of these necklaces in the respiratory mucosa is about twice that of similar structures within the olfactory mucosa (Table I). Table I gives also the diameters of these necklace particles.

Microvilli in both epithelium types have P-faces containing many intramembranous particles (Table I, Figs. 45, 46, 47 and 48).

It is interesting to see that the P-faces of the respiratory cilia beyond the ciliary necklaces are virtually devoid of particles (Fig. 47), whereas corresponding olfactory fracture faces contain many – apparently randomly distributed – particles along their whole lengths observed, thus including ciliary tapers and vesicles (Figs. 45, 46, 49 and 50). The highest particle density is observed in the ciliary tapers (Table I), while nerve-ending body, proximal cilium part and ciliary vesicle show lower particle densities (Table I). E-faces of all structures

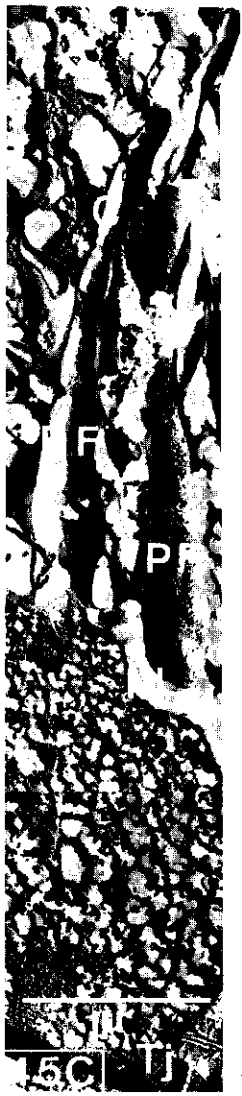

FIG. 45C.

studied are virtually devoid of particles (Table I and clearly demonstrated by Fig. 45C). A vesiculated ciliary tip (Fig. 49) also seems to be devoid of particles. The ratio of the particle density on the olfactory P-face as compared to its density on the respiratory P-face is about 19. This value, based on data presented in the Tables I and XIII, clearly indicates the difference between the two cilium types with respect to particle densities.

Figure 51 shows fracture faces of the unmyelinated olfactory axon bundles which are embedded in Schwann sheaths. The axonal fracture faces also contain particles. Particle counts here gave 2,800 $\pm$ 1,700 particles per μm^2 (aver-

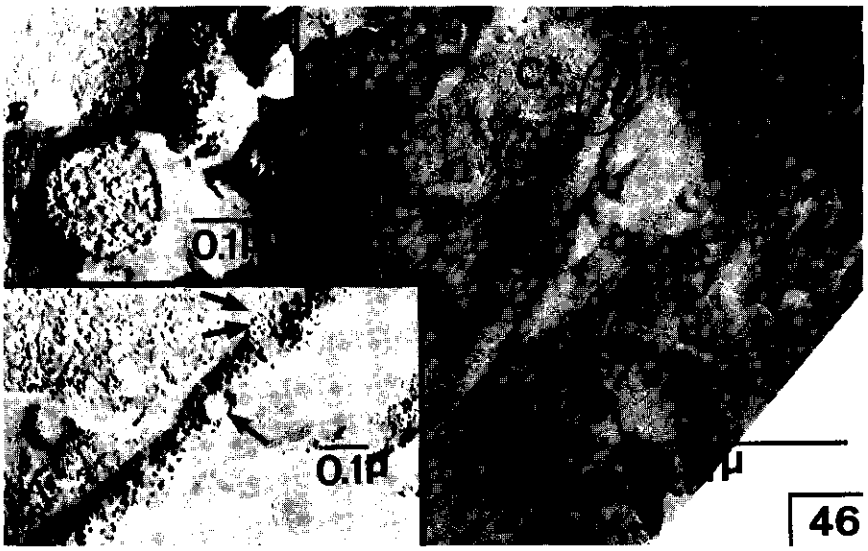

FIG. 46. Nerve ending with olfactory cilia (calf, cribriform plate). The insets depict the encircled parts of the main photograph. Cilia (C), including their tapering region (Ct), are fractured. The upper inset shows a cilium fractured perpendicular to the region where tapering starts; both diameters can be seen in this cross-section. The lower inset shows very distinctly the presence of a large number of particles.

It is also shown that some regions are devoid of particles (arrow). Another area seems to secrete something into the mucus (two arrows). Nl: ciliary necklace.

age of countings in four areas and based on only two photographs). Comparing Figs. 45 and 36 with 51 shows that the particle dimensions in the axonal membrane have a more heterogeneous appearance than those in the nerve ending ciliary membrane. The axons are separated from each other by a small layer of Schwann cell material, although their membranes may in some instances also lie close together. In spite of this, no evidence was obtained for the existence of specific junction or pore formations between axons. The fracture faces of the surrounding Schwann cells (Fig. 51, arrow) also appear to contain particles.

2.3.2. *Electron spin resonance studies on sheep olfactory and respiratory nasal mucosa*

2.3.2.1. Order parameters

12- and 16-doxylstearic acid spin labels were incorporated in sheep olfactory and respiratory mucosal samples. It was hoped that these reporter probes would provide information about the molecular environment of the odour receptor area. Since there is no methodology for this type of work, various procedures were tried during the evolution of the experiments.

FIG. 47. Freeze-etch replica of respiratory epithelium (calf, ethmoturbinal). The insets represent encircled areas of the main photograph. Beyond the ciliary necklaces (Nl) ciliary P-fracture faces contain hardly any particles. Microvillar (Mv) P-faces, on the other hand, do contain particles. No axonemal structures within the cilia are distinguishable.

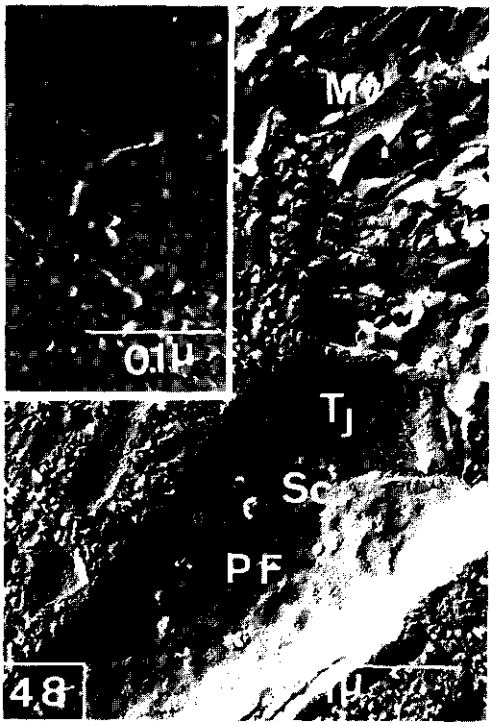

FIG. 48. Freeze-etch replica of a supporting cell (calf). Supporting cell (Sc) microvilli (Mv) contain high particle densities on their P-faces. The cell body density seems to be somewhat lower. Typical tight junction (Tj) ridges of the zonula occludens are clearly present here. The arrow indicates a region where two other cells joined this cell. The inset shows that the tight junction ridges consist of large particles, rather than being continuous. The surface of the cells possesses round patches, suggesting the presence of pinocytotic vesicles or other surface irregularities.

A summary of differences in hyperfine splittings is presented in Table II. This Table presents values for S, which is an order parameter (SEELIG, 1970; SEELIG and HASSELBACH, 1971). When S approaches 0, the probe environment is very isotropic (mobile), while when S approaches 1, this environment is anisotropic (rigid). S is expressed in terms of spectral parameters arising out of the anisotropic averaging of the nitroxide's principal axes:

$$S = \frac{T_{//} - T_{\perp}}{T_{zz} - T_{xx}} \quad 0 < S < 1 \quad T_{zz} - T_{xx} = 26.7 \quad G \text{ (SEELIG, 1970)} \qquad (1)$$

T is expressed in Gauss (G); T_{zz} and T_{xx} are obtained from the nitroxide parameter and $2T_{//}$ and $2T_{\perp}$ correspond to the separation of the two outer hyperfine extrema and the two inner hyperfine lines in the recorded first derivative spectra respectively.

TABLE I. Freeze-etch observations on surface structures of bovine olfactory and respiratory nasal epithelia.

Structure	Particles/$\mu m^2 \times 10^{-3}$		K_p[1]	Particle diameter nm	Other observations
	P-face	E-face			
a. Olfactory nerve ending swelling	3.4	–	–	–	–
b. Olfactory cilium, proximal segment	4.3 ± 2.6^{4}[2]	–	–	–	–
c. Olfactory cilium, distal segment	6.0 ± 2.0^{9}	–	–	–	–
d. Olfactory cilium, vesicle	3.1 ± 1.1^{5}	–	–	–	–
Olfactory cilium, necklace	–	–	–	12 ± 2^{4}	Strand number: 7 ± 2^{6} Strand spacing 84 ± 23^{3} nm
Average (*a-d*) on nerve ending[3]	5.7	0.5 ± 0.3^{5}	10.4	11 ± 2^{12}	–
Supporting cell microvilli	1.8 ± 1.0^{3}	0.2	9.0	9 ± 0^{2}	–
Respiratory cilium	0.3 ± 0.3^{7}	0.02	15.0	10 ± 2^{3}	–
Respiratory cilium, necklace	–	–	–	10 ± 2^{5}	Strand number: 5 ± 1^{9} Strand spacing: 173 ± 6^{3}
Respiratory microvilli	2.8 ± 2.1^{7}	Not clearly observed	–	10 ± 1^{4}	–

[1]) K_p: Particle density on P-face/particle density on E-face (SATIR, 1974).
[2]) Means are presented with their standard deviations; superscripts indicate the number of samples.
[3]) The density value on the P-faces is the average particle density over the total nerve ending surface. This surface is calculated in Table XIII.

FIG. 49. Two ciliary tapers, one of them with a tip, which is apparently devoid of particles. This tip contains a rim, which might be part of the cap structure seen in Fig. 39. The other cilium (arrow) contains a small vesicle with a few particles.

Most high field dips of the first derivative spectra caused by label immobilization did not appear clearly. Therefore we estimated these dips (essential for the calculation of $2T_{//}$) by visual extrapolation (See Fig. 52). This procedure diminishes accuracy and gives a lower $T_{//}$-value and thus lower S-values than would be the case if the hyperfine splittings were calculated properly. Since this error is made consistently we assume that the relative values of Table II may permit a tentative interpretation.

Table II shows order parameters, calculated on spectra recorded from label incorporated tissue slices, orientated perpendicular, respectively parallel to the direction of the magnetic field. Order parameters are calculated for the two label environments present, the nonaqueous (*a*) and the aqueous (*b*). The difference in *S* between these two environments is evident (see also Fig. 52). Table II furthermore presents *S*-values, calculated on tissue dispersions in Pasteur pipettes. Here *S*-values are intermediate to those for *a* and *b*. In these experiments we used both spin label types, 12- and 16-doxylstearic acid, while in the slide experiments only the label 12-doxylstearic acid has been used.

FIG. 50.(*A*) Olfactory mucus layer containing many ciliary vesicles (*B*) One vesicle, including a part of an adhering ciliary taper appears to be covered with many particles.

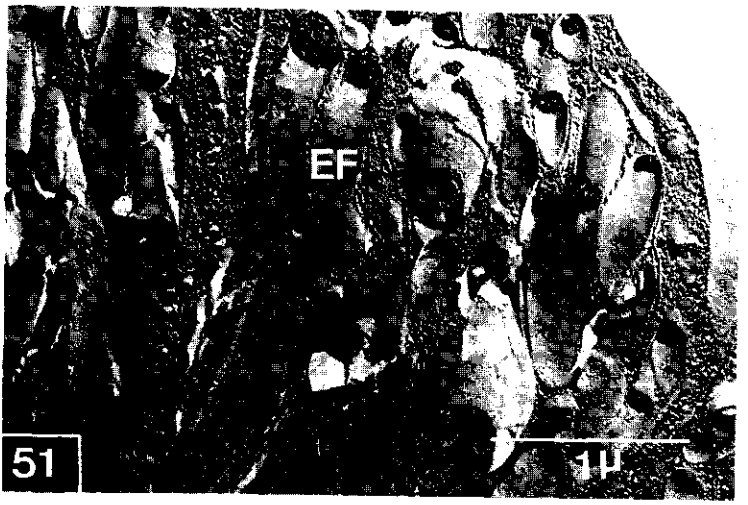

FIG. 51. Olfactory axon bundles at the base of the epithelium. P-faces contain slightly more particles than E-faces. The fracture face of the Schwann sheath (arrow) contains particles too.

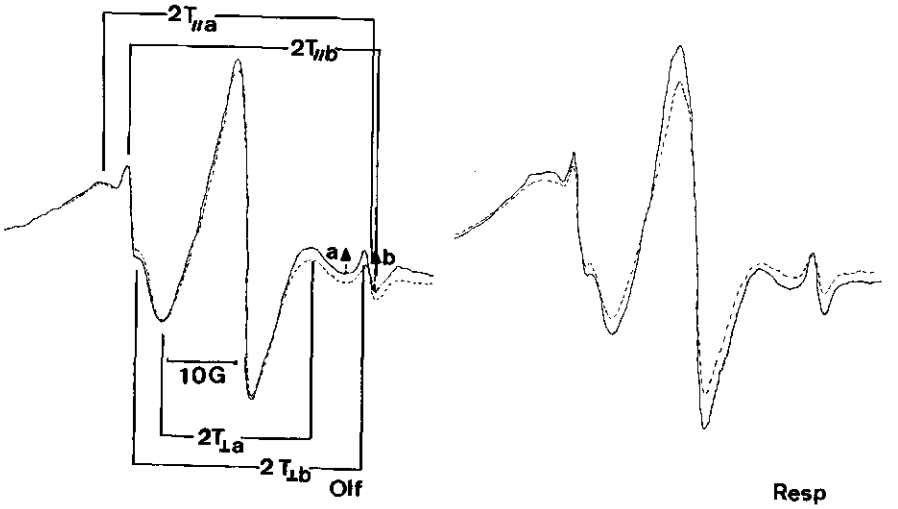

FIG. 52. ESR spectra of 12-doxylstearic acid (5.10^{-4} M) labeled sheep olfactory (Olf) and respiratory (Resp) nasal mucosa. The incubation was carried out in a Krebs-C physiological salt solution for about 20 hours at 4°C. The solid lines represent spectra recorded perpendicular with respect to the magnetic field, while the dashed lines are the spectra recorded parallel to this field. Peak hights *a* and *b* represent the relative label incorporation in more hydrophobic, respectively more aqueous mucosal environments. The separation of the outer hyperfine extrema is $2T_{//}$ while the separation of the two inner hyperfine extrema is $2T_{\perp}$. Both extrema are presented for both label environments (*a* and *b*). Note that the *a*/*b* ratio is higher in the olfactory, than in the respiratory mucosa.

TABLE II. Order parameters (S) for sheep olfactory and respiratory nasal mucosa, without and with odorous stimulation.

Label	Slide experiments								Pasteur pipette experiments			
	12-doxylstearic acid								12-doxylstearic acid		16-doxylstearic acid	
Slide orientation in magnetic field	Perpendicular				Parallel							
Label environment as identified by peak type[1]	a		b		a		b					
Epithelium type[2] / Treatment	Olf	Resp	Olf	Resp	Olf	Resp	Olf	Resp	Olf	Resp	Olf	Resp
Krebs-C physiological solution	0.30 ± 0.03[3]	0.30 ± 0.01[2]	0.06 ± 0.003[4]	0.06[4] [1]	0.33 ± 0.03[8]	0.29 ± 0.02[2]	0.08 ± 0.01 [4]	0.06 ± 0.004[2]	0.14 ± 0.02[5]	0.06 ± 0.03[5]	0.10 ± 0.02[2]	0.10
Tris-HCl, pH = 7.6	–	[5] –	–	–	–	–	–	–	–	–	0.12	0.11
Krebs-C plus 10^{-5} M butyric acid	0.30	–	0.07	–	–	–	–	–	–	–	–	–
Krebs-C plus 10^{-3} M butyric acid	–	–	–	–	–	–	–	–	–	–	0.14	0.11
Krebs-C plus 10^{-2} M butyric acid	–	–	–	–	–	–	–	–	–	–	0.12	–
Tris-HCl plus 10^{-3} M butyric acid	–	–	–	–	–	–	–	–	–	–	0.11	0.10
Krebs-C plus droplet CCl_4 in	0.26	–	–	–	0.31 ± 0.01[2]	–	–	–	–	–	–	–

Krebs-C plus (+)-citronellol	0.28 ±0.02[4 6)]	–	0.05[2]	–	0.31 ±0.03[4]	–	0.06 ±0.004[2]	–	0.13 ±0.03[3 7)]	0.10[2]	0.12[8)]	0.12
Tris-HCl plus (+)-citronellol	–	–	–	–	–	–	–	–	–	–	0.11[8)]	0.11

[1]) *S*-values for the hydrophobic label environments are presented in column *a*, while *S*-values for more aqueous label environments are presented in column *b*.

[2]) Olf: olfactory mucosa; Resp: respiratory mucosa.

[3]) Means are presented with their standard deviations; superscripts indicate the number of samples.

[4]) Where no superscript is presented, the sample consisted of one observation only.

[5]) – : No observations.

[6]) (+)-Citronellol added by means of CO_2.

[7]) (+)-Citronellol added in a 1/50 (v/v) ratio.

[8]) (+)-Citronellol added in a 1/150 (v/v) ratio.

The S-value of the aqueous environment, surrounding the olfactory mucosa was 0.06 (one observation). All order parameters are somewhat lower, then they are in reality. This is due to difficulties with the determination of the high field dips in the outer extrema ($2T_{//}$).

Although especially on the respiratory side, not enough data are presented to provide definite answers, Table II does indicate a slightly greater anisotropicity for probe environments in the olfactory mucosa than in the respiratory mucosa (see also Fig. 52).

In the slide experiments, odorants applied under very unphysiological conditions (see MATERIALS AND METHODS) alter the probe environments so that these become slightly more isotropic. These preliminary results certainly need confirmation. A distinct pattern for the effects of odorants on the order parameters of the dispersed samples cannot be seen in Table II. A specific behaviour towards odorous compounds for either of the two epithelium types under investigation could not be found. This is in agreement with the results of other authors (DODD, 1974; BANNISTER et al., 1975). The more anisotropic behaviour of the olfactory mucosa as compared to the respiratory mucosa means that the olfactory mucosa provides a more anisotropic environment for the nitroxide spin label. Suspensions surrounding the mucosal samples during label incubation are very isotropic (see the remark at the bottom of Table II).

The orientation of the tissues slices within the magnetic field did not seem to influence the spectra very much. Likewise it appears that the *S*-values for both label environments (*a* and *b*) do not differ for both tissue types. Furthermore, no differences could be detected between the environments of the two label types used in the dispersion experiments (Table II).

2.3.2.2. Label incorporation ratios

Both mucosa types (Fig. 52) consist of an aqueous and a hydrophobic environment for the stearic acid spin probe. In the first environment the label tumbles relatively more freely than in the latter. Relative values for these tumbling ratios can be calculated (HUBBELL and MCCONNELL, 1968) and compared. According to HUBBELL and MCCONNELL (1968) the sharp signal $-b-$ is due to an equilibrium of the label in the solution surrounding the membrane fraction with the membrane incorporated label, which gives peak *a*. This equilibrium could also exist between hydrophilic membrane fractions (surface proteins, polysaccharides e.g.) or the surrounding mucus and hydrophobic membrane moieties (phospholipids, hydrophobic proteins). The present results should be interpreted with care, since actual ratios are better described by peak surfaces than by peak heights. However, these surfaces are difficult to calculate because they overlap (HOLMES, 1973).

Fig. 52 shows spectra of the C12-label in olfactory and respiratory mucosa and shows that relatively more label is incorporated in the aqueous moiety of the respiratory mucosa than in that moiety of the olfactory mucosa. This behaviour is very consistent (Table III) and seems to be independent of odorous stimulation. The differences of Table III are more explicit and consistent than those of Table II. The ratio (Q) of the relative incorporation in both mucosa types is higher for the olfactory mucosa than for the respiratory mucosa. Q has been calculated as follows:

$$Q = \frac{a_o/b_o}{a_r/b_r} \tag{2}$$

a_o = height of the high field peak, caused by label incorporation in hydrophobic environments (probably membranous) of restricted label mobility, within the olfactory mucosa;
a_r = the same, but for respiratory mucosa;
b_o = height of the high field peak, caused by label incorporation in more aqueous environments – in which the label can tumble more freely – within the olfactory mucosa;
b_r = the same, bur for respiratory mucosa.

For odour stimulated olfactory mucosa a similar parameter (Q_o) has been used:

$$Q_o = \frac{a_o/b_o}{a_o'/b_o'} \tag{3}$$

Q_o = incorporation ratio for unstimulated versus odour stimulated olfactory mucosa;
a_o and b_o are described above;
a_o' and b_o' are the same, but for odour stimulated olfactory mucosa.

Since we do not have data on odour-stimulated respiratory mucosa in these slide experiments, this ratio could not be calculated for this type of mucosa.

A parameter, τ_c, the rotational correlation time inversely related to the tumbling rate of the nitroxide molecule, can be calculated for both mucosal types suspended in Pasteur pipettes, with and without odorous stimulation. A low correlation time corresponds to a fast tumbling rate. Correlation times may vary between 10^{-10} and 10^{-7} seconds respectively (SNIPES and KEITH, 1970; review by HOLMES, 1973). In order to calculate these correlation times we used the formula employed by SNIPES and KEITH (1970):

$$\tau_c = 6.5 \times 10^{-10} \times W_0 \times \{(h_0/h_{-1})^{1/2} - (h_0/h_{+1})^{1/2}\} \tag{4}$$

W_0 = line width of the central line of the first derivative ESR spectrum in Gauss (G);
h_0 = peak height of the central line of the first derivative ESR spectrum;
h_{-1} and h_{+1} = peak heights of the high and low field lines respectively;
τ_c is expressed in seconds.

The ratio of added label per quantity wet tissue was kept constant for both epithelium types: 5.10^{-4} M label and 100 mg wet tissue/ml incubation medium. Due to the aqueous environment, spin labels tumble more freely and consequently the spectra are narrower and less well resolved. Therefore separate areas of label incorporation cannot be distinguished any more. The values of these correlation times are probably dominated by the same mucosal fractions,

TABLE III. Relative intensities of the high field spectral lines of tissue, incorporated spin label and correlation times of label in tissue suspensions for both sheep olfactory and respiratory mucosa, without and with odorous stimulation.

Label	Parameter	a/b[1]		Q[2]	Q_O[3]	
	Epithelium type / Treatment	Olfactory mucosa	Respiratory mucosa			
12-doxyl-stearic acid	Krebs-C physiological solution	0.68 ± 0.11^{9}[4]	0.28 ± 0.02^{2}	2.4	–	
	Krebs-C plus 10^{-5} M butyric acid	0.37[5]	–	–	1.8	
	Krebs-C plus droplet CCl_4 in loading tube	0.62	–	–	1.1	
	Krebs-C plus (+)-citronellol[6]	1.98 ± 0.31^{4}	–	–	0.34	
	Parameter	Correlation times $\tau_c \times 10^{-10}$ (secs)		P[7]	P_O[8]	P_R[9]
	Epithelium type / Treatment	Olfactory mucosa	Respiratory mucosa			
	Krebs-C physiological solution	7.0 ± 2.0^{5}	1.8 ± 0.1^{4}	3.9	–	–
	Krebs-C plus (+)-citronellol[10]	13.2 ± 1.3^{3}	7.7 ± 0.7^{2}	1.7	0.53	0.23
16-doxyl-stearic acid	Krebs-C physiological solution	2.6^{2}	1.8	1.4	–	–
	Krebs-C plus (+)-citronellol[11]	26.0	4.4	5.9	0.10	0.41
	Krebs-C plus 10^{-3} M butyric acid	1.7	0.8	2.1	1.5	2.2
	Krebs-C plus 10^{-2} M butyric acid	2.5	–	–	1.0	–
	Tris-HCl, pH = 7.6	2.4	1.4	1.7	–	–
	Tris-HCl plus (+)-citronellol	3.7	2.5	1.5	0.65	0.56
	Tris-HCl plus 10^{-3} M butyric acid	1.8	1.1	1.6	1.3	1.3

[1]) a/b: Ratio, which represents the relative label incorporation in more hydrophobic (*a*) and more aqueous (*b*) mucosal environments. All values are calculated for a perpendicular sample orientation with regard to the magnetic field.

[2]) Q: Ratio representing the *a*/*b* ratio for olfactory mucosa, as compared to the ratio for respiratory mucosa (see page 73).

[3]) Q_O: A ratio representing the a/b ratio for unstimulated olfactory mucosa as compared to the ratio for odour stimulated olfactory mucosa.

[4]) Means are presented with their standard deviations; superscripts indicate the number of samples.

[5]) Where no superscript is presented, the sample consisted of one observation only.

[6]) (+)-Citronellol added by means of CO_2.

[7]) P: *A ratio representing the τ_c-value for olfactory mucosa, versus the τ_c-value for respiratory mucosa* (see page 75).

[8]) P_O: A ratio representing the τ_c-value for unstimulated olfactory mucosa, versus the τ_c-value for odour stimulated olfactory mucosa.

[9]) P_R: A ratio representing the τ_c-value for unstimulated respiratory mucosa, versus the τ_c-value for odour stimulated respiratory mucosa.

All these ratios are calculated for the most obvious combinations; for example 16-doxylstearic acid incubated mucosa in Tris-HCl without and with butyric acid stimulation.

[10]) (+)-Citronellol added in a 1/50 (v/v) ratio.

[11]) (+)-Citronellol added in a 1/150 (v/v) ratio.

which dominate the spectra in the slide experiments. Therefore we devised the following ratio:

$$P = \tau_{c_o}/\tau_{c_r} \tag{5}$$

in which τ_{c_o} is the correlation time for unstimulated olfactory mucosa and τ_{c_r} the same for respiratory mucosa. This P factor is probably affected by the same mucosal moieties as factor Q of formula (2). This means that when the olfactory mucosa contains more hydrophobic than aqueous label environments as compared to the respiratory mucosa, both, Q and P ratios have a value which is larger than one. Only the relative values of these ratios with respect to one can be compared and not their absolute values.

Similar ratios may be obtained for unstimulated versus odour-stimulated olfactory (P_O), or respiratory (P_R) mucosa:

$$P_O = \tau_{c_o}/\tau_{c_o}' \tag{6}$$

$$P_R = \tau_{c_r}/\tau_{c_r}' \tag{7}$$

τ_{c_o}' = correlation time in odour-stimulated olfactory mucosa;

τ_{c_r}' = correlation time in odour-stimulated respiratory mucosa.

Table III shows that both Q and P have positive values, whether the mucosae are odour-stimulated or not. The τ_c-values support conclusions based on calculations of the order parameter S (Table II), thus indicating that the label environment in the olfactory mucosa is more anisotropic than in the respiratory mucosa. The slide experiments suggest that this effect might be caused by the presence of a more hydrophobic mucosal fraction within the olfactory mucosa than in the respiratory mucosa. The mucosal area attached to the glass slide probably does not play a major role in evoking these differences. In both mucosal types the lamina propria consists mainly of collagen. Also, the scraped samples in the Pasteur pipette experiments should contain much less collagen, than the tissue slices and they still have similar relative values with respect to one as the Q-values in the slide experiments.

That areas in between both surfaces did not contribute much to the spectra, was shown by scraping label incorporated respiratory epithelium, in which case most of the signal disappeared.

Q_O, P_O and P_R ratios show that the equilibrium of label partition between hydrophobic and hydrophilic mucosal moieties, shifts to the hydrophobic side when hydrophobic odorous compounds are used ((+)-citronellol; Fig. 53) and to the hydrophilic side, when a hydrophilic odorant (butyric acid: Fig. 54; Table III) is used. This was found for both labels (12- and 16-doxylstearic acid) and both mucosa types (olfactory and respiratory) used (Table III). It cannot be excluded, however, that the effects found are simply due to the fact that the odorants acted as solvents for the spin labels, since the odour concentrations used are much higher than would be the case under physiological conditions. On the other hand such a solvent mechanism (which occurs here at an

exaggerated scale) could also be involved in the actual perception mechanism.

The effect of odorous stimulation could be partially reversed by soaking butyric acid (10^{-1} M)-stimulated olfactory mucosa for two hours in Krebs-C. Stimulation was carried out by dipping the mucosal sample for a short time (about one second) in the odorous solution. The reversing of the *a*/*b* ratio is shown in Fig. 54. The odour concentrations applied were extremely high, but since the tissue sample was only exposed to this concentration for such a short moment the results may nevertheless be valid. The tissue sample used in this experiment was about four days old (it was kept at 4 °C). Storage does not necessarily interfere with or obstruct physiological processes of the olfactory

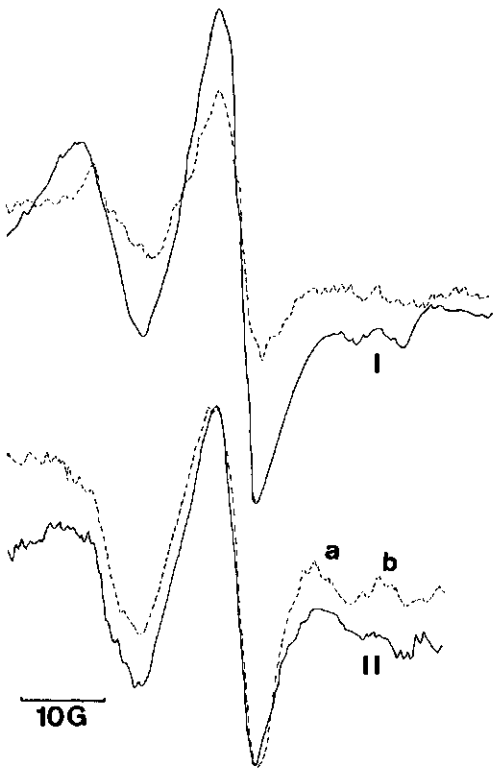

FIG. 53. ESR spectra representing the influence of the odorous compound (+)-citronellol on the partition of 12-doxylstearic acid spin label between non-aqueous (*a*) and aqueous (*b*) environments within sheep olfactory tissue. The solid lines represent spectra recorded perpendicular with regard to the magnetic field, while the dashed lines are the spectra recorded parallel to this field. Spectra of the non-stimulated olfactory mucosa (I) are compared with spectra of the odour-stimulated olfactory mucosa (II). The mucosal sample was label incubated for 20 hours at 4 °C in Krebs-C. After recording of the unstimulated spectrum, odorant was applied as a vapour by means of carbon dioxide. Note the shift of spin label towards the hydrophobic environment after odour stimulation, by the relative increase of peak *a*.

epithelium. This is indicated by the observation that concentration dependent electro-olfactogram (EOG) experiments can be conducted on frogs for four to five days (P. DUYVESTEYN, Pers. Comm.). ASH et al. (1966) noted that rabbit

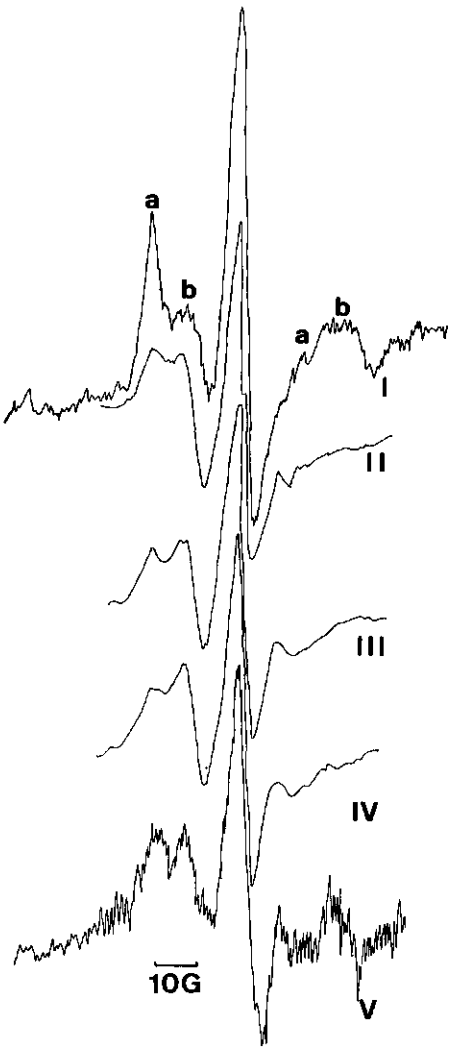

FIG. 54. ESR spectra of the influence of the water soluble odorous compound 1-butyric acid upon sheep olfactory mucosa. The mucosal sample was four days old. The spin label used was 12-doxylstearic acid (10^{-3} M). Incubation occurred in the presence of 5% bovine serum albumine (Fraction V) at 4°C and lasted 20 hours. The incubation medium was Krebs-C physiological solution.
The final 1-butyric acid concentration in the solution surrounding the tissue sample was 10^{-1} M which is very high. The spectra, however, were recorded in the loading tube, containing air (Fig. 44). The sample was exposed to odorant by dipping it in the odorous solution. In I-IV it was left in the loading tube between recordings. The partition of the label between non-aqueous and aqueous label environments is represented by the peak heights of *a*, respectively *b*.
I. Spectrum of unstimulated olfactory mucosa;
II. Spectrum recorded two minutes after exposing the sample to the odorous solution;
III. Spectrum recorded five minutes after exposure;
IV. Spectrum recorded ten minutes after exposure;
V. Spectrum recorded two hours after exposure to the odorous solution. Here the sample was soaked in Krebs-C during this period, which also resulted in label loss, giving a poorer resolution of the spectrum.
Note the gradual peak reversal from I to IV; it takes some time for the label to shift to the aqueous environment. The effect is partially reversed by the two hours soaking procedure (V). It should be noted that butyric acid changed the pH of the physiological solution markedly (from about 7 to 4); such an effect, however, might also be involved in the actual stimulation mechanism. Comparing this figure with Fig. 53 learns that the effect of the water soluble odorous compound 1-butyric acid, is the opposite of that of the water insoluble odorant (+)-citronellol.

bipolar olfactory cells remained intact for at least 14 days at temperatures of 0–4 °C.

2.3.3. *ESR studies on odorant interacted model membranes*

Pilot studies, using phospholipid multibilayers (LIBERTINI et al., 1969; SMITH, 1971), did not show any shift in the order parameters h_{-1}/h_0 or h_{+1}/h_0 (SMITH, 1971; ELETR et al., 1973) under the influence of added odorants, neither in dry nor in wet multibilayers. The used phospholipids were phosphatidylcholine (Lipid Products, Redhill, Surrey) and a mixture of bovine brain phospholipids prepared according to KATES (1972). The odorants were musk ambrette, phenyl acetic acid and vanillin (International Flavors and Fragances, Naarden). 16-Doxyl stearic acid was the spin probe. Probe/phospholipid ratios were 1/200 and odorant/phospholipid ratios were between $1/10^4$ and $1/10^{-2}$. These ratios were based on molecular weights (Mol/Mol), presuming an average phospholipid molecular weight of 750. Antioxidant (0.004% BHT = butyrated hydroxy-toluene) was added in all experiments. The findings that odorous compounds did not alter label environments within model membranes and that such compounds did not differentiate between olfactory and respiratory mucosal samples with respect to label emvironments for spin probes in these mucosae show that it is diffecult to find specific effects of such odorous compounds, using the ESR technique with stearic acid spin labels. Other labels, however, might be more profitable.

Recently BANNISTER et al. (1975) using odorous spin labels, have confirmed our conclusion: they also could not differentiate between odour treatments of olfactory and respiratory mucosa.

2.4. DISCUSSION

2.4.1. *Junctional complexes as seen by the freeze-etch technique*

The existence of typical ridges, which form tight junction complexes have been extensively described and reviewed by several authors (STAEHELIN et al., 1969; STAEHELIN, 1974; CLAUDE and GOODENOUGH, 1973; WADE and KARNOVSKY, 1974; ORCI and PERRELET, 1975). They have also been found in mouse respiratory (SLEYTR et al., 1972) and mouse and frog olfactory mucosa (KERJASCHKI et al., 1972; STOCKINGER et al., 1974; ALTNER and ALTNER, 1974a, b; KERJASCHKI and HÖRANDNER, 1976). Recently we also observed such ridges in rat olfactory mucosa. Frequently these tight junctions are found in combination with gap junctions (ORCI and PERRELET, 1975). In the bovine olfactory epithelium this combination could not be found sofar, though in both mouse (KERJASCHKI and HÖRANDNER, 1976) and in rat, according to our own observations, such a joint occurrence has been found. CLAUDE and GOODENOUGH (1973) have shown that there might be a relation between the number of strands and epithelium leakiness. Following their system the olfactory epithelium could belong to an epithelium type depicting intermediary leakiness (ALTNER

and ALTNER, 1974b) or, alternatively, the junctional belts could be very tight (KERJASCHKI and HÖRANDNER, 1976). The latter authors argue in their critical evaluation of the work of ALTNER and ALTNER (1974b) that conclusions concerning leakiness by ALTNER and ALTNER are based on insufficient observations. The number of strands, six to eight, which has been found in the tight junctions of the olfactory epithelium of the mouse by KERJASCHKI and HÖRANDNER (1976) agrees with the number of strands we have found both in bovine and in rat (unpublished observations). Therefore, according to CLAUDE and GOODENOUGH (1973), the junctions pertaining to the zonula occludens of the olfactory epithelium could be classified as 'very tight' (KERJASCHKI and HÖRANDNER, 1976). However, recently MARTINÈZ-PALOMO and ERLIJ (1975) and MØLLGÅRD et al. (1976) provided evidence against a direct relationship between the number of strands and the leakiness of such junctions. Conclusions concerning such relationships should be considered with great care and should always be supported by electrophysiological evidence.

2.4.2. *Axons*

Unmyelinated axons, as present in the peripheral olfactory system, are rare in vertebrates, although they do occur in some other nervous tissues such as in human bladder (ORCI and PERRELET, 1975). These unmyelinated axons allow direct observation of the axonal membrane, while in myelinated axons generally the membranous fracture face of the surrounding Schwann cells is seen. The fracture faces of both cell types contain a heterogeneous particle population, with an appearance which is rather similar in fracture faces of the axons and the Schwann cell axonal sheaths. Freeze-etch particles in several myelin sheath types have recently been described extensively by PINTO DA SILVA and MILLER (1975), thus solving a long standing dispute about the presence of particles in these sheaths. The particle heterogeneity probably reflects the variety of processes occurring on and in the axonal membranes, such as involvement in action potential generation and conduction (Na^+- and K^+-ion channels). Most evident is that the particle distribution at this level is very different from that at the ciliary level. Similarly KERJASCHKI and HÖRANDNER (1976) showed that the nerve ending membrane contains a much higher particle density than the membranes of the dendrite fracture faces deeper in the epithelium. Once more we can confirm their observation in mice by our observations in rat. Both findings reflect different functions at different levels of the peripheral olfactory nerve.

Specialized junctional structures could not be detected at the axonal level. Our recent work in the rat confirms the findings in the bovine system mentioned earlier. Gap junctions at olfactory dendrites have not been found (ALTNER and ALTNER, 1974b; KERJASCHKI and HÖRANDNER, 1976). The latter authors did find gap junctions between supporting cells, suggesting electrical contact between these cells. Sensory cells, however, are considered as electrically insulated from adjacent cells, as no gap junctions can be found. Our observations at the axonal level support this hypothesis.

2.4.3. *Microvilli*

Supporting cells in the olfactory epithelium and respiratory columnar cells both possess microvilli. The latter cell type thus contains microvilli as well as cilia. The microvilli from these two cells contain intramembranous particles as do many other types of microvilli (STAEHELIN et al., 1969; SLEYTR et al., 1972; ORCI and PERRELET, 1975). HÖRANDNER et al. (1974) indicated the presence of rod shaped particles on the apical surfaces of the supporting cells. We observed a similar particle type in microvillar and apical membrane fracture faces of supporting cells in rat olfactory epithelium, though in the bovine these particles appear to be globular instead of rod shaped. In rat, microvilli of the respiratory epithelium also appear to contain a globular particle type. HÖRANDNER et al. (1974) only found rod shaped particles in the apical surface of the supporting cells but not on microvillous intramembranous fracture faces. In the latter structures they only found globular structures. The difference in particle shape could reflect a functional difference between the plasma membranes of nerve cell, supporting cell and respiratory cell. The rod shaped particles could represent a metabolic condition as well as a species linked phenomenon. Such rod shaped particles have also been found in microvillous cells in the toad urinary bladder which are rich in mitochondria (WADE, 1976). WADE ascribes this particle shape to a possible effect of aldosterone stimulation.

2.4.4. *Ciliary necklaces*

Necklace like structures have been found in basal regions of all types of cilia (GILULA and SATIR, 1972; BERGSTROM et al., 1973), for instance in mouse nasal respiratory (SLEYTR et al., 1972; KERJASCHKI and HÖRANDNER, 1976) and olfactory cilia (KERJASCHKI et al., 1972; STOCKINGER et al., 1974; KERJASCHKI and HÖRANDNER, 1976). Even retinal rods contain analogous structures (RÖHLICH, 1975). The present work shows that bovine olfactory and nasal respiratory cilia also exhibit these necklace structures. Strand numbers and spacing may differ for both types of cilia (Table I); in rat, however, only strand numbers differ. The structure of the ciliary necklaces is described in detail, as observed in SEM and TEM studies, in Chapter I.

2.4.5. *Ciliary fracture faces above the necklace*

Motile cilia, in general, contain only a few particles within the fracture faces belonging to the membranes of these cilia (FLOWER, 1971; GILULA and SATIR, 1972; BERGSTROM et al., 1973; ORCI and PERRELET, 1965). Mouse nasal respiratory cilia, for instance, have been found to contain a low particle density within their intramembranous fracture faces (SLEYTR et al., 1972; KERJASCHKI and HÖRANDNER, 1976). The same seems to be the case for bovine (MENCO et al., 1976 and the present study) and rat respiratory cilia (unpublished). It is therefore concluded, that the feature of particle densities, which are much higher in the olfactory membranes than in respiratory cilia (a factor 19 difference), cannot be considered as characteristic for motility of cilia. Independently, KERJASCHKI and HÖRANDNER (1976) observed similarly a density dif-

ference in mouse nasal epithelia. Our preliminary studies show that the situation in rat appears to be identical. It seems likely that most mammalian species contain olfactory cilia with high particle densities in comparison with respiratory cilia.

Some earlier freeze-etch studies of olfactory epithelium have not revealed the existence of such particles (KERJASCHKI et al., 1972; STOCKINGER et al., 1974; ALTNER and ALTNER, 1974a, b).

Since olfactory cilia form part of the olfactory sensory system (see Chapter 1), it seems reasonable to assume that these particles have a function in the sensory process. However, that olfactory cilia may play a major role in the odour reception process has been challenged by TUCKER (1967), although recently evidence is accumulating that the role which these cilia play might be most important. BRONSHTEIN and MINOR (1977) showed that upon removal of ciliary membranes with Triton X-100 the electro-olfactogram (EOG) also disappears, and that this response reappears with the reappearance of the cilia. Furthermore, Dr. C. MASSON (Pers Comm.), using freeze-fracture methods in the frog, provided evidence that the density of the ciliary intramembranous particle population may be related to the EOG and that both are altered by changes in the physiological condition of the frog. Discrepancies in correlation between ciliary lengths and EOG-response as found for the newt transferred from water to land (SHIBUYA and TAKAGI, 1963) may be explained by a change in particle concentrations. These particles provide evidence for the existence of receptor proteins in the olfactory nerve ending plasma membranes. Such evidence is supported by recent electrophysiological studies, using chemical modification techniques on frog electro-olfactograms (EOG's) (GETCHELL and GESTELAND, 1972; MENEVSE et al., 1977). Furthermore, recent work by HOLLEY et al. (1976), using single unit responses in frog, does indicate the presence of a ligand-binding like receptor mechanism. Their data indicate the presence of a common receptor for several odorous compounds used. P. DUYVESTEYN (Pers. Comm.) assumes a similar mechanism on the basis of electro-olfactograms. The possibility of such mechanisms being involved in chemoreception, has been considered previously with reference to taste (MENCO et al., 1974b; JAKINOVICH, 1976; JAKINOVICH and GOLDSTEIN, 1976; JAKINOVICH and OAKLEY, 1976).

GENNINGS et al. (1976, 1977) provide some direct biochemical evidence for the presence of a possible olfactory receptor protein. These workers conducted binding studies on sex specific steroids in pig nasal tissues. In the olfactory mucosa they found a protein fraction, which appeared to be absent in the respiratory mucosa. This fraction showed a specific binding behaviour towards sex specific androstenones.

Particle densities in the P-faces of ox olfactory cilia appear to be four to six times higher than such densities in mouse (KERJASCHKI and HÖRANDNER, 1976; MENCO et al., 1976). Densities found by KERJASCHKI and HÖRANDNER were in the region of 840 particles/μm^2. Their estimation is based on a much larger sample than the one we used. Our current studies in the rat indicate a situation

rather similar to that in mouse. Particle densities might reflect species specific differences.

Countings on respiratory cilia and particle diameters performed by KERJASCHKI and HÖRANDNER show results similar to the ones in Table I. The low particle density in the ciliary vesicles might indicate that these vesicles are made after particle insertion. The expanding membrane surface causes a dilution of the particles. In rat we frequently observed vesicles, which are totally devoid of particles, though the adjacent cilium fragment contains many particles. Origin and function of these vesicles are disputed (OKANO, 1965; REESE, 1965; SEIFERT, 1970; NAESSEN, 1971; see also Chapter 1).

E-faces of both cilia and microvilli are practically devoid of particles (Table I) in both epithelium types. This is the case in most other membrane types (BRANTON, 1971).

2.4.6. *Results of freeze-etch and spin label experiments in relation to other receptor systems*

It is conceivable that proteinaceous particles in the olfactory cilia have a receptor function analogous to rhodopsin, the receptor protein in the visual system. HONG and HUBBELL (1972), CHEN and HUBBELL (1973), JAN and REVEL (1974), MASON et al. (1974) and OLIVE and RECOUVREUR (1974) conducted various types of experiments from which could be concluded that freeze-etch particles within the rod outer segment receptor membrane (CLARK and BRANTON, 1968; LEESON, 1970, 1971; ROZENKRANZ, 1971) contain rhodopsin. Rod outer segments are also of ciliary origin (Chapter 1). JAHNKE (1975) found that taste buds from the papillae foliatae of the rabbit contain in the taste pore microvilli which possess extremely high intramembranous particle densities and suggests that these particles are associated with the tastant receptor.

Similarly the cholinergic receptor of the electrical organ of *Torpedo marmomata* is probably associated with specific intramembranous particles (CARTAUD and BENEDETTI, 1973; CARTAUD, 1974; CHANGEUX et al., 1975). Very recently changes in particle densities in white adipose plasma membranes induced by lipogenic hormones were demonstrated by means of freeze-fracture techniques (CARPENTIER et al., 1976).

The kinocilium of the guinea pig vestibular organ hardly contains any particles above its necklace (JAHNKE, 1976). Stereocilia, both in guinea pig (JAHNKE, 1976) and in lizard (BAGGOR-SJÖBÄCK and FLOCK, 1977) do contain a high intra-membranous particle density, but in contrast to the kinocilium, they cannot be considered to be real cilia. Stereocilia do not contain the axonemal 9(2) + 2 structure or any of its derivatives. Since equilibrium receptors and hearing are considered to be a type of mechanoreception (VINNIKOV, 1974), a receptor protein is not necessarily involved in this system. This contrasts with chemo- and photosenses.

Electron spin resonance studies of excitable tissues have been conducted first by HUBBELL and MCCONNELL (1968). With this technique again, the visual system is the sensory system which has been investigated most extensively.

VERMA et al. (1973) and PONTUS and DELMELLE (1975a) provided evidence for a relation between bleaching of vertebrate visual pigments and changes in the environment of spin probes in rod outer segments; light appears to increase the fluidity of the disk membrane. MASON et al. (1974), using freeze-etch techniques, found that, upon illumination, rod outer segment particles were translocated from the internal hydrophilic disk area to hydrophobic disk regions. The relation between photobleaching and particle translocation is directly proportional. NICKEL and MENZEL (1976) applying the same methods to insect photoreceptors, could not detect such a relationship.

Rhodopsin incorporated within phosphatidylcholine bilayers markedly inhibits hydrocarbon motion as phosphatidylcholine spin labels indicated (HONG and HUBBELL, 1972). Using freeze-fracture techniques, these workers showed that this anisotropicity could be explained by the presence of incorporated rhodopsin. PONTUS and DELMELLE (1975b) employing lipid deletion methods from rod outer segments, came to similar conclusions. These studies on vision, though still controversial, indicate that the freeze-etch and the electron spin resonance technique allow some predictions on the presence of receptor proteins and the physiological function at the molecular level of this sensory organ.

The protozoan *Tetrahymena pyriformis* contains in some cases somatic cilia with high particle densities (SATTLER and STAEHELIN, 1974; SEKIYA et al., 1975). In addition to a propagation function, these cilia in a unicellular organism may also have sensory functions. NOZAWA et al. (1974), using stearic acid spin labels, found that the cilia in this organism were the most anisotropic organelles out of a variety of organelles investigated. Here too membrane anisotropicity could be caused by intramembranous particles. Alternatively, lipid compositions could be responsible.

In the olfactory system no specific correlates have been detected between spin probe motility and odorous stimulation (DODD, 1974; BANNISTER et al., 1975). Neither the present study, nor similar work by Dr. L. H. BANNISTER and collaborators at Guy's Hospital Medical School, London (Pers. Comm.) could provide such information. However, odorants did affect label environments, but the effects found were similar for both epithelium types (Table III). Odorants applied in unphysiologically high concentrations shifted label moieties to more hydrophobic (in the case of hydrophobic odorants), or more aqueous (when applying hydrophilic odorous compounds) mucosal environments in both tissue types.

It is interesting to note, however, that both tissues did seem to provide different environments for the stearic acid spin probes. These environments are more hydrophobic and anisotropic in the olfactory than in the respiratory nasal mucosa. These effects, as in the visual system and in *Tetrahymena* cilia, could be ascribed to an abundance of intramembranous particles within the ciliary membranes of the olfactory cells. Particles present in the microvilli of adjacent supporting cells may also be involved. Cilia of respiratory cells contain few particles in comparison to those of olfactory cells (Table I). Therefore,

these particles are presumably responsible for the anisotropic and hydrophobic environments provided for the spin label in the olfactory mucosa. Alternatively the lipid composition could be very different for the two epithelium types. Furthermore, various other structural aspects of the mucosa, in particular structures present in the mucus layer, could be responsible for the differences found. Conclusions concerning this matter can only be very tentative, since our data are very crude. Isolation of the structures involved is necessary in order to provide more definite answers. Anyhow, electron spin resonance information and freeze-etch data do not seem to contradict each other. In agreement with KERJASCHKI and HÖRANDNER (1976) we suppose that the nerve ending intramembranous particles play an important role in the receptive and/or transductive system.

3. QUANTITATIVE ANALYSES OF CILIATED AND MICROVILLI BEARING SURFACE STRUCTURES OF THE BOVINE OLFACTORY AND NASAL RESPIRATORY EPITHELIUM

3.1. Introduction

Several sensory systems, for example the visual system of vertebrates (Pirenne, 1962; Vinnikov, 1974), show morphological variations which parallel functional diversity. It is possible that olfactory receptors too show structural variations, which are important in odour quality recognition (Le Gros Clark, 1957; Mozell, 1971; Moulton, 1976), but apart from data on fishes (Bannister, 1965; Breipohl, 1973a; see also review by Hara, 1975) no proper evidence has been provided to support this hypothesis. However, there are some indications that the olfactory epithelium, at least in rabbit, contains a gradient of nerve ending densities (Allison and Warwick, 1949).

Current observation techniques, such as scanning, high-voltage transmission and freeze-etch electron microscopy, make a comprehensive survey of various parameters of the olfactory area possible.

In this chapter quantitative features of nerve endings will be analyzed in order to determine whether or not heterogeneous nerve ending type populations occur in mammals. Moreover, we wish to compare nerve ending densities in different olfactory areas. If differences do exist, they are probably difficult to assess by superficial observations only. Statistical treatments have to be applied in order to discover small differences. If different types of nerve endings are present, the question arises whether or not they show a uniform distribution over the olfactory area. Furthermore, ciliary and microvillar structures will be compared in respiratory and olfactory mucosae.

The possibility that certain areas of the olfactory epithelium are connected to corresponding areas within the olfactory bulb should not be excluded (Moulton, 1976), although this problem is beyond the scope of the present investigation.

Furthermore, intramembranous particles as seen by the freeze-etch technique (Chapter 2) allow a presentation of a possible receptor population.

3.2. Materials and methods

The quantitative observations are based on 61 light, 228 thin and thick section transmission electron, 235 scanning electron and 49 freeze-etch replica transmission electron microscopic micrographs. The preparation of the samples is described in Chapters 1 and 2. Micrographs were taken at different magnifications. Only the light microscope was properly calibrated. The electron micro-

scopes were assumed to be reliable in this respect. Most statistical evaluations are based on the SPSS (Statistical Package for the Social Sciences) programs of NIE et al. (1975). The freeze-etch micrographs are not included in the statistical evaluations of Tables IV–XII, but rather treated as a separate item.
The parameters included in the statistical analyses are:

1. Nerve ending density per cm^2 divided by 10^6;
2. Nerve ending diameter in μm;
3. Olfactory cilia; diameter of the proximal segments in μm;
4. Olfactory cilia; diameter of the distal segments (tapers) in μm;
5. The length of the proximal segments of the olfactory cilia in μm;
6. The maximum observed length of the distal segments (tapers) of the olfactory cilia in μm;
7. Ciliary vesicle; diameter in μm;
8. Supporting cell microvilli; diameter in μm;
9. Ciliary necklace; the number of strands;
10. The number of olfactory cilia per nerve ending;
11. The number of fibrogranular microtubuli particles per pool diameter in nerve ending cross-sections (Fig. 30);
12. The height of the olfactory epithelium in μm;
13. The height of the olfactory mucus layer containing nerve ending structures in μm;
14. The height of the respiratory mucus layer containing respiratory cilia and microvilli in μm;
15. The height of the respiratory epithelium in μm;
16. The diameter of the respiratory cilia in μm;
17. The length of the respiratory cilia in μm;
18. The diameter of the respiratory microvilli in μm.

These parameters are used throughout Tables VI–X. All measurements were done with the aid of a ruler, graded in millimeters, on photographic prints. To ascertain that most of the structure of interest in a particular photograph was included in the observation, sectioned structures, such as nerve endings, were measured so as to incorporate the whole diameter; therefore the largest diameters in the photographs were taken. Likewise, cilium lengths are maximum lengths observed. No corrections have been made for the plane of sectioning; scanning micrographs do not need such corrections anyway. The number of cilia per nerve ending was only counted in scanning micrographs, and in transmission micrographs of sections equal or thicker than the nerve ending diameter. Therefore, micrographs made with the aid of a high-voltage electron microscope were most suitable for such counts on transmission observations. This procedure ensures that the majority of the cilia are observed, as is the case for micrographs obtained with the scanning electron microscope.

Nerve ending densities were calculated with the following formulas:

1. *Transmission electron microscopy*: Density calculations are based on one dimensional observations, using:

$$(a \times M)/(10^4 \times X) \text{ nerve endings}/\mu m \quad (8)$$

which gives:

$$D = (a \times M)^2/X^2 \text{ nerve endings/cm}^2 \text{ epithelium} \quad (9)$$

a = number of nerve endings counted over a certain distance, X, on the photograph;
M = total magnification on photograph;
D = nerve ending density.

2. *Scanning electron microscopy and transmission electron microscopy on sections parallel to the epithelium surface*: Density calculations are based on two dimensional observations. When the sample was not tilted in the microscope the following formula was used:

$$D = (a \times M^2)/(X \times Y) \text{ nerve endings/cm}^2 \text{ epithelium}, \quad (10)$$

whereas when the sample was tilted over an angle of α° this formula was modified as follows:

$$D = (a \times M^2 \times \cos\alpha)/(X \times Y) \text{ nerve ending/cm}^2 \text{ epithelium} \quad (11)$$

X = width of the area on the photograph on which the density is calculated;
Y = height of this area;
α = tilting angle.

It is assumed that in this way a correction has been made for irregularities in the observed surface. No corrections have been made for tissue shrinking during the preparations, since the necessary measurements are very difficult to perform. Besides, shrinking supposedly does not affect the relative dimensions of the structures of interest.

3.3. Results

3.3.1. *Evaluation of measurements on some nasal structures*

Various anatomical parameters have been determined in tissue samples of different areas of the bovine nose. The areas which will be compared with each other include:

1. Different types of epithelium surface such as the olfactory and respiratory epithelium as well as the epithelium in between these tissues: the transitional epithelium (Table VIII).

2. Different areas within the olfactory epithelium, such as the nasal septum, the cribriform plate and the nasal turbinates will be compared (Table IX).

3. In addition comparisons will be made between the nasal epithelia of very young calves and adult animals (Table VII).

Student's t-test was applied to the results of the various comparisons. The degree of correlation between certain parameters indicates whether or not these parameters represent related structures. These relationships will be

presented in a separate table (Table X).

At the end of this chapter the quantitative information collected with section and scanning studies will be combined with information from freeze-etch studies in order to provide estimates for possible receptor populations (Tables XIII and XV).

3.3.2. *Some parameters not included in the comparative evaluations*

3.3.2.1. General cellular appearances of bovine respiratory and olfactory epithelia

Table IV presents some dimensions of cells and cell layers of the two epithelium types. Data are given on respiratory columnar cells, olfactory supporting and nervous cells, atypical brush cells and glandular structures occurring in both epithelium types. The observations on glandular structures are based on a limited number of observations only, and should therefore not be considered to be very accurate. The dimensional differences between the several hair types are obvious, especially for cilia as compared to microvilli and brush cell hairs. The brush cell hairs, however, are morphologically very different from microvilli (see Chapter 1). The figures referring to this cell type are based on observations of brush cells in both epithelium types including their transitional area. The diameter of olfactory nerve axons appears to be the same in freeze-etch and thin section studies. Counts in thin sections of five axons gave a mean microtubular subfiber number of 6 ± 1 subfibers per axon.

Apices of nervous and brush cells are considerably smaller in diameter than the apices of respiratory columnar and olfactory supporting cells.

3.3.2.2. Ciliary microtubule (axoneme) and membrane dimensions

Cilia of both epithelium types do not seem to differ much in their microtubular doublet dimensions (Table V). The diameter of the olfactory taper singlets is approximately identical to those of the other olfactory and respiratory singlet fibers. Their subfibers also contain the same number (13) of microtubular subunits as the central fibers of the $9(2) + 2$ configuration (Fig. 37, inset; KERJASCHKI and HÖRANDNER, 1976; KERJASCHKI, 1976).

The inner limiting membrane lamina is thicker than the outer one in olfactory cilia (as measured in Fig. 37, inset). These dimensions could not be measured in the respiratory epithelium.

3.3.3. *Effect of the observation method on some dimensions and frequencies of epithelium structures of bovine olfactory and respiratory mucosae*

Table VI gives the means, including their standard deviations, and the number of observations of all anatomical features, which have been measured in both epithelium types with the various microscopic methods.

It was found that all dimensions (except the diameter of the nerve endings) appear larger in the scanning electron microscope, than in transmission micrographs. This may be due to the fact that the samples prepared for the SEM

TABLE IV. Some densities and dimensions of structure within the bovine nasal respiratory and olfactory epithelium.

1. *Cellular dimensions* (μm)

	Respiratory columnar cell	Olfactory supporting cell	Olfactory receptor cell	Atypical brush cell
Nerve ending size (terminal swelling)	–	–	Diameter: 1.3 μm (from 326 measurements); height: 2.8 μm (maximum height observed)	–
Diameter of cellular apices	3.8 ± 0.8^{6} (light cell) 2.2 ± 0.8^{3} (dark cell)	2.6 ± 1.0^{8}	1.4 ± 0.4^{17} (dendrites)	1.4^{2}
Cell body, diameter	–	–	4.7 ± 0.6^{8}	–
Axon, diameter	–	–	Thin section: 0.15 ± 0.01^{7}; freeze-etch: 0.19 ± 0.10^{10}	–
Cilia and hairs[2]):	Cilia	Microvilli	Cilia, proximal parts	Hairs
Diameter:	0.10 ± 0.06^{131}	0.08 ± 0.04^{207}	0.20 ± 0.05^{324}	0.10 ± 0.03^{6}
Length:	6.4 ± 2.3^{52}		1.8 ± 0.7^{176}	2.4 ± 1.2^{7}

2. *Glandular densities and dimensions* (μm)

	Olfactory	Respiratory
Density:		
glands/cm^2 × 10^{-4}	2.1[3])	3.9 ± 2.8^{6}
Diameters glandular openings	34 ± 3^{2}	16 ± 9^{7}

[1]) Dimensions and densities are presented with their standard deviations. The superscripts indicate the number of observations on which counting was carried out.

[2]) For more information concerning cilia and microvilli, see Tables VI–X, XVI and XVII.

[3]) No superscript indicates just one observation. This convention will be maintained for following tables.

have a metal coating. The average difference between the various diameters is about 30 nm, or one-sided 15 nm, which is in the order of magnitude of the metal coating. With respect to the diameter of the nerve ending itself the thickness of the layer of metal added to that diameter because of sample coating is negligible. Consequently, pooling of data obtained with both methods may

TABLE V. Dimensions of microtubular and some membranous structures of bovine nasal respiratory and olfactory cilia (nm).

Structure	Olfactory	Respiratory
Outer diameter doublet	30.7 ± 4.6^{11} [1)]	33.4 ± 4.2^{8}
Inner diameter doublet subfiber	8.8 ± 0.7^{12}	8.7 ± 2.0^{7}
Outer diameter singlet	16.5 ± 3.5^{4}	25.8 ± 3.4^{4}
Inner diameter singlet	9.5 ± 1.5^{3}	12.2 ± 2.8^{3}
Outer diameter taper singlet	21.6 ± 5.2^{5}	not present
Inner diameter taper singlet	10.3 ± 2.0^{4}	not present
Length dynein arms	not present	15.9 ± 3.2^{8}
Taper membrane: Outer limiting lamina	1.5	–
Space between inner and outer limiting laminae	2.0	–
Inner limiting lamina	4.0	–
Total membrane diameter	7.5	–

[1]) Dimensions are presented with their standard deviations. The superscripts indicate the number of observations on which counting was carried out.

introduce a considerable source of error for almost all dimensions smaller than the nerve ending diameter. When correlation coefficients (BYRKIT, 1975), calculated according to Pearson (parametric) and Spearman (non-parametric), are compared (Table X) it is concluded that it is allowed to pool these results, since both testing methods gave approximately identical results. Therefore, the rest of this chapter will mainly consider the pooled results, although the separate items are also presented and will be considered where necessary. Although this pooling may introduce errors in the presentation, these errors are amply compensated by the improvement in the clarity of the presentation. Due to the lack of sufficient data we decided not to include the freeze-etch results in the tests. Some parameters, such as epithelium and mucus heights, can be determined better by light microscopy than with electron microscopical techniques.

3.3.4. *Olfactory versus respiratory cilia*

Another observation to be noticed from Table VI is that the diameter of the proximal part of the olfactory cilium is slightly larger than the diameter of the respiratory cilium. This feature has been observed with SEM, TEM as well as when using freeze-etch methods. Ciliary diameters determined on freeze-etch micrographs are intermediate to the values found with the other two techniques. Although being consistent, this difference in diameter between the two cilia types is not statistically significant within reasonable limits ($P \leqslant 0.05$). This

TABLE VI. Quantification of some anatomical features of bovine nasal respiratory and olfactory epithelia with four microscopic methods.

Features	Light (1)	TEM (2)	SEM (3)	Pooled (1, 2, 3)[1]	Freeze-etch
Nerve ending density/cm^2 $\times 10^{-6}$	4.7 ± 2.8^{46}[2]	8.6 ± 5.7^{95}	5.0 ± 3.8^{130}	6.2 ± 4.8^{271}	–
Nerve ending diameter[3]	1.6 ± 0.3^{42}	1.3 ± 0.4^{137}	1.2 ± 0.3^{147}	1.3 ± 0.4^{326}	–
Olfactory cilium, proximal segment, diameter	0.27	0.18 ± 0.04^{167}	0.23 ± 0.05^{156}	0.20 ± 0.05^{324}	0.22 ± 0.05^{4}
Olfactory cilium, distal segment, diameter	–	0.06 ± 0.02^{111}	0.11 ± 0.04^{96}	0.08 ± 0.04^{207}	0.06 ± 0.03^{7}
Olfactory cilium, proximal segment, length	1.5 ± 0.2^{2}	1.5 ± 0.6^{85}	1.9 ± 0.7^{89}	1.7 ± 0.7^{176}	1.7 ± 0.3^{3}
Olfactory cilium, distal segment, maximal length observed	–	28	27	28	4
Olfactory cilium, vesicle, diameter	–	0.5 ± 0.4^{37}	1.2 ± 0.3^{3}	0.6 ± 0.4^{40}	0.5 ± 0.1^{7}
Supporting cell microvillus, diameter	–	0.06 ± 0.04^{138}	0.10 ± 0.04^{115}	0.08 ± 0.04^{253}	0.11 ± 0.01^{2}
Number of ciliary necklace strands[4]	–	7.3 ± 0.8^{21}	6.5 ± 2.4^{4}	7.2 ± 1.2^{25}	7.0 ± 2.1^{6}
Olfactory cilia/nerve ending	–	12.8 ± 4.5^{58}	12.3 ± 2.8^{130}	12.5 ± 3.4^{188}	–
Granules microtubuli pool/nerve ending cross-section	–	25 ± 7^{11}	–	25 ± 7^{11}	–
Olfactory epithelium, height	102 ± 20^{16}	72 ± 28^{2}	–	99 ± 23^{18}	–
Olfactory mucus, height	6.1 ± 3.9^{38}	4.8 ± 2.3^{50}	3.4 ± 1.1^{22}	4.9 ± 3.0^{110}	6.4
Respiratory mucus, height	5.4 ± 1.8^{19}	5.7 ± 1.4^{25}	–	5.6 ± 1.6^{44}	–
Respiratory epithelium, height	68 ± 17^{16}	41	–	33 ± 18^{17}	–
Respiratory cilium, diameter	0.24	0.16 ± 0.04^{53}	0.22 ± 0.05^{77}	0.19 ± 0.06^{131}	0.18 ± 0.03^{7}
Respiratory cilium, length	7.0 ± 2.2^{16}	5.4 ± 2.3^{21}	7.2 ± 2.0^{15}	6.4 ± 2.3^{52}	–
Respiratory microvillus, diameter	–	0.07 ± 0.03^{19}	0.18 ± 0.08^{6}	0.10 ± 0.06^{25}	0.07 ± 0.01^{8}
Number of photographs observed	61	228	235	524	10
Percentage of total number of photographs	11	43	46	100	–

[1]) Values obtained by freeze-etch methods are not included in the pooled column.
[2]) Means are presented with their standard deviations; superscripts indicate the number of samples.
[3]) Dimensions are presented in micrometers (μm).
[4]) This line gives strand numbers for the olfactory cilia alone. The number of necklace strands in the respiratory cilia determined with transmission methods was 6.8 ± 1.0^{4} and with freeze-etch methods 5.3 ± 0.5^{9}. In the next tables the TEM values are pooled with those of olfactory cilia. Table VIII shows that there are no significant differences between the strand numbers in the two cilia types as observed with section techniques.

TABLE VII. Comparison of the means of some micro-anatomical measurements of nasal olfactory and respiratory epithelia in adult and juvenile bovines, employing three microscopic methods.

Features	Cow; 30% of the observed photographs				Calf; 70% of the observed photographs			
	Light	TEM	SEM	Pooled	Light	TEM	SEM	Pooled
Nerve ending density/ $cm^2 \times 10^{-6}$	3.5 ±0.9 [a 1)]	8.8 ±1.1 [a]	4.8 ±0.6 [a]	6.1 ±0.6 [a]	4.8 ±0.4 [a]	8.5 ±0.7 [a]	5.0 ±0.4 [a]	6.2 ±0.3 [a]
Nerve ending diameter[2])	1.48 ±0.10[a]	1.16 ±0.06 [b]	1.15 ±0.05 [a]	1.17 ±0.04 [b]	1.67 ±0.05[a]	1.40 ±0.04 [a]	1.15 ±0.03 [a]	1.34 ±0.03 [a]
Olfactory cilium, proximal segment, diameter	– [3)]	0.157±0.005[b]	0.215±0.007[a]	0.188±0.006[b]	–	0.182±0.004[a]	0.229±0.005[a]	0.204±0.003[a]
Olfactory cilium, distal segment, diameter	–	0.061±0.005[a]	0.097±0.007[b]	0.078±0.005[a]	–	0.061±0.003[a]	0.114±0.004[a]	0.085±0.003[a]
Olfactory cilium, proximal segment, length	–	1.14 ±0.06 [b]	1.43 ±0.09 [b]	1.29 ±0.06 [b]	–	1.69 ±0.09 [a]	2.15 ±0.09 [a]	1.92 ±0.06 [a]
Olfactory cilium, distal segment, maximal length observed	–	–	–	18	–	–	–	28
Olfactory cilium, vesicle, diameter	–	0.73 ±0.55 [a]	0.94 [a]	0.80 ±0.32 [a]	–	0.54 ±0.06 [a]	1.31 ±0.16 [a]	0.58 ±0.07 [a]
Supporting cell microvillus, diameter	–	0.047±0.004[b]	0.085±0.007[a]	0.064±0.005[b]	–	0.067±0.004[a]	0.098±0.004[a]	0.081±0.003[a]
Number of ciliary necklace strands	–	6.6 ±0.3 [b]	–	6.6 ±0.3 [a]	–	7.5 ±0.2 [a]	–	7.3 ±0.3 [a]
Olfactory cilia/nerve ending	–	12.0 ±0.6 [a]	12.8 ±0.4 [a]	12.6 ±0.3 [a]	–	13.0 ±0.8 [a]	12.1 ±0.3 [a]	12.4 ±0.3 [a]
Granules microtubuli pool/ nerve ending cross-section	–	–	–	–	–	–	–	–
Olfactory epithelium, height	98 ±2 [a]	92	–	97 ±2 [a]	103 ±6 [a]	52	–	100 ±7 [a]
Olfactory mucus, height	6.0 ±0.7[a]	5.1 ±0.5 [a]	3.4 ±0.7 [a]	5.1 ±0.4 [a]	6.1 ±0.7[a]	4.6 ±0.4 [a]	3.4 ±0.3 [a]	4.9 ±0.3 [a]
Respiratory mucus, height	9.3 ±0.1[a]	5.8 ±0.5 [a]	–	6.3 ±0.5 [a]	5.0 ±0.3[b]	5.6 ±0.3 [a]	–	5.3 ±0.2 [b]
Respiratory epithelium, height	78 [a]	–	–	60 ±19 [a]	67 ±5 [b]	–	–	67 ±5 [a]
Respiratory cilium, diameter	–	0.174±0.010[a]	0.223±0.007[a]	0.208±0.006[a]	–	0.156±0.006[a]	0.216±0.012[a]	0.184±0.007[b]
Respiratory cilium, length	9.4 ±0.1[a]	5.1 ±1.0 [a]	6.8 ±0.6 [a]	6.4 ±0.5 [a]	6.6 ±0.6[a]	5.7 ±0.6 [a]	8.5 ±0.7 [a]	6.4 ±0.4 [a]
Respiratory microvillus, diameter	–	0.069±0.008[a]	0.199±0.028[a]	0.110±0.018[a]	–	0.079±0.012[a]	0.075 [b]	0.079±0.011[a]

[1]) Since Table VI gives an impression of the number of samples, the sample means in this table are presented with their standard errors. Differing superscripts indicate significant differences with Student's t-test ($P \leq 0.05$) between cow and calf sample means, within one microscopic method, and for the pooled results; *a* represent a higher mean than *b*.

is the case for all the three microscopical methods mentioned. The number of necklace strands at the basal regions of the cilia might be slightly lower for respiratory cilia than for olfactory cilia (a difference of about one strand).

3.3.5. *Effect of age on olfactory and respiratory epithelium structures*

Various structural dimensions and frequencies in juvenile and adult nasal tissues are compared in this section. From the data presented in Table VII it appears that the dimensions of most olfactory nerve ending structures are significantly smaller ($P \leqslant 0.05$) in the adult than in the young animal; the same applies to supporting cell microvilli. Frequency parameters, such as the nerve ending density and the number of cilia per nerve ending, do not seem to differ significantly within these limits. Dimensions, such as the height of the epithelium and the mucus layer, also do not differ between the two age groups within the limits set. The various parameters pertaining to the respiratory epithelium too, do not differ with age. Therefore, it may be concluded that the nerve ending shrinks slightly with age or, alternatively or additionally, that in older animals smaller nerve endings are formed. The basic morphology remains identical.

3.3.6. *Comparison between olfactory and respiratory epithelia*

Table VIII presents comparisons of some anatomical features of olfactory, respiratory and transitional epithelia. No significant differences ($P \leqslant 0.05$) between nerve endings belonging to the olfactory epithelium and those in the transitional zone (between olfactory and respiratory epithelium) can be detected. Moreover, there is no evidence for the existence of a gradient of nerve ending densities in the transition zone. The only detectable difference between the olfactory and the transition areas concerns the height of the olfactory mucus. It may be concluded that the transition area is apparently not characterized by gradual changes; there exists a fairly abrupt transition from olfactory into respiratory epithelium. This region may be better described as an irregular border line than as a zone (see Figs. 15 and 16 in Chapter 1).

3.3.7. *Comparison of various olfactory regions*

There was no good reason to assume a priori that the olfactory epithelium is completely identical in its microstructure throughout its whole surface. Therefore we have made quantitative comparisons with regard to various parameters of the nasal septum, the cribriform plate and the nasal turbinates. This crude selection includes three fairly distinct areas.

Dimensions and frequencies of the various parameters within those areas are tabulated in Table IX. Several pronounced differences between the selected areas are observed. They are concerned with nerve ending density, epithelium height and mucus height. These three features all possess maximal values in the septum as compared to the other areas. Moreover, the diameter of the nerve endings is greater in the septum than in the remaining two nasal areas. The respiratory mucus layer is thicker on the ethmoturbinates than on the nasal

septum. Respiratory cilia are also somewhat longer on the ethmoturbinates. Other features of the nerve endings or the supporting cell apical regions, such as the diameter of supporting cell microvilli, do not show significant differences between the three nasal areas.

Ciliary taper and vesicle diameters show different values in the three nasal regions, with maximum values in the turbinates and minima in the septum. The cribriform plate shows intermediate values for these dimensions. Proximal ciliary segments, on the other hand, have an intermediate length on the ethmotubinates, while maximum lengths for these segments are observed on the nasal septum. The diameters of the proximal ciliary segments do not show significant differences between the three regions observed. It is difficult to say if all these slight, though significant ($P \leqslant 0.05$) differences have a physiological meaning (see page 106).

3.3.8. *Number of cilia per nerve ending*

Nerve endings appear to contain between none and 25 cilia. However, it is rather interesting that the average number of cilia observed per nerve ending shows a remarkable constancy. This number is 12–13 (12.5 ± 3.4 in Table VI) and is independent of the age of the animal (Table VII) and the nasal area studied (Tables VIII and IX). Due to obscureness of part of the ciliary population, the real figure is somewhat higher. We assume that about 1/4–2/5 of the cilia remains hidden behind other cilia and the nerve endings themselves, and escape observation in the scanning and the high-voltage electron microscope. After correction for these unobserved cilia we obtain as the actual average number of cilia per nerve ending a figure of about 17. Since the number of cilia per nerve ending determines the actual shape of that nerve ending, there seems no reason to assume the presence of morphological different types of nerve endings. However, this does not exclude the possibility that locally, within a particular region as e.g. the nasal septum, different nerve ending types might exist. Our observations were too crude to allow the detection of systematic differences within the different areas of the peripheral olfactory organ.

3.3.9. *Relationship between the observed structural parameters*

In the preceding sections we have presented quantitative data on several microstructural features of the two epithelium types in animals of two different age groups and of different areas in the nose. It is to be expected that several of the characteristic microanatomical parameters do not vary independently of each other.

In order to determine the relationships between the various parameters selected, we have calculated the correlation coefficients between all parameters. The parameters were compared with each other and all significant correlations ($P \leqslant 0.05$) are presented in Table X.

These correlation coefficients were determined according to Pearson (parametric) and according to Spearman (non-parametric; Byrkit, 1975). Since the correlation coefficients, calculated in both ways, lead to similar results for

the individual microscopic methods and for the pooled observations and since the correlation coefficients calculated in both ways seem rather similar, Table X shows only the results for the pooled data. Furthermore, the fact that both testing methods lead to similar results shows that the t-test, a parametric testing method which has been used in the previous sections, may be regarded as suitable for this work.

Table X shows that significant, though low positive correlations exist between the height of the olfactory epithelium and the nerve ending density, and also between the height of the olfactory epithelium and the height of the surface covering mucus layer of the olfactory epithelium. Furthermore the height of this mucus layer is positively correlated with the nerve ending diameter. However, the nerve ending diameter, in turn, shows a negative correlation with the nerve ending density. There are no other significant correlations between these four parameters. The first three correlations and the last correlation seem to contradict each other. This contradiction might be explained by the weights of the opposing relationships between the nerve ending diameter and the nerve ending density of Table VII (temporal differences: cow versus calf) and of Table IX (spatial differences: three different areas covered with olfactory epithelium are compared). Comparing temporal distributions shows that the nerve ending diameter shrinks with age, while the nerve ending density and the height of the olfactory epithelium and the mucus layer covering that epithelium remain unaffected. Comparing spatial distributions on the other hand, shows that the nasal septum contains a higher density of the nerve endings of olfactory bipolar cells than the cribriform plate or the ethmoturbinates. This higher nerve ending density is accompanied by a greater width of these nerve endings. Furthermore, they are packed in a thicker mucus layer present on a higher epithelium layer in the nasal septum.

Most correlations presented in Table X are found between the various dimensions of olfactory structures. These correlations reach highest values when various ciliary dimensions are compared. The correlations between the dimensions of these olfactory structures vary from approximately 0.2 when nerve ending diameter and diameters of the proximal ciliary segments and supporting cell microvilli are compared, to 0.7 when the length of the proximal cilium segment and the diameter of the ciliary vesicle or the height of the olfactory epithelium and the height of the olfactory mucus are compared. All correlations between these dimensions are positive. Therefore, the correlations may indicate that when the nerve ending grows all other dimensions of the olfactory epithelium increase, while on the other hand all these structures also shrink simultaneously. This situation is partially met in Table VII, in which four out of six dimensions of the nerve ending substructures and the supporting cell microvilli are smaller in cow than in calf. Some of the correlations might also be explained by the presence of spatial differences (Table IX). Two of the dimensions which do not show significant differences between cow and calf (the diameter of the distal segment of the cilium and the ciliary vesicle diameter) are smaller in the nasal septum than in the other two areas. Some other dimen-

TABLE VIII. Comparison of the means of some micro-anatomical measurements on nasal olfactory, respiratory and transitior

Features	Olfactory area; 62% of the observed photographs				Transitional
	Light	TEM	SEM	Pooled	Light
Nerve ending density/ $cm^2 \times 10^{-6}$	5.0 ±0.6 [a1)]	9.0 ±0.7 [a]	4.8 ±0.4 [a]	6.3 ±0.3 [a]	4.2 ±0.5 [a]
Nerve ending diameter[2)]	1.70 ±0.07[a]	1.39 ±0.04 [a]	1.17 ±0.03 [a]	1.31 ±0.02 [a]	1.55 ±0.07[a]
Olfactory cilium, proximal segment, diameter	– [3)]	0.179±0.004[a]	0.221±0.004[b]	0.200±0.003[a]	–
Olfactory cilium distal segment, diameter	–	0.060±0.002[a]	0.107±0.004[a]	0.082±0.003[a]	–
Olfactory cilium, proximal segment, length	–	1.54 ±0.08 [a]	1.93 ±0.08 [a]	1.77 ±0.06 [a]	–
Olfactory cilium, distal segment, maximal length observed	–	–	–	28	–
Olfactory cilium, vesicle, diameter	–	–	–	–	–
Supporting cell microvillus, diameter	–	0.064±0.003[a]	0.094±0.004[a]	0.077±0.003[a]	–
Number of ciliary necklace strands	–	7.3 ±0.2 [a]	–	7.2 ±0.2 [a]	–
Olfactory cilia/nerve ending	–	13.1 ±0.7 [a]	12.4 ±0.3 [a]	12.6 ±0.3 [a]	–
Granules microtubuli pool/ nerve ending cross-section	–	–	–	–	–
Olfactory epithelium, height	108 ±7 [a]	92	–	106 ±7 [a]	95 ±7 [a]
Olfactory mucus, height	7.6 ±0.9[a]	4.9 ±0.4 [b]	3.5 ±0.3 [a]	5.5 ±0.4 [a]	3.8 ±0.3[b]
Respiratory mucus, height	–	–	–	–	6.4 ±0.8[a]
Respiratory epithelium, height	–	–	–	–	65 ±8 [a]
Respiratory cilium, diameter	–	0.130±0.010[b]	–	0.130±0.010[b]	–
Respiratory cilium, length	–	6.2	–	6.2	7.5 ±0.6[a]
Respiratory microvillus, diameter	–	–	–	–	–

[1)] Since Table VI gives an impression of the number of samples, the sample means in this table are presented with their stan the three areas under observation, within one microscopic method, and for the pooled results; *a* represents a significant higher n
[2)] Dimensions are presented in micrometers (μm).
[3)] Not enough observations or observations totally lacking, thus preventing a proper comparison of the means.

sions, however, are smaller in one of the other two areas, thus opposing the effects of the temporal differences. The positive correlations may indicate that the temporal differences in that case are more important.

High positive correlations also exist between the diameter of the respiratory cilia and most dimensions of the olfactory cilia and between both mucus heights: the respiratory and the olfactory. Consequently we think that most correlations presented here reflect processes which are concerned with ciliary, and therefore, nerve ending growth or degeneration. These processes might reflect the condition of the nasal epithelia, such as expansion or a pathological pheno-

gion between the two other epithelium types) epithelia, employing three microscopic methods.

area; 20% of the observed photographs			Respiratory area; 18% of the observed photographs			
TEM	SEM	Pooled	Light	TEM	SEM	Pooled
6.8 ±1.2 [a]	5.9 ±0.6 [a]	5.6 ±0.5 [a]	–	–	–	–
1.17 ±0.06 [b]	1.06 ±0.06 [a]	1.23 ±0.04 [a]	–	–	–	–
0.167±0.007[a]	0.244±0.012[a]	0.203±0.008[a]	–	–	–	–
0.064±0.006[a]	0.122±0.009[a]	0.090±0.007[a]	–	–	–	–
1.55 ±0.14 [a]	2.09 ±0.17 [a]	1.67 ±0.12 [a]	–	–	–	–
–	–	27	–	–	–	–
–	–	–	–	–	–	–
0.052±0.006[a]	0.099±0.008[a]	0.078±0.006[a]	–	–	–	–
–	–	–	–	6.8 ±0.5 [a]	–	6.8 ±0.5 [a]
2.3 ±1.0 [a]	11.9 ±0.8 [a]	12.1 ±0.6 [a]	–	–	–	–
–	–	–	–	–	–	–
2	–	90 ±8 [a]	–	–	–	–
4.4 ±0.6 [a]	3.2 ±0.4 [a]	3.9 ±0.3 [b]	–	–	–	–
5.6 ±0.2 [a]	–	5.9 ±0.4 [a]	4.9 ±0.4[a]	5.8 ±0.4 [a]	–	5.4 ±0.3 [a]
–	–	65 ±8 [a]	69 ±5 [a]	–	–	67 ±5 [a]
0.144±0.007[a]	0.233±0.016[a]	0.188±0.012[a]	–	0.177±0.008[a]	0.218±0.007[a]	0.200±0.005[a]
5.6 ±0.6 [a]	8.0 ±0.6 [a]	7.1 ±0.4 [a]	6.6 ±0.8[a]	4.6 ±0.7 [a]	7.0 ±0.6 [a]	6.1 ±0.4 [a]
–	–	–	–	–	–	–

ors. Differing superscripts indicate differences with Student's t-test ($P \leq 0.05$) between the sample means within the lines of .n *b*.

menon. We have no reason to assume that the correlations are related to some specific olfactory feature, such as nerve endings of a different shape. This conclusion is supported by the fact that the number of cilia per nerve ending generally does not show significant correlations with any of the dimensional parameters, thus indicating that smaller or larger nerve endings have the same average number of cilia, and therefore the same contours. Likewise, it has already been shown in Tables VII, VIII and IX that these contours do not vary with age or with the area of the olfactory epithelium. Thus, with respect to the observed number of cilia per nerve ending the results of the t-tests and the cor-

TABLE IX. Comparison of the means of some micro-anatomical measurements on three different areas within the ol

Features	Nasal septum: 42% of the observed photographs				Cribrifc
	Light	TEM	SEM	Pooled	Ligl
Nerve ending density/ $cm^2 \times 10^{-6}$	6.4 ± 1.0 [a1)]	9.8 ±0.9 [a]	6.7 ±1.1 [a]	8.3 ±0.6 [a]	4.2 ±
Nerve ending diameter[2])	1.73± 0.10[a]	1.52 ±0.05 [a]	1.02 ±0.04 [b]	1.39 ±0.04 [a]	1.59 ±
Olfactory cilium, proximal segment, diameter	– [3)]	0.192±0.005[a]	0.209±0.010[b]	0.197±0.005[a]	–
Olfactory cilium, distal segment, diameter	–	0.063±0.003[a]	0.100±0.009[b]	0.073±0.004[b]	–
Olfactory cilium proximal segment, length	–	1.78 ±0.11 [a]	1.95 ±0.15 [a]	1.85 ±0.09 [a]	–
Olfactory cilium, distal segment, maximal length observed	–	–	–	28	–
Olfactory cilium, vesicle, diameter	–	0.51 ±0.06 [a]	–	0.51 ±0.06 [b]	–
Supporting cell microvillus, diameter	–	0.074±0.005[a]	0.082±0.010[a]	0.076±0.004[a]	–
Number of ciliary necklace strands	–	7.3 ±0.2 [a]	–	7.3 ±0.2 [a]	–
Olfactory cilia/nerve ending	–	14.4 ±1.0 [a]	11.9 ±0.5 [a]	12.9 ±0.6 [a]	–
Granules microtubuli pool/ nerve ending cross-section	–	26.3 ±2.5 [a]	–	26.3 ±2.5 [a]	–
Olfactory epithelium, height	130 ±14 [a]	–	–	130 ±14 [a]	95 ±
Olfactory mucus, height	11.2 ±2.0[a]	6.4 ±0.8 [a]	3.7 ±0.4 [a]	6.8 ±0.8 [a]	5.3 ±
Respiratory mucus, height	4.3 ±0.5[a]	5.2 ±0.4 [a]	–	4.9 ±0.3 [b]	–
Respiratory epithelium, height	74 ±7 [a]	–	–	70 ±8 [a]	–
Respiratory cilium, diameter	–	0.194±0.009[a]	0.220±0.007[a]	0.212±0.006[a]	–
Respiratory cilium, length	6.2 ±1.5[a]	4.6 ±0.8 [a]	6.4 ±1.2 [a]	5.5 ±0.6 [b]	–
Respiratory microvillus, diameter	–	0.083±0.009[a]	–	0.083±0.009[a]	–

[1]) Since Table VI gives an impression of the number of samples, the sample means in this table are presented with their s
lines of the three areas under observation, within one microscopic method, and for the pooled results; *a* represents a sig
[2]) Dimensions are presented in micrometers (μm).
[3]) Not enough observations or observations totally lacking, thus preventing a proper comparison of the means.

relation matrix support each other. Also other frequency values, such as the number of particles in the microtubular pool and the number of necklace strands do not show significant correlations with most of the other parameters.

The respiratory epithelium too shows several significant correlations be-

lium: the nasal septum, the cribriform plate and the ethmoturbinates, employing three microscopic methods.

17% of the observed photographs			Ethmoturbinates; 41% of the observed photographs			
TEM	SEM	Pooled	Light	TEM	SEM	Pooled
±1,1 [a/b]	3.9 ±0.4 [b]	5.7 ±0.5 [b]	3.9 ±0.4 [b]	6.4 ±0.9 [b]	4.8 ±0.4 [b]	5.0 ±0.3 [b]
! ±0.06 [b]	1.20 ±0.05 [a]	1.21 ±0.04 [b]	1.62 ±0.07[a]	1.24 ±0.05 [b]	1.18 ±0.03 [a]	1.27 ±0.03 [b]
18±0.004[c]	0.230±0.007[a/b]	0.193±0.007[a]	–	0.171±0.005[b]	0.230±0.006[a]	0.207±0.005[a]
54±0.003[a]	0.120±0.007[a]	0.087±0.006[a]	–	0.063±0.005[a]	0.109±0.004[a/b]	0.094±0.004[a]
) ±0.04 [b]	2.03 ±0.19 [a]	1.55 ±0.12 [b]	–	1.62 ±0.13 [a]	1.91 ±0.10 [a]	1.78 ±0.08 [a/b]
–	–	20	–	–	–	27
3 ±0.55 [a]	–	0.73 ±0.55 [a/b]	–	0.77 ±0.30 [a]	–	0.95 ±0.20 [a]
42±0.003[c]	0.100±0.006[a]	0.072±0.005[a]	–	0.059±0.006[b]	0.097±0.005[a]	0.082±0.004[a]
±0.5 [a]	–	6.5 ±0.5 [a]	–	7.3 ±0.5 [a]	–	6.9 ±0.6 [a]
±0.6 [a]	12.3 ±0.5 [a]	12.2 ±0.4 [a]	–	11.9 ±1.0 [a]	12.5 ±0.3 [a]	12.4 ±0.4 [a]
–	–	–	–	19.0 ±1.0 [a]	–	19.0 ±1.0 [a]
	–	95 ±2 [b]	96 ±6 [b]	52	–	91 ±7 [b]
±0.6 [b]	4.6	4.9 ±0.4 [b]	4.5 ±0.4 [b]	4.0 ±0.4 [b]	3.0 ±0.3 [a]	4.0 ±0.2 [b]
–	–	–	6.0 ±0.5 [a]	6.2 ±0.3 [a]	–	6.1 ±0.3 [a]
–	–	–	62 ±5 [a]	–	–	62 ±5 [a]
00	–	0.100	–	0.148±0.006[b]	0.222±0.011[a]	0.186±0.008[b]
	–	6.2	7.3 ±0.4 [a]	6.0 ±0.7 [a]	7.6 ±0.5 [a]	7.0 ±0.3 [a]
–	–	–	–	0.060±0.008[a]	–	0.111±0.021[a]

. Differing superscripts indicate significant differences with Student's t-test ($P \leq 0.05$) between the sample means within the mean than *b* which on its turn represents a significantly higher mean than *c*.

tween the dimensions of its anatomical elements. Some of the correlations are difficult to understand, e.g. the number of cilia per nerve ending (olfactory phenomenon) is correlated with the diameter of the respiratory cilia. All correlations presented in Table X are low and most of the variance remains un-

TABLE X. Pearson and Spearman correlation coefficients of several olfactory and respiratory epithelium surface featur

Features	Nerve ending density/cm² × 10^{-6}		Nerve ending diameter		Olfactory cilium, proximal segment, diameter		Olfactory cilium, distal segment, diameter		Olfactory cilium, proximal segment, length		Olfactory cilium, vesicle, diameter		Sup cell vill n
	1[1]	2[2]	1	2	1	2	1	2	1	2	1	2	1
Nerve ending diameter	–[3]	–											
Olfactory cilium, proximal segment, diameter	–0.33[4] 212 [5] ⩽0.01[6]	–0.32 212 ⩽0.01	0.22 275 ⩽0.01	0.20 275 ⩽0.01									
Olfactory cilium, distal segment, diameter	–0.32 131 ⩽0.01	–0.31 131 ⩽0.01	–	–	0.59 185 ⩽0.01	0.63 185 ⩽0.01							
Olfactory cilium, proximal segment, length	–0.16 127 ⩽0.05	–	0.26 165 ⩽0.01	0.26 165 ⩽0.01	0.42 174 ⩽0.01	0.46 174 ⩽0.01	0.33 132 ⩽0.01	0.38 132 ⩽0.01					
Olfactory cilium, vesicle, diameter	–	–0.44 21 ⩽0.05	–	–	0.39 30 ⩽0.05	0.35 30 ⩽0.05	–	–	0.67 13 ⩽0.01	0.65 13 ⩽0.01			
Supporting cell microvillus, diameter	–0.20 161 ⩽0.05	–0.21 161 ⩽0.01	0.18 206 ⩽0.01	0.12 206 ⩽0.05	0.51 235 ⩽0.01	0.50 235 ⩽0.01	0.43 151 ⩽0.01	0.45 151 ⩽0.01	0.28 123 ⩽0.01	0.36 123 ⩽0.01	0.42 32 ⩽0.01	–	
Number of ciliary necklace strands	–	–	–	–	–	–	–	–	–	–	–	–	–
Olfactory cilia/ nerve ending	–	–	0.16 182 ⩽0.05	–	–	–	–	–	–	–	–	–	–
Granules microtubuli pool/nerve ending cross-section	–	–	–	–	–	–	–	–	–	–	–	–	–
Olfactory epithelium, height	0.50 18 ⩽0.05	–	–	–	–	–	0	0	–	–	0	0	0
Olfactory mucus, height	–	–	0.28 100 ⩽0.01	0.28 100 ⩽0.01	–	–	–	–	0.28 37 ⩽0.05	–	–	–	–
Respiratory mucus, height	–	–	–	–	–	–	–	–	–	–	0	0	–
Respiratory epithelium, height	–	–	–	–	0	0	0	0	0	0	0	0	0
Respiratory cilium, diameter	–	–	–	–	0.75 28 ⩽0.01	0.69 28 ⩽0.01	–	0.40 19 ⩽0.05	–	0.65 14 ⩽0.01	0	0	0.6 28 ⩽0.0
Respiratory cilium, length	–	–	–	–	–	0.61 9 ⩽0.05	–	–	–	–	0	0	–
Respiratory microvillus, diameter	0	0	0	0	0	0	0	0	0	0	0	0	0

[1]) Pearson correlation coefficients, relating actual values.
[2]) Spearman correlation coefficients, relating rank numbers.
[3]) –: Correlation not significant.
[4]) Values of correlation coefficients of significant correlations.

bservations of three microscope techniques.

of e	Olfactory cilia/nerve ending		Granules microtubuli pool/nerve ending cross-section		Olfactory epithelium, height		Olfactory mucus, height		Respiratory mucus, height		Respiratory epithelium, height		Respiratory cilium, diameter		Respiratory cilium, length	
2	1	2	1	2	1	2	1	2	1	2	1	2	1	2	1	2
0[7]																
0	0	0														
0	0	0	0	0												
–	–	–	0	0	0.70 17 ⩽0.01	0.57 17 ⩽0.01										
0	–	–	0	0	–	–	0.66 12 ⩽0.01	–								
0	0	0	0	0	0	0	–	–	–	0.51 16 ⩽0.05						
–	0.53 14 ⩽0.05	0.71 14 ⩽0.01	0	0	0	0	0.87 12 ⩽0.01	0.62 12 ⩽0.05	–	–	0	0				
0	–	–	0	0	–	–	–	–	–	–	–	–	–	–		
–	0	0	0	0	0	0	0	0	–	–	0	0	0.37 25 ⩽0.05	0.45 25 ⩽0.01	–	–

ıple number used for the computation of the significant correlations.
ıificance level (two levels: $P \leqslant 0.01$ or $P \leqslant 0.05$).
:orrelation could not be computed.

explained. An important part of this unexplained variance is probably caused by variations in preparation and observation methods.

3.3.10. *Revised determinations of nerve ending densities*

Since Table IX shows pronounced differences in nerve ending densities over the three observed areas with respect to the microscopic method used, we thought it important to try to eliminate as much as possible the effects of the observation method on these determinations, in order to obtain a proper idea of the importance of the 'area effect' on the nerve ending density. Especially the discrepancy between density counts executed on micrographs made with the TEM and the HVEM and micrographs made with the SEM and the light microscope made a closer investigation essential. The recalculated results are presented in Tables XI and XII.

The results obtained with three different observation methods and presented in Table IX show significant higher densities in the nasal septum than in the other two areas of the olfactory epithelium. We thought that the discrepancy between the three methods might be caused by the range of microscope magnifications used for the density determinations. Especially at high magnifications the picture might be distorted. High magnifications were used more frequently in the TEM than in the SEM studies. Therefore Table XI presents densities, determined with the three methods, but now employing final magnifications (on the photographs) smaller than 10,000 (10 K). Furthermore, medians and modes, as determined from curves of density values versus frequency of occurrence of the densities in question, are presented. Table XI shows that after these transformation procedures density values obtained from TEM photographs approach much better the values obtained with the other two microscopic methods than in Table IX. Standard errors, although based on a smaller number of observations at microscopic magnifications smaller than 10 K remained identical or became slightly smaller after this transformation when compared to the original data. Since these differences occur only in the first decimal, these standard errors are not presented in Table XI for the sake of clarity.

The modified mean, the median and the mode all show that the septum contains the highest nerve ending density, at least in the calf, and probably also in the adult. The results on septal densities in the cow in the TEM observations are only based on a small sample. SEM results, however, show the same tendency in this respect as in calf. Furthermore, the nerve ending density appears to increase slightly when approaching the olfactory-respiratory borderline. This gradient is determined for the ethmoturbinates only.

Table XII summarizes the results of Table XI. The same trends can be seen as in the previous table. This table also shows that, with the three transformed determination methods, the nerve ending density in the adult animal is only 80% of that of the juvenile, which contrasts with the results presented in Table VII.

TABLE XI. Nerve ending densities (per $cm^2 \times 10^{-6}$) in cow and calf of four olfactory areas determined by different microscopic methods and calculated in different ways.

Statistic	Age	Light				TEM				SEM			
		Septum	Cribriform plate	Turbinate	Turbinate, transition zone	Septum	Cribriform plate	Turbinate	Turbinate, transition zone	Septum	Cribriform plate	Turbinate	Turbinate, transition zone
< 10K, Mean [1]	Cow	–	4^{5} [2]	–	–	2^{1}	6^{4}	–	–	4^{4}	3^{3}	3^{14}	–
	Calf	6^{14}	5^{4}	3^{6}	4^{17}	7^{14}	6^{2}	5^{6}	4^{10}	5^{11}	4^{12}	3^{17}	6^{12}
Median	Cow	–	2^{4}	–	–	3^{4}	8^{18}	–	–	5^{7}	3^{9}	4^{20}	–
	Calf	6^{15}	5^{4}	2^{6}	4^{17}	8^{42}	4^{3}	5^{12}	6^{12}	5^{19}	4^{22}	4^{36}	6^{18}
Mode	Cow	–	3^{4}	–	–	4^{4}	4^{18}	–	–	6^{7}	3^{9}	4^{20}	–
	Calf	7^{15}	4^{4}	3^{6}	4^{17}	8^{42}	4^{3}	5^{12}	5^{16}	5^{19}	4^{21}	4^{36}	6^{18}
Means Tables VIII and IX		6^{15}	4^{8}	4^{6}	4^{17}	10^{46}	9^{21}	6^{12}	7^{16}	7^{26}	4^{30}	5^{56}	6^{18}

[1]) Means calculated for all magnifications smaller than 10,000 × on the photographic prints.
[2]) Superscripts indicate the number of samples.

TABLE XII. Nerve ending densities (per $cm^2 \times 10^{-6}$) of four olfactory areas of cow and calf calculated by averaging the density values obtained by the three microscopic methods of Table XI.

Statistic	Age	Septum	Cribriform plate	Turbinate	Turbinate, transition zone	Total average
< 10K, Mean[1]	Cow	$3^{2)}$	4^3	3^1	–	$4^{6\ 3)}$
	Calf	6^3	5^3	4^3	5^3	5^{12}
Median	Cow	4^2	4^3	4^1	–	4^6
	Calf	6^3	4^3	4^3	5^3	5^{12}
Mode	Cow	5^2	5^3	4^1	–	4^6
	Calf	7^3	4^3	4^3	5^3	5^{12}
Pooled means of Tables VIII and IX		$8^{87\ 4)}$	6^{59}	5^{84}	6^{51}	6^{61} (cow) 6^{210} (calf)

[1]) Means calculated for all magnifications smaller than 10,000 × on the photographic prints.

[2]) The superscripts indicate the number of variables (nasal areas) in Table XI from which the pooled mean, medians and modes are calculated.

[3]) This column serves to indicate possible nerve ending density differences between cow and calf. Superscripts in this column are the summated superscripts within the observed line.

[4]) Superscripts in this line indicate the number of samples.

3.3.11. *Volumes and surface areas of nerve ending structures and particle frequencies*

In Table XIII estimations of volume and surface area of the various substructures of the olfactory nerve endings are presented. The nerve ending swellings themselves and the ciliary vesicles are considered to be spherical, while the other ciliary structures are considered to be cylindrical. Since exact ciliary lengths could not be determined in this study we took as a minimum length of the ciliary taper 30 μm, a figure which was met in Fig. 43. As a maximum length 100 μm may be considered. This value is based on estimations of SEIFERT (1970) and observations of REESE (1965). For both values the various entities are calculated. All calculations are based on dimensions presented in Table VI and particle counts in Table I (Chapter 2). As the total number of cilia per nerve ending we took 17 (page 94).

Table XIII clearly shows the enormous surface area represented by the ciliary tapers in comparison to the other nerve ending structures. The contribution of these tapers to the particle population (present in the nerve ending fracture faces, as seen by freeze-etch techniques) is therefore much higher than the contribution of the other nerve ending structures. This uneven relation

TABLE XIII. Volume, surface area and particle concentration, based on freeze-etch data of olfactory nerve ending structures.

Structures	Volume[1]) μm^3		Surface[1]) μm^2		Particles $\times 10^{-3}$/ structure[2])	
	1 cilium	nerve ending[3])	1 cilium	nerve ending	1 cilium	nerve ending
Nerve ending swelling	–	1.2	–	' 5	–	18
Cilium, proximal segment	0.05	0.9	1.1	18	5	78
Cilium, distal segment: 30 μm[4])	0.15	2.6	7.5	128	45	769
100 μm	0.50	8.5	25.1	427	151	2564
Cilium, vesicle[5])	0.04	0.6	0.3	6	1	18
Cilium, total: 30 μm distal segments	0.24	4.1	9.0	152	51	865
Cilium, total: 100 μm distal segments	0.59	10.0	26.5	451	156	2660
Nerve ending total: 30 μm distal segments	–	5.3	–	157	–	883[6])
Nerve ending total: 100 μm distal segments	–	11.2	–	457	–	2689[7])

[1]) Volume and surface values are calculated from data presented in Table VI (the pooled column).

[2]) Particle quantities are based on data presented in Tables I and VI.

[3]) Dimension and particle concentrations for the nerve endings are based on a total of 17 cilia per nerve ending.

[4]) Distal ciliary segments of 30 μm are a minimum estimate, based on own observations (Fig. 43); 100 μm is a maximum estimate based on literature (REESE, 1965; SEIFERT, 1970).

[5]) Values for the ciliary vesicles are based on the presence of 5 such vesicles per nerve ending.

[6]) Assuming an 11 nm particle diameter, these particles occupy 53% of the total nerve ending surface.

[7]) Assuming an 11 nm particle diameter, these particles occupy 56% of the total nerve ending surface.

is even enhanced by the presence of higher particle densities in the tapers (Table I). When the particle diameter measures 11 nm, it follows that the particles occupy between 53% (for the 30 μm tapers) and 56% (for the 100 μm tapers) of the total nerve ending surface. Cilia possess between 50,000 (for a 30 μm taper) and 160,000 (for a 100 μm taper) particles.

3.4. Discussion

3.4.1. *Nerve ending density*

3.4.1.1. Nerve ending density gradients within the nasal olfactory area

The present chapter is concerned with the problem whether or not different receptor cell types can be recognized in the olfactory mucosa, and with distributions of nerve endings in different olfactory regions. It turns out that nerve ending densities in septal areas are 1.5–2 times higher than in the cribriform plate and the nasal turbinates (Tables IX, XI and XII).

Presumably the higher nerve ending density in the septal epithelium is related to the fact that the septum is the nasal region which makes contact with the incoming air stream first. The higher nerve ending density may increase the sensitivity of the tissue in this region towards odours.

Tables XI and XII also show that, at least in the nasal turbinates, the nerve ending density in the transitional region close to the respiratory area is somewhat higher than the density elsewhere in the turbinates. These regions, located more anterior, are also better exposed to incoming air streams. In this case too the well exposed situation could explain the higher nerve ending density. In this respect the possibility that a high nerve ending density compensates for a decrease of ciliary segments in areas close to the respiratory area is worth to be considered. The highest densities, however, have been found in septal areas.

Allison and Warwick (1949) described in the nasal septum of the rabbit a gradient from anterior to posterior regions, amounting from 8.1×10^6 nerve endings/cm^2, via 11.5×10^6 nerve endings/cm^2 to 14.0×10^6 nerve endings/cm^2. In bovine turbinates, we found a gradient in the opposite direction. Allison and Warwick's data are based on a total of 21 observations, while our calculations are based on a total of 125 observations on the turbinates, made with three different microscopic methods.

3.4.1.2. Relation between age and nerve ending density

Table XII shows that nerve ending densities in calf are probably somewhat higher than in the adult animal. Mulvaney and Heist (1971a), in rabbit, observed the same tendency. These authors report a decrease in nerve ending density of about 30% during growth of the animal. In the bovine we observed a maximal decrease with age of about 20%. Mulvaney and Heist (1971a) based their conclusions on 9 observations; our figures are derived from 156 observations (Tables XI and XII; < 10 K lines). The fact that the nerve ending density does not seem to alter very much during growth of the animal has important implications (see also Chapter 1: pages 25, 30–34 and 47). It means that expansion of the tissue as seen in Fig. 1 is due either to an increase in the total number of nerve endings or to a differentiation into patches with nerve endings. The latter hypothesis leads to a situation in adult animals, where nasal areas

which contain nerve endings alternate with areas characterized by ciliated respiratory or squamous cells. Both processes increase of the olfactory surface area and splitting up of this area into patches may even occur concurrently. Evidence for the occurrence of the second process is indicated by the fact that, especially in adult animals, whole areas could not be identified as olfactory tissue. KOLB (1975) encountered the same problem in the roe, another ungilate. We also found respiratory cells within the olfactory regions in adult animals. Because of these experiences the majority of our observations were made on calf tissue. In addition to these facts, a density decrease seems to occur with age. This decrease may be caused by a shrinking of the nervous cell apical part, coupled with an increase of the apical part of the supporting cells. Alternatively or additionally the changes observed may be due to the disappearance of some nerve cells which die and which are not replaced.

3.4.1.3. Density differences within a limited region

In agreement with KOLB (1975) we noticed a great variation spread in nerve ending densities, as can be deducted from the large standard deviations in Table VI. In some samples densities of up to 30×10^6 nerve endings/cm^2 were found, while other areas contained densities of less than 10^6 nerve endings/cm^2. Therefore local variations might be of greater importance than the overall regional differences analyzed here. It is difficult to assess these local differences quantitatively with a reasonable degree of accuracy.

3.4.1.4. A literature survey of olfactory nerve ending densities

Table XIV presents a survey of densities for olfactory nerve endings for various animals through all classes of vertebrates. These values do not show a clear evolutional or any other kind of pattern. Densities for the dog, for example, are the lowest of all values presented in Table XIV. However, dogs are known to possess an excellent olfactory acquity (MOULTON and MARSHALL, 1976a, b). KOLB (1971) suggests that the size of the nervous cell may compensate for low densities. Dogs do have more cilia per nerve ending (OKANO et al., 1967) than the other animals tabulated in Table XIV, but this value is only a very crude estimate. Taking into account that the dog is a very useful animal for olfactory research, we think that both values, density and the number of cilia per nerve ending, need to be reinvestigated for this animal.

It should be kept in mind that, in view of the very different results obtained in the rabbit by different investigators, the variation of these values may be attributed to a great extent to the investigator rather than to the animal.

3.4.2. *The number of cilia per olfactory nerve ending and ciliary dimensions*

3.4.2.1. A literature survey

Table XIV also presents a survey of the numbers of cilia per nerve ending found for various animals, through all classes of vertebrates. Most authors report ranges instead of average values for this number. It appears from Table

TABLE XIV. Literature survey of densities of nerve endings of bipolar olfactory cells in the olfactory epithelium and the number of cilia borne by these nerve endings in various animals.

Animal classes	Species	Nerve ending density/cm^2 $\times 10^{-6}$	Authors	Olfactory cilia/nerve ending	Authors
Mammals	Cat	10	FERRON (1973)	10–40	ANDRES (1969)
	American marter	8	FERRON (1973)	–	–
	Dog	1.2–1.7	MÜLLER (1955)	100–150	OKANO et al. (1967)
	Rabbit	12	ALLISON and WARWICK (1949)	–	–
		9	HEIST et al. (1967)	30–60	HEIST et al. (1967)
		19–43	MULVANEY and HEIST (1971a)	–	–
	Cat, dog, rabbit	8–30	SEIFERT (1970)	–	–
	Rat	6	MENCO (Unpublished)	30	MENCO (Unpublished)
	Bat	2–3	KOLB (1971)	7–9	KOLB (1971)
	Roe	3	KOLB (1975)	–	–
	Pig	6.2	GASSER (1956)	–	–
	Ox	2–10 Mean: 6.2	Present paper	0–25 Mean: 17	Present paper
	Squirrel monkey	–	–	8–20	DE LORENZO (1970)
	Guinea pig	8–10	KANDA et al. (1973)	Many	KANDA et al. (1973)
	Man	3	KANDA et al. (1973)	3–6	KANDA et al. (1973)
	Mole	–	–	1–5	GRAZIADEI (1966)
Birds	Domestic duck	2.5	GRAZIADEI and BANNISTER (1967)	8–10	GRAZIADEI and BANNISTER (1967)
	Seagull	5	DRENCKHAHN (1970)	7–13	DRENCKHAHN (1970)
Reptiles	Lizard	–	–	10	KRATZING (1975)
Amphibians	Frog	8	GETCHELL (1973)	6–12	BLOOM (1954)
		1.5	MENCO (Unpublished)	6–10	MENCO (Unpublished)
				6–8	REESE (1965)
	Mudpuppy	–	–	4–8	FARBMAN and GESTELAND (1974)
Fish	Eel	4	TEICHMANN (1959)	4–8	SCHULTE (1972)
	10 Other species	8–10	TEICHMANN (1954)	–	–
	Goldfish	–	–	4–7	BREIPOHL et al. (1973a)
	Several other species			4–6	BANNISTER (1965)
		–	–	12	SCHULTE and HOLL (1971)
				1–18	BERTMAR (1973)
	Cyprinodonts	40–50	ZEVEKE et al. (1976)	5–8	ZEVEKE et al. (1976)

XIV that these values are generally higher in higher vertebrates, especially mammals, than in lower vertebrates. There is no obvious relationship between the number of cilia per nerve ending and the nerve ending density. It may be that most values have been determined too crudely. It may also be that the nerve ending surface and nerve ending density show some kind of a proportional relationship. In that case not only the number of cilia per nerve ending has to be considered, but also the total lengths of the cilia. These lengths are difficult to determine.

3.4.2.2. The number of cilia per nerve ending in the bovine

Ranges of the number of cilia per nerve ending in the bovine were rather similar to those for other macrosmatic animals: 0–25 cilia per nerve ending. However, in our case (as is shown in Tables VI–IX) the average number of cilia per nerve ending that could be observed is constant (about 12) giving a real average of about 17 cilia per nerve ending (page 94). The present data are the first, to our knowledge, to show this consistency in nerve ending outline.

Other structural parameters presented in this chapter are chiefly related to development and degeneration of nerve ending structures. No evidence could be found for the existence of different nerve ending types. This leads to the conclusion that odour discrimination probably occurs at a submicroscopical level.

3.4.2.3. The relation between ciliary outgrowth and age

With increasing age of the animal, there is a decrease in the ciliary diameter (Table VII), but due to difficulties in determining the total length of the cilium, it is not allowed to conclude that this decrease in girth is accompanied by an increase in length of the cilium. We thought that this difference, as a function of the age of the animal, might reflect differing rates of transport of ciliary structure precursors. In fact it accounted for approximately 6 μm out of about 100 μm ciliary taper outgrowth.

3.4.2.4. The number of cilia per unity of surface

Assuming that outgoing cilia compensate for incoming cilia in length and surface area, it can be calculated that a circular area, with a radius of 5 μm contains about 5,000 μm of ciliary segments. This calculation is based on the following formula:

ciliary length within an area equals length of one cilium, times number of cilia per nerve ending, times number of nerve endings within the observed area (12)

The ciliary length used was 60 μm, a value which is intermediate between minimum and maximum values used elsewhere in this paper; the number of cilia per nerve ending is 17 and the number of nerve endings within the observed area is about 5 (based on 6.2×10^6 nerve endings/cm^2 in Table VI). A ciliary lenth of 60 μm allows cilia from nerve endings within a radius of 65 μm

(including the radius of the observed area) to cross or touch the observation area. In the surrounding area we find about 825 nerve endings. It does not seem unlikely that about 500–600 of those each send on an average 2 to 3 cilia to and/or through the observation area, which measures 80 μm^2. This means that about $3 \times 500 = 1{,}500$ 'foreign' cilium segments cross the boundary. Furthermore, we can calculate that the number of autochtonic ciliary segments present in the observation area is about 5 (number of nerve endings in this area) $\times$ 17 (number of cilia per nerve ending) = 85. Thus only about 5% (85 out of 1,500) of the ciliary segments is autochtonic (for a two dimensional representation see the summary: Fig. 56C).

When we assume, furthermore, that the cilia of the 5 autochtonic nerve endings have about 5 μm of their length per cilium within the observation area, it follows that about $5 \times 5 \times 17 = 425$ μm of ciliary length originates from autochtonic nerve endings. This is only about 10% (425 out of 5,000 μm) of the total ciliary length within the observation area, whereas the remainder belongs to cilia from elsewhere. These calculations indicate that mutual contacts at ciliary levels are probably not casual, but might even be a necessity for an adequate functioning of the system. Real junctional structures between cilia have not been found sofar, also not in our recent freeze-etch work in rat, in spite of the fact that we have looked very carefully for such structures.

3.4.3. *Nerve ending surfaces with respect to epithelium surface*

Calculations have learned that nerve endings at a density of 6.2×10^6 nerve endings/cm^2 and with ciliary tapers of either 30 μm, 60 μm or 100 μm correspond to nerve ending surfaces of respectively 10, 18 and 28 cm^2/cm^2 epithelium surface, assuming the presence of 17 cilia per nerve ending (see also Table XIII). Minimum surface areas, when we assume that nerve endings bear cilia which remain just within the reach of the cilia of adjacent nerve endings, would be 0.06, 0.03 and 0.02 cm^2/cm^2 epithelium surface respectively, at nerve ending densities of 3.5×10^4, 8.8×10^3 and 3.2×10^3 nerve endings/cm^2 respectively. The actual nerve ending density is 200–2,000 times greater, which means that the actual nerve ending densities are much higher than would be necessary to span the whole olfactory area. The vast nerve ending surface area above the epithelium surface offers the possibility for the existence of some kind of interaction at ciliary levels, although the ciliary membrane may be electrically isolated from ciliary membranes nearby.

3.4.4. *Estimations of receptor populations*

3.4.4.1. Particle densities at cilium surface

Table XIII shows that, depending on its length, one may expect the presence of 50,000–155,000 particles per cilium. OTTOSON and SHEPHERD (1967) predicted binding site quantities of 160,000 per 100 μm cilium in frog. This value shows a striking agreement with the number of particles we have calculated: 156,000 per 100 μm cilium surface. Furthermore, the number of binding sites

for the odorous compound p-dimethyl-amino-benzaldehyde (DMBA) on frog olfactory cilia is about 400,000 (GUSEL'NIKOV et al., 1974). Frog cilia have a length of about 200 μm (REESE, 1965), which means that a 100 μm cilium segment contains 200,000 binding sites for this compound. From OTTOSON's and GUSEL'NIKOV's observations, and combined with our own calculations, we might conclude that one particle corresponds to one binding site. However, one must be very careful when drawing this important conclusion, since GUSEL'NIKOV and coworkers did not carry out adequate controls on other cilium types. These workers prepared their cilia according to KOROLEV and FROLOV (1973). The poor quality of the electron micrographs provided by the latter authors raises some doubt with respect to the preparation methods employed. The morphological evidence presented, furthermore, does not seem to prove conclusively that GUSEL'NIKOV et al. (1974) were dealing with olfactory cilia and mucus fluid alone. Moreover, it is probably not permitted to make direct comparisons between frog and bovine olfactory cilia. However, the evidence presented in this section indicates that the particles seen by freeze-etch methods may very well represent odour binding sites.

The text under Table XIII shows that about 55% of the nerve ending surface in this animal is occupied by particles. The remaining intra-membranous area most likely consists of phospholipids.

3.4.4.2. Particle concentrations

In Chapter 2 (page 82) evidence is provided that the particles in the olfactory nerve ending membranes, could have receptor functions analogous to that of rhodopsin in the visual system (DAEMEN, 1973; EBREY and HONIG, 1975). If this is the case, it would be interesting to calculate the particle concentration in the mucus layer which covers the olfactory epithelium. A major assumption we have to make is that all particles consist of the same protein species. Table XV presents such calculations. These calculations were possible because we have data from freeze-etch methods, combined with a quantitative analyses of morphological data obtained by other microscopic methods, all on the same animal. Line *A* in Table XV is derived from Table XIII. For the calculation of the particle concentration in the mucus the following formula was used:

$$C = \frac{D \times \{4\pi \times (p_a.r_a^2 + m.p_d.r_d^2) + 2\pi \times n(p_b.r_b.h_b + p_c.r_c.h_c)\}}{N_{Av} \times (H-V)} \times 10^6\, mMol \qquad (13)$$

C = particle concentration in mMolar in the mucus;
D = nerve ending density in nerve endings/cm^2: 6.2×10^6;
p = particle density in particles/μm^2 (Table I);
r = structure radius in μm (Table VI);
m = number of ciliary vesicles per nerve ending: 5;
n = average number of cilia per nerve ending: 17;
h = length of ciliary segment (Table VI);

TABLE XV. Minimum and maximum particle concentration estimates in the olfactory nerve endings, in the olfactory mucus layer and with respect to odorous stimulation at threshold values[1]). Nerve ending concentration with respect to odorous stimulation at threshold values.

Parameter		Taper length		Remarks
Number	Nature	30 μm (minimum estimate)	100 μm (maximum estimate)	
A.	Particle concentration in nerve ending	2.8×10^{-1} mMol or 1.7×10^{17} particles/ml	4.0×10^{-1} mMol or 2.4×10^{17} particles/ml	These values are based on the last two lines of Table XIII.
B.	Mucus volume above 1 cm^2 epithelium	4.3×10^{-4} ml	3.5×10^{-4} ml	Mucus volumes are corrected for the presence of nerve ending and microvillous structures. It is assumed that the total microvillous volume is identical to that of the total nerve ending volume for both estimates. These volume values are used in the calculations of the rest of this Table.
C.	Particle concentration in the mucus	2.2×10^{-2} mMol or 1.3×10^{16} particles/ml Reduction factor: A/C = 13	7.8×10^{-2} mMol or 4.7×10^{16} particles/ml Reduction factor: A/C = 5	The ciliary abundance is clearly indicated by the values of the reduction factors: they compare particle concentrations in the mucus, with those in the nerve endings.
D.	Particle concentration if these particles were, with identical densities as their presence on nerve ending structures, free swimming in the mucus	7.0×10^{-1} mMol Reduction factors: D/A = 3 D/C = 32	7.5×10^{-1} mMol Reduction factors: D/A = 2 D/C = 10	D and E clearly indicate the high particle concentrations actually present in the mucus and in the nerve endings. Since with respect to the presence of long tapering cilia the maximum reduction factor is only 108, it could be possible that these tapers simulate a fluid which contains such particles in colloidal suspension. However, these particles need to be present on the tapers, since they form part of the nervous receptor structures. The particle concentration in the nerve ending

E.	Maximum particle concentration possible, assuming a 11 nm particle diameter	2.4 mMol Reduction factors: E/A = 9 E/C = 108	2.4 mMol Reduction factors: E/A = 6 E/C = 31	
F.	Odorant concentrations at threshold present in the mucus[2])	6.9×10^{-9} mMol or 4.2×10^{9} molecules/ml Number of particles per odour molecule: A/F = 4.1×10^{7} C/F = 3.1×10^{6}	8.5×10^{-9} mMol or 5.1×10^{9} molecules/ml Number of particles per odour molecule: A/F = 4.6×10^{7} C/F = 9.2×10^{6}	This item indicates the vast excess of proteinaceous particles over odorous molecules, present at threshold values in the olfactory mucus. This may indicate that a high receptor versus low substrate ligand-binding process is a basic principle in olfaction.
G.	Receptor cell nerve ending concentration present in the mucus	1.3×10^{10} nerve endings per ml G/F = 3.1	1.3×10^{10} nerve ending per ml G/F = 2.6	The receptor cell nerve ending concentration approaches the odorous threshold concentrations much closer than the nerve ending particle concentrations. This indicates the possibility for a one to one interaction between odorous molecules and receptor cells: Only one molecule is necessary to excite a nervous cell.

[1]) Odorant concentrations are taken from STUIVER (1958), who used merceptans to determine threshold values in human subjects.
[2]) Since we assumed a different mucus volume for both taper estimates, the odorous molecules are more concentrated in a mucus containing 100 μm tapers, than in a mucus containing 30 μm tapers.

N_{Av} = Avogadro's number: 6.023×10^{23};
H = mucus volume (ml) including volumes of nerve ending and supporting cell distal structures above 1 cm^2 epithelium surface: 4.9×10^{-4} ml;
V = volume of nerve ending structures above 1 cm^2 epithelium surface area: 0.6×10^{-4} ml for 30 μm distal ciliary segments and 1.4×10^{-4} ml for 100 μm distal ciliary segments, assuming that microvillous structures have the same volume as nerve ending structures;
a, b, c and d are the nerve ending swelling, the proximal ciliary segment, the distal ciliary segment and the ciliary vesicle respectively.

The factor within the outer parentheses gives the number of particles per nerve ending (Table XIII and page 104). The comments in Table XV indicate that a high proportion of the mucus volume is occupied by olfactory membrane particles.

In the case of photoreceptors, freeze-etch investigations by CHEN and HUBBELL (1973) indicated that the particle concentration as determined by this method is about 19 times lower than the rhodopsin concentration as determined by X-ray analyses (BLAISE et al., 1969).

From combination of microspectrophotometric data on rhodopsin concentrations in rod outer segments (DAEMEN, 1973) with observations of particle densities in frog outer segments (ROZENKRANZ, 1970) one may infer that the particle concentration is about 13 times lower than the rhodopsin concentration. Both calculations indicate that the particles in the visual system most likely consist of a number of rhodopsin subunits. Similar findings have been reported for MN-glycoprotein in phospholipid bilayers. Here each intra-membranous particle contains 10–20 monomers (SEGREST et al., 1974). The same situation might be the case in the olfactory system. In that case receptor protein populations could be a factor 10 or more higher than the particle concentrations given in Table XV.

In Section 3.4.4.1. it was suggested that the particles each might represent one binding site. The present discussion, however, leads to the idea, that each particle represents a multireceptor complex. It is hoped that biochemists will settle this point in the near future.

3.4.4.3. Odour sensitivity with respect to particle concentrations

Odour concentrations in Line F (Table XV) are based on STUIVER's (1958) work who calculated that at threshold about 9×10^6 mercaptan molecules were present in one human nasal cavity with an olfactory surface area of 5 cm^2. If one assumes that nerve ending and supporting cell microvillous structures have the same volume in the cow as in man and that the height of the mucus layer is also identical one obtains (using Avogadro's number) the molar values of Line F.

Approaching the odour reception mechanism from the viewpoint of receptor availabilities, and using threshold data of various authors, we come to a similar conclusion as STUIVER (1958) and MOULTON and MARSHALL (1976b): a single

receptor cell may detect one odorous molecule. However, the number of binding sites can exceed odour concentrations at threshold by a factor 10^6–10^8 or possibly even more (previous section), which implies a high efficiency for the olfactory organ!

3.4.5. *Implications of the present findings for the peripheral olfactory process*

Our studies did not provide evidence for the presence of morphological different receptor cells, therefore any odour discrimination may occur at submicroscopical levels.

Particles which could be part of receptor proteins or protein complexes are present in high concentrations within the ciliary membranes and in the rest of the nerve ending. With the surrounding phospholipids they form a fluid mosaic membrane structure (SINGER and NICOLSON, 1972; SINGER, 1975). The long distal ciliary segments, which contain the great majority of these particles float in a probably aqueous mucus layer. They form a fluid phase with an enormous surface area packed with particles, thus optimizing the receptor process (Table XV).

Many layers of receptor containing membranes are present, comparable to the situation in visual cells which consist of many layers of rhodopsin containing membranes within each outer segment (JAN and REVEL, 1974; references Chapter 2). In the olfactory system, however, these membranes belong to different cells. In both cases the membranes surround structures of axonemal origin (THURM, 1969; BARBER, 1974; VINNIKOV, 1974).

It is conceivable that interactions occur between adjacent olfactory cilia through contacts, thus activating the conductive system of a number of surrounding nervous cells. However, this would tend to reduce, rather than increase discrimination of odours, unless odour reception is based on a non-specific receptor which acts with different affinities towards odorants. Sofar, our freeze-etch results did not indicate the presence of specialized junctions between adjacent cilia, although ultrathin sections did show close interaction and even fusion between ciliary segments (Fig. 40). If ciliary communication exists, a messenger should be present. This messenger should be non-specific. Carnosine, which is found in high quantities in the olfactory pathway (MARGOLIS, 1974, 1975), might be considered as a possible candidate. Ciliary communication or not, the message could anyhow be translated and transferred according to mechanisms involving cyclic nucleotides and microtubular proteins (ATEMA, 1975; OLSEN, 1975; Chapter 1 of this paper).

Furthermore, the quantitative observations have indicated that odour receptors may interact with high affinity towards odours. The binding process is probably best described by a low substrate versus high receptor interaction. This would mean that odour receptors can be better compared with hormone receptors than with enzymes (KAHN, 1976).

We have tried to provide some quantitative data concerning odour receptor structures. Although these data are indispensable (GRAZIADEI, 1974a), their interpretation seems to stress the need for biochemical analysis once more.

4. ATTEMPTS TO ISOLATE OLFACTORY NERVE ENDING PROCESSES FROM BOVINE OLFACTORY MUCOSA

4.1. INTRODUCTION

In order to conduct biochemical studies, it is necessary to obtain relatively pure fractions of olfactory nerve ending structures. This means that other cellular and subcellular structures should be removed as good as possible. Since no specific markers for the olfactory receptor cell nerve ending membranes are known at present, such isolation procedures are difficult.

An adequate plasma membrane marker for metazoan sensory receptors is only known for the visual system : the protein rhodopsin (DAEMEN, 1973; EBREY and HONIG, 1975). Furthermore, the receptive structures, the outer segments, are easily obtained here (MIKI et al., 1974). In other systems the receptors can be isolated by using their specific binding properties. This procedure allows the isolation of e.g. cholinergic receptors (CHANGEUX et al., 1975) and receptors for hormones (KAHN, 1976).

Recent biochemical work on taste showed competition for sweet compounds in taste bud plasma membranes, while such competition could not be found in the epithelium surrounding the buds (LUM and HENKIN, 1976). In the latter report, dissociation-constant rank orders are consistent with electrophysiological work. Sofar, this study is to our knowledge the most convincing biochemical work carried out on any of the vertebrate peripheral chemical senses. For the olfactory organ no such studies are available at present.

When we started our investigations, a method for obtaining plasma membrane fractions from olfactory nerve endings had been developed (KOCH and NORRING, 1969). This method was based on procedures developed by WHITTAKER (1965) for obtaining synaptosomes. As main biochemical marker, the presence of Na^+-K^+-ATPase in plasma membranes was used. KOCH and NORRING (1969) also supplied some electron microscopical evidence for the presence of plasma membranes with ciliary fragments attached in their fractions.

The main purpose of the present investigation was to develop better methods for obtaining olfactory receptor processes. The presence of ciliary fragments was used as a morphological marker.

To date this objective has not been achieved. We think, however, that a description of our attempts might be of some help to future workers, and prevent them from falling in the same traps we encountered.

4.2. Materials and methods

4.2.1. *Obtaining samples of olfactory tissue*

Bovine heads were obtained from local slaughterhouses. The heads were cut sagittally and the required mucosal area was sampled. This dissection and all isolation procedures were done at a temperature of 4 °C. After dissection, the samples were subjected to a variety of treatments in order to obtain a subcellular fraction enriched specifically in plasma membrane vesicles and ciliary fragments originating from the olfactory nerve endings. All isolation attempts, except those described in Sections 4.2.3.6. and 4.2.3.8., were done on adult bovine material. In 4.2.3.6. sheep mucosal samples were used, while in Section 4.2.3.8. juvenile bovines were used.

This isolation process consists of two major steps: *1.* the preparation of the required organelles and *2.* the relative enrichment of these receptor-bearing organelles. Although the first objective could not be attained to a satisfactory degree, purification procedures – following the preparation – were begun on our crude cellular suspensions.

4.2.2. *Preparation of samples for morphological characterization*

Since no specific biochemical marker for the peripheral olfactory receptor structures is known, a morphological marker was selected. We used the relative enrichment in ciliary fragments as observed by electron microscopy. The characterization procedure was very time consuming. Therefore the number of experiments on which our observations are based is necessarily limited. The preparation of the samples used for characterization in the electron microscope was carried out as described in Chapter 1. The only difference was that the samples were routinely spun down in a Coleman centrifuge (about 15,000 × g: 2 to 3 minutes) after each step of the sample preparation. The Araldite blocks were sectioned at different levels (Breese and Zacharia, 1974).

Occasionally negative staining methods were used, which entailed staining of the samples with 1% phospho-tungstic acid brought to pH = 7.0 with KOH. Bovine serum albumine (Fraction V; 0.01%) was also added.

The tissue remaining after this preparation procedure was usually examined, both by transmission and by scanning electron microscopy.

4.2.3. *Isolation procedures*

The various isolation steps described in this chapter, are labeled with letters *A* through *P*.

4.2.3.1. Scraping the mucosa

After removal of the mucosal samples from the nasal turbinates and the nasal septum their surfaces were scraped (Koch and Norring, 1969). The scraped material was homogenized in an isotonic solution (0.32 M sucrose in 0.05 M Trizma base-HCl, pH = 7.6). The samples were further treated according to Koch and Norring (1969). The same fractions that contained

ciliary fragments in their preparation were subjected to electron microscopy in our procedure (*A*).

4.2.3.2. Variations in ionic strength and pH of sampling solutions

An isotonic physiological solution, Krebs-D (KREBS, 1950), pH = 6.8, was used to rinse gently the olfactory mucosal tissue samples (*B*). The remaining tissue samples were vigorously shaken with a wrist-action shaker in the same Krebs-D solution (*C*). Tissue samples were then vigorously shaken for three minutes in a hypotonic phosphate buffer (0.05 M, pH = 7.4) supplemented with 0.05 M $CaCl_2$. After this shaking, the suspension was made isotonic with 0.03 M sucrose (*D*). Suspensions *B*, *C* and *D* were filtered through cheese cloth with a pore diameter of 450 μm. The filtrates were then centrifuged at 15,000 $\times$ g (4 °C; 20 minutes) in a Sorvall SS-34 centrifuge. The pellets consisted of a red bottom layer and a yellowish top layer. The two layers were separated with a spatula, thus giving a total of six samples.

Supernatants were centrifuged at 65,000 $\times$ g for 90 minutes in the same solutions as used previously. The 9 pellets, as well as the remaining tissue samples, were subjected to electron microscopy.

4.2.3.3. Ficoll density gradients as function of the sampling method

Mucosal samples of the bovine olfactory area were soaked in 2.5 mM Hepes buffer, pH = 7.0. The buffer was made isotonic with mammalian Ringer (*E*). ASH and SKOGEN (1970) employed such a soaking method, except they used sucrose instead of Ringer to make the sampling medium isotonic.

Instead of soaking, mucosal samples were vigorously shaken with the same sampling solution (*F*).

Mucosal samples were again vigorously shaken in the same sampling buffer/Ringer solution. This time the solution was made viscous with 30% Ficoll, which we thought might result in a more gentle shaking action while hardly affecting the osmolarity of the medium (*G*).

Suspensions *E*, *F* and *G* were filtered through cheese cloth (pore diameter: 450 μm). The filtrate *G* was then diluted by a factor five with Hepes/Ringer and spun at 60,000 $\times$ g for 1 hour (4 °C). This action was thought to remove most of the Ficoll.

Suspensions *E*, *F* and *G* were then supplemented with Hepes/Ringer to 50 ml and dehydrated in dialyzing tubing with Aquaside (Calbiochem). We thought this to be a more gentle action to concentrate the sample than differential centrifugation and we hoped to isolate intact structures by this procedure. A disadvantage of this method was that the buffered medium was also concentrated, which increased the ionic strength of the fluid medium surrounding the suspended samples.

Hepes/Ringer was added to the concentrates in order to bring them to a level of 5 ml and, subsequently, these suspensions were gently homogenized with a loose pestle Potter homogenizer (5 strokes). The samples obtained

were then layered upon a 5.7%–45.5% (w/w) continuous Ficoll gradient, made up in the same buffered Ringer solution in 30 ml centrifuge tubes. Centrifugation at 30,000 × g lasted for 135 minutes and was carried out in a Beckman 50-2L ultracentrifuge.

The centrifugation resulted in two bands for the suspensions *F* and *G* (shaken suspensions), and in one band for the soak suspension (*E*). However, the soak suspension was lost while trying to punch the tube. All three tubes contained sediments.

The two remaining tubes were frozen in liquid nitrogen and the bands and intermediate layers were sliced with an electrically heated metal wire along with the tubes. The obtained samples were washed in Hepes/Ringer at 35,000 × g. The supernatants were washed once more at 60,000 × g. Both centrifugations lasted 60 minutes. The main objective for these washings was to remove the Ficoll, which might otherwise have interfered with the microscopic observations. The pellets resulting from both washings were pooled. The washings may have nullified initial beneficial effects of the Aquaside dehydration.

Along with the four bands obtained, the pellets, the dialysates and the initial suspensions were all subjected to electron microscopy.

4.2.3.4. Differential centrifugation

Tissue samples were left to stand (soaked) for 1 hour in 0.02 M Hepes/Ringer, pH = 7.0. Subsequently, they were shaken on a wrist-action shaker for 30 minutes and then sonicated for 30 seconds at setting 2 with a MSE sonicator. This sequence was chosen in order to collect as much of the required sample (ciliary structures) as could be hoped for.

After filtration through cheese cloth, the resulting suspension was subjected to differential centrifugation. The following sequence of g-values was used: 480 × g, (twice, with pellets pooled), 3,050 × g, 9,750 × g and 25,000 × g. The supernatant obtained from the previous centrifugation was spun at the next g-value. All spins lasted 20 minutes, and samples for electron microscopic observation were taken from all stages (*H*).

The method used is similar to the one developed by KOROLEV and FROLOV (1973), who also employed sonication and subsequent differential centrifugation in order to obtain olfactory cilia from frog olfactory mucosa.

A Sorvall SS-34 and a Beckman 50-2L centrifuge were used in the experiments described above.

4.2.3.5. Differential and density gradient centrifugations

At this stage the possibility of contamination of the olfactory samples with respiratory tissue was realized, therefore the sample dissection was restricted to nasal areas which were selected more carefully than had been done previously. The preparation steps were the same as under *H* (4.2.3.4.). After the cheese cloth filtration the resultant suspension was subjected to differential centrifugation. Now the following sequence of g-values was employed for 20 minutes each 1,000 × g, 5,500 × g and 60,000 × g, using the same centrifuges

as employed above.

The 5,500 × g pellet was subjected to a continuous Ficoll gradient (11.5%–31.5%, w/w). Densities were measured by the refractive indices once the centrifugation was finished (PRICE, 1974).

Centrifugation was carried out in 30 ml centrifuge tubes at 30,000 × g and lasted two hours. Two bands were obtained which were washed at 60,000 × g in order to remove the Ficoll. The samples were then suspended with a whirlmixer and loosely homogenized with a Potter homogenizer (5 strokes).

The suspensions of the two bands thus obtained were subjected to a second gradient (13%–34% Ficoll, w/w). Both gradients were prepared in the dissecting medium. This centrifugation was carried out at 55,000 × g and lasted 12 hours. No clear bands could be distinguished. The samples were obtained by aspiration with a Pasteur pipette. Isodense fractions obtained after the second centrifugation on the two bands of the first gradient were combined.

After washing the samples at 60,000 × g for 30 minutes, eight final fractions together with 13 samples obtained in previous stages were subjected to electron microscopical examination (*I*).

4.2.3.6. Methods adapted from isolation procedures for motile cilia and rod outer segments

A. MENEVSE (Pers. Comm.) developed isolation methods for olfactory cilia which were adapted from methods for isolating motile cilia types (see review GOLDSTEIN, 1974) (*J*). He also attempted to isolate the material of interest using methods which were developed for the isolation of rod outer segments (MIKI et al., 1974) (*K*). Samples obtained in this way by MENEVSE were also subjected to an electron microscopical investigation. This work was done on sheep tissue.

4.2.3.7. Millipore adhesion of the epithelium surface and zinc sulfate disruption

The epithelium surface was adhered to a millipore filter (pore width 0.45 μm, 2.5 cm filter diameter; DØVING in: OTTOSON, 1970). The material which adhered to the filter was scraped off and subjected to a differential centrifugation (*L*).

Tissue samples were gently shaken in a buffered solution (2.5 mM Hepes/Ringer, pH = 7.0) supplemented with 5% $ZnSO_4$. The shaking lasted two hours (*M*). The substance collected from the millipore filters and the $ZnSO_4$ suspension were each subjected to differential centrifugation. The following sequence of g-values was employed: 1,500 × g and 9,750 × g. Each centrifugation lasted 20 minutes.

The pellets obtained were examined by electron microscopy. Ultrathin sectioning and negative staining methods were used in this case. Millipore filters, before and after scraping of the sample, were examined both by transmission and scanning electron microscopy.

4.2.3.8. Adhesion of the epithelium surface to a china tile with and without freezing

Tissue samples were with their nerve ending sides attached to a china tile. The material remaining on the tile after removal of the mucosal leaflet was collected and examined (*N*).

The same removal and collection procedure was carried out after liquid nitrogen had been poured over the tissue sample (*O*), and also the epithelium surface had been scraped with a scalpel blade while the mucosal sample was in frozen condition due to liquid nitrogen treatment (*P*).

4.2.4. *Determination of the degree of purification of olfactory processes using morphological methods*

The degree of purification was calculated by means of an estimation of the surface area occupied by ciliary segments of olfactory origin as a function of the total area covered by tissue fragments and occupying one hole of a 400 mesh electron microscope copper grid.

The area (*S*) of such a grid hole occupied with tissue material can be described as follows:

$$S = b \times A \tag{14}$$

in which A is the surface area of the grid hole and b the fraction of that area, which is occupied with material of tissue origin. A equals about 2,000 μm^2 and b was roughly estimated to be 1/4. The area occupied by sectioned material is thus about 500 μm^2.

Furthermore we assume, in order to facilitate calculations, that the number of ciliary cross-sections roughly equals the total number of oblique and longitudinal sections within a certain area and that the surface covered by the oblique and longitudinal sections occupies five times the area covered by cross-sections. Designating the area occupied by a cross-section by a leads to:

$$(a + 5a)/2 \tag{15}$$

as the average area occupied by one ciliary section. Table VI (TEM column) gives 0.17 μm as the average diameter of a cilium. This value lays in between the diameters of cilia of olfactory and respiratory origin, and it gives as average area occupied by one ciliary segment 0.068 μm^2.

We estimate that about 1 out of 10 ciliary sections is of olfactory origin (*O*), while the other 9 segments are of respiratory (*R*) origin. The fraction of ciliary segments of olfactory origin, as compared to all ciliary segments present can now be represented by the following equation:

$$O/(O + R) \tag{16}$$

This equation provides a correction for contamination with other ciliary segments. We obtain for this equation 0.1. Respiratory columnar cells have many more cilia than olfactory nerve endings, as may be seen in the photographs of Chapter 1. In addition, in respiratory cilia, the 9(2) + 2 axonemal

structure is maintained over distances which are about 4 times longer than the proximal segments of the olfactory cilia as concluded from TEM observations (Table VI). Consequently, contamination of our preparations with a few respiratory cells may result in great difficulties to recover ciliary fragments of olfactory origin.

When we find a total of n ciliary fragments per hole area of a 400 mesh grid, it can be calculated that these n fragments occupy a certain fraction (in %) of the total amount of tissue, present within an open grid area:

$$\frac{1}{b \times A} \times \frac{a + 5a}{2} \times \frac{O}{O + R} \times n \times 100\% \qquad (17)$$

The three factors at the left of n are constants and have been discussed above. If N is the number of hole areas used for one observation, we obtain factor P for the degree of relative enrichment of sectioned material of olfactory ciliary origin:

$$P = 1/N \sum_{i=1}^{i=N} 0.0014 \times n_i\%, \text{ with } N = 10\text{–}90 \text{ (usually about 20)} \qquad (18)$$

This factor does not include fragments of ciliary taper origin, since we were not able to recognize such structures in our preparations. Furthermore, this formula assumes the presence of an equal fraction of non-recognizable ciliary fragments in all samples observed.

This enrichment factor is a crude approximation of the degree of purification, but, as will be shown in the section on results, even a factor 100 difference would not change our results drastically. In view of the many approximations, no statistics were applied in this chapter, but large standard deviations would certainly be found. The main purpose of defining an enrichment factor P was to provide a means to select fractions which seemed most promising for future work.

4.2.5. *Materials*

Unless specifically mentioned all chemicals were obtained either from British Drug Houses or from Sigma Inc. and were of analytical grade.

4.3. Results

4.3.1. *Account of the presentation of the results*

The number of methods described in the previous section (Materials and methods) indicates that the aim of this study, the isolation and proper identification of olfactory receptor processes, was not reached. In view of the negative results, they will not be described in detail. Some implications will be mentioned

which may be of relevance for similar studies.

The same heading and lettering system (*A* through *P*) as used in the MATERIALS AND METHODS section will be followed.

4.3.2. *Isolation procedures*

4.3.2.1. Scraping the mucosa

We consistently followed the isolation method developed by KOCH and NORRING (1969) for obtaining plasma membrane fractions from rabbit olfactory nerve endings, yet hardly any fraction gave ciliary fragments in the case of bovines and sheep. This situation is similar to the situation described by the authors cited above for rabbit.

Adenyl cyclase and Na^+-K^+-ATPase were used as enzymatic markers for the presence of plasma membranes (DODD, 1974; MENEVSE et al., 1974). The results show that these enzymes are present in the olfactory mucosa. However, since we cannot separate between different plasma membrane fractions it is not possible to specify in which type and region of cells specific activities occur (MENCO et al., 1974a) (*A*).

4.3.2.2. Variations in ionic strength and pH of sampling solutions

Cilia and nerve ending vesicles were collected mainly by employing centrifugal forces of 15,000 $\times$ g. Yields of ciliary fragments were extremely low. The red pellets obtained with 15,000 $\times$ g centrifugation contained more nerve ending and respiratory cell fragments than the yellow pellets on top of the red ones. No significant difference in ciliary yield was observed between the three sampling methods used, to know rinsing with isotonic Krebs-D (*B*), shaking with isotonic Krebs-D physiological solution (*C*) or shaking with a hypotonic buffer solution (*D*).

The yellow pellets contained about 12 ciliary fragments per 400 mesh grid hole area, which gives (Formula 18) a relative enrichment of about 0.016%, which is negligible.

4.3.2.3. Ficoll density gradients as function of the sampling method

The band obtained from the soaked sample (*E*) was lost, while trying to punch the tube.

Mucosal samples shaken with Hepes/Ringer gave a band containing 26 ciliary sections per 400 mesh grid hole area, which gives a purification factor, *P*, of about 0.035% (*F*). Material obtained from mucosal samples which were shaken in the same solutions as above but made more viscous with Ficoll gave, after gradient centrifugation, bands which hardly contained any recognizable ciliary sections (*G*).

4.3.2.4. Differential centrifugation

We wanted to get a better approximation of the most efficient g-value for

sedimenting ciliary fragments, which would allow to subject the sediment (*H*) more profitably to a density gradient centrifugation.

From the range of g-forces applied, the greatest quantity of ciliary fragments was obtained at 3,050 × g (15, with $P = 0.020\%$), while the 9,750 × g pellet contained about 13 ciliary sections ($P = 0.018\%$). The fractions obtained in this experiment contained fewer nerve ending and columnar cell fragments than the methods employed previously. This is probably due to the sonication, which may also have destroyed many cilia.

4.3.2.5. Differential and density gradient centrifugations

From the results of experiment *H* we concluded that the most efficient g-value for sedimenting ciliary fragments is between 3,050 × g and 9,750 × g and therefore we used 5,500 × g in the present experiment (*I*). The greatest enrichment that could be obtained now was located in the pellet which went through the second gradient. About 50 ciliary sections were found per 400 mesh grid hole area, giving an enrichment of $P = 0.068\%$. A representative sample is shown in Fig. 55. Most ciliary fragments here are probably of respiratory origin, as is concluded from the presence of dynein containing arms on the microtubular doublet subfibers (Chapter 1). Much of the remaining material in this section appears to be of mitochondrial origin.

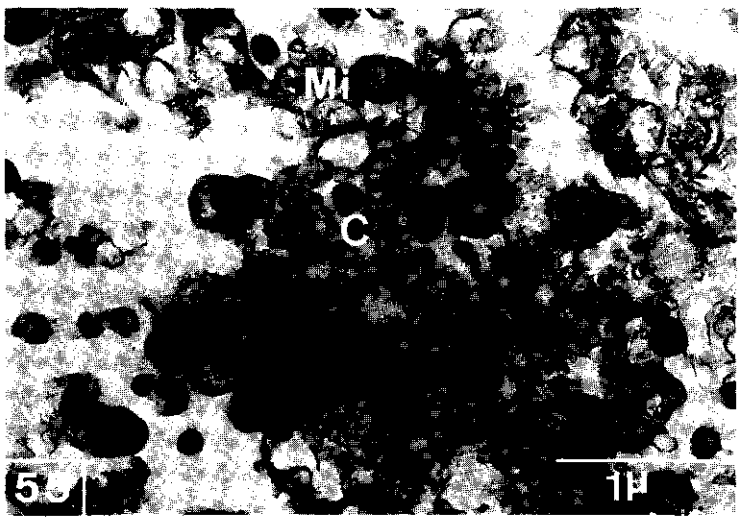

FIG. 55. Gradient fraction, containing ciliary fragments. This fraction comprised the pellet of a continuous Ficoll density gradient (55,000 × g for 12 hours). The medium surrounding this pellet contained about 34% Ficoll, which was dissolved in 0.02 M Hepes supplemented with Ringer (mammalian), pH = 7.0. This was one of the better fractions. Note the variety in cell organelles other than cilia (C)-mitochondria (Mi) in particular. Most cilia seem to have sedimented with the same g-forces as mitochondria.

4.3.2.6. Methods adapted from isolation procedures for motile cilia and rod outer segments

Neither isolation attempts based on methods for the isolation of motile cilia (GOLDSTEIN, 1974) by A. MENEVSE (*J*), nor attempts adapted from methods for the isolation of vertebrate rod outer segments (MIKI et al., 1974) were very promising. However, the latter method yielded many columnar respiratory cells bearing cilia, which showed that the initial dissection method also raises important problems. Therefore it was tried to improve our dissection methods as described in the next paragraphs.

4.3.2.7. Millipore adhesion of the epithelium surface and zinc sulfate disruption

DØVING (in OTTOSON, 1970) adhered epithelium surfaces to filter paper and showed, without quantitative assessment, that the filter paper did contain many ciliary sections, presumably of olfactory origin. However, they might also be of respiratory origin. We have used millipore filters since much of the material is absorbed within the filter material in case of paper filters. Millipore filters would perhaps absorb more of the material at the filter surface than inside. It is easier to recover the absorbed material from the surface, e.g. by scraping with a spatula.

The filters were gently pressed on the epithelium surface. Even though the material adhering to the filters was subjected to two differential gradient steps after removal by means of scraping, no significant enrichment was obtained (*L*). When the filters, before and after scraping, were examined by scanning and transmission electron microscopy only a few ciliary fragments were seen.

Preliminary experiments were carried out in order to investigate if the millipore filter adhered samples contained reasonable amounts of microtubular proteins. Microtubular proteins might be a suitable biochemical marker for receptor fractions. The experiments involved subjection of the samples to SDS-(sodium dodecyl sulfate) polyacrylamide gel electrophoresis (WEBER and OSBORN, 1969) and a colchicine binding assay (LAGNADO et al., 1971). However, sofar no microtubular proteins were detected in reasonable amounts, indicating that these proteins were either not present in detectable amounts in our preparations or lost or denatured during the separation procedure.

Shaking mucosal samples in a buffered solution with 5% $ZnSO_4$ did not prove to be successful (*M*). The $ZnSO_4$ treatment was conducted in view of the fact that animals become anosmic after irrigation of the olfactory area with this compound. Nerve endings and other structures are lost because of such treatments (MULVANEY and HEIST, 1971b; MATULIONIS, 1975, 1976).

4.3.2.8. Adhesion of the epithelium surface to a china tile with and without freezing

The epithelium surface adhered to a china tile before (*N*) and after freezing with liquid nitrogen (*O*). Collection of the material left on the tile after removal of tissue leaflets did not give reasonable amounts of the required structures.

Freezing the mucosal sample with liquid nitrogen and subsequent gentle scraping of the sample surface also proved to be inefficient (*P*).

4.3.2.9. Examination of remains of tissue samples

It proved to be difficult, using both scanning and transmission electron microscopy, to draw conclusions concerning the success of isolation procedures from observations on remaining mucosal surfaces after the preparation. Usually no differences could be seen between treated and untreated samples. This may have been due to damage which occurred to the epithelium layer during sample preparation. Alternatively, mucus could, at least in scanning microscope observations, obscure the epithelium surface. Pathological features cannot be excluded either, especially in adult animals.

Many apparently glandular openings were revealed in scanning microscope observations after vigorous shaking of the samples. The shaking might have ruptured the mucosal structures drastically, so that the epithelium layer and perhaps also layers underneath were removed, thus leading to exposure of mucosal features of the lamina propria.

4.4. Discussion

4.4.1. *Evaluation of possible disadvantages of the observation methods*

The negative results presented indicate that the isolation of peripheral olfactory processes is difficult. The most gentle methods applied, e.g. adhesion of the epithelium surface to a china tile, hardly produced any ciliary processes.

Part of the failures might be ascribed to inadequate sample preparation methods for electron microscopic observations. The use of the minifuge during fixation and embedding procedures may have led to a loss of isolated material. On the other hand Araldite blocks containing samples were sectioned at several levels. Perhaps the uptake of fixed material in agar-agar would have led to a reduced loss of material.

If considerable enrichment was obtained we should have noticed this despite the arguments mentioned here.

4.4.2. *Critical analysis of various methods used*

4.4.2.1. Scraping mucosal surfaces

The application of Koch and Norring's (1969) method yielded few ciliary sections. Scraping the mucosa presumably gives a great variety of plasma membrane elements, containing only small amounts of nerve ending processes. The mucus layer, which houses the receptor structures, occupies only 6% of the total epithelium height. Probably, scraping not only removes epithelium material, but also large amounts of underlaying tissue.

Plasma membrane markers, such as Na^+-K^+-ATPase, cannot be considered as typical for nerve ending membranes only. Consequently Koch's later re-

sults (KOCH, 1972, 1973; KOCH and DESAIAH, 1974; KOCH and GILLILAND, 1977), showing different response-patterns of this ATPase as a result of odorous interaction with plasma membrane preparations of various areas of the olfactory organ, probably cannot be interpreted to reflect only reactions of nerve endings, but represent activities common to mucosal structures. Unless it is shown that various enzymatic activities of nerve ending plasma membranes are specifically stimulated or inhibited by odorous compounds, no conclusions can be drawn about the relation between the presence of these enzymes and the receptor process.

Similar considerations may be made with reference to the work of DODD (1970, 1971) and KOYAMA et al., (1971). The former author used KOCH's isolation procedure and showed that different animals have different activities of the enzyme Na^+-K^+-ATPase in crude fractions of peripheral olfactory origin (DODD, 1970). It was also shown that odorous compounds affect the fluorescence of the membrane probe 1-anilino-8-naphthalene sulphonate (ANS) (DODD, 1971), which was incorporated in such plasma membrane preparations. The two latter publications contain no micrographs. KOYAMA et al., (1971) devised a method rather similar to the one developed by KOCH and NORRING (1969). They sampled bovine peripheral olfactory structures by scraping. No ciliary structures are present in their electron micrographs. Consequently, adenyl cyclase activities in samples collected by scraping (BITENSKY et al., 1972; KURIHARA and KOYAMA, 1972; MENEVSE et al., 1974) are also concerned with plasma membrane fractions of the total mucosa and not of the nerve endings alone.

4.4.2.2. Isolation procedures involving soaking of mucosal samples

Soaking the olfactory mucosa in an isotonic medium (ASH, 1968, 1969; ASH and SKOGEN, 1970) seemed more promising than sampling techniques involving scraping according to light micrographs (ASH and SKOGEN, 1970). The light micrographs revealed that only the layer containing nerve endings had been removed by the soaking technique. Sofar no electron micrographs of the tissues treated in this way have been published but publication of such photographs has been announced (ASH and SKOGEN, 1970). The primary aim of ASH and SKOGEN's work was not to obtain fractions enriched in nerve endings. They showed ascorbic acid to be a cofactor of a protein which in some way is involved in odour reception. Drs. D. J. SAATHOFF and W. D. ELLIS in the laboratories of the Honeywell Corporation, Minnesota (Pers. Comm.) showed that the response involving ascorbic acid was non-specific and that this response could be obtained equally well and sometimes even better in a number of other tissues, including brain, liver and kidney. DODD and CASH (1974) suggest that the primary function of the ascorbic acid in the olfactory mucosa is to act as an antioxidant, and that it does not play a direct role in the transduction mechanism, but that it may inhibit lipofuscin formation.

4.4.2.3. Sampling techniques involving sonication of mucosal tissue

KOROLEV and FROLOV (1973) used sampling techniques which involved sonication and subsequent differential centrifugation. They claim to have obtained fractions enriched in ciliary structures from frog olfactory mucosa. The morphological evidence provided for the presence of such cilia in their fractions seems to be based on one electron micrograph of one cilium. GUSEL'NIKOV et al. (1974) showed by differential spectrophotometry that mucus fractions and ciliary samples obtained by the method of KOROLEV and FROLOV (1973) contain proteins with different sensitivities towards odorants.

4.4.3. *Implications of the present critiques for previous studies on the biochemistry of olfaction*

Since, as has been described above, most previous studies on the biochemistry of peripheral olfactory processes were based on tissue material obtained by similar methods as the ones we have employed, it seems doubtful whether these studies were dealing indeed with material adequately enriched with nerve ending structures. Therefore some reservations have to be made when interpreting the results of these biochemical investigations, designed to elucidate the nature of primary receptor processes.

4.4.4. *Relevance of anatomical information for biochemical studies*

Results on anatomical details of the olfactory mucosa as described in the previous three chapters have some relevance for biochemical studies on olfaction. Mapping studies (HEIST et al., 1967; MULVANEY and HEIST, 1970) have shown that the epithelium is present on extremely complex nasal turbinates, and that even within these restricted areas olfactory areas alternate with respiratory areas. Nasal turbinates are very convoluted, which makes it difficult to remove undamaged epithelium from this region. Moreover, the attachment of the olfactory mucosa to the underlying bone of the turbinates seems to be tighter than in the case of respiratory epithelium. When the olfactory mucosal layer is removed a ribbed bony surface remains. This surface is less ribbed in the respiratory area.

Once mucosal samples from olfactory origin have been dissected, it will probably not be an easy task to isolate the receptive processes. Scanning electron micrographs, like Fig. 17, and high-voltage transmission electron micrographs (Figs. 41 and 43) clearly illustrate the complexity of the surface layer containing the nerve endings. Distal processes of cilia and microvilli of supporting cells form an intensively dense carpet, in which all kinds of other structures such as granular masses (Fig. 24) and a variety of vesicles (Figs. 40 and 41) seem to be entangled. Furthermore, distal ciliary segments and microvilli have an identical diameter (Table VI). It seems most unlikely that, without the aid of substances with specific binding properties, microvillous structures can be easily separated from the distal segments of olfactory cilia. The isolation of complete ciliary structures seems even more unfeasible, since it is virtual-

ly impossible to disentangle such a complex morphological structure, without damaging the required structures. We were unable to identify in our preparations the ciliary tapers, which probably possess most of the receptive surface area. This is indicated by our results (Chapter 3) and the conclusions of KERJASCHKI and HÖRANDNER (1976): particles embedded in the ciliary membranes are supposed to represent receptor proteins. These proteins could conceivably be used as a marker. Therefore we think that, despite the practical objections mentioned above, it seems promising to aim for the isolation of ciliary tapers in future biochemical work. It seems also advisable to use juvenile instead of adult animals in this research, since unwanted pathological and other morphological aberrations are less likely to occur in juveniles (Chapters 1 and 3).

Biochemical studies on olfaction should also involve a study of the supporting cells. In Chapter 2 we have shown that bovine microvilli contain globular particles in their membranous fracture faces, while the analogous fracture faces in rat contain rod shaped particles. In mouse (KERJASCHKI and HÖRANDNER, 1976) the rod shaped particles are limited to the membranous fracture faces above the tight junctions and do not involve the microvilli. These differences could be species specific, but they could just as well represent different metabolic conditions. Recently evidence is accumulating that the shape of the supporting cells and their microvilli might be sex dependent. SAINI and BREIPOHL (1976) showed that supporting cells have a different appearance in male and female Rhesus monkeys. Furthermore, the shape of these cells in the female changes during the menstrual cycle. This work provides morphological evidence for differing olfactory sensitivities in males and females (see also KOELEGA and KÖSTER, 1974).

Moreover, TAKAGI and OKANO (1974) and OKANO and TAGAKI (1974) present evidence that in the bullfrog supporting cell apical parts detach from those supporting cells upon stimulation with odorants (such as chloroform) which elicit a positive electro-olfactogram.

These apical parts contain secretory granules which disintegrate in the mucus. In all these studies the effects on the bipolar sensory cells were less pronounced. Although the role of the supporting cells remains uncertain these studies show that they are sensitive to changing circumstances. Therefore a study of the biochemistry of olfaction should involve these cells as well.

Future isolation attempts should probably involve cellular separation methods. Digestive enzymes such as hyaluronidase and collagenase might be used to dissolve the mucus and to loosen cellular connections. These enzymes have been successfully applied to disperse ciliated cells of the frog pharyngeal epithelium (WILSON et al., 1975). After these digesting procedures the several cell types, such as olfactory bipolar and supporting cells and respiratory columnar cells, have to be separated. Centrifugal elutriation (FLANGAS, 1974) might provide a means to obtain this objective. Elutriation uses cell size, rather than cellular densities as means of separation. Once a reasonable pure fraction of olfactory bipolar cells has been obtained, methods can be applied to snap

off the ciliary structures (BLUM, 1971; GOLDSTEIN, 1974). Like other types of cilia (BLUM, 1971), olfactory cilia probably possess a basal breaking point.

Dispersion methods have been applied to rabbit olfactory epithelium (ASH et al., 1966), but to our knowledge this work has not been continued. These authors showed that the medium containing the dispersed cells consisted of approximately equal amounts of respiratory columnar cells and supporting cells and bipolar receptor cells together.

Tissue cultures (HEIST et al., 1967; FARBMAN, 1973; FARBMAN and GESTELAND, 1974b, 1975) could also serve as a starting point for separation procedures. Sofar they have only been used in electrophysiological work.

4.4.5. *Alternative approaches*

MARGOLIS (1972) identified a soluble protein, which occurs at high concentrations in olfactory pathways. He found that this protein, which seems to be involved in the carnosine metabolism (MARGOLIS, 1974), is most likely mainly synthesized in the olfactory epithelium (MARGOLIS and TARNOFF, 1973; MARGOLIS, 1975). However, the occurrence of this protein is not limited to olfactory epithelium, because it is also found in the bulbus. This protein, together with microtubular proteins, could serve as a biochemical marker when isolating structures from the peripheral olfactory system.

GENNINGS et al. (1974, 1976, 1977) have used sex-specific pheromones in pig and found that the olfactory mucosa contained a fraction with specific binding behaviour towards these pheromones. Affinity-labeling could be used when isolating structures, in which this protein is present.

MENEVSE et al. (1977) used protection and photoaffinity techniques in an electrophysiological approach and found evidence for selective labeling of olfactory receptors. Similar techniques could be applied in future isolation attempts. Techniques to isolate specific plasma membrane regions of one cell, as is desirable in studies of this type, have only recently been initiated (see review NEVILLE, 1975), and are currently used in simpler systems than the olfactory organ.

However elegant some of the above approaches are, without a thorough morphological characterization of remaining tissue material and obtained fractions, such as the one devised for the isolation of taste buds by LUM et al. (1976), no convincing biochemical work can be performed on the olfactory system.

SUMMARY

Nervous extensions, belonging to bipolar sensory cells and directed towards the nasal lumen, contain receptors for odorous molecules. Little is known concerning the nature of these receptors. No biological receptor system is known which interacts with such a great variety of compounds as the odour receptor system. Unfortunately, at the present stage biochemical studies of this interesting organ are limited due to various technical problems. These biochemical studies require sufficient amounts of tissue at a suitable level of purity. Lack of sufficient quantities of tissue combined with laborious preparation procedures have caused great difficulties in studying the biochemistry of

TABLE XVI. Some morphological features of the bovine olfactory epithelium compared within three different groupings[1]).

	Height olfactory epithelium μm	Nerve ending density per $cm^2 \times 10^{-6}$	Observed number of cilia per nerve ending
I. *Age groups:*			
a) adult	97 ± 2^{a} [2)]	6.1 ± 0.6^{a}	12.6 ± 0.3^{a}
b) juvenile	100 ± 7^{a}	6.2 ± 0.3^{a}	12.4 ± 0.3^{a}
II. *Transition from olfactory to respiratory epithelium:*			
a) olfactory normal	106 ± 7^{a}	6.3 ± 0.3^{a}	12.6 ± 0.3^{a}
b) olfactory transition	90 ± 8^{a}	5.6 ± 0.6^{a}	12.1 ± 0.6^{a}
III. *Different areas within the olfactory epithelium*			
a) septum	130 ± 14^{a}	8.3 ± 0.6^{a}	12.9 ± 0.6^{a}
b) cribriform	95 ± 2^{b}	5.7 ± 0.5^{b}	12.1 ± 0.4^{a}
c) ethmoturbinates	91 ± 7^{b}	5.0 ± 0.3^{b}	12.4 ± 0.4^{a}
IV. All data[3])[4])	$99 \pm 5(23^{18})$	$6.2 \pm 0.3(4.8^{271})$	$12.5 \pm 0.3(3.4^{188})$

[1]) The presented values are pooled from observations on 524 micrographs, obtained by light microscopy, and by thin and thick section transmission and scanning electron microscopy.

[2]) The means are presented with their standard errors. Differing superscripts indicate significant differences between the values within the column of one grouping (I, II and III) with $P \leqslant 0.05$ as calculated with Student's t-test.

[3]) The numbers between the brackets represent the standard deviations of the means depicted. The superscripts indicate the number of observations.

[4]) A significant, although low correlation (0.5 with $P \leqslant 0.05$) exists between the epithelium height and the nerve ending density. Significant correlations between epithelium height or nerve ending density, and the number of observed cilia per nerve ending could not be detected.

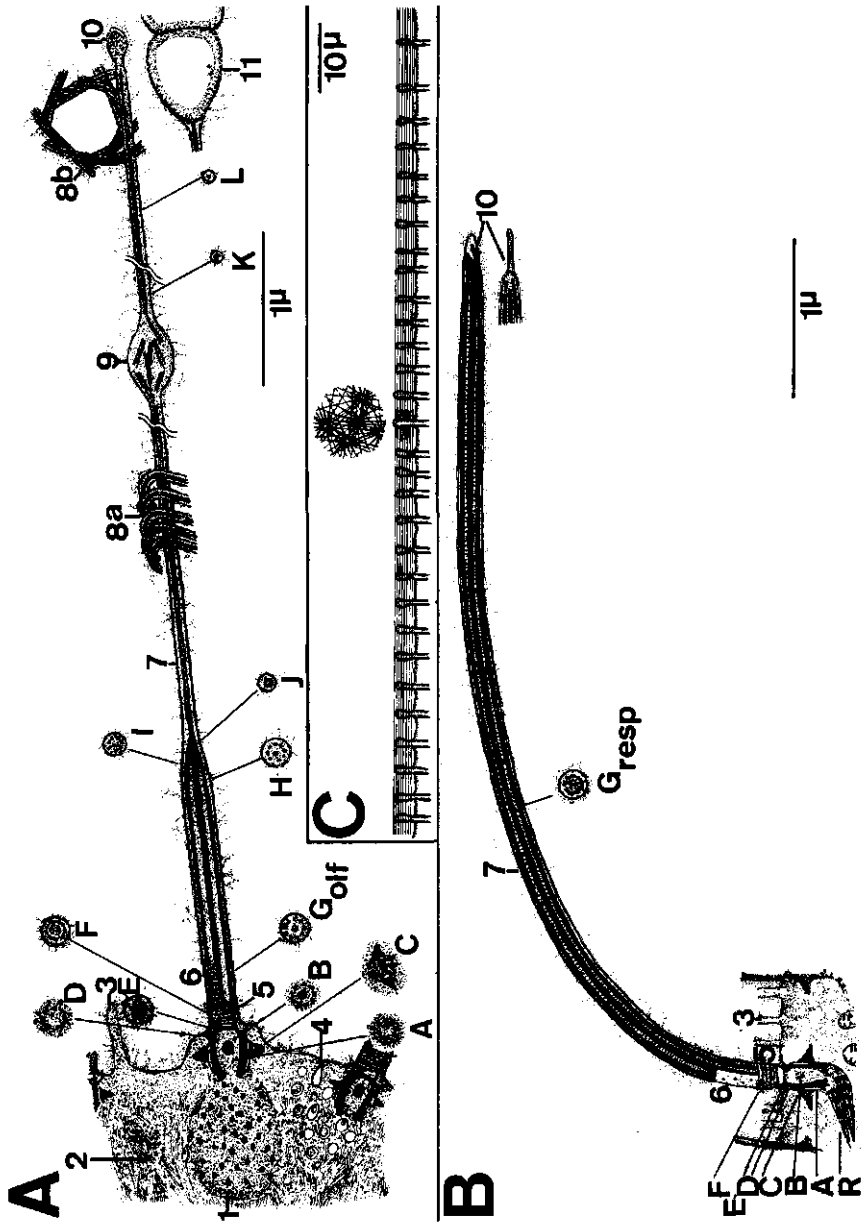

FIG. 56. Diagrammatic representations of an olfactory cilium (**A**) and a respiratory cilium (**B**), and of nerve ending densities, and lengths and number of olfactory cilia (**C**). The three diagrams are drawn to scale. In (**C**) nerve ending densities are presented according to the

mean density of Table XVI. Cilia are drawn according to average (proximal segments) and estimated (distal segments) length (Table XVII). The circular diagram shows about 85 ciliary sections (5 nerve endings, each containing 17 cilia) from autochtonic nerve endings. We estimated that these form only 5%–10% of the total amount of ciliary segments in such an area. The linear diagram in **56C** shows that the cilia of one nerve ending may extend over approximately 15 other nerve endings. Cilia are drawn over 60 μm. (Chapter 3.) All features drawn in Figs. **56A** and **B** are present in the photographs of Chapters 1 and 2. *A-E*: basal body cross-sections; *F-H*: cross-sections through proximal ciliary segments and analogous respiratory ciliary regions; *I-L*: cross-sections through distal ciliary segments; G_{olf} and G_{resp}: a most common cross-section through an olfactory and respiratory cilium. Note the absence of arm-shaped structures on the doublet subfibers in the olfactory cilium. R: rootlet of the basal body of the respiratory cilium.
1: fibrogranular microtubuli pool; *2*: nerve ending microtubuli; *3*: nerve ending microvilli; *4*: endocytotic vesicles; *5*: ciliary necklaces; *6*: P-membranous fracture faces depicting intramembranous particles. Many particles are present in these faces of the olfactory cilia, while only few are present in the respiratory cilia. The P-face represents the inner membranous lamina. *7*: adhering mucus; *8a* and *b*: some formations of the distal ciliary segments as observed by high-voltage electron microscopy; *9*: vesicle formations of the distal segments; *10*: ciliary tips; *11*: vesiculated tip, which is in contact with a tip of another cilium.

the peripheral olfactory system (Chapter 4). The present study deals with bovines and occasionally sheep since their olfactory area is large and samples were readily available.

However, no morphological data on this tissue, essential to support biochemical analyses, were available for these animals when we started this study. Therefore morphological studies were begun. Olfactory tissue was compared consistently with ciliated nasal respiratory mucosal tissue. The following observation methods were used: light microscopy, thin and thick section transmission and scanning electron microscopy. Thick sections were examined at 1,000 kV in an AEI-EM7 high-voltage electron microscope. We hoped, in vain however, that this technique would enable us to see olfactory cilia over their whole length. High-voltage techniques had not been applied previously to this tissue. Some photographs prepared with this technique and with the scanning electron microscope are presented as stereopairs (Chapter 1). In addition freeze-etch techniques have been applied (Chapter 2) to both epithelium types.

The olfactory epithelium is a pseudostratified epithelium covered with a mucus layer of about 5 μm which contains nerve endings from olfactory dendrites. The bipolar receptor cells themselves possess a more or less constant number of cilia (Table XVI) along with some short microvilli (Fig. 56). The dendrites are embedded in an epithelium layer which also contains supporting cells bearing microvilli, some atypical brush cells (which are also found in the respiratory epithelium), and apical parts of the Bowman glands. Most attention is paid to the mucous surface of this epithelium which contains the cilia and microvilli.

Olfactory cilia in the cow are thought to be immotile in contrast to the cilia of the respiratory epithelium. In other cilium types immotility corresponds with the absence of dynein containing arms on the microtubular doublet subfibers.

TABLE XVII. Morphological and some functional differences between bovine olfactory nerve ending cilia and respiratory columnar cell cilia.

Feature observed	Respiratory cilia	Olfactory cilia
1. *Shape*	Cylindrical	Cylindrical, as respiratory cilia over 1.7 μm, then via a conical part taper to a smaller diameter which they maintain for the rest of their length
2. *Basal body*	Striated rootlets present	Striated rootlets absent
3. *Shape tip*	Usually conical with a blunt tip; sometimes short tapers deprived of microtubuli are present	Club-shaped, containing a cap, or vesiculated
4. *Origination*	From a flat cellular surface	From a spherical dendritic nerve ending surface
5. *Mutual orientation*	Parallel	Radial, with the distal segments tapering parallel in bundles
6. *Length*	6.4 μm	Proximal 9(2) + 2 microtubular part: 1.7 μm; distal part: 28 μm (longest distance measured), but could be 50 μm (SEIFERT, 1970) to 200 μm (REESE, 1965)
7. *Diameter*	0.19 μm	Initial part: 0.20 μm Distal part: 0.08 μm
8. *Length/diameter-ratio*	About 34	Could be 1000 to 2000
9. *Cilia per cell*	Numerous; not counted; in any case many more than on olfactory cells	12.5 (observed) About 17 (after correction)
10. *Vesiculation*	Occasionally observed	Frequently observed along their whole length, including tips
11. *Microtubular structures*	Normal 9(2) + 2 microtubular subfibers over their whole length; dynein containing arms present	Proximal normal 9(2) + 2 subfibers, though the doublets here do not possess dynein containing arms. Beyond the proximal part the cilia taper via intermediary stages to distal streamers containing just one or two microtubular subfibers.
12. *Matrix*	Electron-lucent	Electron-dense
13. *Membrane freeze-fracture faces: Particle density:*		
P-face:	0.3×10^3 particles/μm^2	5×10^3 particles/μm^2
E-face:	0.02×10^3 particles/μm^2	0.5×10^3 particles/μm^2
14. *Particle diameter*	11 nm	12 nm
15. *Number of necklace strands*	About 6	About 7
16. *Strand spacing*	173 nm	84 nm
17. *Diameter strand particles*	10 nm	12 nm
18. *Environment provided for stearic acid nitroxide spin probes as measured by electron spin resonance*[1])	Less hydrophobic More isotropic	More hydrophobic More anisotropic
19. *Action*	Motile (LUCAS and DOUGLAS, 1934)	Sensory; probably involved in the odorous perception. The particles, as seen by freeze-etch methods might represent receptor sites.

[1]) These results are obtained from sheep nasal mucosa, and should be considered with great care, since they are only of a very preliminary nature.

Therefore dynein, a Mg^{++}-activated ATPase, and the arms which contain this enzyme, are thought to be responsible for ciliary motion. The arms were observed in respiratory cilia, but not in the axonemal structures of olfactory cilia (Fig. 56, Table XVII and Chapter 1).

In Fig. 56 and Table XVII several other differences between the two cilia types are presented. These tabulations may help to properly identify olfactory cilia during isolation procedures (Chapter 4). At the moment no identification techniques other than microscopy are available. Despite these tabulations proper identification, especially on cross-sections, remains difficult. This is due to the fact that respiratory cilia are present in a vast abundance on the columnar cells while the dendritic nerve endings contain much less olfactory cilia. Apart from that, respiratory cilia contain the normal 9(2) + 2 axonemal structure over distances which are about four times greater than the proximal segments of the olfactory cilia. We calculated that our isolation did not exceed an enrichment of 0.07% in proximal segments of olfactory cilia as percentage of the rest of the cellular material present in the sections on the microscope grids (Chapter 4).

Scanning electron microscopic observation of the nerve endings with proximal cilium segments is frequently accompanied by a loss of the distal ciliary segments. This might be caused by the sample preparation method used. However, the nerve endings themselves can be clearly observed by this technique (Chapter 1). Although often tapers too could be seen clearly with this method, they were observed optimally with high-voltage transmission techniques (Chapter 1). This technique also revealed many empty areas surrounded by ciliary tapers (Fig. 56). These areas might represent expanded air-membrane interfaces. The air might have contained odorous compounds. Conceivably these areas could facilitate odorous interaction since the odorant molecule, which is usually amphiphilic with a large hydrophobic moiety, might pass the watery mucus in such airsacks. Alternatively, these bubbles could have been caused by passing secretion or tissue degradation products. Furthermore the high-voltage technique as well as the scanning technique showed clearly the complexity of the mucus layer which contains ciliary tapers and supporting cell microvilli.

Cilia often contain vesicles (Fig. 56), at least in the olfactory cells. These vesicles might be a feature of ciliary degradation, but they might also represent a functional stage. Sometimes vesicles belonging to different tapers seem to fuse (Chapter 1). Fracture faces of the membranes of such vesicles contain particles like the rest of the cilium (Chapter 2). Recently, however, we observed in rat that these vesicles are frequently devoid of particles in contrast with the rest of the cilium. Therefore different types of vesicles may exist.

Ciliary necklaces have been observed with all techniques applied, including scanning electron microscopy.

Table XVI summarizes the most interesting results of a thorough statistical analysis of a number of photographs (524) from samples prepared with various methods with the exception of freeze-etching (Chapter 3). The purpose of this

analysis was to establish the presence of morphological differences in nerve ending types and to investigate on a quantitative basis the possibility of variations in nerve ending density.

Three different groupings were investigated: (*a*) adult as compared to juvenile tissues; (*b*) olfactory as compared to respiratory epithelium and (*c*) three morphological different areas of the olfactory epithelium were compared to each other. The number of observed cilia per nerve ending (12–13) is remarkably constant in the olfactory tissues and seems to be independent of the groupings examined. In fact, there are probably about 17 of them present per nerve ending, since part of the cilia remains obscured behind the visible part of the nerve ending.

The nerve density in the nasal septum shows the greatest deviation from the average (34%). The density is correlated with epithelium height, which is also highest in the septum. The density seems to decrease by about 20% with increasing age, from 5×10^6 nerve endings/cm^2 in calves of a few weeks old till 4×10^6 nerve endings/cm^2 in adults. These figures were obtained by recalculation of densities obtained at microscope magnifications lower than 10K. These calculations gave probably more accurate mean densities than the values of Table XVI. The reduction of the density of nerve endings appears to be too small to be inversely proportional to the expansion of the olfactory areas during growth. Therefore, our findings indicate that new nerve endings are formed postnatally in the olfactory area (Chapters 1 and 3). Occasionally, whole areas of apparently recently formed nerve endings have been observed in adult animals with the scanning method (Chapter 1). Several authors, using radioactive labeling techniques, have shown that formation and regeneration of peripheral olfactory nervous tissue occurs in mature animals.

The statistical analysis also indicates that there is a slight decrease in the size of nerve ending structures with age. Fig. 56C gives a diagrammatic representation of nerve ending densities and the number of cilia per nerve ending and per surface area.

The major conclusion to be drawn from this part of this study is the presence of a rather homogeneous type of nerve ending. If different types do exist, then they must occur in aggregations smaller than the ones studied. If, at that level too, no different types can be found (apart from the normal variation of course), then odorous discrimination can solely be attributed to differences at a submicroscopical, probably molecular level (Chapter 3).

Freeze-etch studies indicate the presence of a dense intramembranous particle population in the P-faces (inner faces) of olfactory cilia. In our experimental animals this density is about a factor of 19 higher than the particle density on the same faces in respiratory cilia (Table XVII; Fig. 56; Chapter 2). As mentioned before, olfactory cilia are probably immotile in contrast with respiratory cilia. From this we conclude that these particles are probably not involved in motility. Rather, it seems attractive to assume that they have a sensory function. The presence of particles in membranes has frequently been associated with the presence of specific proteins. Assuming that the particles

in the olfactory nerve endings contain a single protein species which is involved in odour reception allows an estimation of receptor concentrations present in the mucus layer covering the epithelium. Using the data of Tables XVI and XVII and knowing that the height of the mucus layer is about 5 μm, permits us to calculate particle concentrations. These may vary between 2×10^{-2} mMol (for 30 μm distal ciliary segments) to 8×10^{-2} mMol (for 100 μm distal ciliary segments). We have also calculated that the maximum particle concentration present in a similar mucous volume does not exceed the actual particle concentration by more than a factor 100 when compared to the particle concentrations for 30 μm distal ciliary segments or more than a factor 30 when compared to particle concentrations when only 100 μm distal ciliary segments are present. This indicates that the particle concentrations which are really present are fairly high. Using STUIVER's (1958) threshold data, we calculated that the particle concentration is about 10^7 times higher than the odour concentration at threshold, while the odour molecule/nerve ending density ratio showed, as has been found previously, that a one to one ratio might exist. If the particles contain a multi-unit proteinaceous receptor as seems to be the case for rhodopsin in the visual system, receptor concentrations might even be higher. The great majority of these particles are located in the ciliary tapers (Chapters 2 and 3). The latter provide a fluid membranous environment containing a mosaic of proteins embedded in the phospholipid bilayers. These tapers are connected to the nerve endings themselves, which of course, is essential for transmitting the neural message corresponding to the odorous stimulus. They provide the olfactory organ with an elaborate system which is able to pack a high receptor concentration in such a way that a transmitting function which involves coding and eventually decoding of a message, can be properly fulfilled (Chapter 3).

Microtubuli, present in both cilia, have several possible functions. They provide the necessary support for the receptive membrane and might play a role in ciliary growth and signal transmission. They could play a role in combination with cyclic nucleotides (Chapter 1).

Very preliminary spin label studies, using stearic acid nitroxide spin labels incorporated in the olfactory and respiratory mucosae of sheep indicated that the olfactory mucosa provides environments for label incorporation which are more hydrophobic and anisotropic than similar environments are in the respiratory mucosa. These effects could be caused by the presence of proteinaceous particles which are visible by freeze-etch techniques (Chapter 2). Sofar no differences in behaviour towards odorants could be detected between the two mucosal types. although in both types, the olfactory as well as the respiratory mucosa, water soluble odorants shifted spin label moieties to more aqueous mucosal environments, while more hydrophobic odorous compounds shifted those label moieties to more hydrophobic mucosal environments. The odour concentrations used, however, were very high, as compared to natural conditions.

ACKNOWLEDGEMENTS

It is a pleasure to thank everybody who was involved in the preparation of this work. In the first place I am grateful to Dr. G. H. Dodd (University of Warwick, Coventry, England) and Prof. E. P. Köster (Psychological Laboratory, State University of Utrecht) for providing me with facilities to carry out the present project. I am also indebted to Prof. L. M. Schoonhoven, who enabled me to submit this work in Wageningen. With Dr. L. H. Bannister (Medical School, Guy's Hospital; University of London) I had many most fruitful discussions. I am glad that he will be co-promotor.

The various EM units in Warwick, Nottingham, Birmingham and Utrecht will be pleased to see that the time spent on me was not totally wasted. Thanks to Gerry Smith, Henry Woodgate, Dr. M. Lewis, Dr. P. H. J. Th. Ververgaert, Dr. M. Davey (Nottingham), Ted Bowden, Dr. R. Thornhill, Dr. C. Dow and Ian Ward.

Klaas Smit subjected very skillfully my results to computer analyses: Thank you Klaas. Marion Alhadeff and Bob Yancey thank you for participating in the correction of the English. Thea van Bemmel and Ria Konter are greatfully acknowledged for their typing.

Last but not least I wish to thank the colleagues I met in the various laboratories: Moshen Nemat Gorgani, Paul Duyvesteyn, Adnan Menevse, Chucks Nwanze, Pieter Punter, Janet Lloyd, Pano Ioannou, Tommy Hendriks, John Mottley and everybody else for their moral support.

The British Medical Research Council (MRC) supplied financial support for the major part of this work.

SAMENVATTING

KWALITATIEVE EN KWANTITATIEVE ONDERZOEKINGEN AAN DE OPPERVLAKKEN VAN HET NASALE REUK- EN ADEMHALINGSSLIJMVLIES VAN RUND EN SCHAAP GEBASEERD OP VERSCHILLENDE ULTRASTRUKTURELE EN BIOCHEMISCHE METHODEN

De olfaktorische- of reukzenuwcel behoort tot het bipolaire celtype waarvan de dendrieten eindigen met knopjes waarop een aantal haarvormige uitlopers zijn geïmplanteerd. Deze haartjes, cilia, bevinden zich in de slijmlaag die het reukepithelium bedekt. Vrij algemeen wordt aangenomen dat deze cilia het merendeel van de geurreceptoren bevatten. Er is geen ander biologisch receptorsysteem bekend, dat op een dergelijke verscheidenheid aan stoffen reageert als het geurreceptorsysteem. Over de aard van de geurreceptor is echter weinig bekend doordat men dit systeem tengevolge van gebrekkige isolatiemethoden, nog niet biochemisch heeft kunnen analyseren.

Het reukepithelium is moeilijk uit de nasale holte te verwijderen. Daardoor is het vrijwel onmogelijk een redelijke hoeveelheid materiaal, benodigd voor biochemische analyses aan dit weefsel, te verkrijgen. Bovendien moeten dan nog strukturen die geen receptorfunctie hebben uit het ruwe materiaal verwijderd worden, om een preparaat te verkrijgen dat nagenoeg alleen uit olfaktorische cilia bestaat. Daar we niet beschikken over biochemische merkers die specifiek voor deze cilia zijn, kunnen we voor een karakterisering alleen hun morfologische verschijning gebruiken. Een dergelijke karakterisering aan de hand van submicroscopische kenmerken werd bereikt met behulp van elektronenmicroscopische technieken. (Hoofdstuk 4). In de onderhavige studie zijn voornamelijk koeien en soms schapen gebruikt. Deze keuze werd bepaald door de gunstige grootte van het geurreceptor gebied, dat in de neus van deze dieren gevonden wordt. Een bijkomend voordeel was dat dit materiaal via het slachthuis verkregen kon worden.

Morfologische details, nodig ter ondersteuning van biochemisch werk aan dit type epithelium zijn voor deze diersoorten niet beschikbaar. Wij waren daardoor genoodzaakt alvorens aan een biochemische benadering te beginnen eerst een morfologisch onderzoek uit te voeren. Eigenschappen van het reukepithelium werden vergeleken met het aangrenzend nasale ademhalings- (respiratorisch) epithelium. Beide typen van epithelium dragen cilia.

De morfologische onderzoekingen werden uitgevoerd met behulp van de volgende observatiemethoden: makroskopische observatie, lichtmikroskopie, dunne- en dikke coupe transmissie- en raster-elektronenmikroskopie. De dikke coupes werden bestudeerd in een AEI-EM 7 hoogspannings-elektronenmikroskoop bij 1000 kilovolt. Wij hoopten, zij het tevergeefs, dat deze techniek ons de mogelijkheid zou bieden olfaktorische cilia over hun hele lengte te volgen. Deze techniek werd nog niet eerder op dit weefsel toegepast. Sommige foto's

die met deze mikroskoop en met de raster-elektronenmikroskoop werden vervaardigd zijn stereoskopisch weergegeven (Hoofdstuk 1). Tevens is op beide soorten epithelium de vries-ets replika techniek toegepast (Hoofdstuk 2).

Het olfaktorische epithelium bestaat uit verschillende naast en boven elkaar liggende celsoorten. Het epitheliumoppervlak is bedekt met een slijmlaag van ongeveer 5 μm dik. De knopvormige uiteinden van de dendrieten van de reukzenuw bevatten een betrekkelijk konstant aantal cilia (Tabel XVI) en enige korte eveneens haarvormige microvilli (Fig. 56 en Hoofdstuk 1). De dendrieten worden omgeven door de toppen van omringende steuncellen. De steuncellen dragen eveneens microvilli. Het epithelium bevat verder basale cellen en enige atypische cellen, die door borstelvormige haarbundeltjes zijn gekenmerkt. Dit celtype komt ook in het respiratorische epithelium voor. Voorts worden in het epithelium de toppen van kliertjes van Bowman aangetroffen. Waarschijnlijk kunnen er nog andere celtypes worden onderscheiden, die als voorlopers van sommige van de bovenstaande celtypes kunnen worden opgevat. Onze studie betreft voornamelijk de mucus oppervlakte, met de daarin opgenomen cilia en microvilli (Hoofdstuk 1).

De cilia van het reukepithelium kunnen zich, althans bij de koe, waarschijnlijk niet bewegen, in tegenstelling tot de overeenkomstige cilia van het respiratorische epithelium. In andere typen van cilia gaat een onbewegelijkheid gepaard met de afwezigheid van armpjes die aan de doubletstrukturen van de mikrotubuli in de cilia zitten. Deze armpjes bevatten het enzym dyneine (een magnesium geaktiveerd adenosine-trifosfatase). Dit enzym is verantwoordelijk voor de eigen beweging van dergelijke cilia. Deze armpjes hebben wij waargenomen in respiratorische cilia, maar niet in de olfaktorische cilia (Fig. 56 en Tabel XVII; Hoofdstuk 1).

Fig. 56 en Tabel XVII laten, behalve bovengenoemd verschil, een aantal andere verschillen tussen beide typen van cilia zien. Dergelijke morfologische verschillen zouden kunnen worden gebruikt bij het identificeren van olfaktorische cilia tijdens isolatieprocedures (Hoofdstuk 4). Ondanks de aangegeven verschillen tussen beide ciliumtypes blijft, in het bijzonder wanneer dwarsdoorsneden worden gebruikt, een goede identifikatie van de olfaktorische cilia moeilijk. Een verontreiniging van een olfaktorisch preparaat met slechts een paar respiratorische cellen leidt tot een zeer moeilijk terugvinden van de olfaktorische cilia. Respiratorische cellen bevatten veel meer cilia per cel dan de bipolaire reukcellen. Verder zijn in de respiratorische cilia de negen doublet- en twee singlet subvezels van de interne mikrotubulaire struktuur aanwezig over een afstand die ongeveer vier maal zo lang is als in de cilia van de reukcellen. Deze laatste cilia verdunnen zich na ongeveer 1,7 μm tot segmenten met een doorsnede van ongeveer 0,08 μm (Tabel XVII). Deze dunne segmenten kunnen een lengte hebben van ongeveer 0,1 mm. Deze segmenten blijken moeilijk terug te vinden te zijn bij zuiveringsprocedures. Daarom gebruikten we voor een karakterisering van frakties alleen de dikkere beginstukjes. De genoemde kenmerken van de respiratorische en olfaktorische cilia hebben tot gevolg dat een respiratorische verontreiniging tijdens een olfakto-

rische zuivering zeer hinderlijk is. Een dergelijke verontreiniging blijkt echter niet of nauwelijks te voorkomen te zijn. Wij hebben berekend dat onze pogingen om cilia van de reukzenuwcellen te isoleren slechts een verrijking opleverden van 0,07% ten opzichte van ander cellulair materiaal (Hoofdstuk 4).

Raster-elektronenmikroskopische waarnemingen aan de zenuwuiteinden van de reukcel, welke nog de dikke beginstukjes van de cilia dragen, toonden aan dat dikwijls de dunne ciliumuitlopers verloren waren gegaan . In andere gevallen werden de reukceluiteinden zelf en de dikke beginstukjes van de cilia door de ciliumuitlopers aan het oog onttrokken. In opnames gemaakt met de hoogspannings-transmissie-elektronenmikroskoop werden de drie substrukturen van de zenuwceluiteinden tezamen goed waargenomen (Hoofdstuk 1). Deze techniek liet verder lege gebiedjes zien, omgeven door ciliumuitlopers (Fig. 56 en Hoofdstuk 1). Deze gebiedjes zouden kunnen dienen voor een vergroting van het grensvlak tussen lucht en receptormembraan. Omdat geurmolekulen veelal een wateroplosbaar en een waterafstotend molekuuldeel bevatten is het denkbaar dat via dergelijke luchtzakjes de geurmolekulen gemakkelijker de waterige mucus passeren alvorens met de membraan een interaktie aan te gaan. Ook de membraanmoleculen bestaan uit polaire en apolaire segmenten. De waargenomen 'holtes' zouden overigens ook het gevolg kunnen zijn van een aantal andere verschijnselen, zoals klierafscheiding, weefselafbraak of een pathologische conditie. In ieder geval laten de hoogspannings-transmissie- en de raster-elektronenmikroskoop duidelijk de complexiteit van de mucuslaag met zijn ciliumuitlopers en microvilli zien.

Cilia bevatten veelal blaasjes (Fig. 56), zowel in het olfaktorische als in het respiratorische epitheel. Mogelijk hebben deze blaasjes een funktie bij de afbraak van de cilia. In het olfaktorische systeem zouden ze echter ook betrokken kunnen zijn bij de zintuigfunktie. Soms lijken deze blaasjes, ofschoon deeluitmakend van verschillende cilia (Fig. 56 en Hoofdstuk 1), met elkaar te versmelten. Foto's gemaakt met de vries-ets techniek laten zien dat, evenals de rest van het cilium, de breukvlakken door het membraan van deze blaasjes talrijke partikels bevatten. Bij de rat blijken er naast deze blaasjes met partikels ook blaasjes voor te komen met vrijwel geen partikels, ofschoon de rest van het cilium daar wel mee voorzien is (Hoofdstuk 2). Dit zou kunnen wijzen op het bestaan van meerdere typen blaasjes.

Halssnoerachtige strukturen, die aan de basis van alle bekende typen van cilia worden gevonden komen ook voor in de beide ciliumtypen die wij hebben onderzocht. Soms was deze struktuur zelfs zichtbaar met de raster-elektronenmikroscoop, althans bij olfaktorische cilia. Het beste zijn ze echter zichtbaar te maken met behulp van de vries-ets techniek (Hoofdstuk 2).

Tabel XVI laat de meest interessante resultaten zien van een statistische analyse van metingen aan de hand van 524 mikroskopische opnames gemaakt met alle toegepaste technieken, met uitzondering van de vries-ets techniek (Hoofdstuk 3). Het doel van deze analyse was om de aan- of afwezigheid van heterogene receptorceltypen vast te stellen en voorts om de verdeling van zenuwuiteinden te bepalen in verschillende gebieden van het reukepithelium.

Drie verschillende groeperingen werden onderzocht: I. Volwassen tegenover jonge dieren; II. De gradient van het reukepithelium naar het respiratorische epithelium; III. Drie verschillende gebieden welke zich morfologisch duidelijk onderscheiden zijn met elkaar vergeleken aan de hand van hun olfaktorisch en respiratorisch epithelium.

Gemiddeld blijkt het aantal waarneembare cilia per zenuwuiteinde ongeveer 12 à 13 te zijn. Dit aantal is onafhankelijk van de wijze van groepering. Correctie voor het deel van de cilia dat zich door ligging achter de rest van het zenuwuiteinde aan de waarneming onttrekt, brengt dit aantal gemiddeld op 17.

De dichtheid van de zenuwuiteinden vertoont de grootste afwijking van het gemiddelde op het nasale septum. Deze afwijking bedraagt ongeveer 34% (laatste rij Tabel XVI). Deze dichtheid is gekorreleerd met de hoogte van het epithelium. Deze hoogte, zowel als de mucushoogte zijn beiden het grootst op het nasale septum. De dichtheid van de zenuwuiteinden neemt wellicht enigszins (ongeveer 20%) af met toenemende leeftijd. Deze dichtheidsafname is echter niet voldoende om de groei van het reukgebied met een omgekeerd evenredige zenuwuiteinde verdunning te verklaren. Hoogstwaarschijnlijk wordt het aantal reukcellen postnataal uitgebreid. Deze gedachte vindt steun door de bevinding dat met de raster-elektronenmikroskoop soms gebieden werden waargenomen waarin de zenuwuiteinden een embryonaal uiterlijk vertonen (Hoofdstukken 1 en 3).

Fig. 56C geeft het aantal zenuwuiteinden per oppervlakte-eenheid met het aantal cilia per zenuwuiteinde schematisch weer. De statistische analyse geeft geen aanleiding om het bestaan te veronderstellen van verschillende typen zenuwuiteinden. Dientengevolge is er ook geen aanleiding het bestaan aan te nemen van morfologisch verschillende typen receptorcellen, die verantwoordelijk zijn voor de geurperceptie. Indien er dus al verschillende typen receptorcellen zouden bestaan, dan zouden zij tengevolge van een niet-homogene verspreiding aan waarneming zijn ontsnapt en/of (wanneer zij niet buiten de normale variatie vielen) andere morfologische karakteristieken moeten bezitten, die niet door ons zijn gebruikt. Indien dergelijke verschillen ook niet op andere morfologische niveaus gevonden kunnen worden moet geurdiskriminatie hoogstwaarschijnlijk worden toegeschreven aan variaties in submikroskopische cellulaire eigenschappen. Wellicht is dit niveau molekulair (Hoofdstuk 3).

Breukvlakken in replicas die met de vries-ets techniek werden vervaardigd, lieten zien dat de olfaktorische cilia een hoge partikeldichtheid in hun intra-membraan oppervlakten bezitten. Deze partikelpopulatie is naar het celplasma en dus niet extracellulair gericht. De partikel-dichtheid in overeenkomstige breukvlakken door de membranen van respiratorische cilia is ongeveer 19 maal lager (Tabel XVII en Fig. 56; Hoofdstuk 2). Omdat de cilia van de reukcellen, in tegenstelling tot respiratorische cilia, waarschijnlijk geen eigen beweging hebben, bevatten deze partikels waarschijnlijk geen materiaal dat nodig is om de cilia te laten bewegen. Het is heel wel mogelijk dat zij een rol vervullen bij de zintuigfunktie van het systeem. In de literatuur kon in verschil-

lende gevallen een verband tussen de aanwezigheid van specifieke eiwitten en een bepaalde partikelpopulatie worden aangetoond. Indien we aannemen dat de partikels, welke hier zijn waargenomen, inderdaad een receptor-funktie hebben en dat deze receptor bestaat uit slechts één type eiwit, dan kunnen we een schatting maken van de hoeveelheid receptor welke in de mucus aanwezig is. We maken daarvoor gebruik van de gegevens van de Tabellen XVI en XVII. We hebben berekend dat, uitgaande van een mucushoogte van ongeveer 5 μm, de mucus een partikelconcentratie bevat die varieert tussen 2×10^{-5} Mol (voor 30 μm lange ciliumuitlopers) en 8×10^{-5} Mol (voor 100 μm lange ciliumuitlopers). Verder berekenden we dat de maximale partikelconcentratie, die in een gelijkblijvend mucusvolume mogelijk is, bovenstaande concentraties, afhankelijk van de ciliumuitloper lengte met niet meer dan een factor 100, respektievelijk 30 zal overtreffen. Er zijn dus redenen om de aanwezigheid van hoge concentraties geurreceptor-moleculen in de slijmlaag te veronderstellen.

Met behulp van STUIVER's (1958) berekeningen over de hoeveelheid geurmolekulen die in de olfaktorische ruimte bij een prikkel op drempel-niveau aanwezig zijn, hebben wij berekend dat de partikelconcentratie de geurmolekuulconcentratie met een factor 10^7 overtreft bij deze drempelwaarde. De geurmolekuul/zenuwuiteinde verhouding daarentegen bedraagt ongeveer 1, hetgeen ook door anderen is gevonden. Ieder partikel zou meerdere receptormolekulen kunnen bevatten, zoals bijvoorbeeld het geval is voor overeenkomstige partikels in de membranen van het visuele receptor systeem. Voor het visuele systeem bestaan er duidelijke aanwijzingen dat per partikel meer dan een molekuul rhodopsine, het visuele receptor eiwit, aanwezig is. Als dit ook hier het geval is wordt bovenstaande factor nog groter dan 10^7. De overmaat aan receptor ten opzichte van geurmolekulen (substraat) wijst op een receptorinteraktie die vergelijkbaar is met hormoon-receptor interactie en dus niet op een systeem dan analoog is aan een enzymatische reaktie, waar in het algemeen het substraat in overmaat aanwezig is (Hoofdstuk 3).

Verreweg het grootste deel van de partikels is gelokaliseerd in de ciliumuitlopers (Hoofdstukken 2 en 3). Onder de partikelbevattende membranen bevinden zich de axonemale microtubulaire strukturen. In de respiratorische cilia hebben deze laatste strukturen een funktie bij de beweging van deze cilia; in de olfaktorische cilia voorzien ze misschien in een manier om de geurmembraan te bevestigen. Verder zouden ze een rol kunnen spelen bij de groei van de cilia en zouden ze samen met cyclische nucleotiden betrokken kunnen zijn bij de verwerking van de geurboodschap (Hoofdstuk 1). De cilia zijn verbonden met de zenuwceluiteinden waardoor het door de geurstof opgewekte signaal naar de rest van de zenuwcel wordt doorgegeven. De ciliumuitlopers vormen een efficiënte structuur (in plaats van het alternatief van vrij zwemmende receptoren) om de mucus van een zo hoog mogelijke receptorconcentratie te voorzien.

Verkennend onderzoek waarbij gebruik werd gemaakt van de elektron-spin-resonantie methode en waarbij stearinezuur spin-labels werden toegepast, liet zien, dat de olfaktorische mucosa labelomgevingen bevat, welke meer

hydrofoob en anisotroop (star) zijn dan overeenkomstige labelomgevingen in de respiratorische mucosa. In deze experimenten werd het schaap als proefdier gebruikt. Met deze techniek konden, tot nu toe, ten aanzien van geurstoffen geen verschillen tussen beide mucosatypen worden aangetoond. Wel verschoof in beide typen mucosa, onder invloed van water-oplosbare geurstoffen, spinlabel naar een meer waterige mucosa omgeving, terwijl hydrofobe geurstoffen het omgekeerde deden. Het verschil in label-incorporeringsgedrag tussen de beide epithelium typen zou een gevolg kunnen zijn van de aanwezigheid van partikels, die met behulp van de vries-ets techniek zijn waargenomen.

De hoop wordt uitgesproken dat het voorgaande onderzoek een aantal morfologische karakteristieken heeft opgeleverd die de isolatie van geurreceptoren kunnen vergemakkelijken waardoor daadwerkelijk tot een degelijk biochemisch onderzoek naar de aard van de werking van dit interessante zintuig kan worden overgegaan.

LITERATURE

ADAMS, D. R., 1972. Olfactory and non-olfactory epithelia in the nasal cavity of the mouse, *Peromyscus*. – Am. J. Anat., **133**: 37–49.

ADAMS, D. R. & MCFARLAND, L. Z., 1971. Septal olfactory organ in *Peromyscus*. – Comp. Biochem. Physiol. A. Comp. Physiol., **40**: 971–974.

AFZELIUS, B. A., 1959. Electron microscopy of the sperm tail. – Biophys. Biochem. Cytol., **5**: 269–281.

AFZELIUS, B. A., 1976. A human syndrome caused by immotile cilia. – Science, **193**: 317–319.

AFZELIUS, B. A., ELIASSON, R., JOHNSON, Ø & LINDHOLMER, C., 1974. Lack of dynein arms in immotile human spermatozoa. – J. Cell Biol., **66**: 225–232.

AHLSTRÖM, P., THALMANN, I., THALMANN, R. & ISE, I., 1975. Cyclic AMP and adenylate cyclase in the inner ear. – Laryngoscope, **85**: 1241–1258.

ALLISON, A. C. & WARWICK, R. T. T., 1949. Quantitative observations on the olfactory system of the rabbit. – Brain, **72**: 186–197.

ALTNER, H. & ALTNER, I., 1974a. Cell apices and cell contacts in the vertebrate olfactory epithelium as revealed by freeze fracturing and tracer experiments. – In: Transduction Mechanisms in Chemoreception, Poynder, T. M., ed.: 59–70, Information Retrieval Ltd., London.

ALTNER, H. & ALTNER-KOLNBERGER, I., 1974b. Freeze-fracture and tracer experiments on the permeability of zonulae occludentes in the olfactory mucosa of vertebrates. – Cell Tissue Res., **154**: 51–59.

ALTNER, H. & KOLNBERGER, I., 1975. The application of transmission electron microscopy on the study of the olfactory epithelium of vertebrates. – In: Methods in Olfactory Research, Moulton, D. G., Turk, A. & Johnston Jr., J. W. eds.: 163–190, Acad. Press, London.

AMENDOLEA, L., FILIPO, R. & CORBACELLI, A., 1972. Aspects of the normal human nasal mucosa by scanning electron microscopy. 1. The ciliary epithelium. – Boll. Soc. Ital. Biol. Sper., **48**: 290–292.

ANDRES, K. H., 1969, On the olfactory epithelium of the cat. – Z. Zellforsch., **96**: 250–274.

ANDRES, K. H., 1975. New morphological results for the physiology of smell and taste. – Arch. Oto-Rhino-Laryng., **210**: 1–41.

ANDREWS, P. M., 1974. A scanning electron microscopic study of the extra pulmonary respiratory tract. – Am. J. Anat., **139**: 399–423.

ASH, K. O., 1968. Chemical sensing: An approach to biological molecular mechanisms using difference spectroscopy. – Science, **162**: 452–454.

ASH, K. O., 1969. Ascorbic acid: Cofactor in rabbit olfactory preparations. – Science, **165**: 901–902.

ASH, K. O., BRANSFORD, J. E. & KOCH, R. B., 1966. Studies on dispersion of rabbit olfactory cells. – J. Cell Biol., **29**: 554–561.

ASH, K. O. and SKOGEN, J. D., 1970. Chemosensing: selectivity, sensitivity and additive effects on a stimulant-induced activity of olfactory preparations. – J. Neurochem., **17**: 1143–1153.

ATEMA, J., 1973. Microtubule theory of sensory transduction. – J. Theor. Biol., **38**: 181–190.

ATEMA, J., 1975. Stimulus transmission along microtubules in sensory cells: An hypothesis. – In: Microtubules and Microtubule Inhibitors, Borgers, M. & De Brabander, M., eds.: 247–257, North-Holland Publishing Company, Amsterdam.

BACCETTI, B., BURRINI, A., PALLINI, V., RENIERI, T., ROSATI, F. & MENCHINI FABRIS, G. F., 1975. The short-tailed human spermatozoa. Ultrastructural alterations and dynein absence. – J. Submicrosc. Cytol., **7**: 349–359.

BAGGOR-SJÖBÄCK, D. & FLOCK, Å., 1977. Freeze-fracturing of the auditory basillar papilla in the lizard *Calotes versicolor*. – Cell Tiss. Res., **177**: 431–443.

BAKHTIN, E. K., 1975. On the origin and possible role of microvesicles in olfactory receptor cells. – Tsitologiya, **17**: 898–901.

BANDMAN, U., RYDGREN, L. & NORBERG, B., 1974. The difference between random movement and chemotaxis. – Exp. Cell Res., **88**: 63–73.

BANNISTER, L. H., 1965. The fine structure of the olfactory surface of teleostean fishes. – Quart. J. Micr. Sci., **106**: 333–342.

BANNISTER, L. H., CLARK, A. D., DUNNE, L. J. & WYARD, S. J., 1975. Electron spin resonance measurements of molecular interactions in mouse olfactory epithelium. – Nature, **256**: 517–518.

BARBER, V. C., 1974. Cilia in sense organs. – In: Cilia and Flagella, Sleigh, M. A., ed.: 403–433, Acad. Press, London.

BARBER, V. C. and BOYDE, A., 1968. Scanning electron microscopic studies of cilia. – Z. Zellforsch., **84**: 269–284.

BEDINI, C., FIASCHI, V. & LANFRANCHI, A., 1976. Olfactory nerve reconstruction in the homing pigeon after resection: Ultrastructural and electrophysiological data. – Arch. Ital. Biol., **114**: 1–22.

BEESTON, B. E. P., 1972. High voltage electron microscopy of biological specimens: some practical considerations. – J. Microscopy, **98**: 402–416.

BERGSTROM, B. H., HENLEY, C. & COSTELLO, D. P., 1973. Particulate flagellar and ciliary necklaces revealed by the use of freeze-etch. – Cytobios, **7**: 51–60.

BERLINER, L. J., ed., 1976. Spin Labeling: Theory and Applications. – Acad. Press, New York.

BERTMAR, G., 1972. Scanning electron microscopy of the olfactory rosette in sea trout. – Z. Zellforsch., **128**: 336–346.

BERTMAR, G., 1973. Ultrastructure of the olfactory mucosa in the homing Baltic sea trout *Salmo trutta trutta*. – Marine Biol., **19**: 74–88.

BITENSKY, M. W., MILLER, W. H., GORMAN, R. E., NEUFIELD, A. H. & ROBINSON, R., 1972. The role of cyclic AMP in visual excitation. – In: Adv. Cyclic Nucleot. Res., **Vol. 1**, Greengard, P., Paoletti, R. & Robinson, G. A., eds.: 317–335, Raven Press, New York.

BLAISE, J. K., WORTHINGTON, C. R. and DEWEY, M., 1969. Molecular localization of frog retinal receptor photopigment by electron microscopy and low-angle X-ray diffraction. – J. Mol. Biol., **39**: 407–416.

BLOCK, E. F. & BELL, W. J., 1974. Ethomeric analysis of pheromone receptor function in cockroaches. – J. Insect Physiol., **20**: 993–1003.

BLOOM, G., 1954. Studies on the olfactory epithelium of the frog and the toad with the aid of light and electron microscopy. – Z. Zellforsch., **41**: 89–100.

BLUM, J. J., 1971. Existence of a breaking point in cilia and flagella. –J. Theor. Biol., **33**: 257–263.

BOZARTH, A. J. & STRAFUSS, A. C., 1974. Ultrastructural characteristics of the submucosal glands of normal bovine respiratory nasal mucosa. – Cornell Vet., **64**: 57–71.

BRANTON, D., 1971. Freeze-etching studies of membrane structure. – Phil. Trans. Roy. Soc. Lond. B, **261**: 133–138.

BRANTON, D., BULLIVANT, S., GILULA, N. B., KARNOVSKY, M. J., MOOR, H., MÜHLETALER, K., NORTHCOTE, D. H., PACKER, L., SATIR, B., SATIR, P., SPETH, V., STAEHELIN, L. A., STEERE, R. L. & WEINSTEIN, R. S., 1975. Freeze-etching nomenclature. – Science, **190**: 54–56.

BREESE, Jr., S. S. & ZACHARIA, T. P., 1974. Methods in electron microscopy. – In: Methods in Molecular Biology., **Vol. 5**: Subcellular Particles, Structures and Organelles, Laskin, A. I. & Last, J. A., eds.: 231–263, Marcel Dekker, New York.

BREIPOHL, W., BIJVANK, G. J., PFEFFERKORN, G. E., 1974a. Scanning electron microscopy of various sensory receptor cells in different vertebrates. – In: Scanning Electron Microscopy, **Vol. 7**: Johari, O. & Corvin, I., eds.: 557–564, I.I.T. Research Institute, Chicago, Illinois.

BREIPOHL, W., BIJVANK, G. J. & ZIPPEL, H. P., 1973a. Scanning electron microscopy of olfactory receptors in *Carassius auratus*. – Z. Zellforsch., **138**: 439–454.

BREIPOHL, W., BIJVANK, G. J. & ZIPPEL, H. P., 1973b. Scanning electron microscopy of the olfactory glands in the goldfish (*Carassius auratus*). – Z. Zellforsch., **140**: 567–582.
BREIPOHL, W., LAUGWITZ, H. & BIJVANK, J., 1974b. Scanning electron microscopical findings on olfactory receptors. – Verh. Anat. Ges., **68**: 793–797.
BREIPOHL, W., LAUGWITZ, H. J. & BORNFELD, N., 1974c. Topological relations between the dendrites of olfactory sensory cells and sustentacular cells in different vertebrates. An ultrastructural study. – J. Anat., **117**: 89–94.
BRONSHTEIN, A. A. & MINOR, A. V., 1977. The regeneration of olfactory flagella and restoration of electro-olfactogram after treatment of the olfactory mucosa with Triton X-100. – Tsitologiya, **19**: 33–39.
BYRKIT, D. R., 1975. Elements of Statistics. An Introduction to Probability and Statistical Inference. – D. Van Nostrand Company, New York.
CAGAN, R. H., 1976. Biochemical studies of taste sensation. II. Labeling of cyclic AMP of bovine taste papillae in response to sweet and bitter stimuli. – J. Neurosci. Res., **2**: 363–372.
CARPENTIER, J.-L., PERRELET, A. & ORCI, L., 1976. Effects of insulin, glucagon and epinephrine on the plasma membrane of the white adipose cell: a freeze-fracture study. – J. Lipid Res., **17**: 335–342.
CARTAUD, J., 1974. Structural organization of the excitable membrane of the *Torpedo marmomata* electrical organ. – In: 8th Int. Congr. Electron Microscopy, Sanders, J. V. & Goodchild, D. J., eds.: 284–285, Austr. Acad. Sci., Canberra.
CARTAUD, J. & BENEDETTI, E. L., 1973. Presence of a lattice structure in membrane fragments rich in nicotine receptor protein from the electric organ of *Torpedo marmomata*. – FEBS Letters, **33**: 109–113.
CHANGEUX, J.-P., BENEDETTI, L., BOURGEOIS, J.-P., BRISSON, A., CARTAUD, J., DEVAUX, P., GRÜNHAGEN, H., MOREAU, M., POPOT, J.-L., SOBEL, A. & WEBER, M., 1975. Some structural properties of the cholinergic receptor protein in its membrane environment relevant to its function as a pharmacological receptor. – Cold Spring Harbor Symp., **40**: 211–230.
CHEN, Y. S. & HUBBELL, W. L., 1973. Temperature- and light-dependent structural changes in rhodopsin-lipid membranes. – Exp. Eye Res., **17**: 517–532.
CHERRY, R. J., DODD, G. H. & CHAPMAN, D., 1970. Small molecule-lipid membrane interactions and the puncturing theory of olfaction. – Biochim. Biophys. Acta, **211**: 409–416.
CLARK, A. W. & BRANTON, D., 1968. Fracture faces in frozen outer segments from the guinea pig retina. – Z. Zellforsch., **91**: 586–603.
CLAUDE, P. & GOODENOUGH, D. A., 1973. Fracture faces of zonulae occludentes from 'tight' and 'leaky' epithelia. – J. Cell Biol., **58**: 390–400.
CONTICELLO, S., BIONDI, S. & MALANNINO, N., 1973. A cytological study of the olfactory epithelium in the guinea pig. – Clin. Otorinolaring., **25**: 162–171.
CUSCHIERI, A. & BANNISTER, L. H., 1974. Some histochemical observations on the mucosubstances of the nasal glands of the mouse. – Histochem. J., **6**: 543–558.
CUSCHIERI, A. & BANNISTER, L. H., 1975. The development of the olfactory mucosa in the mouse: electron microscopy. – J. Anat., **119**: 471–498.
DAEMEN, F. J. M., 1973. Vertebrate rod outer segment membranes. – Biochim. Biophys. Acta, **300**: 255–288.
DALEY, D. L. & VANDE BERG, J. S., 1976. Apparent opposing effects of cyclic AMP and dibutyryl-cyclic GMP on the neuronal firing of the blowfly chemoreceptors. – Biochim. Biophys. Acta, **437**: 211–220.
DAVIES, J. T., 1971. Olfactory theories. – In: Handbook of Sensory Physiology, **Vol. IV**: Chemical Senses, **Part 1**: Olfaction, Beidler, L. M., ed.: 322–350, Springer-Verlag, Berlin.
DE LORENZO, A. J. D., 1970. The olfactory neuron and the blood-brain barrier. – In: Taste and Smell in Vertebrates, Wolstenholme, G. E. W. & Knight, J. eds.: 151–176, J. & A. Churchill, London.
DODD, G. H., 1970. The adenosine triphosphate activities of the olfactory mucosae of some

common animals. – Comp. Biochem. Physiol., **36**: 633–637.
DODD, G. H., 1971. Studies on olfactory receptor mechanisms. – Biochem. J., **123**: 31p-32p.
DODD, G. H., 1974. Structure and function of chemoreceptor membranes. – In: Transduction Mechanisms in Chemoreception, Poynder, T. M., ed.: 103–113, Information Retrieval Ltd., London.
DODD, G. & CASH, C., 1974. Lipofuscins, ascorbic acid and the olfactory pigment. – Proc. 1st ECRO Congress, Orsay, France: 33.
DRENCKHAHN, D., 1970. On the regio olfactoria and nervus olfactorius in the gull, *Larus argentatus*. – Z. Zellforsch., **106**: 119–142.
EBREY, T. G. and HONIG, B., 1975. Molecular aspects of photoreceptor function. – Quart. Rev. Biophys., **8**: 129–184.
ECHLIN, P., 1975. Sputter coating techniques for scanning electron microscopy. – In: Scanning Electron Microscopy, **Vol. 8**, Johari, O. & Corvin, I., eds.: 217–224, I.I.T. Research Institute, Chicago, Illinois.
EDELSON, P. J. & FUDENBERG, H. F., 1973. Effect of vinblastine on the chemotactic responsiveness of normal human neutrophils. – Infection Immunity, **8**: 127–129.
ELETR, S., ZAKIM, D. & VESSEY, D. A., 1973. A spin-label study of the role of phospholipids in the regulation of membrane-bound microsomal enzymes. – J. Mol. Biol., **78**: 351–362.
ERNST, L. K. & PUSHKARSKII, V. G., 1975. The biological indication of odors in cows: Review. – S-Kh. Biol., **10**: 563–567.
FARBMAN, A. I., 1973. Differentiation of olfactory mucosa in organ culture. – Anat. Rec., **175**: 317.
FARBMAN, A. I. & GESTELAND, R. C., 1974a. Fine structure of olfactory epithelium in the mud puppy. – Am. J. Anat., **139**: 227–244.
FARBMAN, A. I. & GESTELAND, R. C., 1974b. Developmental and electrophysiological studies of olfactory mucosa in organ culture. – Proc. 1st ECRO Congress, Orsay, France: 31.
FARBMAN, A. I. & GESTELAND, R. C., 1975. Developmental and electrophysiological studies of olfactory mucosa in organ culture. In: Olfaction and Taste, V, Denton, D. & Coghlan, J. P., eds.: 107–110, Acad. Press, New York.
FARVARD, P. & CARASSO, N., 1973. The preparation and observation of thick biological sections in the high voltage electron microscope. – J. Microscopy, **97**: 59–81.
FAWCETT, D. W., 1975. The mammalian spermatozoon. – Develop. Biol., **44**: 394–436.
FERRON, J., 1973. A comparative morphological study of the olfactory organ of several carnivorous mammals. – Naturaliste Canad., **100**: 525–541.
FISHER, K. & BRANTON, D., 1975. Application of the freeze-fracture technique to natural membranes. – Methods Enzymol., **32**: 35–44.
FLANGAS, A. L., 1974. Bulk separations of rat brain cells by centrifugal elutriation. – Prep. Biochem., **4**: 165–177.
FLOWER, N. E., 1971. Particles within membranes: a freeze-etch view. – J. Cell Sci., **9**: 435–441.
FRISCH, D., 1967. Ultrastructure of mouse olfactory mucosa. – Am. J. Anat., **121**: 87–119.
FURUTA, M., ICHITANI, Y., FUKAZAWA, M., TSUKISE, A., OKANO, M. & SUGAWA, Y., 1975. Ultrastructure of olfactory mucosa of newborn rats. – Bull. Coll. Agr. & Vet. Med., Nihon Univ., **32**: 202–212.
FURUTA, M., TSUKISE, A., OKANO, M. & SUGAWA Y., 1974. Ultrastructure of kitten olfactory mucosa. – Bull. Coll. Agr. & Vet. Med., Nihon Univ., **31**: 229–240.
GASSER, H. S., 1956. Olfactory nerve fibers. – J. Gen. Physiol., **39**: 473–496.
GENNINGS, J. N., GOWER, D. B. & BANNISTER, L. H., 1974. Studies on the metabolism of the odoriferous ketones, 5α-androst-16-en-3-one and 4, 16-androstadien-3-one by the nasal epithelium of the mature and immature sow. – Biochim. Biophys. Acta, **369**: 294–303.
GENNINGS, J. N., GOWER, D. B. & BANNISTER, L. H., 1976. Preliminary characterisation of an olfactory receptor to 5α-androst-16-en-3-one in the sow. – Proc. 2nd ECRO Congress, Reading, England: 27.
GENNINGS, J. N., GOWER, D. B. & BANNISTER, L. H., 1977. Studies on the receptors to 5α-

androst-16-en-3-one and 5α-androst-16-en-3α-ol in sow nasal mucosa. – Biochim. Biophys. Acta, **496**: 547–556.
GETCHELL, M. L. & GESTELAND, R. C., 1972. The chemistry of olfactory reception: Stimulus-specific protection from sulfhydryl reagent inhibition. –Proc. Nat. Acad. Sci. U.S., **69**: 1494–1498.
GETCHELL, T. V., 1973. Analyses of unitary spikes recorded extracellularly from frog olfactory receptor cells and axons. – J. Physiol., **234**: 533–551.
GIBBONS, I. R., 1965. Chemical dissection of cilia. – Arch. Biol. (Liège), **76**: 317–352.
GILULA, N. B. & SATIR, P., 1972. The ciliary necklace. A ciliary membrane specialization. – J. Cell Biol., **53**: 494–509.
GLAUERT, A. M., 1974. The high voltage electron microscope in biology. – J. Cell Biol., **63**: 717–748.
GLAUERT, A. M. & GLAUERT, R. H., 1958. Araldite as an embedding medium for electron microscopy. – J. Biophys. Biochem. Cytol., **4**: 191–194.
GOLDSTEIN, S. F., 1974. Isolated, reactivated and laser-irradiated cilia and flagella. – In: Cilia and Flagella, Sleigh, M. A., ed.: 111–130, Acad. Press, London.
GORIDIS, C., COQUIL, J. F., CAILLA, H. L. & URBAN, P. F., 1975. Cyclic nucleotides and photoreceptor function of vertebrate retina. – Proc. 10th FEBS Meeting, **41**: 151–163.
GRANT, C. W. M. & MCCONNELL, H. M., 1974. Glycophorin in lipid bilayers. – Proc. Nat. Acad. Sci. U.S., **71**: 4653–4657.
GRAZIADEI, P. P. C., 1966. Electron microscopic observations of the olfactory mucosa of the mole. – J. Zool. (Lond.), **149**: 89–94.
GRAZIADEI, P. P. C., 1970. The mucous membranes of the nose. – Ann. Otol. Rhinol. Laryngol., **79**: 433–442.
GRAZIADEI, P. P. C., 1971a.Topological relations between olfactory neurons. – Z. Zellforsch., **118**: 449–466.
GRAZIADEI, P. P. C., 1971b. The olfactory mucosa of vertebrates. – In: Handbook of Sensory Physiology, **Vol. IV**: Chemical Senses, **Part 1**: Olfaction, Beidler, L. M., ed.: 27–58, Springer-Verlag, Berlin.
GRAZIADEI, P. P. C., 1973a. The ultrastructure of vertebrates olfactory mucosa. – In: The Ultrastructure of Sensory Organs, Friedman, I., ed.: 267–305, North-Holland Publishing Company, Amsterdam.
GRAZIADEI, P. P. C., 1973b. Cell dynamics in the olfactory mucosa. – Tissue & Cell, **5**: 113–131.
GRAZIADEI, P. P. C., 1974a. The olfactory organ of vertebrates: A survey. – In: Essays on the Nervous System, Bellairs, R. & Gray, E. G., eds.; 191–222, Clarendon Press, Oxford.
GRAZIADEI, P. P. C., 1974b. The olfactory and taste organs of vertebrates: a dynamic approach to the study of their morphology. – In: Transduction Mechanisms in Chemoreception, Poynder, T. M., ed.: 3–14, Information Retrieval Ltd., London.
GRAZIADEI, P. P. C., 1975. Application of scanning electron microscopy and autoradiography in the study of olfactory mucosa. – In: Methods in Olfactory Research, Moulton, D. G., Turk, A. & Johnston Jr., J. W., eds.: 191–240, Acad. Press, London.
GRAZIADEI, P. & BANNISTER, L. H., 1967. Some observations on the fine structure of the olfactory epithelium in the domestic duck. – Z. Zellforsch., **80**: 220–228.
GRAZIADEI, P. P. C. & GRAZIADEI, G. A. M., 1976. Olfactory epithelium of *Necturus maculosus* and *Ambystoma tigrinum*. – J. Neurocytol., **5**: 11–32.
GUSEL'NIKOV, V. I., KOROLEV, A. M. & FROLOV, O. YU., 1974. Interaction of odorants and the olfactory hairs of the frog in vitro. – Dokl. Akad. Nauk. SSSR. Ser. Biol., **216**: 448–451.
HARA, T. J., 1975. Olfaction in fish. – Progr. Neurobiol., **5**: 271–335.
HARTMAN, H., 1975. The centriole and the cell. – J. Theor. Biol., **51**: 501–509.
HEIST, H. E. & MULVANEY, B. D., 1968. Centriole migration. – J. Ultrastruct. Res., **24**: 86–101.
HEIST, H. E., MULVANEY, B. D. & LANDIS, D. J., 1967. Odor sensing cell ultrastructure by

electron microscopy. – Air Force Office of Scientific Research Contract No. AF 49(638)-1618. Honeywell Corporate Research Center, Honeywell Inc., Hopkins, Minnesota.
HOLLEY, A., 1975. Odour perception. – La Recherche, **6**: 629–639.
HOLLEY, A., DELALEU, J. Cl., REVIAL, M. F. & JUGE, A., 1976. Quantitative stimulation of frog olfactory receptors: Concentration-response relationships – Proc. 2nd ECRO Congress, Reading, England: 42.
HOLMES, D. E., 1973. Drug-induced changes in electron spin resonance spectra from spin-labeled membranes. – Molec. Pharmacol., **1 Pt. 2**: 601–635.
HONG, K. & HUBBELL, W. L., 1972. Preparation and properties of phospholipid bilayers containing rhodopsin. – Proc. Nat. Acad. Sci. U.S., **69**: 2617–2621.
HÖRANDNER, H., KERJASCHKI, D. & STOCKINGER, L., 1974. Rodshaped particles in epithelial free surface membranes. – In: 8th Int. Congr. Electron Microscopy, Sanders, J. V. & Goodchild, D. J., eds.: 210–211, Austr. Acad. Sci., Canberra.
HUBBELL, W. L. & MCCONNELL, H. M., 1968. Spin-label studies of the excitable membranes of nerve and muscle. – Proc. Nat. Acad. Sci. U.S., **61**: 12–16.
INOUE, F., 1974. Scanning electron microscopic findings of nasal mucosa. – Otol. Fukuoka, **20**: 202–220.
JACKSON, R. T. & LEE, C.-C., 1965. Degeneration of olfactory receptors induced by colchicine. – Exp. Neurol., **11**: 483–492.
JAHNKE, K., 1975. In discussion: ROLLIN, H. Function and disturbances of the sense of taste. – Arch. Oto-Rhino-Laryng., **210**: 225.
JAHNKE, K., 1976. The fine structure of freeze-fractured intercellular junctions in the guinea pig inner ear. – Acta Oto-Laryng., Suppl., **336**: 5–40.
JAKINOVICH Jr., W., 1976. Stimulation of the gerbil's gustatory receptors by disaccharides. – Brain Res., **110**: 481–490.
JAKINOVICH Jr., W. & GOLDSTEIN, I. J., 1976. Stimulation of the gerbil's gustatory receptors by monosaccharides. – Brain Res., **110**: 491–504.
JAKINOVICH Jr., W. & OAKLEY, B., 1976. Stimulation of the gerbil's gustatory receptors by polyols. – Brain. Res., **110**: 505–513.
JAN, L. Y. & REVEL, J.-P., 1974. Ultrastructural localization of rhodopsin in the vertebrate retina. – J. Cell Biol., **62**: 257–273.
JEFFERY, P. K. & REID, L., 1975. New observations of rat airway epithelium: a quantitative and electron microscopic study. – J. Anat., **120**: 295–320.
JOST, P., WAGGONER, A. S. & GRIFFITH, O. H., 1971. Spin labeling and membrane structure. – In: Structure and Function of Biological Membranes, Rothfield, L. I. ed.: 83–144, Acad. Press, London.
JOURDAN, F., 1975. Ultrastructure of the olfactory epithelium of the rat: receptor polymorphism. – C. R. Acad. Sc. Paris, **280**: 443–446.
KAHN, C. R., 1976. Membrane receptors for hormones and neurotransmitters. – J. Cell Biol., **70**: 261–286.
KANDA, T., KITAMURA, T., KANEKO, T. & TIZUMI, O., 1973. Scanning electron microscopical observations on the olfactory epithelium of guinea pig and human being. – J. Otolaryngol., Japan, **76**: 30.
KARNOVSKY, M. J., 1965. A formaldehyde fixative of high osmolality for use in electron microscopy. – J. Cell Biol., **27**: 137A–138A.
KATES, M., 1975. Techniques of Lipidology: Isolation, Analysis and Identification of Lipids. – Laboratory Techniques in Biochemistry and Molecular Biology, **Vol. 3, Part 2**, Work, T. S. & Work, E., eds., North-Holland Publishing Company, Amsterdam..
KEITH, A. D., SHARNOFF, M. & COHN, G. E., 1973. A summary and evaluation of spin labels used as probes for biological membrane structure. – Biochim. Biophys. Acta, **300**: 379–419.
KERJASCHKI, D., 1976. The central tubuli in distal segments of olfactory cilia lack dynein arms. – Experienta, **32**: 1459–1460.
KERJASCHKI, D. & HÖRANDNER, H., 1976. The development of mouse olfactory vesicles and

their cell contacts: A freeze-etching study. – J. Ultrastruct. Res., **54**: 420–444.
KERJASCHKI, D., SLEYTR, U. & STOCKINGER, L., 1972. Surface structures of nerve-endings in the olfactory epithelium as seen by freeze-etching. – Die Naturwissenschaften, **59**: 314–315.
KOCH, R. B., 1972. Biochemical studies of olfactory tissue: Responses of ATPase activities to octanol and ascorbic acid. – Chem.-Biol. Interactions, **4**: 195–208.
KOCH, R. B., 1973. Biochemical studies on olfactory mucosa. – In: Pharmacology and the Future of Man, **Vol. 5**, Maxwell, R. A., ed.: 31–46, Karger, Basel.
KOCH, R. B. & DESAIAH, D., 1974. Preliminary studies on rat olfactory tissue: Effects of odorants on Na^+-K^+-ATPase activity. – Life Sci., **15**: 1005–1016.
KOCH, R. B. & GILLILAND, T. I., 1977. Responses of Na^+-K^+-ATPase activities from dog olfactory tissue to selected odorants. – Life Sci., **20**: 1051–1062.
KOCH, R. B. & NORRING, N. L., 1969. Fractionating of olfactory tissue homogenates. Isolation of a concentrated plasma membrane fraction. – J. Neurochem., **16**: 145–157.
KOELEGA, H. S. & KÖSTER, E. P., 1974. Some experiments on sex differences in odor perception. – Ann. N.Y. Acad. Sci., **237**: 234–246.
KOLB, A., 1971. Examinations by light and electron microscope of the cavum nasi and olfactory epithelium in some kinds of bats. – Z. Saügetierkd., **36**: 202–213.
KOLB, A., 1975. Light microscopic studies on the olfactory epithelium of the roe (*Capreolus capreolus*). – Anat. Anz., **137**: 417–428.
KONIJN, T. M., 1974. Chemotactic effect of cyclic AMP and its analogues in the *Acrasieae*. – Antibiot. Chemoter. (Basel), **19**: 96–110.
KOLNBERGER, I. & ALTNER, H., 1971. Ciliary-structure precursor bodies as stable constituents in the sensory cells of the vomero-nasal organ of reptiles and mammals. – Z. Zellforsch., **118**: 254–262.
KOROLEV, A. M. & FROLOV, O. Yu., 1973. A method of isolating frog olfactory cilia. – Fiziol. Zh. SSSR. Im. I.M. Sechenova, **59**: 176–179.
KOYAMA, N. & KURIHARA, K., 1972. Effects of odorants on lipid monolayers from bovine olfactory epithelium. – Nature, **236**: 402–404.
KOYAMA, N., SAWADA, K. & KURIHARA, K., 1971. Isolation and some properties of plasma membranes from bovine olfactory epithelium. – Biochim. Biophys. Acta, **241**: 42–48.
KRATZING, J. E., 1972. The structure of olfactory cilia in a lizard. – J. Ultrastruct. Res., **39**: 295–300.
KRATZING, J. E., 1975. The fine structure of the olfactory and vomeronasal organs of a lizard (*Tiliqua scincoides scincoides*). – Cell Tissue Res., **156**: 239–252.
KREBS, H. A., 1950. Body size and tissue respiration. – Biochim. Biophys. Acta, **4**: 249–269.
KURIHARA, K. & KOYAMA, N., 1972. High activity of adenyl cyclase in olfactory and gustatory organs. – Biochem. Biophys. Res. Comm., **48**: 30–34.
LAGNADO, J. R., LYONS, C. & WICKREMASINGHE, G., 1971. The subcellular distribution of colchine-binding protein ('microtubule protein') in rat brain. – FEBS Letters, **15**: 254–260.
LEESON, T. S., 1970. Rat retinal rods: freeze-fracture replication of outer segments. – Canad. J. Ophthal., **5**: 91–107.
LEESON, T. S., 1971. Freeze etch studies of rabbit eye. II. Outer segments of retinal photoreceptors. – J. Anat., **108**: 147–157.
LE GROS CLARK, W., 1957. Inquiries into the anatomical basis of olfactory discrimination. – Proc. Roy. Soc., **146**: 299–319.
LENZ, H., 1972. Stereoscopic demonstration of cilia in human nasal mucosa with the scanning electron microscope. – Z. Laryng. Rhinol., **51**: 618–632.
LENZ, H., 1976. The olfactory region and the course of the fila olfactoria through the lamina cribosa and dura mater in the scanning-electron-microscope. – Arch. Oto-Rhino-Laryng., **213**: 455–456.
LEVANDOVSKY, M., HAUSER, D. C. R. & GLASSGOLD, J. M., 1975. Chemosensory responses of a protozoan are modified by antitubulins. – J. Bacteriol., **124**: 1037–1038.

LEWIS, E. R. & NEMANIC, M, K., 1973. Critical point drying techniques. – In: Scanning Electron Microscopy, **Vol. 6**, Johari, O. & Corvin, I., eds.: 768–774, I.I.T. Research Institute, Chicago, Illinois.
LIBERTINI, L. J., WAGGONER, A. S., JOST, P. C. & GRIFFITH, O. H., 1969. Orientation of lipid spin labels in lecithin multilayers. – Proc. Nat. Acad. Sci. U.S., **64**: 13–19.
LOCKÉ, M. & KRISHNAN, N., 1971. Hot alcoholic phosphotungstic acid and uranyl acetate as routine stains for thick and thin sections. – J. Cell Biol., **50**: 550–557.
LOCKE, M., KRISHNAN, N. & MCMAHON, J. T., 1971. A routine method for obtaining high contrast without staining sections. – J. Cell Biol., **50**: 540–544.
LOO, S. K., 1977. Fine structure of the olfactory epithelium in some primates. – J. Anat., **123**: 135–146.
LOWE, G. A., 1974. The occurrence of ciliary aggregations on the olfactory epithelium of two species of gadoid fish. – J. Fish Biol., **6**: 537–539.
LOWE, G. A. & MACLEOD, N. K., 1975. The ultrastructural organization of olfactory epithelium of two species of gadoid fish. – J. Fish Biol., **7**: 529–532.
LUCAS, A. M. & DOUGLAS, L. C., 1934. Principles underlying ciliary activity in the respiratory tract. II. A comparison of nasal clearance in man, monkey and other mammals. – Arch. Otolaryngol., **20**: 518–541.
LUM, C. K. L. & HENKIN, R. I., 1976. Sugar binding to purified fractions from bovine taste buds and epithelial tissue. Relationships to bioactivity. – Biochim. Biophys. Acta, **421**: 380–394.
LUM, C. K. L., WHITTAKER, N. F. & HENKIN, R. I., 1976. Preparation and isolation of a taste bud-derived fraction from bovine circumvallate papillae. – Biochim. Biophys. Acta., **421**: 353–361.
MARGOLIS, F. L., 1972. A brain protein unique to the olfactory bulb. – Proc. Nat. Acad. Sci. U.S., **69**: 1221–1224.
MARGOLIS, F. L., 1974. Carnosine in the primary olfactory pathway. – Science, **184**: 909–911.
MARGOLIS, F. L., 1975. Biochemical markers of the primary olfactory pathway: a model neural system. – Adv. Neurochem., **1**: 193–246.
MARGOLIS, F. L. & TARNOFF, J. F., 1973. Site of biosynthesis of the mouse brain olfactory bulb protein. – J. Biol. Chem., **248**: 451–455.
MARGULIS, L., 1973. Colchicin-sensitive microtubules. – Int. Rev. Cytol., **34**: 333–361.
MASON, W. T., FAGER, R. S. & ABRAHAMSON, E. W., 1974. Structural response of vertebrate photoreceptor membranes to light. – Nature, **247**: 188–191.
MARTÍNEZ-PALOMO, A. & ERLIJ, D., 1975. Structure of tight junctions in epithelia with different permeability. – Proc. Nat. Acad. Sci. U.S., **72**: 4487–4491.
MATULIONIS, D. H., 1975. Ultrastructural study of mouse olfactory epithelium following destruction by $ZnSO_4$ and its subsequent regeneration. – Am. J. Anat., **142**: 67–89.
MATULIONIS, D. H., 1976. Light and electron microscopic study of the degeneration and early regeneration of olfactory epithelium in the mouse. – Am. J. Anat., **145**: 79–99.
MATULIONIS, D. H. & Parks, H. F., 1973. Ultrastructural morphology of the normal nasal respiratory epithelium of the mouse. – Anat. Rec., **176**: 65–83.
MENCO, B. P. M., 1976. The movement of frog olfactory cilia. – Film for TELEAC-foundation, Utrecht, Holland.
MENCO, B. P. M., DODD, G. H., DAVEY, M. & BANNISTER, L. H., 1976. Presence of membrane particles in freeze-etched bovine olfactory cilia. – Nature, **263**: 597–599.
MENCO, B., MENEVSE, A. & DODD, G., 1974a. Studies on olfactory cilia. – Proc. 1st ECRO Congress, Orsay, France: 32.
MENCO, B., SCHOONHOVEN, L. M. & VISSER, J., 1974b. Qualitative and quantitative analyses of electrophysiological responses of an insect taste receptor. – Proc. Koninkl. Nederl. Akademie van Wetenschappen, Series C, **77**: 157–170.
MENEVSE, A., CHENG, L., MENCO, B. & DODD, G., 1974. Adenyl cyclase activities of olfactory and gustatory plasma membranes. – Proc. 1st ECRO Congress, Orsay, France: 32.
MENEVSE, A., DODD, G. & POYNDER, M., 1976. Adenylate cyclase as the basis of the olfactory

transduction mechanism. – Proc. 2nd ECRO Congress, Reading, England: 76.
MENEVSE, A., SQUIRREL, D., DODD, G. & POYNDER, M., 1977. A chemical-modification approach to the olfactory code. – Biochem. Soc. Trans., **5**: 191–194.
MIKI, N., KEIRNS, J. J., MARCUS, F. R. & BITENSKY, M. W., 1974. Light regulation of adenosine 3′, 5′ cyclic monophosphate levels in vertebrate photoreceptors. – Exp. Eye Res., **18**: 281–297.
MINOR, A. V. & SAKINA, N. L., 1973. The role of cyclic adenosine-3′-5′-monophosphate in olfactory reception. – Neirofiziologia, **5**: 415–422.
MØLLGÅRD, K., MALINOWSKA, D. & SAUNDERS, N. R., 1976. Lack of correlation between tight junction morphology and permeability properties in developing chorion plexus. – Nature, **264**: 293–294; Nature, **267**, 1977: 182–183.
MOOR, H., WALDNER, H. & FREY-WYSSLING, A., 1961. A new freezing ultramicrotome. – J. Biophys. Biochem. Cytol., **10**: 1–13.
MOOSEKER, M. S. & TILNEY, L. G., 1975. The organization of an actin filament-membrane complex: filament polarity and membrane attachment in the microvilli of intestinal epithelial cells. – J. Cell Biol., **67**: 725–743.
MORAN, D. T. & VARELA, F. G., 1971. Microtubules and sensory transduction. – Proc. Nat. Acad. Sci. U.S., **68**: 757–760.
MOULTON, D. G., 1974. Dynamics of cell populations in the olfactory epithelium. – Ann. N.Y. Acad. Sci., **237**: 52–61.
MOULTON, D. G., 1975. Cell renewal in the olfactory epithelium of the mouse. – In: Olfaction and Taste, V, Denton, D. A. & Coghlan, J. P., eds.: 111–114, Acad. Press, New York.
MOULTON, D. G., 1976. Spatial patterning of response to odors in the peripheral olfactory system. – Physiol. Rev., **56**: 578–593.
MOULTON, D. G. & BEIDLER, L. M., 1967. Structure and function in the peripheral olfactory system. – Physiol. Rev., **47**: 1–52.
MOULTON, D. G., ÇELEBI, G. & FINK, R. P., 1970. Olfaction in mammals – two aspects: proliferation of cells in the olfactory epithelium and sensitivity to odours. – In: Taste and Smell in Vertebrates, Wolstenholme, G. E. W. & Knight, J., eds.: 227–250, J. & A. Churchill, London.
MOULTON, D. G. & MARSHALL, D. A., 1976a. The performance of dogs in detecting α-ionone in vapor phase. – J. Comp. Physiol., A, **110**: 287–306.
MOULTON, D. G. & MARSHALL, D. A., 1976b. Quantitative analysis of nasal air flow in dogs sniffing odors. – Proc. 2nd. ECRO Congress, Reading, England: 24.
MOZELL, M. M., 1971. Spatial and temporal patterning. – In: Handbook of Sensory Physiology, **Vol. IV**: Chemical Senses, **Part 1**: Olfaction, Beidler, L. M., ed.: 205–215, Springer-Verlag, Berlin.
MÜLLER, A., 1955. Quantitative studies on dog olfactory epithelium. – Z. Zellforsch., **41**: 335–350.
MULVANEY, B. D. & HEIST, H. E., 1970. Mapping of olfactory cells. – J. Anat., **107**: 19–30.
MULVANEY, B. D. & HEIST, H. E., 1971a. Centriole migration during regeneration and normal development of olfactory epithelium. – J. Ultrastruct. Res., **35**: 274–281.
MULVANEY, B. D. & HEIST, H. E., 1971b. Regeneration of rabbit olfactory epithelium. – Am. J. Anat., **131**: 241–251.
MYGIND, N. & BRETLAU, P., 1973. Scanning electron microscopic studies of the human nasal mucosa in normal persons and in patients with perennial rhinitis. 1. Cilia and microvilli. – Acta Allergologica, **28**: 9–27.
NAESSEN, R., 1971. The 'receptor surface' of the olfactory organ (epithelium) of man and guinea pig. A descriptive and experimental study. – Acta Oto-Laryng., **71**: 335–248.
NEGUS, V., 1958. The Comparative Anatomy and Physiology of the Nose and Paranasal Sinuses. – E. & S. Livingstone, Edenburgh.
NEVILLE Jr., D. M., 1975. Isolation of cell surface membrane fractions from mammalian cells and organs. – In: Methods in Membrane Biology, **Vol. 3**, Korn, E. D., ed.: 1–49, Plenum Press, New York.

NICKEL, E. & MENZEL, R., 1976. Insect UV-, and green-photoreceptor membranes studied by the freeze-fracture technique. – Cell Tissue Res., **175**: 357–368.
NIE, N. H., HADLAI HULL, C., JENKINS, J. G., STEINBRENNER, K. & BENT, D. H., 1975. Statistical Package for the Social Sciences (SPSS). – 2nd edition, McGraw-Hill Book Company, New York.
NØRREVANG, A. & WINGSTRAND, K. G., 1970. On the occurrence and structure of choanocyte-like cells in some *Echinoderms*. – Acta Zool. (Stockh.), **51**: 249–270.
NOZAWA, Y., IIDA, H., FUKUSHIMA, H., OHKI, K. & OHNISHI, S., 1974. Studies on *Tetrahymena* membranes: Temperature-induced alterations in fatty acid composition of various membrane fractions in *Tetrahymena pyriformis* and its effect on membrane fluidity as inferred by a spin label study. – Biochim. Biophys. Acta, **367**: 134–147.
OKANO, M., 1965. Fine structure of the canine olfactory hairlets. – Arch. Histol. Jap., **26**: 169–185.
OKANO, M., FURUTA, M., TSUKISE, A. & SUGAWA, Y., 1974. Ultrastructure of olfactory epithelium in embryonic chicks. – In: 8th Int. Congr. Electron Microscopy, Sanders, J. V. & Goodchild, D. J. eds.: 314–315, Austr. Acad. Sci., Canberra.
OKANO, M. & SUGAWA, Y., 1965. Ultrastructure of the respiratory mucous epithelium of the canine nasal cavity. – Arch. Histol. Jap., **26**: 1–21.
OKANO, M. & TAKAGI, S. F., 1974. Secretion and electrogenesis of the supporting cell in the olfactory epithelium. – J. Physiol., **242**: 353–370.
OKANO, M., TSUKISE, A. & SUGAWA, Y., 1973. Ultrastructure of puppy olfactory mucosa. – Bull. Coll. Agr. & Vet. Med., Nihon Univ., **30**: 113–129.
OKANO, M., WEBER, A. F. & FROMMES, S. P., 1967. Electron microscopic studies of the distal border of the canine olfactory epithelium. – J. Ultrastruct. Res., **17**: 487–502.
OKUDA, M. & KANDA, T., 1973. Scanning electron microscopy of the nasal mucous membrane. – Acta Oto-Laryng., **76**: 283–294.
OLEY, N., DEHAN, R. S., TUCKER, D., SMITH, J. C. & GRAZIADEI, P. P. C., 1975. Recovery of structure and function following transection of the primary olfactory nerves in pigeons. – J. Comp. Physiol. Psychol., **88**: 477–495.
OLIVE, J. & RECOUVREUR, M., 1974. Structural organization of mammalian retinal photoreceptors. – In: 8th Int. Congr. Electron Microscopy, Sanders, J. V. & Goodchild, D. J., eds.: 196–197, Austr. Acad. Sci., Canberra.
OLSEN, R. W., 1975. Filamentous protein model for cyclic AMP-mediated cell regulatory mechanisms. – J. Theor. Biol., **49**: 263–287.
ORCI, L. & PERRELET, A., 1975. Freeze-etch Histology. – Springer-Verlag, Berlin.
OTTOSON, D., 1970. Electrical signs of olfactory transducer action. – In: Taste and Smell in Vertebrates, Wolstenholme, G. E. W. & Knight, J., eds.: 343–356, J. & A. Churchill, London.
OTTOSON, D. & SHEPHERD, G. M., 1967. Experiments and concepts in olfactory physiology. – In: Sensory Mechanisms, Progress in Brain Research, **Vol. 23**, Zotterman, Y., ed.: 83–138, Elsevier Publishing Company, Amsterdam.
PEDERSEN, H. & MYGIND, N., 1976. Absence of axonemal arms in nasal mucosa cilia in Kartagener's syndrome. – Nature, **262**: 494–495.
PINTO DA SILVA, P. & MILLER, R. G., 1975. Membrane particles on fracture faces of frozen myelin. – Proc. Nat. Acad. Sci. U.S., **72**: 4046–4050.
PIRENNE, M. H., 1962. Rods and cones. – In: The Eye, **Vol. II**, Davson, H., ed.: 13–29, Acad. Press, London.
PITELKA, D. R., 1974. Basal bodies and root structures. – In: Cilia and Flagella, Sleigh, M. A., ed.: 437–469, Acad. Press, London.
PONTUS, M. & DELMELLE, M., 1975a. Light induced change in rod outer segment membrane fluidity. – Vision Res., **15**: 145–147.
PONTUS, M. & DELMELLE, M., 1975b. Fluid lipid fraction in rod outer segment membrane. – Biochim. Biophys. Acta., **401**: 221–230.
POYNDER, T. M., ed., 1974. Transduction Mechanisms in Chemoreception. – Information

Retrieval Ltd., London.
PRICE, C. A., 1974. Zonal centrifugation. – In: Methods in Molecular Biology. **Vol. 5**: Subcellular Particles, Structures and Organelles, Laskin, A. I. & Last, J. A., eds.: 155–230, Marcel Dekker, New York.
PROCTOR, D. F. & SWIFT, D. L., 1971. The nose- a defence against the atmospheric environment. – In: Inhaled Particles, **Vol. III**, Walton, W. H., ed.: 59–70, Unwin Brothers Ltd., Surrey, England.
REESE, T. S., 1965. Olfactory cilia in the frog. – J. Cell Biol., **25**: 209–230.
REESE, T. S. & BRIGHTMAN, M. W., 1970. Olfactory surface and central olfactory connections in some vertebrates. – In: Taste and Smell in Vertebrates, Wolstenholme, G. E. W. & Knight, J., eds.: 115–149, J. & A. Churchill, London.
RÖHLICH, P., 1975. The sensory cilium of retinal rods is analogous to the transitional zone of motile cilia. – Cell Tissue Res., **161**: 421–430.
ROTER DIRKSEN, E., 1971. Centriole morphogenesis in developing ciliated epithelium of the mouse oviduct. – J. Cell Biol., **51**: 286–302.
ROZENKRANZ, J., 1970. On the fine structure of the frog's rod outer segments, observed by the freeze-etching technique. – Z. Zellforsch., **111**: 228–262.
SAINI, K. D. & BREIPOHL, W., 1976. Surface morphology in the olfactory epithelium of normal male and female Rhesus monkeys. – Am. J. Anat., **147**: 433–446.
SATIR, P., 1974. Freeze-fracture particle arrays in membrane interactions. – In: 8th Int. Congr. Electron Microscopy, Sanders, J. V. & Goodchild, D. J., eds.: 240–241, Austr. Acad. Sci., Canberra.
SATTLER, C. A. & STAEHELIN, L. A., 1974. Ciliary membrane differentiations in *Tetrahymena pyriformis*. *Tetrahymena* has four ciliary types. – J. Cell Biol., **62**: 473–490.
SCHULTE, E., 1972. Studies of the regio olfactoria in the eel, *Anguilla anguilla* L. I. Fine structure of the olfactory epithelium. – Z. Zellforsch., **125**: 210–228.
SCHULTE, E. & HOLL, A., 1971. Ultrastructure of the olfactory epithelium of *Calamoichthys calabaricus* J. A. Smith (Pisces, Brachiopterygii). – Z. Zellforsch., **120**: 261–279.
SEELIG, J. 1970. Spin label studies of oriented smectic liquid crystals (A model system for bilayer membranes). – J. Am. Chem. Soc., **92**: 3881–3887.
SEELIG, J. & HASSELBACH, W., 1971. A spin label study of sarcoplasmic vesicles. – Eur. J. Biochem., **21**: 17–21.
SEGREST, J. P., GULIK-KRZYWICKI, T. & SARDET, C., 1974. Association of the membrane-penetrating polypeptide segment of the human erythrocyte MN-glycoprotein with phospholipid bilayers: I. Formation of freeze-etch intramembranous particles. – Proc. Nat. Acad. Sci. U.S., **71**: 3294–3298.
SEIFERT, K., 1970. The ultrastructure of the olfactory epithelium in macrosmatics. An electron microscopical investigation. – Normale und Pathologische Anatomie, **Heft 21**, Bargmann, W. & Doerr, W., eds., Georg Thieme Verlag, Stuttgart.
SEKIYA, T., KITAJIMA, Y. & NOZAWA, Y., 1975. Freeze-fracture studies of various membrane components isolated from *Tetrahymena pyriformis* cells. – J. Electron Microsc., **24**: 155–165.
SHIBUYA, T. & TAKAGI, S. F., 1963. Electrical response and growth of olfactory cilia of the olfactory epithelium of the newt in water and on land. – J. Gen. Physiol., **47**: 71–82.
SHIMAMURA, A. & TOH, H., 1974. Scanning electron microscopic observations of the nasal mucosa in the rabbit. – J. Electron Microsc., **23**: 227.
SINGER, S. J., 1975. Architecture and topography of biologic membranes. – In: Cell Membranes. Biochemistry, Cell Biology & Pathology, Weissmann, G. & Claiborne, R., eds.: 35–53, HP Publishing Co., Inc., New York.
SINGER, S. J. & NICOLSON, G. L., 1972. The fluid mosaic model of the structure of cell membranes. – Science, **175**: 720–731.
SLEIGH, M. A., ed., 1974. Cilia and Flagella. – Acad. Press, London.
SLEYTR, U., KERJASCHKI, D. & STOCKINGER, L., 1972. Freeze etching preparation of tissue fragments with the EPA 100 demonstrated on the nose septum of the mouse. – Mikrosko-

pie, **28**: 257–268.
SMITH, I. C. P., 1971. A spin label study of the organization and fluidity of hydrated phospholipid multibilayers-a model membrane system. – Chimia, **25**: 349–360.
SNIPES, W. & KEITH, A., 1970. Spin labels extend applications of ESR. – Research/Development, **February 1970**, 22–26.
STAEHELIN, L. A., 1974. Structure and function of intercellular junctions. – Int. Rev. Cytol., **39**: 191–283.
STAEHELIN, L. A., MUKHERJEE, T. M. & WYNN WILLIAMS, A., 1969. Freeze-etch appearance of the tight junctions of small and large intestine of mice. – Protoplasma (Wien), **67**: 165–184.
STAHL, W. H., 1973. Compilation of Odor and Taste Threshold Values Data. – ASTM Data Series DS 48, Philadelphia.
STEMPAK, J. G. & WARD, R. T., 1964. An improved staining method for electron microscopy. – J. Cell Biol., **22**: 697–701.
STEPHENS, R. E. & EDDS, K. T., 1976. Microtubules: Structure, chemistry and function. – Physiol. Rev., **56**: 709–777.
STEPHENS, R. E. & LEVINE, E. E., 1970. Some enzymatic properties of axonemes from the cilia of *Pecten irradians*. – J. Cell Biol., **46**: 416–421.
STOCKINGER, L., 1963. The ultrastructure of the ciliated epithelium of the nasal septum of the rat. – Z. Zellforsch., **59**: 443–466.
STOCKINGER, L., KERJASCHKI, D. & HÖRANDNER, H., 1974. A freeze-etch representation of the olfactory epithelium. – Verh. Anat. Ges., **68**: 487–490.
STONE, T. J., BUCKMAN, T., NORDIO, P. L. & MCCONNELL, H. M., 1965. Spin-labeled biomolecules. – Proc. Nat. Acad. Sci. U.S., **54**: 1010–1017.
STUIVER, M., 1958. Biophysics of the sense of smell. – Dissertation Groningen University, Groningen, Holland.
SUMMERS, K., 1975. The role of flagellar structures in motility. – Biochem. Biophys. Acta, **416**: 153–168.
ŠVEJDA, J. & ŠAFÁŘ, V., 1974. The ciliated epithelium in the scanning electron microscope. – Schweiz. Monatschr. Zahnheilkd., **84**: 1341–1355.
TAKAGI, S. F., 1971. Degeneration and regeneration of the olfactory epithelium. – In: Handbook of Sensory Physiology, **Vol. IV**: Chemical Senses, **Part 1**: Olfaction, Beidler, L. M., ed.: 75–94, Springer-Verlag, Berlin.
TAKAGI, S. F. & OKANO, M., 1974. An electrophysiological and electronmicroscopical study of the secretion in the olfactory epithelium. – Gumma Symp. Endocr., **11**: 3–14.
TEICHMANN, H., 1954. Comparative investigations on the nose of fishes. – Z. Morph. Ökol. Tiere, **43**: 171–212.
TEICHMANN, H., 1959. About the performance of the sense of smell in the eel (*Anguilla anguilla* (L.)). – Z. vergl. Physiol., **42**: 206–254.
THEISEN, B., 1973. The olfactory system in the hagfish *Myxine glutinosa*. I. Fine structure of the apical part of the olfactory epithelium. – Acta Zool. (Stockh.), **54**: 271–284.
THORNHILL, R. A., 1967. The ultrastructure of the olfactory epithelium of the lamprey *Lampreta fluviatilis*. – J. Cell Sci., **2**: 591–602.
THURM, U., 1969. General organization of sensory receptors. – In: Rendiconti della Scuola Internazionale di Fisica 'Enrico Fermi', **Vol. 43**, Reichardt, W., ed.: 44–68, Acad. Press, London.
TUCKER, D., 1967. Olfactory cilia are not required for receptor function. – Fed. Proc., **26**: 544.
VANDE BERG, J. S., 1975. Cytochemical localization of phosphodiesterase: axonal, mitochondria and microtubules. – J. Insect Physiol., **21**: 455–461.
VENABLE, J. H. & COGGESHALL, R., 1965. A simplified lead citrate stain for use in electron microscopy. – J. Cell Biol., **25**: 407–408.
VERKLEIJ, A. J. & VERVERGAERT, P. H. J. TH., 1975. The architecture of biological and artificial membranes as visualized by freeze etching. – Ann. Rev. Phys. Chem., **26**: 101–122.

VERMA, S. P., BERLINER, L. J. & SMITH, I. C. P., 1973. Cation-dependent light induced structural changes in visual receptor membranes. – Biochem. Biophys. Res. Comm., **55**: 704–709.

VINNIKOV, YA. A., 1969. The ultrastructural and cytochemical bases of the mechanism of function of the sense organ receptors. – In: The structure and Function of Nervous Tissue, **II**, Bourne, G. H., ed.: 265–392, Acad. Press, New York.

VINNIKOV, YA. A., 1974. Sensory Reception. Cytology, Molecular Mechanisms and Evolution. – In: Molecular Biology, Biochemistry and Biophysics, **Vol. 17**, Kleinzeller, A., Springer, G. F. & Wittmann, H. G., eds., Springer-Verlag, Berlin.

WADE, J. B., 1976. Membrane structural specialization of the toad urinary bladder revealed by the freeze-fracture technique. II. The mitochondria-rich cell. – J. Membrane Biol., **29**: 111–126.

WADE, J. B. & KARNOVSKY, M. J., 1974. The structure of the zonula occludens. A single fibril model based on freeze-fracture. – J. Cell Biol., **60**: 168–180.

WARNER, F. D., 1972. Macromolecular organization of eukaryotic cilia and flagella. – Adv. Cell. Mol. Biol., **2**: 193–235.

WARNER, F. D., 1974. The fine structure of the ciliary and flagellar axoneme. – In: Cilia and Flagella, Sleigh, M. A., ed.: 11–37, Acad. Press, London.

WATERMAN, R. E. & MELLER, S. M., 1973a. Nasal pit formation in the hamster: A transmission and scanning electron microscopic study. – Develop. Biol., **34**: 255–266.

WATERMAN, R. E. & MELLER, S. M., 1973b. Scanning electron microscopic study: Early nasal development in golden hamster. – J. Dent. Res., **52**: 112.

WEBER, K. & OSBORN, M., 1969. The reliability of molecular weight determinations by dodecyl sulfate-polyacrylamide gel electrophoresis. – J. Biol. Chem., **244**: 4406–4412.

WHITTAKER, V. P., 1965. The application of subcellular fractionation techniques to the study of brain function. – Progr. Biophys., **15**: 39–96.

WILSON, G. B., JAHN, T. L. & FONESCA, J. R., 1975. Studies on ciliary beating of frog pharyngeal epithelium in vitro: 1. Isolation and ciliary beat of single cells. – Trans. Amer. Microsc. Soc., **94**: 43–57.

WOLFE, J., 1972. Basal body fine structure and chemistry. – Adv. Cell. Mol. Biol., **2**: 151–192.

YAMAMOTO, M., 1976. An electron microscopic study of the olfactory mucosa in the bat and rabbit. – Arch. Histol. Jap., **38**: 359–412.

YAMAMOTO, M., UCHIDA, K. & ITO, T., 1976. Regeneration of olfactory bipolar neurons in the normal olfactory epithelium of the adult bat. – Okajimas Fol. Anat. Jap., **53**: 291–304.

ZEISKE, E., MELINKAT, R., BREUCKER, H. & KUX, J., 1976. Ultrastructural studies on the epithelia of the olfactory organ of Cyprinodonts (Teleostei, Cyprinodontoidea). – Cell Tissue Res., **172**: 245–267.

ZINGSHEIM, H. P. & PLATTNER, H., 1976. Electron microscopic methods in membrane biology. – In: Methods in Membrane Biology, **Vol. 7**, Korn, E. D., ed.: 1–146, Plenum Publishing Company, New York.